MAGNETIC SURFACE EFFECTS ON SOLAR OSCILLATIONS

Rekha Jain

A Thesis Submitted for the Degree of PhD
at the
University of St Andrews

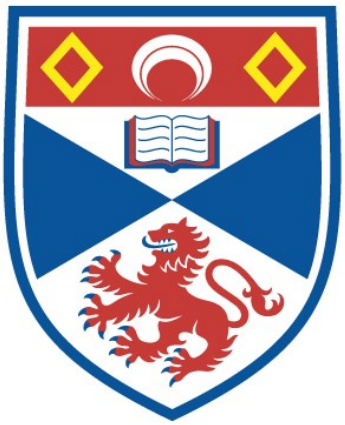

1993

MAGNETIC SURFACE EFFECTS ON SOLAR OSCILLATIONS

Rekha Jain

A thesis submitted for the degree of Doctor of Philosophy at the University of St. Andrews

ProQuest LLC.
789 East Eisenhower Parkway
P.O. Box 1346
Ann Arbor, MI 48106 – 1346

ABSTRACT

This thesis is concerned with the effects of magnetic atmospheres on solar oscillations.

The behaviour of magnetohydrodynamic surface waves propagating on a single magnetic interface is discussed ignoring the effects of gravity. The effects of non-parallel propagation (where the wave vector is at an angle to the magnetic field direction) are considered.

The effects of chromospheric magnetic fields on solar p- and f-modes in a stratified atmosphere are examined for three different models. In the first of these models, the chromosphere is assumed to be isothermal and permeated by a uniform and horizontal magnetic field. A dispersion relation for the p-modes trapped below such an atmosphere is derived. Asymptotic and numerical solutions for the p-modes are discussed in detail. An increase in chromospheric magnetic field strength leads to an increase in the frequency of the p-modes, whereas an increase in the chromospheric temperature leads to a decrease in the frequencies of these modes. Comparison with observational data suggests that both these effects may indeed take place.

The second model is set up for magnetic fields which decrease with height in such a way that the Alfvén speed remains constant. In addition to magnetic effects, the effects of non-parallel propagation on p- and f-modes are considered in the presence of such a non-uniform magnetic field. After deriving a very general dispersion relation, various asymptotic and numerical solutions have been obtained and the possible effects of magnetic fields and non-parallel propagation on these modes are examined. The presence of a horizontal non-uniform chromospheric field produces changes in the frequencies of the p- and f-modes, reducing the frequencies of p-modes and increasing the frequency of the f-mode. Besides depending upon magnetic field strength, frequencies also depend on both the mode's order n and its degree l. The effects of non-parallel propagation are found to be most significant for the f-mode and the low order p-modes.

The magnetic structure of the chromosphere has been further generalised by combining the two models described above. In this three layer model, a dispersion relation is derived in a general manner and discussed in detail for the p-modes. The role of magnetoacoustic cut-off frequency is studied. Again, the results are qualitatively similar to those found from observation.

DECLARATION

I, Rekha Jain, hereby certify that this thesis has been composed by myself, that it is a record of my own work, and that it has not been accepted in partial or complete fulfilment of any other degree or professional qualification.

Signature of Candidate.....

Date 26th June '92.

POSTGRADUATE CAREER

I was admitted to the Faculty of Science of the University of St. Andrews under Ordinance General No. 12 in May 1989 and as a candidate for the degree of Ph.D in October 1989.

Signature of Candidate..

Date 26th June '92.

CERTIFICATE

I certify that Rekha Jain has satisfied the conditions of the Ordinance and Regulations and is thus qualified to submit the accompanying application for the degree of Doctor of Philosophy.

Signature of Supervisor ..

Date 26 June 1992

COPYRIGHT

ACKNOWLEDGEMENTS

Discussions on a variety of topics, with folks from various fields of research coming from different educational and cultural backgrounds, is a regular feature of a research student's life in St. Andrews. The inspirations, frustrations, prejudices and occasional triumphs of a large number of people thus run through this thesis, unseen and unacknowledged, except here where I would like to say thanks to this lively group of friends, colleagues and flatmates. Their informal and occasionally incisive wit has made my stay in St. Andrews much more of a pleasure and lot less of a chore than it otherwise might have been. Although I can not recount every individual name here, I am specially proud to have known Drs. Alan Miles, Colin Steele and David Evans.

I owe a special sense of gratitude to my supervisor Dr. B. Roberts for his very tangible contribution. Because of the unpredictable nature of the research work I was involved with, his advice and encouragement came as a beacon light to guide the path of my research. During the course of this work, I have drawn upon both his knowledge as well as profound experience, covering several aspects of solar physics, through many enlightening discussions. His calm, patient and optimistic outlook were always a source of inspiration for me. His enthusiasm and supply of fresh ideas were very encouraging especially when the going was tough and dull (on many occassions it provided a necessary impetus to get back to the calculations !). It has given me immense pleasure to work with him. My thanks to him are as endless as my happiness in getting it all over with.

I would also like to extend my thanks to Prof. E. R. Priest for he always listened and helped !

This happiness of coming to the end of the tunnel is perhaps shared by my family and friends back home too, who made it all possible. Without their love and support none of this could have happened. Coping with an offspring who wanted to study abroad must be a great trial for any parents, but mine managed admirably. I would like to express my gratitude to them.

Financial assistance for this work came from the University of St. Andrews and Committee of Vice Chancellors and Principals. Thanks are also due to them for their generosity.

To
Mom, Dad and Usha,
With love and thanks

'We Dance around in a Ring and Suppose,
But the Secret sits in the Middle and Knows'
.....Robert Frost

CONTENTS

CHAPTER 1

INTRODUCTION

1.1 Solar Oscillations

Throughout history, and indeed pre-history, the Sun has occupied a position of awe and fascination for Mankind. Part of this fascination lies with its obvious role in providing energy. In recent times, however, with the advent of sophisticated instruments, it has been realised that the Sun, with its dynamic atmosphere, can sometimes provide a spectacular sight as any of flares, prominences or sunspots may be present. The main reason that the Sun is studied, however, is that it (and in particular its atmosphere) plays an important role in the current understanding of the Universe.

Just as the Earth's atmosphere supports the propagation of sound waves (by consisting of compressible gases), the compressible nature of the Sun's atmosphere (plasma in this case) allows it too to support sound waves. However, as the Sun's atmosphere also contains a significant magnetic field, waves and oscillations other than simple sound waves may also exist.

Sound waves are produced and propagated by the restoring forces provided by the gas or plasma pressure. In the case of magnetic fields, additional restoring forces are provided by the magnetic pressure and tension. Thus, sound waves in the solar atmosphere are influenced and modified by these magnetic forces, the resulting waves being known as *magnetoacoustic waves* or *magnetohydrodynamic waves.*

Solar oscillations have long been studied now, but there still remains a great deal to be understood about them. Since the oscillations and waves in the Sun are controlled by various restoring forces, pressure, buoyancy and magnetic, their study provides an understanding of these basic forces. When more than one restoring force is present, the wave behaviour can become very interesting and its study very complicated. Besides being phenomena of curiosity, solar oscillations can be useful in providing some information about the Sun, information that perhaps cannot be acquired by any other means.

The Sun is an ordinary star among stars and it is believed that many other stars exhibit solar type oscillations and phenomena to a smaller or larger extent. Thus the

understanding of solar oscillations is important for the study of stellar oscillations.

Many of the magnetic atmosphere effects discussed in the following chapters may well take place in atmospheres of Sun-like stars even though it will not be easy to carry out detailed observations due to the remote nature of these stars.

The Sun is unique in that one is able to diagnose properties by remote, yet high resolution optical observations, together with sophisticated analytical and computational work. This combination allows one to infer stellar atmospheric features in detail, impossible to obtain directly even for nearby stars.

Because of the Sun's proximity, solar oscillations are, and surely will be for the forseeable future, the only stellar oscillations that can be investigated in any detail.

1.2 Basic Equations and Definitions

Before discussing the theoretical work on solar oscillations, it is instructive to put together the basic equations and definitions that will be used in the rest of the thesis. All the models studied make use of the magnetohydrodynamic (MHD) equations.

In magnetohydrodynamics, the study of the interaction between a plasma and a magnetic field, certain assumptions are made (e.g. Priest, 1982). The plasma is considered as a single continuous fluid and is assumed to be in thermodynamic equilibrium. It is also assumed that all velocities are very small compared to the speed of light and hence that relativistic effects can be neglected. The plasma is assumed to be compressible and of infinite conductivity. The equations that describe its motion are (e.g., Priest, 1982):

$$\rho\left[\frac{\partial \mathbf{v}}{\partial t}+(\mathbf{v}\cdot\nabla)\,\mathbf{v}\right] = -\nabla p+\frac{1}{\mu}(\nabla\times\mathbf{B})\times\mathbf{B}+\rho\mathbf{g}\,, \tag{1.1}$$

$$\frac{\partial \rho}{\partial t}+\rho\nabla\cdot\mathbf{v}+\mathbf{v}\cdot\nabla\rho = 0, \tag{1.2}$$

$$\frac{\partial p}{\partial t}+\mathbf{v}\cdot\nabla p = \frac{\gamma p}{\rho}\left(\frac{\partial \rho}{\partial t}+\mathbf{v}\cdot\nabla\rho\right)\,, \tag{1.3}$$

$$\frac{\partial \mathbf{B}}{\partial t} = \nabla\times(\mathbf{v}\times\mathbf{B})\,, \tag{1.4}$$

$$\mathbf{j} = \frac{1}{\mu}\nabla\times\mathbf{B}\,, \tag{1.5}$$

$$\nabla \cdot \mathbf{B} \;=\; 0\,. \tag{1.6}$$

Here ρ represents the density and p the pressure of the plasma, $\mathbf{v}$ is the Eulerian velocity field, $\mathbf{B}$ is the magnetic field, $\mathbf{j}$ is the vector current density, γ is the ratio of specific heats (specific heat at constant pressure divided by specific heat at constant volume) and μ is the magnetic permeability. Gravity is denoted by $\mathbf{g}$. Equations (1.1), (1.2) and (1.6) describe the conservation of momentum, mass and magnetic flux. The equation of state is

$$p \;=\; \mathcal{R}\rho T\,, \tag{1.7}$$

where $\mathcal{R}$ ($=\frac{k_B}{m_p}$, where k_B is Boltzmann's constant and m_p is the mean particle mass) is the gas constant.

The following definitions will also be used :

1) The sound speed, c_s, is given by :

$$c_s(z) \;=\; \left(\frac{\gamma p(z)}{\rho(z)}\right)^{1/2}\,; \tag{1.8}$$

2) The Alfvén speed, v_A, is given by :

$$v_A(z) \;=\; \frac{B(z)}{(\mu\rho(z))^{1/2}}\,; \tag{1.9}$$

3) The plasma beta, which is the ratio of plasma to magnetic pressure, is given by :

$$\beta \;=\; \frac{2\mu p}{B^2}\,, \tag{1.10}$$

4)The slow magnetoacoustic or cusp speed is given by :

$$c_T \;=\; \frac{c_s v_A}{(c_s^2+v_A^2)^{1/2}}\,; \tag{1.11}$$

5) The fast magnetoacoustic speed is given by :

$$c_f \;=\; \left(c_s^2+v_A^2\right)^{1/2}\,; \tag{1.12}$$

6) The density scale height (length scale over which density changes) is given by :

$$H = \frac{\rho}{d\rho/dz} ; \tag{1.13}$$

7) The acoustic cut-off frequency of an isothermal atmosphere is given by :

$$\omega_a = \frac{c_s}{2H} ; \tag{1.14}$$

8) The buoyancy (or Brunt Väisälä) frequency ω_g of an atmosphere is given by :

$$\omega_g = \left[\frac{g}{H} - \left(\frac{g}{c_s}\right)^2\right]^{1/2} . \tag{1.15}$$

Use will be made of these quantities in the following sections and chapters.

1.3 Magnetoacoustic Surface Waves

There are several reasons which motivate the study of magnetic surface effects on solar oscillations. In the Sun, the plasma is surrounded or bounded by another plasma (i.e. plasma with different properties) giving rise to surfaces rather than a uniform system. Some of the properties of solar oscillations, which depend crucially on the nature of the plasma and its interaction with the magnetic field on either side of this bounded surface, can differ greatly between neighbouring locations. It is useful to recap the well-known results for a uniform medium as these results provide a basis for the analysis of magnetoacoustic surface waves.

The nature of the waves in a uniform medium can be found by considering equations (1.1) to (1.6) and introducing small perturbations to the equilibrium quantities. Throughout the thesis, it will be assumed that perturbations are sufficiently small that their squares and products may be ignored, i.e. a linear analysis may be carried out. Variables are assumed to be of the form

$$p = p_o + p \exp i\,(\omega t - \mathbf{K}.\mathbf{r}) , \tag{1.16}$$

for an equilibrium value p_o and a perturbation $p \exp i\,(\omega t - \mathbf{K}.\mathbf{r})$; i.e. perturbations are oscillatory in both space and time, with angular frequency ω and wavenumber $K = |\mathbf{K}|$. On analysis equations (1.1) to (1.6) yield (see, for example, Roberts, 1985)

$$\left(\omega^2 - k_z^2 v_A^2\right)\left[\omega^4 - \left(c_s^2 + v_A^2\right) K^2\omega^2 + K^2 k_z^2 c_s^2 v_A^2\right] \;=\; 0\,, \qquad (1.17)$$

where k_z is the z-component of $\mathbf{K}$, and c_s and v_A are the sound and Alfvén speeds (introduced in Section 1.2).

On solving Equation (1.17), three forms of waves are found with velocities equaling or being closely associated with the Alfvén speed, the fast magnetoacoustic speed and the slow magnetoacoustic or cusp speed, these waves being referred to as the Alfvén wave, the fast magnetoacoustic wave and the slow magnetoacoustic wave. Of these, the fast wave propagates in all directions whereas the Alfvén wave and the slow magnetoacoustic wave cannot travel in directions perpendicular to the magnetic field. Thus the effects of these waves depend on the direction of propagation. The speeds of these waves, as well as their degrees of influence, are governed by a parameter giving the degree of magnetism of an atmosphere. The plasma β is such a parameter; high values of β denote a non-magnetic atmosphere while low values indicate that magnetic effects are dominant.

Deep within the photosphere of the Sun, the plasma β is high, i.e. $\beta \gg 1$ (due to the extremely high plasma pressures), whereas in the high corona the plasma is extremely tenuous and the plasma beta is correspondingly low ($\beta \ll 1$). Around the photosphere and low chromosphere, the magnetic and plasma pressures are roughly equal and $\beta \approx 1$.

Thus the influence of the magnetic field is a function of height within the atmosphere - an effect of stratification. In addition to this stratification, however, the solar atmosphere is highly structured, i.e. the magnetic field is confined (by convection effects) to a large number of thin flux tubes. In these flux tubes, $\beta \approx 1$ and magnetic effects and acoustic effects are roughly comparable, whereas away from these tubes $\beta \gg 1$ and magnetic fields are less significant.

Equation (1.17) can be expressed in the form

$$\left(\frac{\omega}{K}\right)^4 - \left(c_s^2 + v_A^2\right)\left(\frac{\omega}{K}\right)^2 + \cos^2\theta c_s^2 v_A^2 \;=\; 0\,, \qquad (1.18)$$

which can easily be solved to find the speeds of the magnetoacoustic waves. In Equation (1.18), θ is the angle between the direction of propagation, $\mathbf{K}$, and the direction of the equilibrium magnetic field lines. In particular, the behaviour for extremely large or small values of the plasma beta can be found. For very small beta the slow and fast

speeds tend to the values $(v_A^2 \cos^2\theta)^{1/2}$ and $\left(c_s^2 + v_A^2 \sin^2\theta\right)^{1/2}$, whereas in the case of very large beta these speeds tend to $(c_s^2 \cos^2\theta)^{1/2}$ and $\left(v_A^2 + c_s^2 \sin^2\theta\right)^{1/2}$. For the special case of parallel propagation ($\theta = 0$) for extreme values of β the fast speed is $\max(v_A, c_s)$ while the slow speed is $\min(v_A, c_s)$.

Thus, for a uniform medium, three fundamental types of waves exist, namely the Alfvén wave, the slow magnetoacoustic wave and the fast magnetoacoustic wave. However, the assumption of uniformity is not generally valid; and in the Sun, there exist discontinuities (or at least regions of rapid change) in the density, pressure, temperature and magnetic field. Such discontinuities take the form of two dimensional sheets, separating two different parts of the atmosphere. These discontinuities modify the waves referred to above and, in fact, magnetoacoustic waves propagate along such surfaces and are given the title magnetoacoustic surface waves.

Obviously, abrupt positional changes in such quantities as density, pressure, temperature or magnetic field are not physically reasonable but as far as the propagation of a wave is concerned if the region where a physical quantity varies is much less than the wavelength of the relevant wave, then the effect that this gradual interface has on the wave is closely similar to the effect that a sharp interface produces.

There exist many candidates for surface waves. One candidate is the running penumbral wave (see Giovanelli, 1972; Zirin and Stein, 1972 for the first observations). Such waves are seen to emanate from the umbrae of sunspots and, in fact, they move along the boundary between the penumbrae and the underlying plasma. Nye and Thomas (1974, 1976) modelled these as magnetoacoustic gravity modes (magnetoacoustic waves influenced by gravity), whereas Small and Roberts (1984) modelled such waves as fast magnetoacoustic surface waves.

Other possible applications of surface waves include coronal heating (Ionson (1978, 1985); Rae and Roberts (1981); Hollweg (1985, 1987a,b); Lee and Roberts (1986)), helioseismology (Deubner and Gough (1984), Christiansen-Dalsgaard, Gough and Toomre (1985), Leibacher et al (1985)), magnetospheric physics (Southwood and Hughes (1983) and references therein) and laboratory applications.

A particularly simple discontinuity producing a surface wave is the one where the magnetic field takes on different values in the two sides of the interface. The speed of the surface wave lies in the interval between the Alfvén speeds on the two sides of the discontinuity (Kruskal and Schwarzchild, 1954; Dungey and Loughhead, 1954; Chandrasekhar, 1961). Adding in compressibility allows two surface waves to exist (Roberts, 1981).

The inclusion of gravity adds complexity to the surface wave velocities. In the

presence of gravity, a further term, a function of the difference in density across the interface is present in the expression for the phase speed ω/k. In extreme cases, this term may cause ω to be imaginary, i.e. the interface is unstable (e.g. a dense fluid resting above a less dense fluid with the magnetic fields being weak).

A study of magnetoacoustic surface waves on a solitary planar interface is carried out in Chapter 2. It must be remembered, however, that for solar applications, interfaces are affected by curvature and furthermore waves can be influenced by more than one interface (see Chapter 5). However, before looking at curved or multiple interfaces, it is necessary to understand the simple cases.

In summary, magnetic structuring in the solar atmosphere takes place due to the surfaces of discontinuity on either side of which the plasma and magnetic properties vary. Magnetohydrodynamic surface waves can exist on discontinuities in the magnetic field, plasma density, pressure or temperature.

1.4 Helioseismology

1.4.1 A Brief History

In 1960, it was discovered that the Sun undergoes a regular oscillatory motion with a dominant period of 5 minutes and a velocity amplitude of ~ 1 ms^{-1}. These oscillations were inferred from the Doppler images of the Sun obtained at Mount Wilson Observatory (Leighton 1960; Leighton et al. 1962). This discovery was later confirmed by Evans and Michard (1962). Over the next decade or so, several studies were made of the characteristics of the oscillations, and of their causes. These oscillations were observed to be of reduced power amplitude in regions of strong magnetic field.

Early observations were difficult to interpret because power spectral analysis techniques were, at the time, restricted to a single dimension. A major breakthrough towards the understanding of the oscillations came in 1966 when the two dimensional power spectrum was first applied to the problem (Mein, 1966). In this spectrum, also known as diagnostic diagram, the observed power is plotted as a function of the horizontal wavelength and the frequency of the wave. Application of these diagrams to the solar oscillations then demonstrated that the oscillations were evanescent in the solar atmosphere.

Many models were put forward to explain these observations. The earliest model was of a rising granule acting like a piston, providing an impulse to the atmosphere which then continued to oscillate. Since the acoustic waves emitted by this process should be isotropically propagating both horizontally and vertically, this model was ruled out as observations had shown that the solar 5-minute oscillations were primarily

vertical motions. Other models included either gravity or acoustic waves trapped in various regions of the Sun, ranging from the convection zone to the transition region. Each of these models predicted a different pattern of power in the diagnostic diagram.

The trapping of gravity waves was ruled out because the observations showed at least two patches of power in the evanescent acoustic wave region of the diagram. Ulrich (1970) and, subsequently, Leibacher and Stein (1971), by the models of acoustic wave trapped below the photosphere, predicted a characteristic, parabolic pattern of dispersion curves in the diagnostic $k-\omega$ (wavenumber-frequency) diagram. According to these models, the parabolic ridges arise from the interference of acoustic waves trapped in the temperature structure inside the Sun. In time the observers improved the resolution of the observations and decreased the noise in the diagnostic diagram by observing larger areas for longer time spans, and began to find slanted ridges of power (Deubner, 1972). Finally, Deubner (1975) was able to make sufficiently high quality observations which undoubtedly showed the presence of several well-separated ridges of power, hence confirming the trapped acoustic wave models. An example of a present day high quality diagnostic diagram is shown in Figure 1.1.

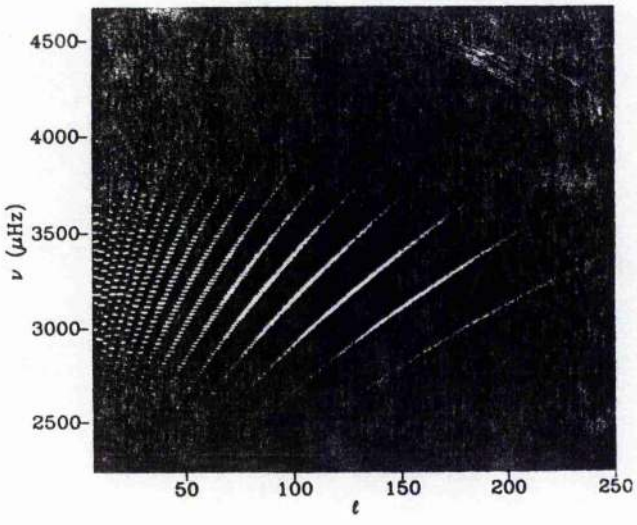

Figure 1.1: A diagnostic ($k-\omega$ or $l-\nu$) diagram of the solar p-mode oscillations. The power in this two dimensional spectrum is distributed in individual peaks that are aligned along curved ridges. Each peak corresponds to an individual mode with a specific l and n value, where l is the spherical harmonic degree and n is the radial order of the mode. Each ridge contains modes with equal values of n (figure courtesy Dr. J. W. Harvey, from Duvall et. al, 1987).

The trapping of acoustic waves is understood in the following way. The acoustic waves below the solar surface will propagate away in all directions if there is any disturbance in the fluid. Deeper in the Sun, waves whose path of propagation is not oriented precisely vertically (i.e. if the propagation path is at a non-zero angle to the vertical), will be refracted sideways and eventually upwards by the increasing sound-speed (increasing with temperature and depth). On the other hand, just below the photosphere, the pressure scale height rapidly decreases outwards to a value less than the wavelength of the waves, reflecting them back downwards. These two reflection points define a cavity within which the waves are trapped. The position of the lower reflection point depends on the number of vertical nodes of the wave. The interference of waves propagating around the cavity will give rise to a standing wave pattern such that the energy density outside the cavity vanishes.

The condition for a standing wave is that the wave should return to its starting point after a whole number of reflections at the surface and it should not undergo any phase change (i.e. it should be in phase with the initial wave). The more often a wave returns to the surface on its round trip of the Sun, the less deeply it penetrates before being turned back. Thus some of these standing waves cover the whole of the Sun, while others only the outer regions (see Figure 1.2). It was realised that by measuring the frequencies of these waves, it is possible to deduce the variation of sound speed from the surface to the deeper regions and in turn find out the temperature and density at various depths. Thus the importance of helioseismology was finally realised.

Three dimensional standing wave patterns (also called as normal modes) can be set up for approaching and receding areas on the surface of the Sun. The velocity pattern in a mode can be divided into radial and angular parts. The mode structure in the radial direction is represented by *radial order* n. The angular part being a spherical harmonic introduces two mode numbers, *spherical harmonic degree* l and *azimuthal order* m. Thus l and m describe the spatial variation. The number of nodes around the azimuth (a great circle through the poles) depends on the degree l and the number of nodes around the equator depends on m. If the Sun were not rotating, then the modes of the same l and n, but different m, would have the same frequency. But the Sun rotates and the small differences in frequency between modes of different m contain information about the rotational velocity.

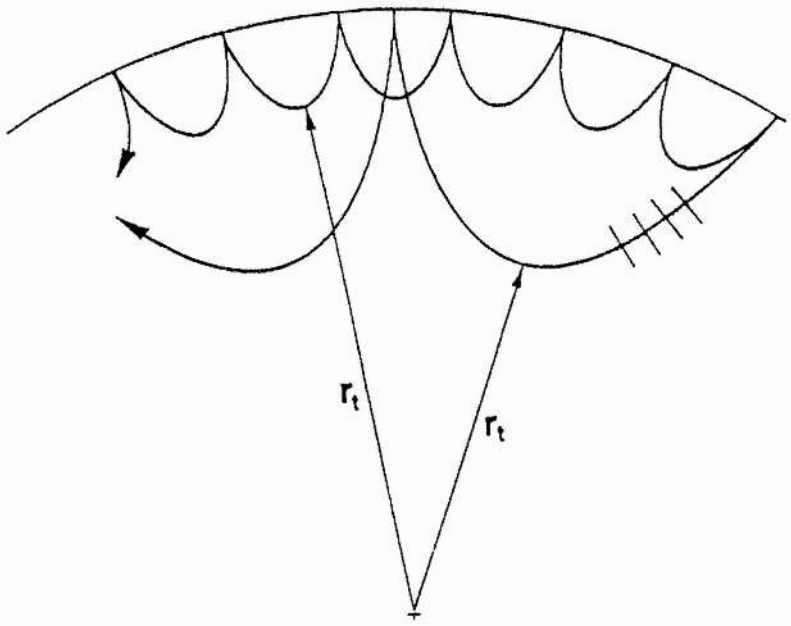

Figure 1.2: Schematic illustration of the propagation of the sound wave in the Sun. Due to the increase of the sound speed with depth, the deeper parts of the wave fronts move faster. Notice that waves with a smaller wavelength, corresponds to a higher value of the degree l, penetrate less deeply (figure courtesy, Christensen Dalsgaard and Berthomieu, 1991).

1.4.2 General Description

Generally these 5-minute oscillations are discussed either as plane waves or as spherical harmonics. The spherical harmonic description is most appropriate for global modes which *feel* the spherical geometry of the Sun. Normally this description is most relevant for low l modes. In this description, the radial component of a mode of oscillation is described by an eigenfunction ξ in polar coordinates (r, θ, ϕ) where r is the radius, θ is the colatitude, and ϕ is the longitude. The eigenfunction is

$$\xi(l, m, n) = A_{ln}(r) Y_l^m(\theta, \phi) e^{i\omega_{mnl}t}, \tag{1.19}$$

where $A_{ln}(r)$ is the radial dependence of the eigenfunction, n is the number of radial nodes. A spherical harmonic is represented by $Y_l^m(\theta, \phi) = P_l^m(\cos\theta)e^{im\phi}$ where

$P_l^m(\cos\theta)$ is the associated Legendre function.

As mentioned earlier, the spherical harmonic degree l is the total number of nodal lines on the solar surface. The azimuthal order m is the number of nodal lines around the equator of the coordinate system. This equator is generally chosen as the solar rotation equator. The value of m is restricted to be between $+l$ and $-l$, thereby giving $2l+1$ values of m to each mode for one value of l. If $m = 0$, then the mode is called a *zonal* mode; if $m = l$, the mode is a *sectoral* mode. The remaining modes are *tesseral*. The cyclic frequency ω_{lmn} depends on the mode with values l, m and n. It is given by $\nu = \omega/2\pi = 1/P$, where P is the period of the mode. Measurement of ν provides the basic data of helioseismology.

The radial equation for adiabatic oscillations, ignoring the perturbation to the gravitational potential, is given by (see Deubner and Gough, 1984)

$$\frac{d^2\Psi}{dr^2} + \left[\frac{\omega^2 - \omega_a^2}{c_s^2} - \left(1 - \frac{\omega_g^2}{\omega^2}\right)\frac{l(l+1)}{r^2}\right]\Psi = 0\,, \tag{1.20}$$

where

$$\Psi = c_s^2\rho_o^{1/2}\mathrm{div}A\,,\quad \omega_a^2 = \frac{c_s^2}{4H^2}(1-2H')\,,\quad H = \frac{\rho_o}{\rho_o'}\,,\quad \omega_g^2 = g\left(\frac{1}{H} - \frac{g}{c_s^2}\right)\,. \tag{1.21}$$

The dash ($'$) denotes differentiation with respect to r; ω_a^2 is a generalisation of Lamb's acoustic cut-off frequency. H is the density scale height, and ω_g is the buoyancy (Brunt Väisälä) frequency. Thus, it is clear from Equation (1.20) that the behaviour of the mode is determined by the variation of the characteristic frequencies ω_g and ω_a and also $l(l+1)/r$ with r.

In the plane wave approximation, the modes are considered to be local waves, not affected by the curved shape of the Sun. This approximation is not valid for very small values of l, or for long wavelengths. In this representation, the eigenfunction becomes

$$\Psi(k_h, n) \equiv A_{ln}(x)e^{i(\omega t - k_h x)}\,, \tag{1.22}$$

where k_h is the horizontal wavenumber and x is the displacement in a horizontal coordinate system on the solar surface. The plane parallel equivalent of Equation (1.20) is given by

$$\frac{d^2\Psi}{dx^2} + \left[\frac{\omega^2 - \omega_a^2}{c_s^2} - \left(1 - \frac{\omega_g^2}{\omega^2}\right)k_h^2\right]\Psi = 0\,. \tag{1.23}$$

Comparing Equations (1.20) and (1.23), it is clear that modes in the spherical case are equivalent to modes in the plane parallel case when the horizontal wavenumber k_h is related to spherical degree l by

$$k_h = [l(l+1)]^{1/2}/R_{Sun} , \tag{1.24}$$

where R_{Sun} is the solar radius. The wavenumber k_h is related to λ_h, the horizontal wavelength of the wave, by $k_h = \frac{2\pi}{\lambda_h}$. This plane wave description will be used in the remainder of the thesis.

1.5 The P-mode Dispersion Relation

It is useful to examine the dispersion relation for p-modes in a plane parallel atmosphere, assuming a linear temperature profile for the convection zone.

Consider the equilibrium values of pressure, temperature and density to be $p_o(z)$, $T_o(z)$ and $\rho_o(z)$, respectively, and their perturbations to be $p(z)$, $T(z)$ and $\rho(z)$.

The undisturbed state ($\mathbf{v} = 0$, $\partial/\partial t = 0$) of the atmosphere in the absence of a magnetic field is taken to be

$$p_o'(z) = g\rho_o(z) , \tag{1.25}$$

stating that the gas pressure p_o is stratified by gravity. Here z is directed vertically downwards, and the dash ($'$) denotes differentiation with respect to depth z. Gravity acts in the z direction of a cartesian coordinate system x, y, z. Thus $\mathbf{g} = g\hat{\mathbf{z}}$. The presence of gravity also leads to an imposed *length-scale* in the system. This length scale is the density scale height $H = \rho_o/\rho_o'$.

Since the waves are of small amplitude, the basic equations (1.1) to (1.3) can be linearised :

$$\rho_o \frac{\partial \mathbf{v}}{\partial t} = -\nabla p + \rho g\hat{\mathbf{z}} , \tag{1.26}$$

$$\frac{\partial \rho}{\partial t} + \nabla \cdot (\rho_o \mathbf{v}) = 0, \tag{1.27}$$

$$\frac{\partial p}{\partial t} + \mathbf{v} \cdot \nabla p_o = c_s^2 \left(\frac{\partial \rho}{\partial t} + \mathbf{v} \cdot \nabla \rho_o \right) , \tag{1.28}$$

where

$$c_s^2 = \frac{\gamma p}{\rho} . \tag{1.29}$$

Equation (1.25), when combined with gas law (1.7), gives

$$p_o(z) = p_o(0) exp\left[\int_0^z \frac{dz}{\Lambda}\right] , \tag{1.30}$$

where $\Lambda(z) = p_o(z)/\rho_o(z)g = \mathcal{R}T_o(z)/g$ is the pressure scale height in the atmosphere.

Introducing the variable (see Lamb, 1932)

$$\Delta = \text{div } \mathbf{v} \tag{1.31}$$

and considering the three dimensional motion with

$$\mathbf{v} = (v_x(z), v_y(z), v_z(z))\, e^{i(\omega t - k_x x - k_y y)} , \tag{1.32}$$

for frequency ω and horizontal wavenumbers k_x and k_y, it is possible to obtain the following pair of first order differential equations by using equations (1.26)-(1.28) (see Appendix A3, Section 2) :

$$(\omega^2 - K^2 c_s^2)\Delta = gK^2 v_z + \omega^2 \frac{dv_z}{dz} , \tag{1.33a}$$

and

$$(\omega^4 - g^2 K^2) v_z = g(K^2 c_s^2 - \gamma\omega^2)\Delta - \omega^2 c_s^2 \frac{d\Delta}{dz} , \tag{1.33b}$$

where $K = \left(k_x^2 + k_y^2\right)^{1/2}$ and now $c_s^2 = \gamma p_o(z)/\rho_o(z)$.

Equations (1.33a) and (1.33b) describe acoustic waves in a stratified medium. They also describe gravity waves, and their unstable counterpart, namely convection. The acoustic and gravity waves are commonly referred to as p- and g-modes.

Eliminating v_z between (1.33a) and (1.33b) gives the following equation (also called Lamb's Equation) :

$$\frac{d^2\Delta}{dz^2} + \left\{\frac{c_s^2 I + \gamma g}{c_s^2}\right\}\frac{d\Delta}{dz} + \left\{\frac{(\omega^2 - K^2 c_s^2)}{c_s^2} - \frac{gK^2}{\omega^2}\left[\frac{c_s^2 I - (\gamma - 1)g}{c_s^2}\right]\right\}\Delta = 0. \tag{1.34}$$

Consider a linear temperature profile for $z \geq 0$. The sound speed profile for this is of the form

$$c_s^2(z) \;=\; c_o^2\left(1+\frac{z}{z_o}\right)\;,\;\; z \geq 0\,, \tag{1.35}$$

where $z_o = \{c_o^2/c_s'^2\}_{z=0}$ is the temperature scale-height at $z=0$ (where $c_s = c_o$).

From Equations (1.25) and (1.30) it is possible to show that

$$\frac{p_o(z)}{p_o(0)} = \left(1+\frac{z}{z_o}\right)^{m+1}\;, \qquad \frac{\rho_o(z)}{\rho_o(0)} = \left(1+\frac{z}{z_o}\right)^{m}\;, \tag{1.36}$$

where

$$m+1 = \frac{z_o}{\Lambda_o} = \frac{\gamma g}{(c_s^{2'})}\,. \tag{1.37}$$

The density scale height H and the buoyancy frequency ω_g are given by

$$H = \frac{(z+z_o)}{m}\;, \qquad \omega_g^2 = \left(m - \frac{(m+1)}{\gamma}\right)\frac{g}{(z+z_o)}\;, \tag{1.38}$$

whereas the acoustic cut-off frequency is given by

$$\omega_a^2 = \frac{c_s^2}{4H^2} = \frac{m^2 c_o^2}{4z_o(z_o+z)}\,. \tag{1.39}$$

For the linear temperature profile the solution to Equation (1.34) was shown by Lamb (1932) to be

$$\begin{aligned}\Delta(z) = e^{-K(z+z_o)}\{&\mathcal{A}_1 M\left(-a, m+2, 2K(z+z_o)\right)\\ &+\mathcal{A}_2 U\left(-a, m+2, 2K(z+z_o)\right)\}\,,\end{aligned} \tag{1.40}$$

where $\mathcal{A}_1$ and $\mathcal{A}_2$ are arbitrary constants, and M and U are confluent hypergeometric functions (Abramowitz and Stegun, 1965). The parameter a is given by

$$2a \;=\; \frac{\omega^2}{gk_x}\frac{m+1}{\gamma} + \left(m - \frac{m+1}{\gamma}\right)\frac{gk_x}{\omega^2} - (m+2)\,. \tag{1.41}$$

It is necessary to specify the upper and lower boundaries to the atmosphere in order to progress further. Consider a *polytrope* corresponding to $\Lambda_o = c_o^2 = 0$ with the atmosphere vanishing at $z = 0$ (upper boundary). With $z_o = 0$ the solution (1.40) gives finite Δ and v_z at $z = 0$ if $\mathcal{A}_2$ is chosen to be zero. Thus,

$$\Delta(z) = e^{-K(z+z_o)} M\left(-a, m+2, 2K(z+z_o)\right) . \tag{1.42}$$

A lower boundary can be specified by imposing a base to the atmosphere at the depth $z = z_c$ and requiring that $v_z = 0$ at the base. On introducing the notation $\Omega^2 = \omega^2/gK$, Equation (1.42) and (1.33b) then gives the dispersion relation (see also Speigel and Unno 1962; Roberts, 1988)

$$2\Omega^2 \frac{M'\left(-a, m+2, 2Kz_c\right)}{M\left(-a, m+2, 2Kz_c\right)} = 1 + \Omega^2 - \frac{\Omega^2(m+1)}{Kz_c} , \tag{1.43}$$

where M' denotes the derivative of $M(-a, m+2, x)$ with respect to x. The parameter a in terms of Ω^2 is written as

$$2a = \Omega^2 \frac{(m+2)}{\gamma} + \left(m - \frac{m+1}{\gamma}\right) \frac{1}{\Omega^2} - (m+2) . \tag{1.44}$$

The dispersion relation (1.43) can be solved numerically. One special case, however, is that when $Kz_c \gg 1$. As the right hand side of Equation (1.43) is finite when $Kz_c \gg 1$, it is necessary that the left hand side must also be finite. This can be achieved if both the numerator and the denominator are finite.

Using the following result (Abramowitz and Stegun, 1965; p.504)

$$M(a, b, z) \sim \frac{\Gamma(b)}{\Gamma(a)} e^z z^{a-b} , \quad |z| \gg 1 , \tag{1.45}$$

for gamma function Γ, it is possible to show that

$$M(-a, m+2, 2Kz_c) \sim \frac{\Gamma(m+2)}{\Gamma(-a)} e^{2Kz_c} (2Kz_c)^{-(a+m+2)} . \tag{1.46}$$

As $Kz_c \to \infty$, $e^{2Kz_c} 2Kz_c^{-(a+m+2)} \to \infty$ and so $M(-a, m+2, 2Kz_c)$ will also tend to infinity unless $\Gamma(m+2)/\Gamma(-a)$ tends to zero. Since a gamma function (in this case $\Gamma(m+2)$) cannot become zero, it is necessary that $\Gamma(-a)$ is very large, i.e. $-a$ is close to zero or a negative integer. A similar situation applies for the term $M'(-a, m+2, 2Kz_c)$. Hence a constraint on parameter a is that it is close to zero or a positive integer. Thus,

$$a \to n-1\,, \qquad n = 1, 2, 3, ... \tag{1.47}$$

From Equation (1.44) this becomes

$$(m+1)\Omega^4 - \gamma(m+2n)\Omega^2 + (\gamma - 1)m - 1 \;=\; 0\,. \tag{1.48}$$

As Equation (1.48) is quadratic in Ω^2 there exist two solutions of Ω^2; these two solutions correspond to the p-modes and the g-modes. Under the condition $(\gamma - 1)m < 1$ (i.e. $\omega_g^2 < 0$) the g-modes are unstable (i.e. convective sets in). The borderline (between stable and unstable g- modes) case is described by $\omega_g^2 = 0$, i.e.

$$\gamma \;=\; 1 + \frac{1}{m}\,. \tag{1.49}$$

For the borderline case $\omega_g = 0$ (*adiabatic stratification*) the p-modes satisfy

$$\Omega^2 = \Omega_n^2 \equiv 1 + \frac{2n}{m}\,, \tag{1.50}$$

that is,

$$\omega^2 = \omega_n^2 \equiv gK\left(1 + \frac{2n}{m}\right)\,. \qquad n = 1, 2, 3, ...\,. \tag{1.51}$$

Relation (1.51) indicates that the p-modes form parabolae in the $\omega - K$ plane (see Figure 1.3). An alternative approach to obtain the relation (1.51) is to use WKB theory (see Roberts, 1988; Evans, 1990).

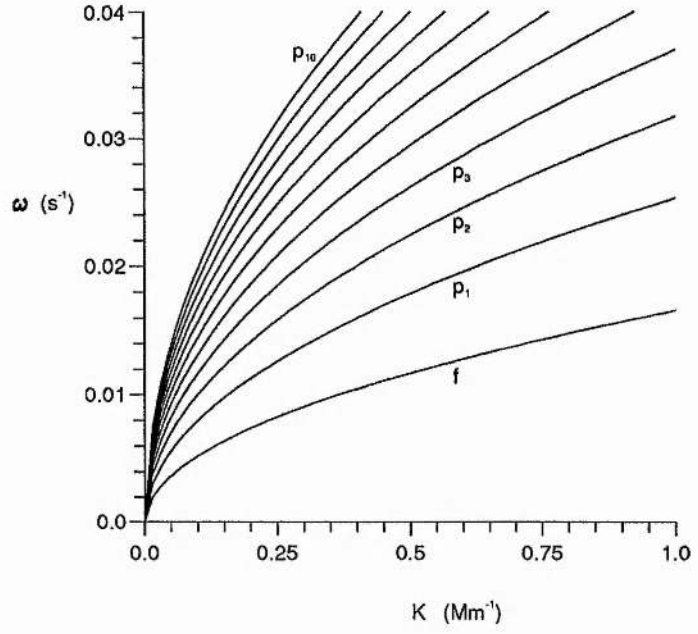

Figure 1.3: The angular frequency ω as a function of wavenumber K for the f-mode and the first ten p-modes. The frequency and wavenumber are related by the dispersion relation (1.51). For this figure the value of γ is taken to be 5/3.

Thus, summarising, the modes given by Equation (1.51) are acoustic waves trapped inside the Sun's atmosphere. Since pressure is the restoring force for acoustic waves, these modes are described as *p-modes*. When the model atmosphere is not marginally stable then another sequence of low frequency modes arise. These have buoyancy as the restoring force. Modes for a stable atmosphere are gravity modes and hence denoted *g-modes*, whereas for an unstable atmosphere these are simply convective modes that do not propagate. Observations of g-modes require very long periods of uninterrupted viewing since their amplitudes are smaller than p-modes and they are more closely spaced than p-modes.

There is a third important global oscillation called the *fundamental* or *f-mode*. This mode forms a case intermediate (due to its frequency) between p- and g-modes because of its relation $\omega^2 = gK$ and is related to the surface waves that exist on the Earth's oceans. Such modes are incompressible in nature and the dispersion relation is entirely independent of the temperature structure of the atmosphere. These modes are discussed further in Chapter 4.

Observations of p-modes are believed to be extremely reliable and hence much of the theoretical work in helioseismology has been concentrated on p-modes. Recently several authors have focussed on the effects of the Sun's rotational velocity and magnetic field on the p-mode frequencies. The progress made in determining accurately the sound speed and its variation with depth is amazing. The influence of magnetism on the p-mode frequency is briefly discussed in the following section.

1.6 Magnetic Effects

There are three important regions in which magnetic field effects can be examined - strong fields around the base of the convection zone; fibril fields below the photosphere and the chromospheric canopy fields. Much attention has been given to the first two regions.

The study of a uniform magnetic field at the base of the convection zone, made by Campbell and Roberts (1986) and Roberts and Campbell (1986), suggested that the changes in the strength of the field over the solar cycle could explain the frequency change observed by Woodard and Noyes (1985). The calculations also suggest that a field strength of $5 \times 10^5 - 10^6$G at the base of the convection zone would be necessary.

The high degree modes have their turning points above the base of the convection zone, and hence these modes will be unaffected by such magnetic fields.

The effect of a toroidal magnetic field just below the convection zone have been considered by Vorontsov (1986), Gough and Thompson (1986) and Thompson (1988) in order to explain the splitting in the frequencies.

Models for fibril fields and their interaction with acoustic waves have been investigated by Bogdon and Zweibel (1985), Zweibel and Bogdan (1986), Bogdan and Cattaneo (1989) and Zweibel and Däppen (1989). Zweibel and Bogdan considered a statistical ensemble of scatterers (i.e. the flux tubes) and the average effect this has on the acoustic wave frequencies. They suggested that frequency changes of 0.1 % to 0.3 % are possible.

Investigations of chromospheric canopy fields and their effects on the frequencies of f- and p-modes have been carried out by Campbell and Roberts (1989) and Evans and Roberts (1990). Such fields are expected to influence the frequencies of the modes trapped near the surface (i.e intermediate or high l modes). The model of Campbell and Roberts consists of a field-free convection zone with temperature increasing linearly with depth in this region. On top of this region, is an isothermal gas with a horizontal magnetic field whose strength decreases exponentially with height (giving a constant Alfvén speed). This region represents the chromospheric canopy field. Such a model

may give a *lower* bound to the effects that occur in reality. Campbell and Roberts (1989) found that the effect of such a magnetic atmosphere on p-modes is to decrease their frequencies. The f-mode, however, shows an increase in frequency.

The work by Evans and Roberts (1990) included a chromosphere with a uniform field rather than an exponentially decreasing one. This model allows the Alfvén speed to increase exponentially with height. One expects an Alfvén speed profile in the Sun to lie somewhere between these two cases. The work of Evans and Roberts is complementary to the work of Campbell and Roberts in being another extreme of the real magnetic field profile on the Sun and in that sense may provide an *upper* bound to the effects that actually occur in reality. Evans and Roberts found that the frequencies of f- and p-modes increased with an increase in magnetic field strength. They also assessed the effect of a variable canopy height (the region immediately below the canopy being field-free and isothermal).

The study undertaken in this thesis aims mainly at the effects of a magnetic field in the solar surface layers on the p- and f-modes. As mentioned earlier, it is likely that these magnetic fields change the frequencies of p- and f-modes. The other point of interest lies in the recent evidence of changes in the frequencies of p-modes over the solar cycle. The most prominent global variation in the solar cycle is that of a magnetic field. The models discussed in this thesis thus have the same equilibrium configurations as in Campbell and Roberts (1989) and Evans and Roberts (1990). The work presented in Chapters 3 and 4 generalises these two models.

The development of helioseismology has seen, over the years, an interplay between studies of acoustic waves and the manner in which these waves are influenced by the atmosphere of the Sun. Research in helioseismology is becoming increasingly important for a better understanding of many basic fields of astronomy and astrophysics, such as the stellar atmospheres and their associated stellar magnetic activity cycles.

1.7 Outline of the Remaining Chapters

The subsequent material is organised to enable the reader to understand various models developed as a logical study rather than a chronological one. Several assumptions are emphasized at various stages, and deduced from these are equations basic to the study of solar oscillations.

Although the time consuming, complicated algebra in obtaining various results is omitted, important mathematical rigor is not compromised.

The lengthy numerical analysis is not described in full detail, but a close interrelationship between various asymptotic and numerical results was established wherever it

was possible to do so.

Although this thesis deals with basic models, it is expected that the approach and coverage will interest and appeal to people working in related areas. For those desiring to do more specialised work in this area, it may provide sufficient background !

The discussion of magnetoacoustic surface waves is presented in Chapter 2 (see also Jain and Roberts, 1991). First the basic model is described and the wave equations and the dispersion relation derived. The surface waves are discussed for various sets of parameters.

Chapter 3 considers a model for investigating the influence of a uniform horizontal chromospheric magnetic field on p-mode frequencies. A general dispersion relation is derived and solved analytically in the limit of small horizontal wavenumber, and numerically for the more general case. The results are compared with the relevant observations.

Chapter 4 deals with a model analysing the influence of a non-uniform horizontal chromospheric field (non-uniform in such a way that the Alfvén speed remains constant) on f- and p-mode frequencies. Like the model of Chapter 3, this model divides the atmosphere into two layers. This model also takes into account the effects of non-parallel propagation. The governing equations are derived in a general way and various interfacial aspects are discussed. A dispersion relation is derived and solutions are obtained both analytically (for small horizontal wavenumber) and numerically (for the more general case). A comparison is made between these two solutions. A possibility for the existence of magnetoacoustic surface waves in the presence of gravity is discussed (see also Jain and Roberts, 1990).

The model of Chapter 3 appears to have a defect, namely the unlimited increase in Alfvén speed with height. In order to overcome this shortcoming, a more general three layer model is described in Chapter 5. This model consists of a third isothermal layer, resting on top of the two layers investigated in Chapter 3. The third layer is equivalent to the chromospheric region considered in Chapter 4. A complicated dispersion relation results for the three layer model, the complexity making its numerical solution rather involved. Advantages and disadvantages of the model are then assessed.

Finally, some concluding remarks and suggestions for further work are presented in Chapter 6.

CHAPTER 2

MAGNETIC SURFACE EFFECTS IN THE ABSENCE OF GRAVITY

2.1 Introduction

The increasing interest in the study of wave propagation in a magnetically structured atmosphere, motivated by the observed inhomogeneous nature of the solar atmosphere, has highlighted many important properties of magnetoacoustic surface waves. Magnetoacoustic surface waves can exist on discontinuities in the magnetic field (strength or direction) or plasma density, pressure or temperature. In the solar atmosphere, for example, discontinuities (or at least rapid changes) in the magnetic field arise on the edges of sunspots or intense flux tubes.

A discussion of magnetohydrodynamic surface waves at a single interface, in an incompressible medium, may be found in Chandrasekhar (1961); see also Kruskal and Schwarzschild (1954) and Gerwin (1967). The phase-speed of such a wave is given by

$$c_k = \left(\frac{\rho_o v_A^2 + \rho_e v_{Ae}^2}{\rho_o + \rho_e} \right)^{1/2} \tag{2.1}$$

where ρ_o and v_A are the density and Alfvén speed on one side of the interface and ρ_e and v_{Ae} are their respective values on the other side. The investigation of waves in flux tubes also gives rise to the speed c_k (see, for example, the reviews by Spruit, 1983; Spruit and Roberts, 1983; Thomas, 1985; Roberts, 1986; Ryutova, 1990).

Surface waves in compressible media have been discussed by various authors. Wentzel (1979) and Roberts (1981) formulated the magnetoacoustic surface wave problem for a magnetic field which is uniform in the direction of the field but varies in the perpendicular direction, considering in particular the case of a single magnetic interface. The detailed properties of magnetoacoustic surface waves on such an interface have been investigated by Uberoi (1982) and Somasundaram and Uberoi (1982) for non-parallel propagation and by Miles and Roberts (1989) for the case of parallel propagation.

Somasundaram and Uberoi (1982) investigated the effects of compressibility on the propagation of surface waves, allowing for different magnetic field strengths on the two sides of the interface. They were concerned with the longitudinal phase-speeds of the surface waves at various propagation angles. Miles and Roberts (1989) discussed longitudinal phase-speeds and penetration depths of surface waves on a magnetic interface, one side of which is field-free. They also investigated the associated pressure perturbations and motions for a variety of field strengths and sound speeds. In another context, Cadez and Okretic (1989) have discussed the possibility of surface wave energy leakage, which may occur in the case of a two-step configuration. A study of phase-speed diagrams, which can yield information on the spectrum of modes that a magnetic structure can support, was carried out by Rae and Roberts (1983).

An application of magnetoacoustic surface waves, namely running penumbral waves, was suggested by Small and Roberts (1984). Running penumbral waves were first observed by Giovanelli (1972) and Zirin and Stein (1972), and have been modelled by Nye and Thomas (1974, 1976) and Cally and Adam (1983) as magnetoacoustic-gravity modes (see also Zhugzhda and Dzhalilov (1984)).

Magnetoacoustic surface waves clearly play a prominent role in any discussion of waves in a structured atmosphere. They may gain an additional importance in view of their possible role in the heating of the corona (Ionson, 1978; Wentzel, 1979; Rae and Roberts, 1981; Lee and Roberts, 1986; Hollweg, 1986, 1987a,b, 1990; Davila, 1990).

Such is the relevance of magnetoacoustic surface waves to solar phenomena. It is important to assess, what observational evidence there is for the occurrence of surface waves in the Sun and the effects of magnetic interfaces on Solar oscillations in general. Although there are no confirmed identifications of surface waves, various phenomena are strong candidates for being such. As mentioned above, the running penumbral waves observed emanating from sunspots may be examples of surface waves. Another possibility is the f-mode, a buoyancy driven mode lying below the pressure driven p-mode parabolae in the $\omega - k$ diagram (see Chapter 1). The 'f' stands for fundamental, a notation introduced by Cowling (1941). The f-mode has approximate frequency $\omega = (gk)^{1/2}$ where g is the local gravitational acceleration and k is the horizontal wavenumber. The f-mode has been observed both at high (see Libbrecht and Kaufman, 1988; Tarbell et. al., 1988; Libbrecht, Woodard and Kaufman, 1990) and at low horizontal wavenumber k (Rabaey, Hill and Barry, 1988). The f-modes are believed to be independent of thermal stratification in the atmosphere. It may be that the discontinuities in magnetic fields in the photosphere and lower chromosphere cause the angular frequency ω of these modes to be modified slightly. Although the p-modes are standing waves (unlike the f-modes which are surface waves), the local magnetic fields

may influence their frequencies.

Thus, the topic of magnetic surfaces and their effects on different types of solar waves is quite interesting but at the same time can become very complicated if the propagation of waves on more than one interface is considered and the gravitational stratification is also included. It is therefore advisable first to look at simple magnetic structuring namely a single magnetic interface ignoring the complications introduced by gravity. Once some insight into the effects of magnetic structuring is obtained, the inclusion of gravity would be considered in the following chapters.

It is of interest, then, to consider the properties of surface waves, and to assess the dependence of phase-speeds on various field strengths. In this *chapter* the subsection 'parallel propagation ($\theta = 0$)' is concerned with the propagation of magnetoacoustic surface waves on a magnetic interface, the propagation being in a direction parallel to the magnetic field. Remaining sections deal with the non-parallel propagation of magnetoacoustic surface waves at a single interface one side of which is field-free.

2.2 The Wave Equations

Magnetohydrodynamic wave propagation can be considered in an ideal, perfectly conducting and compressible plasma. The effects of gravity are ignored here, though included in subsequent chapters. The basic equations of ideal magnetohydrodynamics are taken in the form (see Chapter 1)

$$\frac{\partial \rho}{\partial t} + \rho \nabla \cdot \mathbf{v} + \mathbf{v} \cdot \nabla \rho = 0, \tag{2.2}$$

$$\rho \left[\frac{\partial \mathbf{v}}{\partial t} + (\mathbf{v} \cdot \nabla)\, \mathbf{v} \right] = -\nabla p + \frac{1}{\mu} (\nabla \times \mathbf{B}) \times \mathbf{B}\,, \tag{2.3}$$

$$\frac{\partial \mathbf{B}}{\partial t} = \nabla \times (\mathbf{v} \times \mathbf{B})\,, \qquad \nabla \cdot \mathbf{B} = 0\,, \tag{2.4}$$

$$\frac{\partial p}{\partial t} + \mathbf{v} \cdot \nabla p = \frac{\gamma p}{\rho} \left(\frac{\partial \rho}{\partial t} + \mathbf{v} \cdot \nabla \rho \right)\,, \tag{2.5}$$

$$p = \mathcal{R}\, \rho\, T\,, \tag{2.6}$$

where p, ρ, and T are the pressure, density, and temperature of the gas with velocity

v and magnetic field $\mathbf{B}$; γ is the ratio of specific heats, μ is the magnetic permeability, $\mathcal{R}(=\frac{k_B}{m_p}$ where k_B is Boltzmann's constant, and m_p is the mean particle mass) is the gas constant.

The equlibrium field is assumed to be of the form $\mathbf{B} = B_o(z)\hat{\mathbf{x}}$, lying parallel to the x-axis and varying in strength in the z-direction. The equilibrium gas pressure $p_o(z)$ is related to the equilibrium magnetic pressure $B_o^2(z)/2\mu$ by

$$\frac{d}{dz}\left(p_o + \frac{B_o^2}{2\mu}\right) = 0 . \tag{2.7}$$

To investigate the propagation of small amplitude plane waves the perturbations in the flow, pressure, etc. are written in the form

$$\mathbf{v} = \mathbf{v}(z)\exp\ i(\omega t - k_x x - k_y y), \qquad p = p_o(z) + p(z)\exp\ i(\omega t - k_x x - k_y y) . \tag{2.8}$$

Here ω is the angular frequency and k_x and k_y are the wave numbers in the x- and y- directions, defining a wave vector $\mathbf{K} = (k_x, k_y, 0)$ in the $x-y$ plane. The wave numbers are $k_x = K\cos\theta$ and $k_y = K\sin\theta$, for angle of propagation θ to the applied field; $K = (k_x^2 + k_y^2)^{1/2}$. The sound speed in the basic state of density $\rho_o(z)$ is $c_s(z) = \{\gamma p_o(z)/\rho_o(z)\}^{1/2}$ and the Alfvén speed is $v_A(z) = \left\{B_o(z)/(\mu\rho_o(z))^{1/2}\right\}$. It is also useful to define the total perturbed pressure $P_T = p + B_o B_x/\mu$, the sum of the perturbed gas pressure and the perturbed magnetic pressure (for a field perturbation B_x in the direction of the unperturbed magnetic field).

Equations (2.2)-(2.6), when linearised about the equilibrium (2.7), give rise to a second order ordinary differential equation for the z-component of velocity (Goedbloed 1971; Roberts 1981):

$$\frac{d}{dz}\left\{\frac{\rho_o(z)(k_x^2 v_A^2(z) - \omega^2)}{(m^2(z) + k_y^2)}\frac{dv_z}{dz}\right\} - \rho_o(z)\left(k_x^2 v_A^2(z) - \omega^2\right)v_z = 0 , \tag{2.9}$$

where

$$m^2(z) = \frac{(k_x^2 c_s^2(z) - \omega^2)(k_x^2 v_A^2(z) - \omega^2)}{(c_s^2(z) + v_A^2(z))(k_x^2 c_T^2(z) - \omega^2)} , \qquad c_T^2(z) = \frac{c_s^2(z) v_A^2(z)}{(c_s^2(z) + v_A^2(z))} ; \tag{2.10}$$

with v_z and P_T related by

$$P_T = \frac{i\rho_o(z)}{\omega}\frac{(k_x^2 v_A^2(z) - \omega^2)}{(m^2(z) + k_y^2)}\frac{dv_z}{dz} . \tag{2.11}$$

A derivation of (2.9) and (2.11) is given in Appendix A2, Section 1 and Section 2 respectively.

In a uniform medium (for which ρ_o, c_s, v_A, and m^2 are constants), Equation (2.9) becomes

$$(k_x^2 v_A^2 - \omega^2)\left(\frac{d^2 v_z}{dz^2} - (m^2 + k_y^2)v_z\right) = 0 , \tag{2.12}$$

showing that there are two possibilities: either $\omega^2 = k^2 v_A^2$, with $v_z(z)$ arbitrary; or $\omega^2 \neq k^2 v_A^2$ and $v_z(z)$ satisfies

$$\frac{d^2 v_z}{dz^2} - (m^2 + k_y^2)v_z = 0 . \tag{2.13}$$

2.3 Surface Waves On A Magnetic-Magnetic Interface

2.3.1 The Dispersion Relation

One interesting investigation is that of the behaviour of plane waves on an interface which has uniform fields on either side of it (the two uniform fields being different in magnitude). This involves a basic state in which the magnetic field is of the form

$$B_o(z) = \begin{cases} B_e , & z > 0, \\ B_o , & z < 0, \end{cases} \tag{2.14}$$

where B_o and B_e are constants (see Figure 2.1).

The pressure balance condition (Equation (2.7)) yields

$$p_e + \frac{B_e^2}{2\mu} = p_o + \frac{B_o^2}{2\mu} . \tag{2.15}$$

Together with the ideal gas law (2.6), Equation (2.15) implies that

$$\frac{\rho_e}{\rho_o} = \frac{c_o^2 + \frac{\gamma}{2}v_A^2}{c_e^2 + \frac{\gamma}{2}v_{Ae}^2} , \tag{2.16}$$

where $c_e = (\gamma p_e/\rho_e)^{1/2}$ and $v_{Ae} = B_e/(\mu\rho_e)^{1/2}$ are the sound speed and Alfvén speed in the region $z > 0$, and $c_o = (\gamma p_o/\rho_o)^{1/2}$ and $v_A = B_o/(\mu\rho_o)^{1/2}$ are their counterparts when $z < 0$.

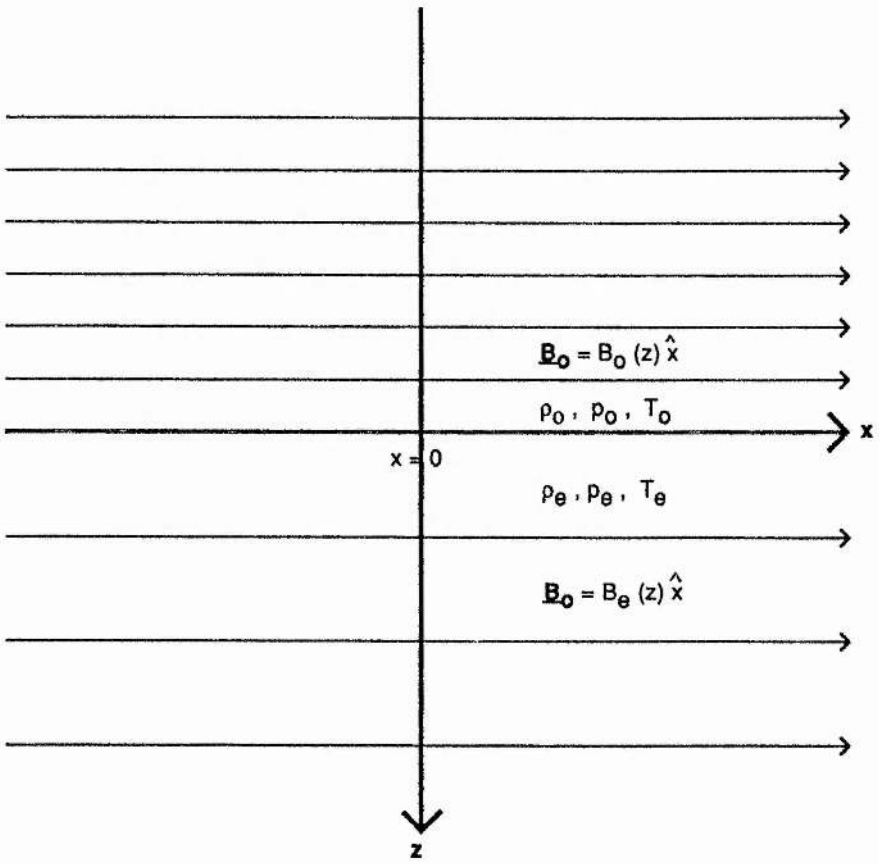

Figure 2.1: The equilibrium atmosphere of a single magnetic interface.

On either side of the discontinuity at $z = 0$, the media are uniform and so Equation (2.12) applies since each of the coefficients ρ_o, c_s, v_A, and m^2 in Equation (2.9) is a constant. Thus, in addition to Alfvén waves, given by the first factor in Equation (2.12), there are magnetoacoustic modes given when Equation (2.13) is applied to the two regions $z > 0$ and $z < 0$. For the region $z < 0$, Equation (2.13) becomes

$$\frac{d^2 v_z}{dz^2} - (m_o^2 + k_y^2) v_z = 0 , \qquad z < 0 , \tag{2.17}$$

while where $z > 0$ it reduces to

$$\frac{d^2v_z}{dz^2} - (m_e^2 + k_y^2)v_z = 0 , \qquad z > 0 . \tag{2.18}$$

Here

$$m_o^2 = \frac{(k_x^2c_o^2 - \omega^2)(k_x^2v_A^2 - \omega^2)}{(c_o^2 + v_A^2)(k_x^2c_T^2 - \omega^2)} , \qquad m_e^2 = \frac{(k_x^2c_e^2 - \omega^2)(k_x^2v_{Ae}^2 - \omega^2)}{(c_e^2 + v_{Ae}^2)(k_x^2c_{Te}^2 - \omega^2)} ; \tag{2.19}$$

note that (for ω^2 and k_x^2 real) m_o^2 and m_e^2 may be positive or negative.

Solving Equations (2.17) and (2.18) subject to the requirement that $v_z(z)$ remains bounded as z tends to $\pm\infty$ yields

$$v_z(z) = \begin{cases} \alpha_e e^{-(m_e^2+k_y^2)^{1/2}z} , & z > 0, \\ \alpha_o e^{(m_o^2+k_y^2)^{1/2}z} , & z < 0, \end{cases} \tag{2.20}$$

where $(m_o^2 + k_y^2)^{1/2} > 0$ and $(m_e^2 + k_y^2)^{1/2} > 0$. The restrictions on $(m_o^2 + k_y^2)^{1/2}$ and $(m_e^2 + k_y^2)^{1/2}$ imply that it is surface waves which are being considered.

It is necessary that both $v_z(z)$ and $P_T(z)$ be continuous across the interface $z = 0$ (see Roberts, 1981). The latter condition is apparent from the integral of the Equation (2.9) across the interface and assures that there are no unbalanced forces at the interface. In fact these two conditions can be seen formally from Equation (2.9). The term inside { } in Equation (2.9) must be continuous, for if it were discontinuous, its derivative would involve the dirac delta function which is not present on the right hand side of Equation (2.9). Hence,

$$\rho_o(z)\frac{(k_x^2v_A^2(z) - \omega^2)}{(m^2(z) + k_y^2)}\frac{dv_z}{dz} \tag{2.21}$$

must be continuous across the interface $z = 0$. Thus $\alpha_e = \alpha_o$ and continuity of P_T at $z = 0$ gives (see Appendix A2, Section 2)

$$\rho_o(k_x^2v_A^2 - \omega^2)(m_e^2 + k_y^2)^{1/2} + \rho_e(k_x^2v_{Ae}^2 - \omega^2)(m_o^2 + k_y^2)^{1/2} = 0 , \tag{2.22}$$

valid for $(m_o^2 + k_y^2)^{1/2}$ and $(m_o^2 + k_y^2)^{1/2}$ both positive. Equation (2.22) is the dispersion relation for surface waves at a single magnetic interface; it has been obtained by Wentzel

(1979) and Roberts (1980, 1981). This Equation can be rewritten in terms of the propagation angle θ as follows:

$$\rho_o(K^2v_A^2\cos^2\theta-\omega^2)(m_e^2+k_y^2)^{1/2}+\rho_e(K^2v_{Ae}^2\cos^2\theta-\omega^2)(m_o^2+k_y^2)^{1/2}=0\ , \quad (2.23)$$

where

$$m_o^2+k_y^2=\frac{(K^2c_o^2\cos^2\theta-\omega^2)(K^2v_A^2\cos^2\theta-\omega^2)}{(c_o^2+v_A^2)(K^2c_T^2\cos^2\theta-\omega^2)}+K^2\sin^2\theta\ , \quad (2.24)$$

$$m_e^2+k_y^2=\frac{(K^2c_e^2\cos^2\theta-\omega^2)(K^2v_{Ae}^2\cos^2\theta-\omega^2)}{(c_e^2+v_{Ae}^2)(K^2c_{Te}^2\cos^2\theta-\omega^2)}+K^2\sin^2\theta\ . \quad (2.25)$$

Equation (2.23) can be re-arranged in the form (Roberts, 1981)

$$\frac{\omega^2}{K^2}=\cos^2\theta\left[v_A^2-\frac{R}{R+1}(v_A^2-v_{Ae}^2)\right]=\cos^2\theta\left[v_{Ae}^2+\frac{1}{R+1}(v_A^2-v_{Ae}^2)\right]\ , \quad (2.26)$$

where

$$R\ =\ \left(\frac{\rho_e}{\rho_o}\right)\left(\frac{m_o^2+k_y^2}{m_e^2+k_y^2}\right)^{1/2}>0 \quad (2.27)$$

is a function of ω^2/K^2 and θ.

2.3.2 Properties of the Modes

It is clear from the form (2.26) of the dispersion relation that the phase-speed, $c_{ph}\equiv\omega/K$, of a magnetoacoustic surface waves lies between $v_A\cos\theta$ and $v_{Ae}\cos\theta(\cos\theta>0)$, and its longitudinal phase-speed, ω/k_x, lies between v_A and v_{Ae}. (In particular, if one side of the interface is field-free, say $v_{Ae}=0$, then the former restriction becomes merely $\omega/K\leq v_A\cos\theta$.) Hence, it follows immediately that *magnetoacoustic surface waves are unable to propagate in a direction perpendicular to the applied magnetic field* (i.e., magnetoacoustic surface waves are unable to propagate when $\theta=\frac{\pi}{2}$). The dispersion relation (2.22), subject to the constraints $(m_o^2+k_y^2)^{1/2}>0$ and $(m_e^2+k_y^2)^{1/2}>0$, may possess either no solution, one solution or two solutions, depending upon the relative values of the sound speeds and the Alfvén speeds in the two media (Roberts, 1981).

Where two waves arise, these are referred to as *slow* and *fast* magnetoacoustic surface waves. Their properties are explored in subsection 'low beta plasma' and thereafter.

Another consequence of Equation (2.26) is that surface waves at an interface are *non-dispersive* (i.e., ω/K is independent of K). This is to be expected since in such a medium no natural length-scale exists, and so the propagation speeds of all waves depend only on θ. Some special cases are as follows.

Incompressible Limit

To begin with, note that for an incompressible plasma the density changes of a moving plasma element are negligible, i.e.

$$\frac{\partial \rho}{\partial t} + \mathbf{v} \cdot \nabla \rho = 0 . \tag{2.28}$$

Thus the continuity Equation (2.2) reduces to $\nabla \cdot \mathbf{v} = 0$. Formally the incompressible limit can be obtained from the compressible equations for a plasma by considering the limit $c_s \to \infty$. If a medium is almost incompressible then the sound waves do propagate extremely fast (i.e. c_s is very large). The incompressible form of Equation (2.21) is obtained by considering the limiting forms of m_e^2 and m_o^2 as c_o, $c_e \to \infty$, i.e. m_o^2, $m_e^2 \to K^2 \cos^2\theta$. Then Equation (2.22) reduces to

$$\frac{\omega^2}{K^2} = c_k^2 \cos^2\theta \; ; \quad i.e., \quad \omega^2 = k_x^2 c_k^2 , \tag{2.29}$$

where c_k is given by Equation (2.1). Equation (2.29) is the dispersion relation for a hydromagnetic surface wave in an incompressible medium. It indicates that the wave propagates along the interface with a speed which is intermediate between the two Alfvén speeds.

Low-β plasma

A possibly more relevant case for solar applications arises when a low-β plasma is considered, corresponding to the Alfvén speeds greatly exceeding the sound speeds on both sides of the interface. The pressure balance condition for a low-β plasma implies that $\rho_o v_A^2 \approx \rho_e v_{Ae}^2$, and Equations (2.24) and (2.25) imply that $m_o^2 + k_y^2 \approx K^2 - \omega^2/v_A^2$ and $m_e^2 + k_y^2 \approx K^2 - \omega^2/v_{Ae}^2$. Thus Equation (2.23) reduces to (Roberts, 1981; Uberoi, 1982)

$$v_{Ae}(v_A^2 \cos^2\theta - c_{ph}^2)(v_{Ae}^2 - c_{ph}^2)^{1/2} + v_A(v_{Ae}^2 \cos^2\theta - c_{ph}^2)(v_A^2 - c_{ph}^2)^{1/2} = 0 . \tag{2.30}$$

Now the phase-speed $c_{ph}\left(= \frac{\omega}{K}\right)$ must lie between $v_A \cos\theta$ and $v_{Ae}\cos\theta$. Additionally, both Alfvén speeds (v_A and v_{Ae}) should be greater than the phase-speed c_{ph}

for the surface wave solutions to be evanescent in the two media ($(v_{Ae}^2 - c_{ph}^2)^{1/2} > 0$ and $(v_A^2 - c_{ph}^2)^{1/2} > 0$). Thus, if v_A is taken to be larger than v_{Ae}, then for a given θ, $v_A \cos\theta > c_{ph}$ and $v_{Ae} \cos\theta < c_{ph} < v_{Ae}$. If $k_y \gg k_x$, then Equation (2.30) reduces to

$$\frac{\omega^2}{K^2} = c_k^2 \cos^2\theta \; ; \quad i.e., \quad \omega^2 = k_x^2 c_k^2 \; . \tag{2.31}$$

A more quantitative description of Equation (2.30) may be given by squaring it, which leads to a quadratic equation in c_{ph}^2:

$$c_{ph}^4 - (v_A^2 + v_{Ae}^2)c_{ph}^2 \; + \; v_A^2 v_{Ae}^2 \cos^2\theta(1 + \sin^2\theta) \; = \; 0 \; . \tag{2.32}$$

Solving Equation (2.32) gives the roots

$$2c_{ph}^2 \; = \; (v_A^2 + v_{Ae}^2) \; \pm \; \left[(v_A^2 + v_{Ae}^2)^2 - 4 \; v_A^2 \; v_{Ae}^2 \; \cos^2\theta \; (1 + \sin^2\theta)\right]^{1/2} \; . \tag{2.33}$$

The positive root is unacceptable since $c_{ph}^2 < v_A^2, v_{Ae}^2$. Thus,

$$2c_{ph}^2 \; = \; (v_A^2 + v_{Ae}^2) \; - \; \left[(v_A^2 - v_{Ae}^2)^2 + 4 \; v_A^2 \; v_{Ae}^2 \; \sin^4\theta\right]^{1/2} \; . \tag{2.34}$$

Now, for small θ (strictly, for $\sin^4\theta \ll 1$) Equation (2.34) gives

$$2c_{ph}^2 \; = \; (v_A^2 + v_{Ae}^2) \; - \; |v_A^2 \; - \; v_{Ae}^2| \left[1 \; + \; \frac{2 \; v_A^2 \; v_{Ae}^2 \; \sin^4\theta}{(v_A^2 - v_{Ae}^2)^2}\right] \; , \tag{2.35}$$

and so

$$c_{ph}^2 \; = \; \min\,(v_A^2, v_{Ae}^2) \; - \; \frac{v_A^2 v_{Ae}^2}{|v_A^2 \; - \; v_{Ae}^2|} \sin^4\theta \; , \tag{2.36}$$

provided v_A is not too close to v_{Ae}^2.

At the other extreme, where the angle of propagation is close to being perpendicular to the magnetic field, $\sin\theta \approx 1$, and Equation (2.34) yields

$$c_{ph}^2 \approx \left(\frac{v_A^2 v_{Ae}^2}{v_A^2 + v_{Ae}^2}\right) \cos^2\theta \, (1 + \sin^2\theta) \; ; \tag{2.37}$$

that is (on noting that $\rho_o v_A^2 \approx \rho_e v_{Ae}^2$),

$$c_{ph}^2 \approx c_k^2 \cos^2\theta \left(1 - \frac{1}{2}\cos^2\theta\right) . \tag{2.38}$$

This confirms an earlier result, namely that surface modes are unable to propagate across the magnetic field (i.e., when $\theta = \pi/2$). Additionally, it may be seen from Equation (2.34) that no surface wave is able to propagate at angle $\theta = 0$, as c_{ph}^2 must lie between v_A^2 and v_{Ae}^2 (see also Roberts, 1981). Altogether, if both sides of the magnetic interface are low-β plasmas then there are no surface waves for either $\theta = 0$ or $\theta = \pi/2$. However, for $0 < \theta < \pi/2$ a (fast) surface mode exists, with phase-speed given by Equation (2.34). By contrast, if only one side of the magnetic interface has a low beta then a surface mode may arise even for $\theta = 0°$; see below.

Parallel propagation ($\theta = 0$)

It is instructive to consider Equation (2.22) for $k_y = 0$, corresponding to the case of parallel propagation:

$$\rho_o(k_x^2 v_A^2 - \omega^2)m_e + \rho_e(k_x^2 v_{Ae}^2 - \omega^2)m_o = 0 . \tag{2.39}$$

Case (a) : $v_A > v_{Ae}$

The condition $m_e > 0$ implies that $\omega/k_x < c_{Te}$ or $\min(c_e, v_{Ae}) < \omega/k_x < \max(c_e, v_{Ae})$, while the condition $m_o > 0$ implies that $\omega/k_x < c_T$ or $\min(c_o, v_A) < \omega/k_x < \max(c_o, v_A)$. Additionally, the longitudinal phase-speed ω/k_x is such that $v_{Ae} < \omega/k_x < v_A$. Thus there arises the possibility of $\omega/k_x < \min(c_e, c_T)$; this is the *slow surface wave*. For $c_o \to \infty$ and $c_e \to \infty$, it can easily be seen from Equation (2.29) that the phase-speed of the slow surface wave tends to c_k, the phase-speed of a surface wave in an incompressible medium.

In Figure 2.2a the dependence of the phase-speed ω/k_x on c_o/c_e is exhibited for the two cases $v_A/c_e = 1.8$ and $v_{Ae}/c_e = 0.4$. It may be noted that there exists a critical value of c_o/c_e below which the surface wave is unable to propagate. The critical value of c_o/c_e is given by the intersection of the curves $\omega/k_x = c_T$ and $\omega/k_x = v_{Ae}$. For the field-free case (i.e., when $v_{Ae} = 0$) the critical value is zero, and the slow surface mode exists for all c_o/c_e.

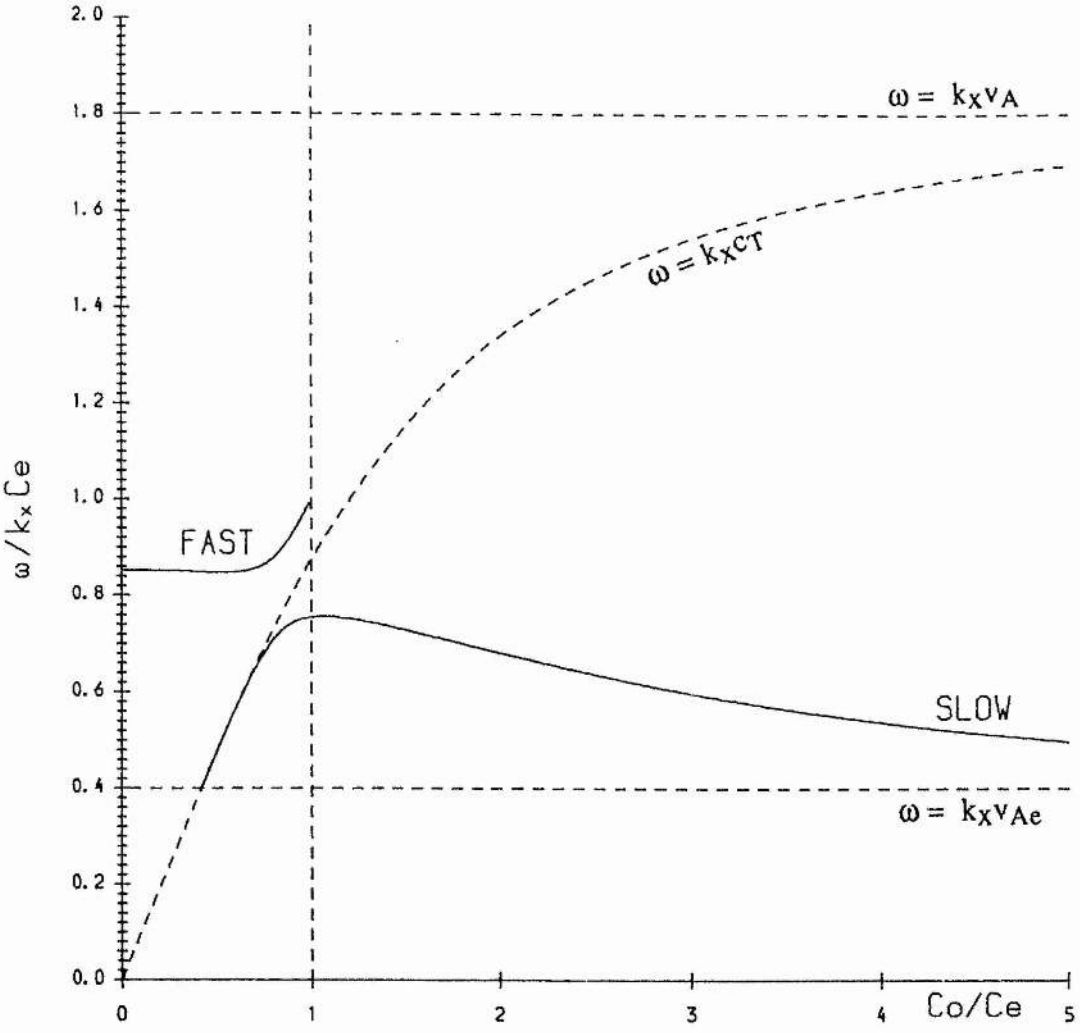

Figure 2.2a: The variation of the phase-speed (in units of the sound speed c_e) of the slow and fast magnetoacoustic surface waves, propagating parallel to the magnetic field, with the parameter c_o/c_e for the case $v_A > v_{Ae}$: specifically $v_A/c_e = 1.8$ and $v_{Ae}/c_e = 0.4$. Here (and elsewhere in the figures) $\gamma = \frac{5}{3}$.

As illustrated in Figure 2.2a, if the β of the plasma is small on one side of the interface but larger on the other side, then either a *fast* mode or a *slow* mode exists or both *slow* and *fast* surface modes co-exist, depending upon the ratio c_o/c_e. When the sound-speed (c_o) of the low-β plasma exceeds the sound speed (c_e) of the high-β plasma, then only the slow surface mode exists. For a low-β situation where $v_A > c_o$

and $v_{Ae} > c_o$, only a fast mode exists

Case(b) : $v_{Ae} > v_A$

The next case considered is that of the evolution from two surface modes to no mode. The longitudinal phase-speed satisfies the condition $v_A < \omega/k_x < v_{Ae}$. The slow surface wave has phase-speed $v_A < \omega/k_x < c_{Te}$. Figure 2.2b shows the variation of ω/k_x as a function of c_o/c_e for $v_A/c_e = 0.4$ and $v_{Ae}/c_e = 1.8$.

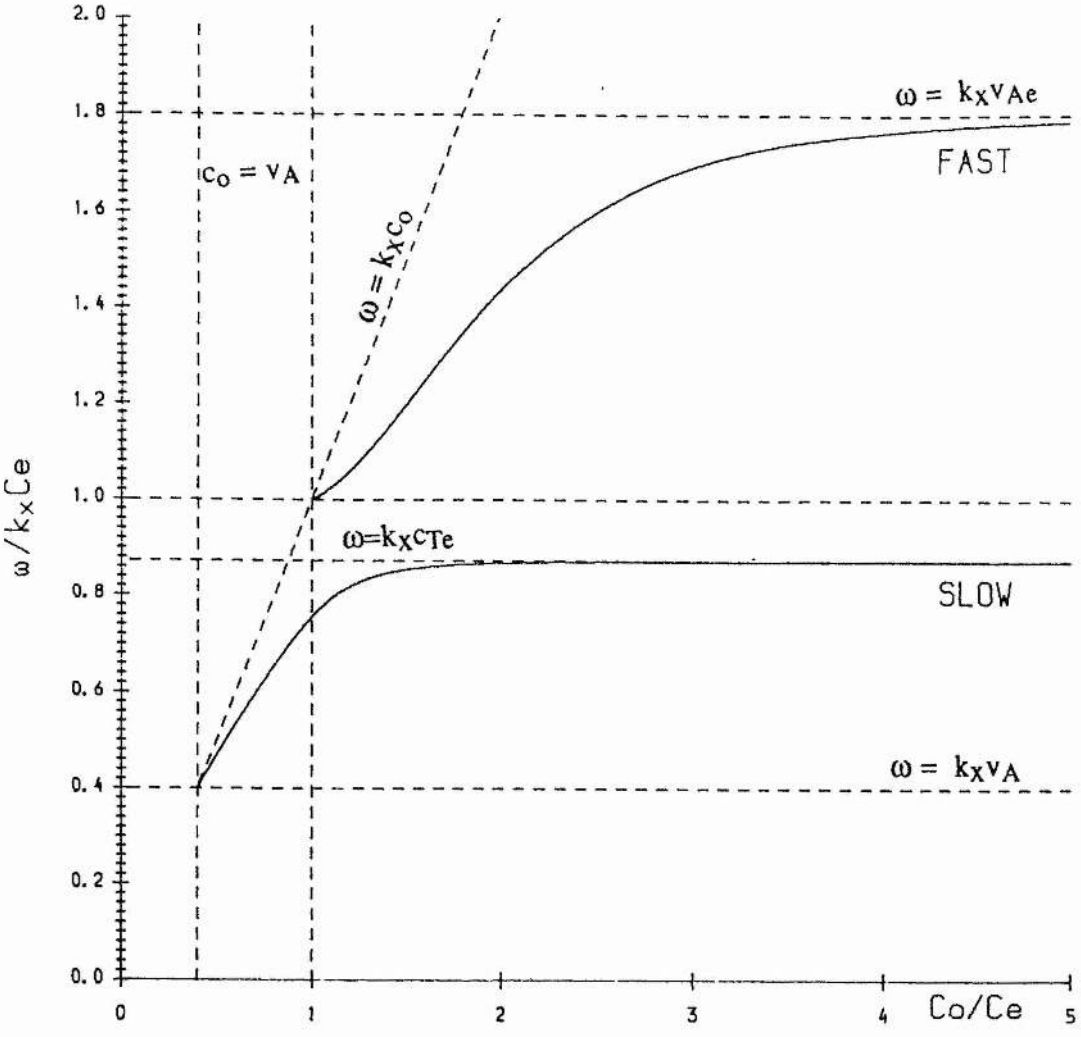

Figure 2.2b: The variation of the phase-speed (in units of the sound speed c_e) of the slow and fast magnetoacoustic surface waves, propagating parallel to the magnetic field, with the parameter c_o/c_e for the case $v_A < v_{Ae}$: $v_A/c_e = 0.4$ and $v_{Ae}/c_e = 1.8$. Observe that both modes have phase-speeds between v_{Ae} and v_A.

In this case, the critical value of c_o/c_e below which the slow surface wave does not exist is given by the intersection of the curve $\omega/k_x c_e = v_A/c_e$ and $c_o/c_e = v_A/c_e$. Figure 2.2b illustrates the earlier conclusion that there are no surface waves when both sides of the magnetic interface are low-β plasmas ($v_{Ae} > c_e$ and $v_A > c_o$). The slow surface wave exists for all values of $c_o > v_A$ and the fast surface wave starts appearing as soon as c_o exceeds c_e. This is to be expected because when $v_{Ae} > v_A$, the condition for the fast mode to exist is $v_{Ae} > c_e$ and $c_e < c_o$.

It is interesting to consider the penetration depths of surface modes, i.e. the distances from the interface to which surface waves are able to penetrate (see also Miles and Roberts, 1989). Fast and slow magnetoacoustic waves penetrate a distance of the order of m_o^{-1} into the region $z < 0$ and a distance m_e^{-1} into the region $z > 0$. Figure 2.3 displays the dependence upon c_o/c_e of penetration depths ($(\lambda m_e)^{-1}$into the region $z < 0$ and $(\lambda m_o)^{-1}$into the region $z > 0$ for a wavelength $\lambda \equiv 2\pi/k$) of the slow and fast magnetoacoustic waves.

Note from Figure 2.3 a,b that as c_o exceeds a critical value (corresponding to $c_o = v_{Ae}$ in Figure 2.3 a and $c_o = v_A$ in Figure 2.3 b), the slow surface modes penetrate more into the weak magnetic field region than into the strong field region, whereas the fast surface modes (when they exist) penetrate more into the strong magnetic field region than into the weak field region.

It may, at first glance, seem that the cases $v_A > v_{Ae}$ and $v_{Ae} > v_A$ refer to the same situation if the regions $z > 0$ and $z < 0$ are reversed. However, the ratios v_A/c_e and v_{Ae}/c_e are kept constant while the ratio c_o/c_e (and hence v_A/c_o and v_{Ae}/c_o) is varied. Clearly, c_o and c_e play different roles; reversal of the regions $z > 0$ and $z < 0$ cannot be carried out.

2.4 Surface Waves On A Magnetic-Nonmagnetic Interface

Consider the case of non-parallel propagation ($\theta \neq 0$) on an interface one side of which is field-free. With $v_{Ae} = 0$, Equation (2.23) reduces to

$$\rho_o(K^2 v_A^2 cos^2\theta - \omega^2)(m_e^2 + k_y^2)^{1/2} - \rho_e\, \omega^2(m_o^2 + k_y^2)^{1/2} \;=\; 0\,, \qquad (2.40)$$

where now

$$m_e^2 \;+\; k_y^2 \;=\; K^2 \;-\; \frac{\omega^2}{c_e^2}\,. \qquad (2.41)$$

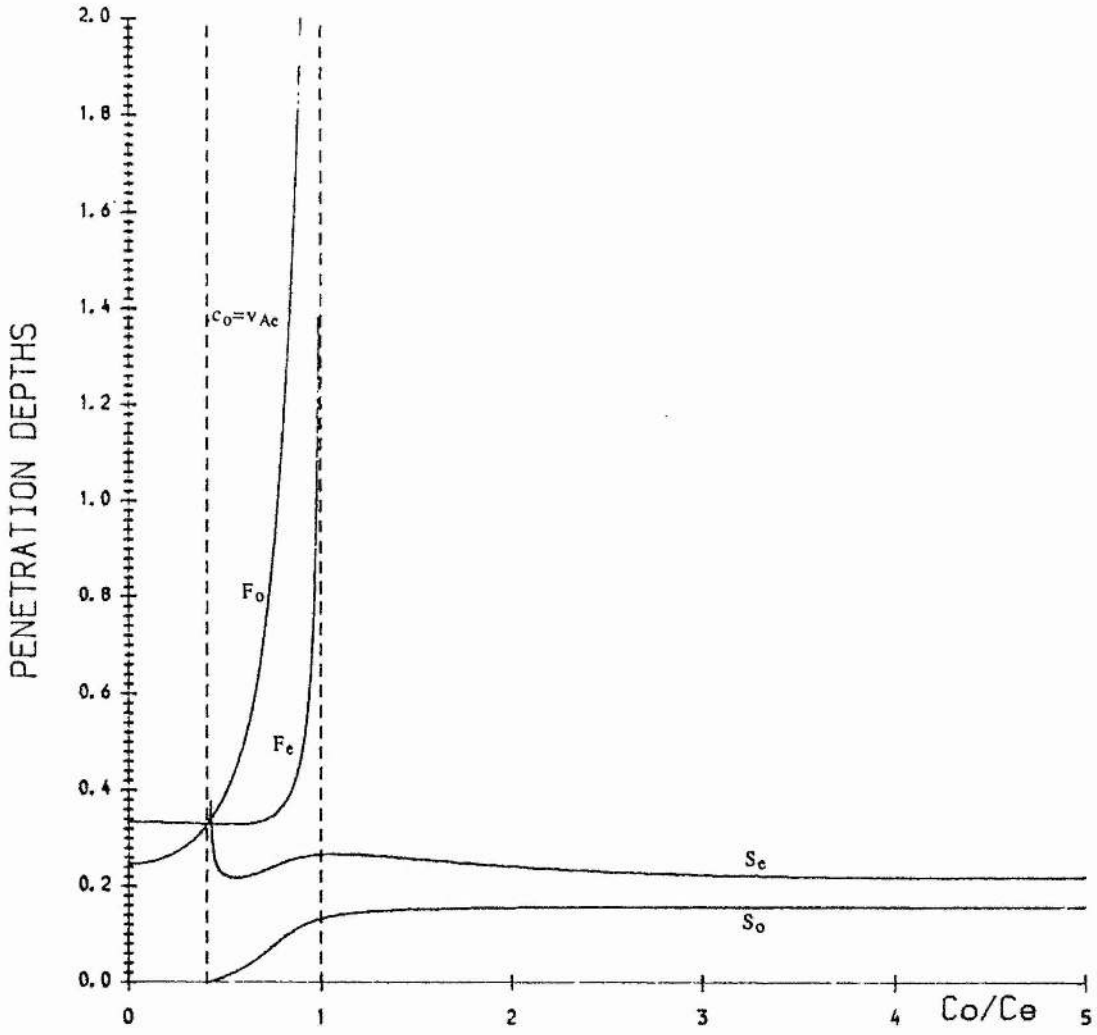

Figure 2.3a: The variation with c_o/c_e of the penetration depths of the slow and fast magnetoacoustic surface waves (propagating parallel to the magnetic field) for $v_A/c_e = 1.8$ and $v_{Ae}/c_e = 0.4$. Depths are measured in units of wavelength $2\pi/k$.'S_o' - slow surface wave into the region (v_A, c_o); 'S_e' - slow surface wave into the region (v_{Ae}, c_e); 'F_o' - slow surface wave into the region (v_A, c_o); 'F_e' - slow surface wave into the region (v_{Ae}, c_e).

Equation (2.40) may be cleared of radicals by squaring, the result being a quartic in $c_{ph}^2 \equiv \omega^2/K^2$ (Roberts, 1981):

$$(c_o^2 + v_A^2)(c_T^2\cos^2\theta - c_{ph}^2)(v_A^2\cos^2\theta - c_{ph}^2)(c_e^2 - c_{ph}^2) =$$

$$\left(\frac{\rho_e}{\rho_o}\right)^2 c_{ph}^4 c_e^2 \left[(c_o^2\cos^2\theta - c_{ph}^2)(v_A^2\cos^2\theta - c_{ph}^2) + \sin^2\theta(c_o^2 + v_A^2)(c_T^2\cos^2\theta - c_{ph}^2)\right], \quad (2.42)$$

with $m_e^2 + k_y^2 > 0$ and $m_o^2 + k_y^2 > 0$. It should be noted that spurious roots may be introduced on squaring; these satisfy Equation (2.42) but not the original dispersion relation (2.40) and its conditions for exponentially decaying solutions.

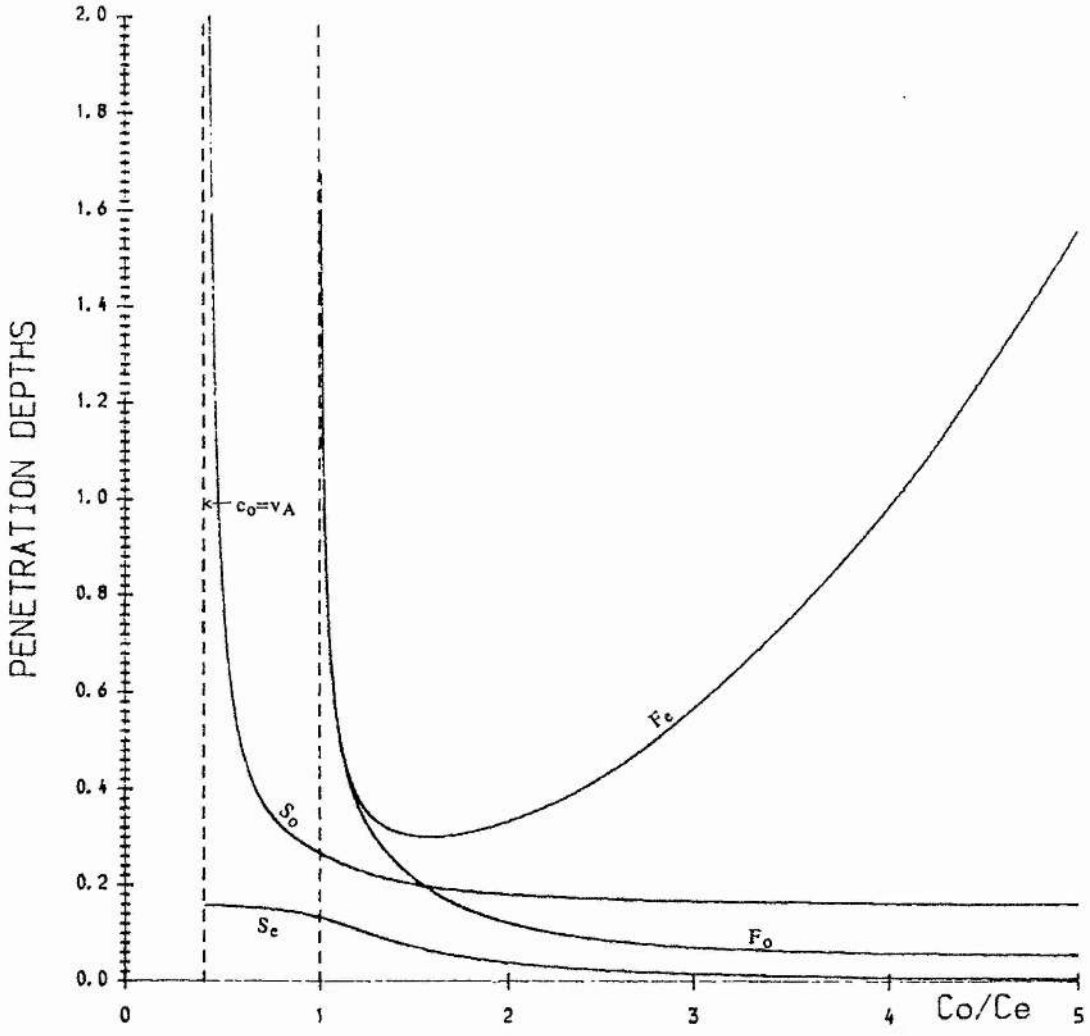

Figure 2.3b: The variation with c_o/c_e of the penetration depths of the slow and fast magnetoacoustic surface waves (propagating parallel to the magnetic field) for $v_A/c_e = 0.4$ and $v_{Ae}/c_e = 1.8$.For notation see Figure 2.3a.

The condition $m_e^2 + k_y^2 > 0$ implies that $c_{ph} < c_e$, and the condition $m_o^2 + k_y^2 > 0$ implies $c_{ph} < c_T \cos\theta$ or $\min(c_o \cos\theta, v_A \cos\theta) < c_{ph} < \max(c_o \cos\theta, v_A \cos\theta)$. Also $c_{ph} \leq v_A \cos\theta$. Thus, there exists the possibility of a slow surface wave with phase-speed $c_{ph} < \min(c_T \cos\theta, c_e)$. In fact, the slow surface wave is present irrespective

of the magnitudes of c_e, c_o, and v_A (Roberts, 1981; Miles and Roberts, 1989). But if $v_A > c_o$ and the field-free medium is warmer than the magnetic medium, (so that $c_e > c_o$), then a fast surface wave may propagate with phase-speed satisfying $c_o \cos\theta < c_{ph} < \min(c_e, v_A \cos\theta)$.

The variation with v_A/c_e of the phase-speed ω/K of surface waves propagating at various angles θ to the applied field is shown in Figure 2.4 for two values of c_o/c_e namely 0.75 (Figure 2.4a) and 1.4(Figure 2.4b).

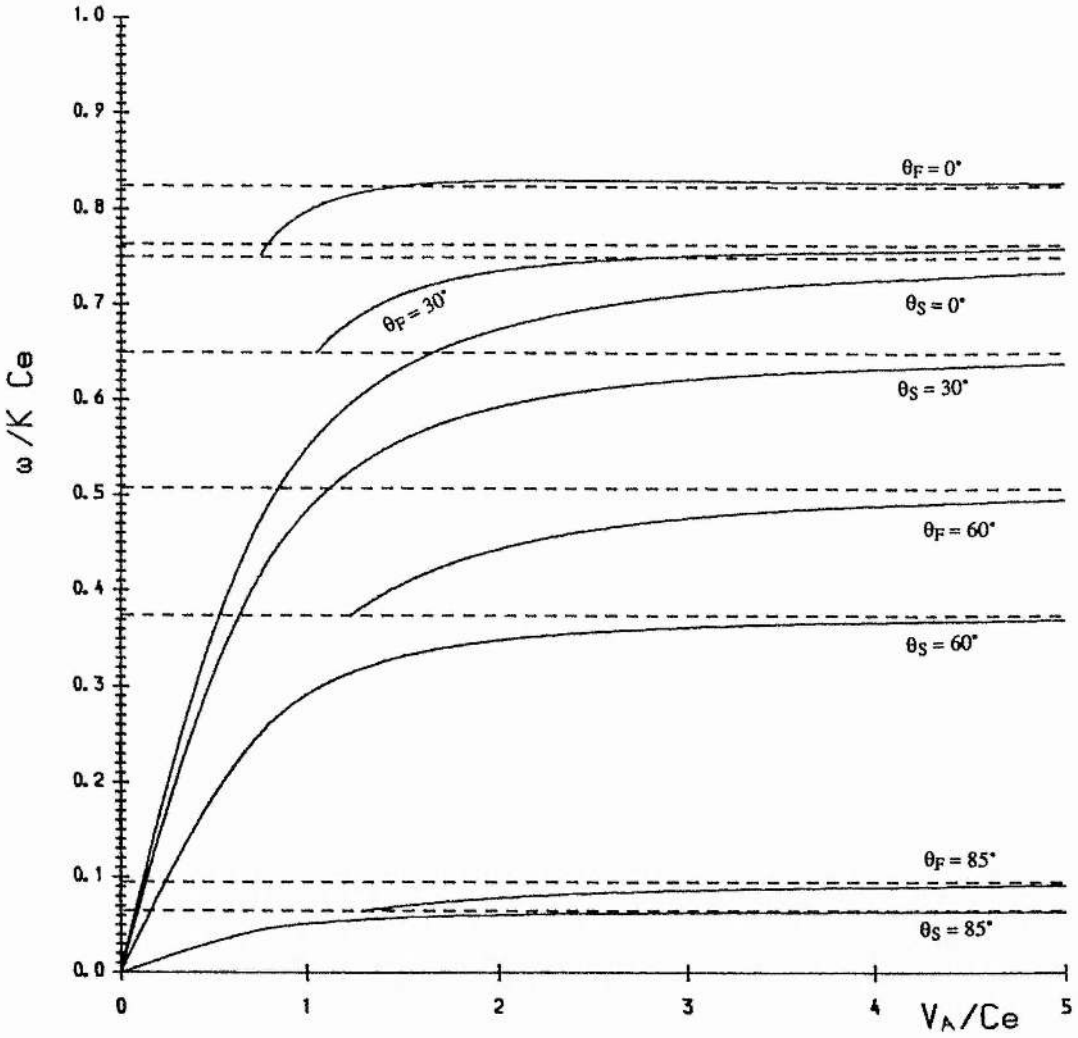

Figure 2.4a: The variation of the dimensionless phase-speed ω/Kc_e of the slow and fast magnetoacoustic surface waves with the parameter v_A/c_e for angles of propagation $\theta = 0°, 30°, 60°,$ and $85°$; $c_o/c_e = 0.75$. The subscript 'S' denotes 'slow' surface wave and 'F' denotes 'fast' surface wave. The fast wave exists only when $v_A > c_o$ and $c_o < c_e$.

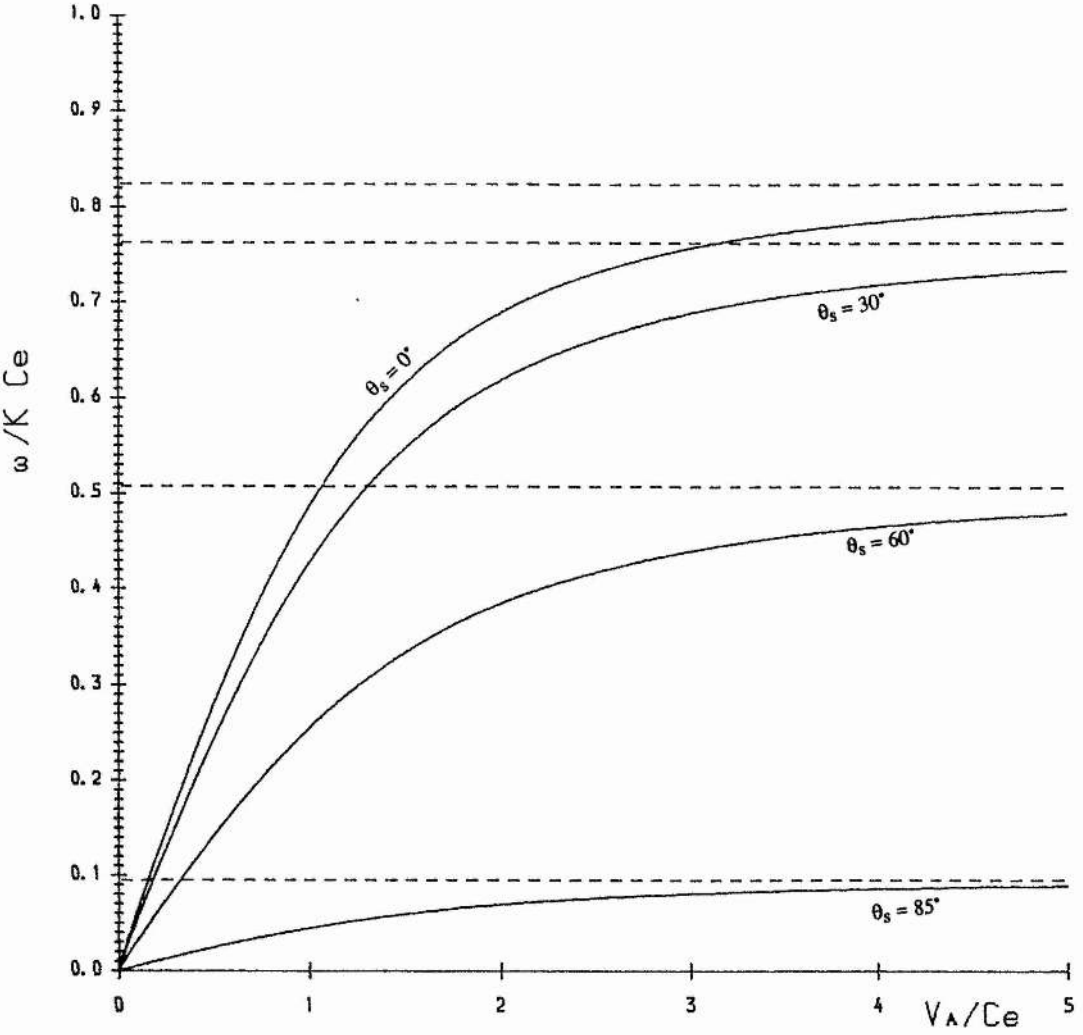

Figure 2.4b: The variation of the dimensionless phase-speed ω/Kc_e of the slow and fast magnetoacoustic surface waves with the parameter v_A/c_e for angles of propagation $\theta = 0°, 30°, 60°$, and $85°$; $c_o/c_e = 1.4$. The subscript 'S' denotes 'slow' surface wave. Note the absence of fast wave since $c_o > c_e$.

It can easily be seen from the figures that fast and slow modes are present together only for $v_A > c_o$. When the gas inside the magnetised region is warmer than the field-free region (i.e., when $c_o > c_e$), the fast wave is absent (Figure 2.4b). Also apparent in Figure 2.4 is that both slow and fast surface waves propagate with phase-speeds

which *decrease* with increasing angle θ, for a given c_o/c_e. Also, $\omega/Kc_e \to 0$ as $\theta \to \pi/2$ for both slow and fast surface waves; this is to be expected since the phase-speed for a surface wave must lie in the range $0 < \omega/K < v_A \cos\theta$ when there is a field-free region on one side of the interface. It may also be noted in Figure 2.4 that for the slow surface wave $\omega/Kc_e \to 0$ as $v_A/c_e \to 0$. For large v_A/c_e the slow wave asymptotes to the smaller of the values $(c_o/c_e)\cos\theta$ and

$$\left\{\frac{2\cos^4\theta}{\gamma^2}\left[\left(1+\frac{\gamma^2}{\cos^4\theta}\right)^{1/2}-1\right]\right\}^{1/2}.$$

The fast surface wave (when permitted to propagate) asymptotes to the larger of these two values.

Figure 2.5 illustrates the dependence of ω/Kc_e on c_o/c_e for two different values of v_A/c_e. Once again, the fast wave propagates only when $c_o < c_e$. Here also the phase-speeds of slow and fast modes *decrease* with increasing θ as a function of c_o/c_e, for a given v_A/c_e.

Figure 2.6 exhibits the dependence on v_A/c_e of the penetration depth for angles $\theta = 0°$ and $60°$, with c_o/c_e taken to be 0.75 (Figure 2.6 a,b) or 1.4 (Figure 2.6 c,d).

For large v_A/c_e, it can be seen that the fast mode penetrates more than the slow mode into either region and both the modes penetrate deeper into the field-free region than into the magnetic region. It is interesting to note the decrease in the penetration depths with the increase in angle θ for large v_A/c_e. Also, the penetration depths of slow and fast surface waves become equal as $\theta \to \pi/2$; since both $(m_o^2+k_y^2)^{-1/2}$ and $(m_e^2+k_y^2)^{-1/2}$ tend to K when θ approaches $\pi/2$; however, as noted earlier, the surface modes cease to propagate in this limit $\left(\frac{\omega}{K} \to 0 \text{ as } \theta \to \frac{\pi}{2}\right)$. For large values of v_A/c_e, the slow surface wave penetration depth asymptotes to $1/\left\{2\pi\left(1-(c_o^2/c_e^2)\cos^2\theta\right)^{1/2}\right\}$ in the field-free medium, and to $\frac{(\gamma/2)\left(c_o^2/c_e^2\right)}{2\pi(1-(c_o^2/c_e^2)\cos^2\theta)^{1/2}}$ in the field medium. The penetration depth of fast surface wave asymptotes (for large v_A/c_e) to $\frac{1}{2\pi\left\{1-\frac{2\cos^4\theta}{\gamma^2}\left[\left(1+\frac{\gamma^2}{\cos^4\theta}\right)^{1/2}-1\right]\right\}^{1/2}}$ in the field-free medium, and to $(2\pi)^{-1}$ in the magnetic medium.

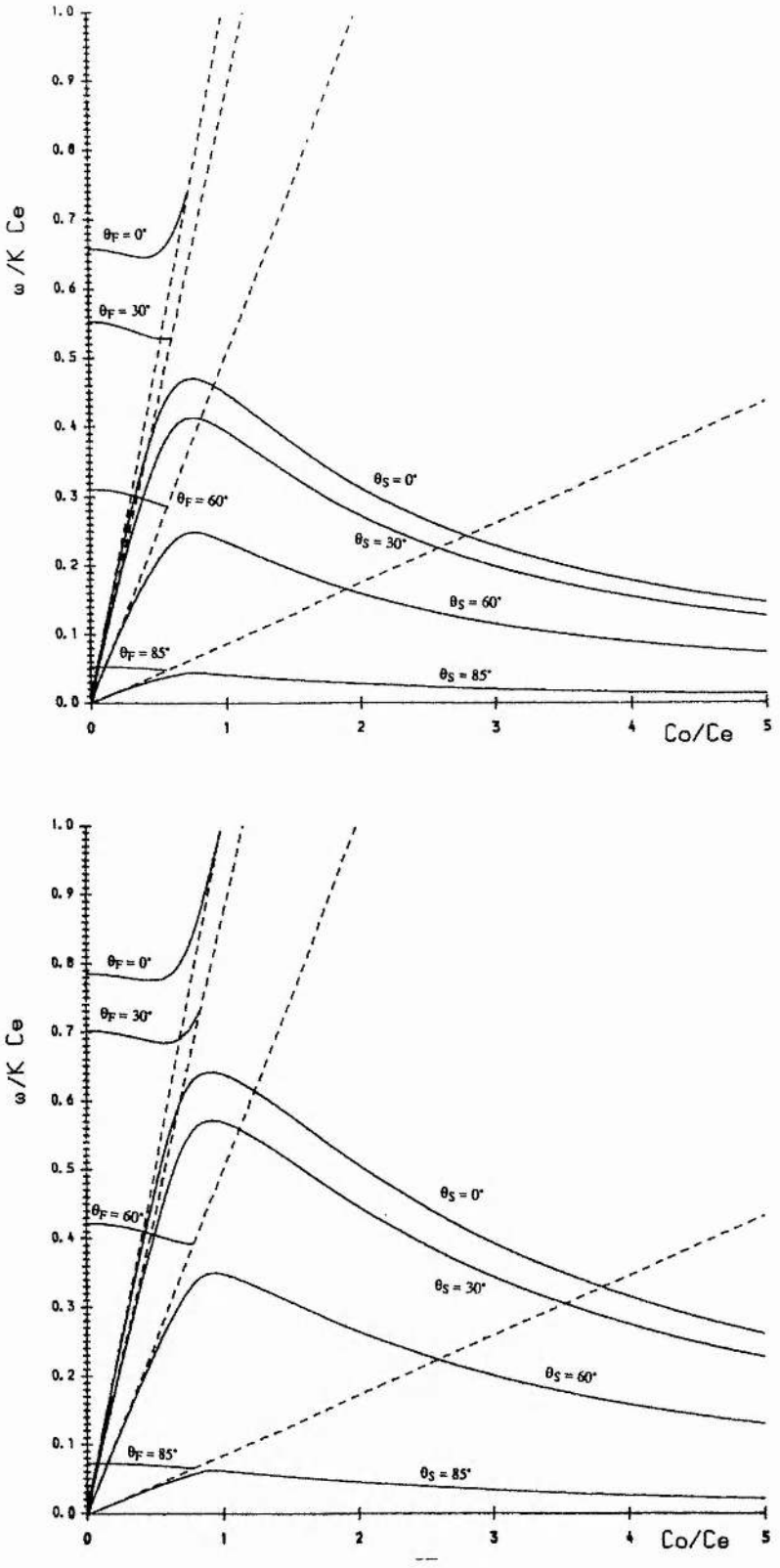

Figure 2.5 The variation of the phase-speed ω/Kc_e of the slow and fast surface waves with the parameter c_o/c_e, for angles of propagation $\theta = 0°, 30°, 60°,$ and $85°$. Cases (a) $v_A/c_e = 0.75$; (b) $v_A/c_e = 1.4$. The sloping asymptotes are the lines $\omega = Kc_o \cos\theta$ for various θ.

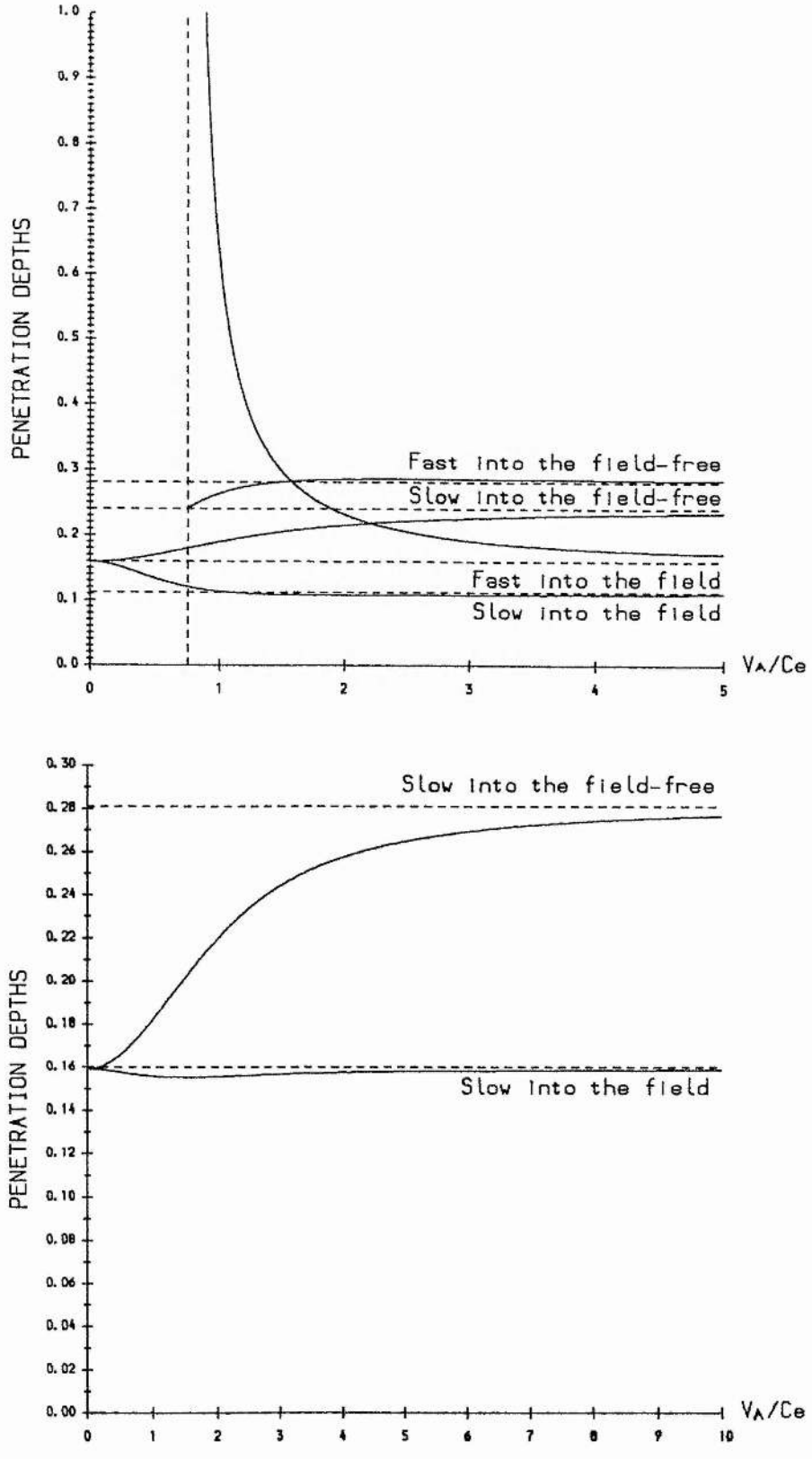
PENETRATION DEPTHS
1.0
0.9
0.8
0.7
0.6
0.5
0.4
0.3
0.2
0.1
0.0
0
1
2
3
4
5
VA/Ce
Fast into the field-free
Slow into the field-free
Fast into the field
Slow into the field
PENETRATION DEPTHS
0.30
0.28
0.26
0.24
0.22
0.20
0.18
0.16
0.14
0.12
0.10
0.08
0.06
0.04
0.02
0.00
0
1
2
3
4
5
6
7
8
9
10
VA/Ce
Slow into the field-free
Slow into the field

Figure 2.6a, b

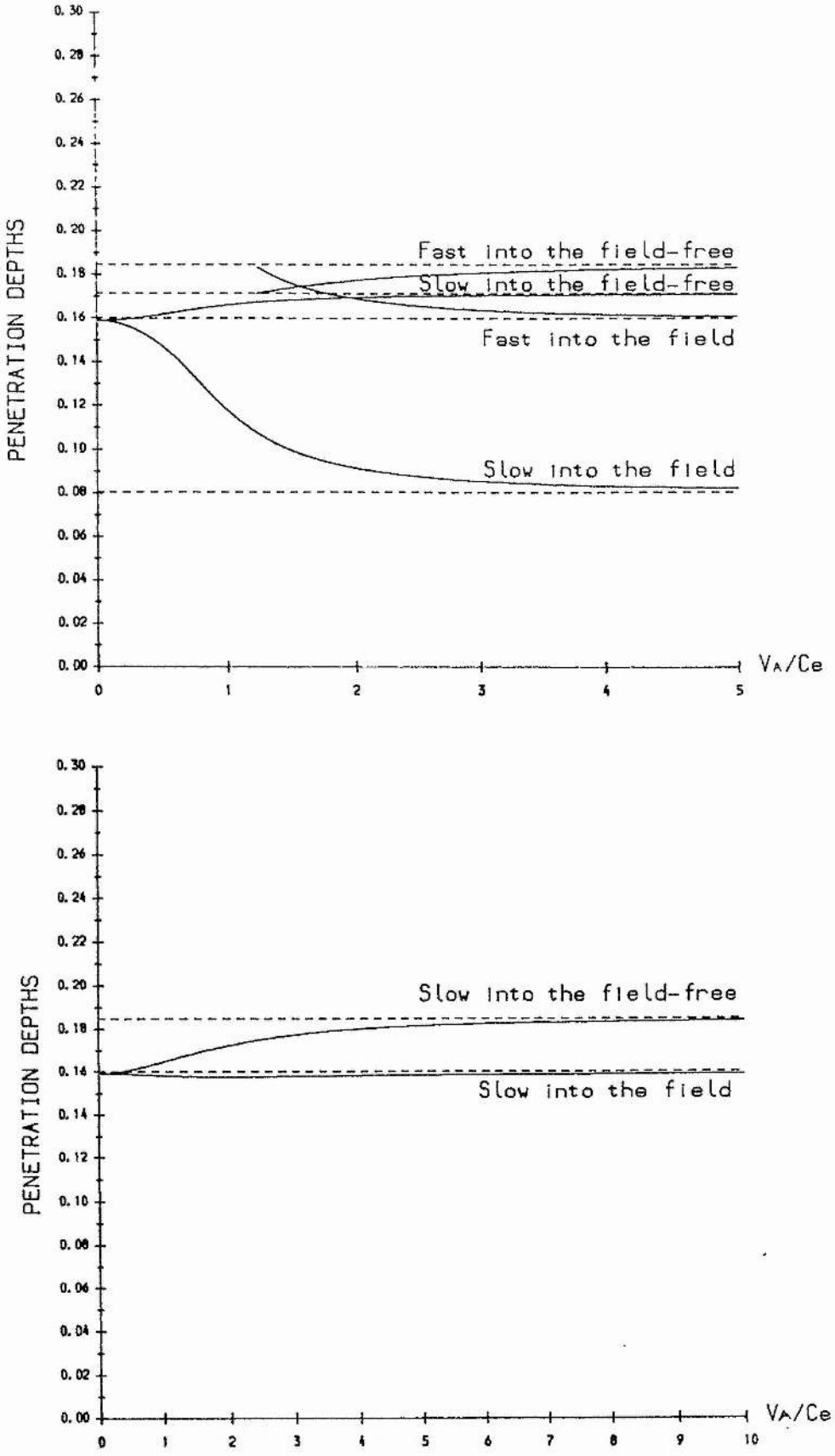

Figure 2.6: The variation with v_A/c_e of the penetration depths (in units of $2\pi/K$) of the fast and slow surface waves into the field-free and magnetic regions for $\theta = 0°$ and $60°$.(a)$\theta = 0°$, $c_o/c_e = 0.75$, (b)$\theta = 0°$, $c_o/c_e = 1.4$; (c)$\theta = 60°$, $c_o/c_e = 0.75$, (d)$\theta = 60°$, $c_o/c_e = 1.4$.

2.5 Summary

In this *chapter* the dispersion relation describing the non-parallel propagation of the surface waves in the absence of gravity is derived for a single magnetic interface. Fast and slow magnetoacoustic surface waves may arise whenever there is a discontinuity in the temperature or density or in the magnetic field. In the incompressible limit the phase-speed of the surface wave is intermediate between the Alfvén speeds on the two sides of the interface and is symmetric (i.e., the surface wave penetrates an equal distance either side of the interface) about the surface of discontinuity. In the case of an interface one side of which is field-free, a slow surface wave can always propagate but a fast surface wave will propagate only if the sound speed in the magnetic region is less than the Alfvén speed and the field-free medium is warmer than the magnetic medium (Roberts, 1981). At a magnetic-magnetic interface, however, both slow and the fast magnetoacoustic surface waves can arise but there exists a critical value of c_o/c_e below which the slow surface wave does not propagate.

At the magnetic, nonmagnetic interface the fast wave penetrates more than the slow surface wave into either medium and both penetrate more into the field-free medium than into the magnetic region for large v_A/c_e.

Any correct interpretations of the magnetic and thermal surface effects on the observed solar modes require inclusion of gravity in the analysis. This chapter can thus be regarded as an initial step which can be followed by the inclusion of gravitational stratification and thus an investigation of surface effects on solar p-modes and, to a lesser extent f-modes.

CHAPTER 3

SURFACE EFFECTS OF A UNIFORM MAGNETIC FIELD ON P-MODES

3.1 Introduction

When the solar 'five minute oscillations' or p-modes (see Chapter 1, Sections 1.4 and 1.6) were first detected in the early sixties the subject was considered by most as an atmospheric discipline. The next ten years saw the presentation of various theoretical works giving a basic understanding of the behaviour of these oscillations. Attempts were made to use observations to explain certain characteristics of the solar atmosphere. However, when it was realized in the seventies that these oscillations were global modes (i.e., they existed in the solar interior as well as the atmosphere), interest moved quickly towards the possibility of doing seismology of the Sun by measuring accurately and interpreting carefully frequencies for the p-modes. Today, these oscillations are used as a tool to infer the physical structure of the solar interior and atmosphere. Theories are developed in detail to reproduce the observed frequencies within the limits of observational uncertainties. Observations are made with high precision to investigate important basic properties of the solar interior.

There are two basic and fundamentally different approaches to the task of reconciling the theoretical and observed frequencies. First, the observed frequencies are compared with theoretical ones that are calculated from solar models derived for various choices of certain physical parameters, and the parameters giving the best fit are then determined. The progress made along these lines indicates that the standard solar model gives a fairly good fit to the observations, but that there remains a small discrepancy between the observed frequencies and theoretically computed ones. On the other hand, the second approach is to determine the functional forms of certain physical quantities, such as the sound velocity distribution, by solving integral equations for the eigenfrequencies. This approach is useful as it may clarify the cause of the discrepancy between the theoretical and observed frequencies. To date no theoretical solar model has been able to reproduce all observed frequencies to the required accuracy, despite a very effective and mathematically accurate treatment.

During the last few years, considerable effort has been made to measure very accurately the frequencies of the p-mode oscillations and to determine if these frequencies vary with the solar cycle. Although extensive and accurate data sets do not yet extend over intervals as long as 11 years, recent observations of the solar p-mode frequencies have led to significant improvements in the quality and the quantity of the observational data sets now available. Recently, Elsworth et al.(1990), Libbrecht and Woodard (1990) and Woodard and Libbrecht (1991) have shown conclusively that solar p-mode frequencies change with time and the measured frequency shifts $\Delta\nu = \nu(1988) - \nu(1986)$ and $\Delta\nu = \nu(1989) - \nu(1986)$ depend strongly on frequency ν and only weakly on degree l. Figure 3.1 displays the frequency shifts determined by Woodard and Libbrecht (1991). The observational results have been averaged over modes of degree l in the range $4 < l < 140$. In this figure, Woodard and Libbrecht have compared p-mode frequencies from 1986 to 1988, 1989. The year 1986 was a period of low solar activity, while 1988 and 1989 were the periods of rising solar activity. Figure 3.1 shows the increase in the frequency shift with frequency up to $\nu \approx 3.9$mHz while the frequency shifts drop sharply above $\nu \approx 3.9$mHz.

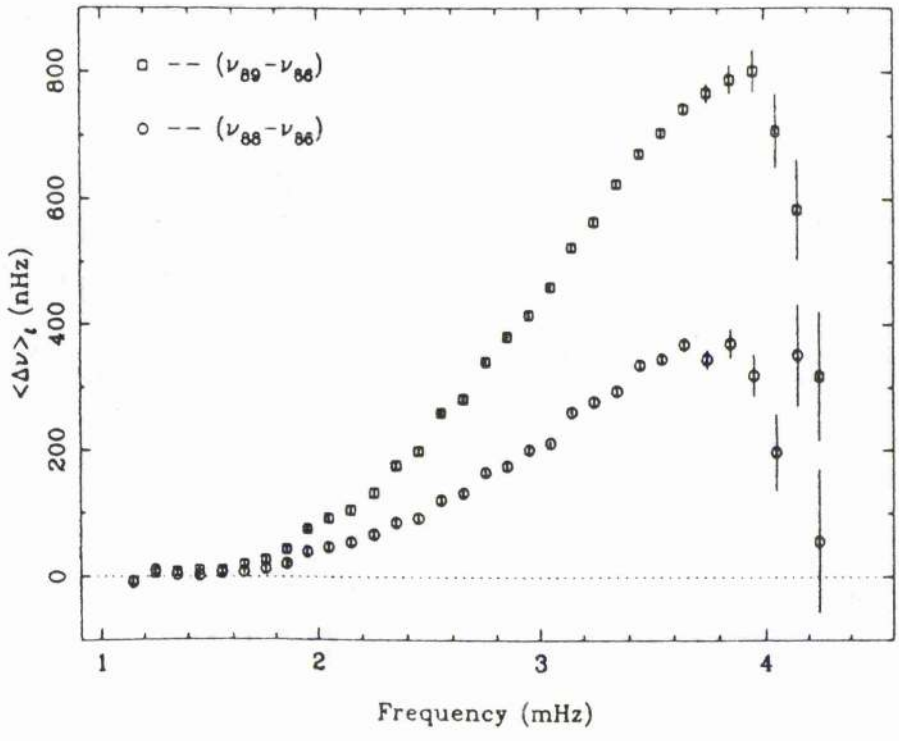

Figure 3.1: The frequency shift as a function of mode frequency for solar p-mode oscillations, using the 1986 mode frequencies as a reference. The 1988 data are denoted by circles; 1989 by squares. The frequency dependence was obtained by averaging over modes in the range $4 < l < 140$ of spherical harmonic degree. (Woodard and Libbrecht, 1991)

An important further development is to determine the physical changes in the Sun that are responsible for these frequency shifts.

The solar p-modes are believed to be acoustic waves trapped in the solar interior cavity, a cavity delimited at its lower extreme by the increasing sound speed in the convection zone and at its upper extreme by the reflective properties of the photosphere and the chromosphere (see chapter 1). The perturbations responsible for the frequency shifts may be located in the upper atmosphere where the p-modes are evanescent. Since the decay rate of eigenmodes with height is determined by this upper atmosphere, its detailed structure is important. Since the magnetic field is a significant part of the chromosphere, its effect on the frequencies of p-modes is of considerable importance.

The importance of a chromospheric canopy magnetic field on frequency shifts in p- and f-modes was first pointed out by Roberts and Campbell (1988), Campbell and Roberts(1989) and Evans and Roberts (1990). The variations in height of a magnetic canopy and its influence on the solar p- and f-modes again confirmed the importance of chromospheric magnetism (Evans and Roberts, 1991). Chromospheric 'canopy' fields here refer to the magnetic fibril fields that fan out at higher levels in the solar atmosphere and form an overlying canopy field. In Campbell and Roberts (1989) this higher level is modelled by a horizontal magnetic field whose strength decreases with height in such a manner as to maintain a constant Alfvén speed. This type of magnetic field perturbation causes the p-mode frequencies to decrease. In Evans and Roberts (1990) the magnetic field is again taken to be horizontal, but, in this case, of constant magnitude. This type of magnetic field configuration produces a positive frequency shift. Goldreich et al. (1991) have affirmed the importance of variations in the photospheric magnetic field strengths. They argued that these variations are responsible for positive frequency shifts at low p-mode frequencies and that the precipitious drop in the shifts at high frequencies is caused by the presence of a chromospheric resonance and an increase in the chromospheric temperature. A perturbation approach to chromospheric field changes has recently been developed by Wright and Thompson (1992).

Thus, various authors have taken chromospheric magnetic fields into account in models predicting p-mode frequencies. All of the papers described above suggest that the study of chromospheric magnetism and its influence on the p-modes is very interesting and encouraging. These studies and various observational works raise the question - can changes in chromospheric magnetic activity over the solar cycle bring about the frequency shifts as observed ? Many facets of chromospheric magnetic fields remain unexplored; hence, the aim of this chapter is to answer the above question by the inclusion of further chromospheric effects.

For this purpose a very simple model is discussed, continuing the investigation

begun by Evans and Roberts (1990). The main objective is to determine the thermal as well as magnetic effects of the chromosphere on the solar p-mode frequencies. The convection zone is modelled as a fluid having a temperature profile that increases linearly with depth. The effects of vertical magnetic flux tubes in the convection zone and of a toroidal magnetic field at the base of the convection zone are neglected. The atmosphere above the temperature minimum is assumed to be isothermal and permeated by a uniform horizontal magnetic field.

3.2 The Model And Dispersion Relation

The model shown in Figure 3.2 is studied in an attempt to find out how the p-mode frequencies are influenced by a horizontal magnetic field situated above the convection zone.

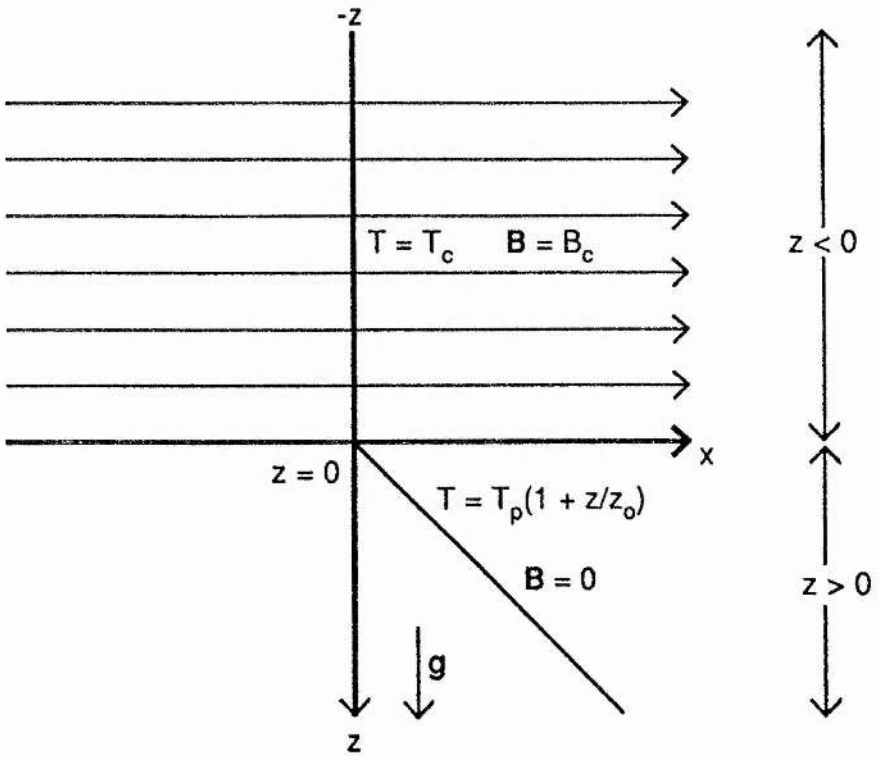

Figure 3.2: The equilibrium atmosphere of the model.

The model makes use of two layers of atmosphere, the upper layer representing the chromosphere and the lower one representing the convection zone. The reference level, $z = 0$, corresponds to the base of the chromosphere (i.e. the temperature minimum). The chromosphere and the convection zone are represented by the regions $z < 0$ and $z > 0$, respectively; i.e., z increases moving downwards and thus measures depth rather than height. The medium is stratified by gravity acting in the positive z-direction. It is assumed that the solar plasma is an ideal, perfectly conducting gas, permeated by a horizontal magnetic field $\mathbf{B} = B_o(z)\hat{\mathbf{x}}$ and that the unperturbed state is in a magnetohydrostatic equilibrium described by the equation :

$$\frac{d}{dz}\left(p_o + \frac{B_o^2}{2\mu}\right) = \rho_o(z)g \, . \tag{3.1}$$

The plasma pressure $p_o(z)$, density $\rho_o(z)$ and temperature $T_o(z)$ are related by the ideal gas law

$$p_o = \mathcal{R}\rho_o T_o \, , \tag{3.2}$$

where $\mathcal{R}$ is the gas constant (see Equation (2.6) Chapter 2). The temperature $T_o(z)$ is taken to increase linearly with depth in the convection zone ($z > 0$) and to be constant in the chromosphere ($z < 0$), i.e.

$$T_o(z) = \begin{cases} T_p\left(1 + \frac{z}{z_o}\right) \, , & z > 0, \\ T_c \, , & z < 0. \end{cases} \tag{3.3}$$

Here, T_p is the temperature at the top of the convection zone and T_c is the temperature in the chromosphere. The temperature scale height at the top of the convection zone is z_o.

The magnetic field is taken to be of the form (see Figure 3.2)

$$B_o(z) = \begin{cases} 0 \, , & z > 0, \\ B_c \, , & z < 0. \end{cases} \tag{3.4}$$

Thus, with $T_o(z)$ and $B_o(z)$ specified by Equations (3.3) and (3.4) respectively, the gas pressure distribution is

$$p_o(z) = \begin{cases} p_p\left(1 + \frac{z}{z_o}\right)^{(m+1)} \, , & z > 0, \\ p_c e^{z/H_c} \, , & z < 0, \end{cases} \tag{3.5}$$

with chromospheric density scale height $H_c(=\mathcal{R}T_c/g)$ and convection zone polytropic index $m\,[=(gz_o/\mathcal{R}T_p)-1]$.

The gas pressure p_p at the top of the convection zone ($z = 0_+$) is related to the pressure p_c at the base of the chromosphere ($z = 0_-$) through continuity of total pressure,

$$p_c + \frac{B_c^2}{2\mu} = p_p \,. \tag{3.6}$$

On using the ideal gas law (3.2), Equation (3.6) may be expressed in terms of the interfacial density ratio as

$$\frac{\rho_c}{\rho_p} = \frac{c_{sp}^2}{(c_{sc}^2 + \frac{\gamma}{2}v_{Ac}^2)} \,. \tag{3.7}$$

Here, $c_{sp} = (\gamma p_p/\rho_p)^{1/2}$ is the sound speed at the top of the convection zone ($z = 0_+$), and $c_{sc} = (\gamma p_c/\rho_c)^{1/2}$ and $v_{Ac} = B_c/(\mu\rho_c)^{1/2}$ are the sound and Alfvén speeds at the base of the chromosphere ($z = 0_-$). The adiabatic index, in both the convection zone and chromosphere is γ, and is assumed to be a constant.

The governing equations (neglecting dissipation and the displacement current) are taken to be (see Chapter 1)

$$\frac{\partial \rho}{\partial t} + \rho\nabla\cdot\mathbf{v} + \mathbf{v}\cdot\nabla\rho = 0, \tag{3.8}$$

$$\rho\left[\frac{\partial \mathbf{v}}{\partial t} + (\mathbf{v}\cdot\nabla)\,\mathbf{v}\right] = -\nabla p + \frac{1}{\mu}(\nabla\times\mathbf{B})\times\mathbf{B} + \rho\mathbf{g}\,, \tag{3.9}$$

$$\frac{\partial \mathbf{B}}{\partial t} = \nabla\times(\mathbf{v}\times\mathbf{B})\,, \tag{3.10}$$

$$\frac{\partial}{\partial t}\left(\frac{p}{\rho^\gamma}\right) + (\mathbf{v}\cdot\nabla)\left(\frac{p}{\rho^\gamma}\right) = 0\,, \tag{3.11}$$

where γ is the adiabatic index. The velocity field is taken to be two dimensional : $\mathbf{v} = (v_x, 0, v_z)$.

Since the typical relative displacement of the solar surface in each mode is only of order 10^{-6} to 10^{-8} (Christensen Dalsgaard, 1986), linear theory is a good approximation for the analysis of the above equations. Thus, for a small displacement, it can be assumed that each physical quantity is changed by a small perturbation from its equilibrium value and the perturbation quantities can be expressed in the form $\mathbf{v} = (v_x(z), 0, v_z(z))\, exp\ i(\omega t - k_x x)$, etc, where ω is the angular frequency and k_x is the wavenumber along the x-axis. After some detailed algebra (see Appendix A3, Section 1), the following governing equation (see also Goedbloed 1971; Adam 1977; Roberts 1985) is obtained:

$$\frac{d}{dz}\left\{\frac{\rho_o(c_s^2+v_A^2)(\omega^2-k_x^2c_T^2)}{(\omega^2-k_x^2c_s^2)}\frac{dv_z}{dz}\right\}$$

$$= \frac{\rho_o g^2 k_x^2}{(\omega^2-k_x^2c_s^2)} - \rho_o(\omega^2-k_x^2v_A^2) - gk_x^2\frac{d}{dz}\left(\frac{\rho_o c_s^2}{(\omega^2-k_x^2c_s^2)}\right)v_z\ , \qquad (3.12)$$

where $c_s(z) = (\gamma p_o(z)/\rho_o(z))^{1/2}$ is the local sound speed, $v_A(z) = B(z)/(\mu\rho_o(z))^{1/2}$ is the local Alfvén speed and $c_T(z) = c_s v_A/(c_s^2+v_A^2)^{1/2}$ is the MHD cusp speed.

For the chromosphere ($z < 0$), which is isothermal with a uniform magnetic field, the governing Equation (3.12) reduces to

$$\{\mathcal{A}_1 + \mathcal{A}_2\ exp(-\mathcal{A}_3 z)\}\frac{d^2v_z}{dz^2} + \mathcal{A}_1\mathcal{A}_3\frac{dv_z}{dz} + \left\{\mathcal{A}_4 - k_x^2\mathcal{A}_2\ exp(-\mathcal{A}_3 z)\right\}v_z = 0, \quad (3.13)$$

where

$$\mathcal{A}_1 = \omega^2 c_{sc}^2\ , \qquad \mathcal{A}_2 = v_{Ac}^2(\omega^2 - k_x^2c_{sc}^2)\ , \qquad \mathcal{A}_3 = \frac{1}{H_c} = \frac{\gamma g}{c_{sc}^2}\ ,$$

$$\mathcal{A}_4 = (\gamma-1)g^2k_x^2 + \omega^2(\omega^2 - k_x^2c_{sc}^2)\ . \qquad (3.14)$$

Here, c_{sc}^2 is the square of the sound speed in the chromosphere ($z < 0$), v_{Ac}^2 is the square of the Alfvén speed at the base of this region, and γ is the adiabatic index in the region $z < 0$.

Under the transformation

$$\xi = -\frac{\mathcal{A}_1}{\mathcal{A}_2}exp\ (\mathcal{A}_3 z)\ , \qquad V = v_z\xi^{-k_x/\mathcal{A}_3}\ , \qquad (3.15)$$

Equation (3.13) reduces to the hypergeometric equation

$$\xi(1-\xi)\frac{d^2V}{d\xi^2} + \{r-(p+q+1)\xi\}\frac{dV}{d\xi} - pqV = 0\ , \tag{3.16}$$

where

$$p+q = \frac{2k_x}{\mathcal{A}_3}+1\ , \quad pq = \frac{k_x}{\mathcal{A}_3}\left(\frac{k_x}{\mathcal{A}_3}+1\right)+\frac{\mathcal{A}_4}{\mathcal{A}_1\mathcal{A}_3^2}\ , \quad r = p+q = \frac{2k_x}{\mathcal{A}_3}+1\ . \tag{3.17}$$

The application of the transformation (3.15) was first noticed by Nye and Thomas (1976) and Adam(1977).

The general solution of Equation (3.16) near $\xi = 0$ is

$$V \;=\; \mathcal{C}_1 F(p,q;r;\xi) \;+\; \mathcal{C}_2\xi^{1-r}F(p-r+1,q-r+1;2-r;\xi)\ , \tag{3.18}$$

where $\mathcal{C}_1$ and $\mathcal{C}_2$ are arbitrary constants and F is the hypergeometric function defined by the Gauss series (Abramowitz and Stegun, 1965; p.556)

$$F(p,q;r;\xi) = 1 \;+\; \frac{pq}{r}\xi \;+\; \frac{p(p+1)q(q+1)}{r(r+1)}\frac{\xi^2}{2!}+\ldots\ldots \qquad |\xi|<1\ . \tag{3.19}$$

In terms of the original variables, Equation (3.16) has the solution

$$\begin{aligned} v_z \;=\; & \mathcal{C}_1 e^{k_x z}F\left(p,q;r;\frac{-\mathcal{A}_1}{\mathcal{A}_2}e^{\mathcal{A}_3 z}\right) \\ & + \mathcal{C}_2 e^{-k_x z}F\left(p-r+1,q-r+1;2-r;\frac{-\mathcal{A}_1}{\mathcal{A}_2}e^{\mathcal{A}_3 z}\right). \end{aligned} \tag{3.20}$$

Since here trapped modes are being considered, both kinetic and magnetic energy densities must vanish in the limit $z \to -\infty$ ($\xi \to 0$), infinitely far from the Sun.

In the chromosphere, the magnetic energy density of the perturbation is

$$E_B \;=\; \frac{(\mathbf{B_o}+\mathbf{B})\,.\,(\mathbf{B_o}+\mathbf{B})}{2\mu} - \frac{\mathbf{B_o}^2}{2\mu}\ , \tag{3.21}$$

which on linearisation gives

$$E_B = \frac{\mathbf{B_o}.\mathbf{B}}{\mu} = \frac{B_x B_o}{\mu} . \tag{3.22}$$

From the linearised form of the induction Equation (see Appendix A3, Equation A3.4), the x-component is given by

$$\frac{\partial B_x}{\partial t} = -B_o \frac{\partial v_z}{\partial z} . \tag{3.23}$$

On Fourier decomposition, Equation (3.23) gives

$$i\omega B_x = -B_o \frac{dv_z}{dz} . \tag{3.24}$$

Thus, equation (3.22) becomes

$$E_B = \frac{i}{\omega} \frac{B_o^2}{\mu} \frac{dv_z}{dz} . \tag{3.25}$$

Using the result (Abramowitz and Stegun, 1965; p.557)

$$\frac{d}{dz} F(p, q; r; z) = \frac{pq}{r} F(p+1, q+1; r+1; z) , \tag{3.26}$$

and Equation (3.20), it is clear that E_B will vanish as $z \to -\infty$ only if $\mathcal{C}_2 = 0$. Thus

$$v_z = \mathcal{C}_1 \left(\frac{-\mathcal{A}_1}{\mathcal{A}_2} \right)^{\frac{k_x}{\mathcal{A}_3}} e^{k_x z} F\left(p, q; r; \frac{-\mathcal{A}_1}{\mathcal{A}_2} e^{\mathcal{A}_3 z} \right) , \qquad z < 0 . \tag{3.27}$$

The solution (3.27) also satisfies the requirement that the kinetic energy density vanishes in the limit $z \to -\infty$.

The hypergeometric Equation (3.16) has three regular singular points at $\xi = 0, 1, \infty$ where

$$\xi = - \frac{\omega^2 c_{sc}^2}{v_{Ac}^2(\omega^2 - k_x^2 c_{sc}^2)} e^{z/H_c} . \tag{3.28}$$

The singularity in the solution (3.18) near $\xi = 0$ is caused by the negative power $(1 - r$, since $r > 1)$ to which ξ is raised. As the constant C_2 has been set equal to 0, this singularity has been removed. The logarithmic singularity at $\xi = 1$ can be avoided if ξ never equals unity. For ξ to equal unity (with $z \leq 0$ and hence $\exp(\mathcal{A}_3 z) \leq 1$), $-\mathcal{A}_1/\mathcal{A}_2$ must be greater than or equal to 1. That is

$$-\frac{\omega^2 c_{sc}^2}{v_{Ac}^2(\omega^2 - k_x^2 c_{sc}^2)} \geq 1 , \tag{3.29}$$

i.e.

$$c_{Tc}^2 \leq \frac{\omega^2}{k_x^2} \leq c_{sc}^2 , \tag{3.30}$$

where

$$c_{Tc}^2 = \frac{c_{sc}^2 v_{Ac}^2}{c_{sc}^2 + v_{Ac}^2} . \tag{3.31}$$

And so the singularity is avoided if

$$\frac{\omega^2}{k_x^2} < c_{Tc}^2 \quad \text{or} \quad \frac{\omega^2}{k_x^2} > c_{sc}^2 . \tag{3.32}$$

The singularity at $\xi = \infty$ corresponds to $\omega^2/k_x^2 = c_{sc}^2$ or $v_{Ac} = 0$. The case $\omega^2/k_x^2 = c_{sc}^2$ is covered by (3.30).

In the convection zone $(z > 0)$ where $\mathbf{B} = 0$, considering $\Delta = \text{div } \mathbf{v}$ as the dependent variable gives the relationship between v_z and Δ (see Appendix A3, Section 2) as

$$(\omega^2 - k_x^2 c_{sp}^2)\Delta = g k_x^2 v_z + \omega^2 \frac{dv_z}{dz} , \tag{3.33a}$$

and

$$(\omega^4 - g^2 k_x^2) v_z = g(k_x^2 c_{sp}^2 - \gamma\omega^2)\Delta - \omega^2 c_{sp}^2 \frac{d\Delta}{dz} , \tag{3.33b}$$

where γ is the adiabatic index and $c_{sp}^2(z)$ is the square of the sound speed in the convection region $(z > 0)$.

Eliminating v_z between (3.33a) and (3.33b) and assuming $\omega^2 \neq gk_x$, the governing equation for Δ can be obtained (Lamb, 1932) as follows

$$\frac{d^2\Delta}{dz^2} + \left\{\frac{c_{sp}^2\prime + \gamma g}{c_{sp}^2}\right\}\frac{d\Delta}{dz} + \left\{\frac{(\omega^2 - k_x^2 c_{sp}^2)}{c_{sp}^2} - \frac{gk_x^2}{\omega^2}\left[\frac{c_{sp}^2\prime - (\gamma-1)g}{c_{sp}^2}\right]\right\}\Delta = 0, \quad (3.34)$$

the prime denoting derivatives with respect to depth z. For the linear temperature profile given by Equation (3.3), the sound speed follows as

$$c_s^2(z) \;=\; c_{sp}^2\left(1 + \frac{z}{z_o}\right)\;,\quad z > 0\;, \quad (3.35)$$

where $z_o = \{c_s^2(z)/c_s'^2(z)\}_{z=0}$ is the temperature scale-height at $z = 0$ (where $c_s = c_{sp}$). For such a profile, Lamb (1932) has shown that Equation (3.34) has solution

$$\begin{aligned}\Delta(z) = e^{-k_x(z+z_o)}\{&\mathcal{C}_4 M\left(-a, m+2, 2k_x(z+z_o)\right)\\ &+\mathcal{C}_5 U\left(-a, m+2, 2k_x(z+z_o)\right)\}\,,\end{aligned} \quad (3.36)$$

where $\mathcal{C}_4$ and $\mathcal{C}_5$ are arbitrary constants, and M and U are Kummer's functions (confluent hypergeometric functions) (Abramowitz and Stegun, 1965; p.504). The parameter a entering in the confluent hypergeometric function is determined by

$$a \;=\; \frac{\omega^2}{gk_x}\frac{m+1}{2\gamma} + \left(m - \frac{m+1}{\gamma}\right)\frac{gk_x}{2\omega^2} - \frac{m+2}{2}\;,\qquad m = \frac{\gamma g}{c_s^2\prime} - 1\;. \quad (3.37)$$

For the special case of adiabatic stratification, $c_{sp}^2 = (\gamma-1)g$ and neither convective motions nor gravity modes can occur; for this case, the polytropic index m reduces to

$$m = \frac{1}{\gamma - 1}\;. \quad (3.38)$$

Now (Abramowitz and Stegun, 1965; p.504)

$$M(a, b, z) \sim \frac{\Gamma(b)}{\Gamma(a)} e^z z^{a-b} \to \infty \text{ as } z \to \infty\;, \quad (3.39)$$

and so Equations (3.33a) and (3.36) show that $C_4 = 0$ in order to have a finite kinetic energy density $\rho_o v^2/2$ as $z \to \infty$. The finite kinetic energy density is required as the modes are trapped in the upper part of the convection zone.

Thus, the solution for the convection zone is

$$\Delta(z) \;=\; e^{-k_x(z+z_o)}\, C_5\, U\left(-a, m+2, 2k_x(z+z_o)\right) \;, \quad (z<0)\,. \tag{3.40}$$

Then, using Equation (3.33b) and the following derivative property of the confluent hypergeometric functions (Abramowitz and Stegun, 1965; p.507)

$$\frac{d}{dz}\left\{U(a,b,z)\right\} \;=\; -aU(a+1,b+1,z)\,, \tag{3.41}$$

Equation (3.40), when expressed in terms of the original variables, becomes

$$\begin{aligned}(\omega^4 - g^2k_x^2)v_z e^{k_x(z+z_o)} \;=\; & C_5\left\{\left[k_x c_{sp}^2(\omega^2+gk_x) - \gamma g\omega^2\right]\; U(-a,m+2,2k_x(z+z_o))\right. \\ & \left. -2a\omega^2 c_{sp}^2 k_x\; U(-a+1,m+3,2k_x(z+z_o))\right\}\,. \end{aligned} \tag{3.42}$$

To obtain the dispersion relation relating ω and k_x, the two solutions for v_z given by Equations (3.27) and (3.42) are matched at the interface $z = 0$. It is necessary that the vertical component of velocity, v_z, be continuous at $z = 0$. Also, integrating Equation (3.12) across the interface yields the condition that

$$\left\{\frac{\rho_o(c_s^2+v_A^2)(\omega^2-k_x^2c_T^2)}{(\omega^2-k_x^2c_s^2)}\right\}\frac{dv_z}{dz} \;+\; \left\{\frac{gk_x^2\rho_o c_s^2}{(\omega^2-k_x^2c_s^2)}\right\}v_z \tag{3.43}$$

be continuous at the interface. Thus, the application of these two conditions to the solutions (3.27) and (3.42) yield the dispersion relation

$$\begin{aligned} & 2a\omega^2 c_{sp}^2 k_x \frac{U\left(-a+1,m+3,2k_xz_o\right)}{U\left(-a,m+2,2k_xz_o\right)} \;+\; \gamma g\omega^2 \;-\; k_x c_{sp}^2(\omega^2+gk_x) \\ & = \frac{(c_{sc}^2+\frac{\gamma}{2}v_{Ac}^2)(g^2k_x^2 \;-\; \omega^4)(\omega^2-k_x^2c_{sc}^2)}{gk_x^2c_{sc}^2 \;+\; (c_{sc}^2+v_{Ac}^2)(\omega^2-k_x^2c_{Tc}^2)\left\{k_x - \frac{pq}{r}\frac{A_1A_3}{A_2}\frac{F\left(p+1,q+1;r+1;\frac{-A_1}{A_2}\right)}{F\left(p,q;r;\frac{-A_1}{A_2}\right)}\right\}}\,. \end{aligned} \tag{3.44}$$

Equation (3.44) is a very general dispersion relation describing magnetoacoustic surface waves (see Chapter 2), modified by gravity, which may propagate along the interface ($z = 0$) between the chromosphere ($z < 0$) and the convection zone ($z > 0$) (see also Roberts, 1981; Miles and Roberts, 1991; Jain and Roberts, 1990; 1991) as well as p- and f- modes. It also includes g-modes and their unstable counterpart (convection). This dispersion relation was also derived earlier by Evans and Roberts (1990) in their investigation of the influence of a uniform chromospheric field on the solar p- and f-modes (for the cases $T_c = T_p$, $B_c \neq 0$ and $T_c \neq T_p, B_c = 0$). Here, the p-modes will be discussed (for all the cases $T_c = T_p$, $B_c \neq 0$; $T_c \neq T_p, B_c = 0$ and $T_c \neq T_p$, $B_c \neq 0$).

The dispersion relation (3.44) can be written in the dimensionless form

$$2a\kappa\Omega^2 \frac{U\left(-a+1, m+3, 2\kappa\right)}{U\left(-a, m+2, 2\kappa\right)} + (m+1)\Omega^2 - \kappa(1+\Omega^2)$$

$$= \left(\frac{T_c}{T_p}\right) \frac{\gamma\Lambda\left(\Lambda\Omega^2 - \kappa\right)(1-\Omega^4)}{\Gamma\left[\Lambda + \phi\left(\frac{1+\beta}{\beta}\right)\left(\Lambda\Omega^2 - \frac{\kappa}{1+\beta}\right)\right]}, \tag{3.45}$$

where

$$\kappa = k_x z_o\,, \quad \Omega^2 = \frac{\omega^2}{g k_x}\,, \quad \beta = \frac{c_{sc}^2}{v_{Ac}^2}\,, \quad \Lambda = \frac{m+1}{\gamma}\frac{c_{sp}^2}{c_{sc}^2}\,, \quad \Gamma = \frac{2\gamma\beta}{\gamma+2\beta}\,,$$

$$\phi = \left\{1 - \beta\Omega^2 \frac{\left[1 + \frac{\gamma-1}{\gamma}\frac{1}{\Omega^2} + \frac{\Omega^2}{\gamma}\right]}{\left[\frac{2\kappa}{\gamma\Lambda} + 1\right]\left[\Omega^2 - \frac{\kappa}{\Lambda}\right]} \frac{F\left(p+1, q+1; r+1; \frac{-\mathcal{A}_1}{\mathcal{A}_2}\right)}{F\left(p, q; r; \frac{-\mathcal{A}_1}{\mathcal{A}_2}\right)}\right\}\,,$$

$$2p\,, 2q = \left(\frac{2\kappa}{\gamma\Lambda} + 1\right) \mp \left\{1 - \frac{4\kappa}{\Omega^2\gamma^2\Lambda}\left[(\gamma-1) + \Omega^2\left(\Omega^2 - \frac{\kappa}{\Lambda}\right)\right]\right\}^{1/2}\,,$$

$$r = \frac{2\kappa}{\gamma\Lambda} + 1\,, \qquad -\frac{\mathcal{A}_1}{\mathcal{A}_2} = -\frac{\Omega^2\beta}{\left(\Omega^2 - \frac{\kappa}{\Lambda}\right)}\,. \tag{3.46}$$

The p-mode frequencies in the presence of a magnetic field and at a particular temperature can be found by solving Equation (3.44) using suitable values of the relevant parameters. Sections 3.3 and 3.4 describe some such developments.

3.3 Asymptotic Solutions To The Dispersion Relation

3.3.1 Solutions for field-free case in the limit as $\kappa \to 0$

The theoretical p-mode frequency shifts for this model can be found by solving Equation (3.44) numerically if the values for all the parameters are supplied. However, additional information can be found out about the solutions to Equation (3.44) by considering several particular limiting cases of the Equation. One such case is the limit that $\kappa(= k_x z_o)$ tends to zero, i.e., the horizontal wavenumber becomes much smaller than z_o^{-1}. The advantage of this (asymptotic) method is that expansions of equations can be solved algebraically to give the frequency shift. Information gained by such an approach can be used to determine which aspects of the modes are of most interest in the numerical solutions (presented in Section 3.4).

An interesting preliminary case to examine is that of a field-free atmosphere. It should be noted that simply setting $B_c = 0$ (and so $v_{Ac} = 0$) in dispersion relation (3.44) does not give the desired dispersion relation since the relevant value for $\mathcal{A}_2$ (see Equation (3.14)) causes ξ to become infinite which is a singularity of Equation (3.16). However, it is still possible to obtain the dispersion relation for the field-free case by taking the limit $\beta \to \infty$ (i.e. $B_c \to 0$) in Equation (3.45) (see Appendix A3, Section 3). Alternatively, the dispersion relation for the field-free case can be obtained by adopting the same method as presented in Section 3.2 but with $B_c = 0$ throughout the calculations. By considering an isothermal atmosphere with $B_c = 0$, the governing Equation (3.12) reduces to

$$\frac{d}{dz}\left\{\frac{\rho_o\omega^2}{(\omega^2 - k_x^2c_s^2)}\frac{dv_z}{dz}\right\} = \left\{\frac{\rho_o g^2 k_x^2}{(\omega^2 - k_x^2c_s^2)} - \rho_o\omega^2 - gk_x^2\frac{d}{dz}\left(\frac{\rho_o c_s^2}{(\omega^2 - k_x^2c_s^2)}\right)\right\}v_z\,, \quad (3.47)$$

which can be arranged into the form

$$\frac{d^2v_z}{dz^2} + \frac{1}{H_c}\frac{dv_z}{dz} + \mathcal{A}v_z \;=\; 0\,, \qquad z < 0\,, \quad (3.48)$$

where

$$\mathcal{A} \;=\; \left(\omega^2 - k_x^2c_s^2\right) + \frac{(\gamma-1)g^2k_x^2}{\omega^2}\,. \quad (3.49)$$

Equation (3.48) has a solution

$$v_z \;=\; C_1 \exp\frac{z}{2H_c}\left[-1+\left(1-4\mathcal{A}H_c^2\right)^{1/2}\right], \qquad z<0\,. \tag{3.50}$$

Matching (3.50) and (3.42) at the interface $z = 0$ and imposing the boundary condition that

$$\left\{\frac{\rho_o c_s^2\omega^2}{(\omega^2-k_x^2c_s^2)}\right\}\frac{dv_z}{dz}+\left\{\frac{gk_x^2\rho_o c_s^2}{(\omega^2-k_x^2c_s^2)}\right\}v_z \tag{3.51}$$

be continuous at the interface $z = 0$ gives the dispersion relation for a field-free case. In dimensionless form, the dispersion relation for a field-free atmosphere is given by (see also Campbell and Roberts, 1989; Evans and Roberts, 1990)

$$2a\frac{U(-a+1,m+3,2\kappa)}{U(-a,m+2,2\kappa)} = -\frac{(m+1)}{\kappa}+\frac{\Omega^2+1}{\Omega^2}+\frac{(m+1)(\wedge\Omega^2-\kappa)(1-\Omega^4)}{\gamma\ X\ \Omega^2}, \tag{3.52}$$

where

$$X = \wedge\kappa+\frac{\gamma\wedge^2\Omega^2}{2}\left[-1+\left\{1-\frac{4\kappa}{\gamma^2\wedge}\left[\frac{(\gamma-1)+\Omega^2(\Omega^2-\frac{\kappa}{\wedge})}{\Omega^2}\right]\right\}^{1/2}\right]. \tag{3.53}$$

(Equation (3.46) gives the definitions of κ, Ω^2 and $\wedge$.)

The expansion of the right-hand side of Equation (3.52) in a Taylor series in κ gives (see Appendix A3, Section 4)

$$\text{rhs. of Equation}(3.52) = 1 \;-\; \frac{a_8\,\Omega^8+a_4\,\Omega^4+\,a_0}{\Omega^2(\Omega^4-1)} \;+\; O(\kappa)\,, \tag{3.54}$$

where

$$a_8=\frac{(m+1)}{\gamma^2\wedge}\,, \quad a_4=-1+2(\gamma-1)a_8\,, \quad a_0=1\;+\;\frac{(m+1)}{\wedge}\frac{(1-2\gamma)}{\gamma^2}\,,$$

$$O(\kappa)=\left[\frac{a_8\,\Omega^8+\left(a_4+1-\frac{(m+1)}{\wedge}\right)\,\Omega^4+\left(a_0-1+\frac{(m+1)}{\wedge}\right)}{\wedge(m+1)\Omega^4(\Omega^4-1)^2}\right]\times$$

$$\left\{\wedge\left(1-\Omega^4\right)\left(\Omega^2+1\right)-1+\frac{(a_8\,\Omega^8+a_4\,\Omega^4+\,a_0)}{\Omega^2\,(\Omega^4-1)}\right\}\kappa\,. \tag{3.55}$$

Thus, Equation (3.52) gives

$$2a\frac{U\left(-a+1,m+3,2\kappa\right)}{U\left(-a,m+2,2\kappa\right)} = 1 \; - \; \frac{a_8\,\Omega^8 + a_4\,\Omega^4 + \; a_0}{\Omega^2(\Omega^4-1)} \; + \; O(\kappa)\,. \tag{3.56}$$

Using the identity (Abramowitz and Stegun, 1965; p.504)

$$U(a,b,z) = \frac{\pi}{\sin\pi b}\left[\frac{M(a,b,z)}{\Gamma(1+a-b)\Gamma(b)} - z^{(1-b)}\frac{M(1+a-b,2-b,z)}{\Gamma(a)\Gamma(2-b)}\right], \tag{3.57}$$

the left-hand side of Equation(3.56) becomes

$$2a\frac{U\left(-a+1,m+3,2\kappa\right)}{U\left(-a,m+2,2\kappa\right)} = -\frac{(m+1)}{\kappa}\left\{\frac{M(-1-a-m,-m-1,2\kappa)-\mathcal{M}_2}{M(-1-a-m,-m,2\kappa)-\mathcal{M}_4}\right\}, \tag{3.58}$$

where

$$\mathcal{M}_2 \;=\; (2\kappa)^{(m+2)}\frac{M(1-a,m+3,2\kappa)\Gamma(1-a)\Gamma(-m-1)}{\Gamma(-a-m-1)\Gamma(m+3)}\,, \tag{3.59}$$

$$\mathcal{M}_4 \;=\; (2\kappa)^{(m+1)}\frac{M(-a,m+2,2\kappa)\Gamma(-a)\Gamma(-m)}{\Gamma(-a-m-1)\Gamma(m+2)}\,. \tag{3.60}$$

Here, it must be assumed that m is not an integer although this assumption has no significance from a physical point of view.

From Equation (3.56),

$$2a\frac{U\left(-a+1,\;m+3,\;2\kappa\right)}{U\left(-a,\;m+2,\;2\kappa\right)} \text{ is finite as } \kappa \to 0\,.$$

But, from Equation (3.58), it would seem that

$$2a\frac{U\left(-a+1,\;m+3,\;2\kappa\right)}{U\left(-a,\;m+2,\;2\kappa\right)} \to \infty \text{ as } \kappa \to 0\,.$$

So, for compatibility with Equation (3.56) it is necessary that $(2\kappa)^{(m+1)}\Gamma(-a) \to \infty$ as $\kappa \to 0$ (see Equations (3.58) and (3.60)). This requires that

$$a \to n-1\,, \qquad n = 1,2,3,... \tag{3.61}$$

Consider the special case of adiabatic stratification. Then, from Equations (3.37) and (3.38)

$$2a \;=\; -(m+2) \;+\; m\Omega_*^2\,, \tag{3.62}$$

where it is assumed that $\Omega^2 \to \Omega_*^2$ and that $\Omega_*^2 \neq 0$ as $\kappa \to 0$. Solutions $\Omega_*^2 = 0$, representing gravity modified surface waves are not of concern here.

Thus,

$$2(n\;-\;1) \;\sim\; -(m\;+\;2) \;+\; m\Omega_*^2\,, \tag{3.63}$$

and so

$$\Omega_*^2 \;\sim\; 1 \;+\; \frac{2n}{m}\,, \quad n = 1,2,3,... \tag{3.64}$$

These are the p-modes. Here $\Omega_*^2 = \omega_*^2/gk_x$ and so the cyclic frequency $\nu_*(=\omega_*/2\pi)$ is referred to as the 'mode frequency'.

In order to obtain the first order correction to (3.64), set

$$\Omega^2 \;\sim\; \Omega_*^2 \;+\; \delta_o(2\kappa)^s\,, \tag{3.65}$$

with s and δ_o to be determined. Using Equations (3.37), (3.38) and (3.65)

$$a \;\sim\; -\frac{(m+2)}{2} \;+\; \frac{m(\Omega_*^2 + \delta_o\,(2\kappa)^s)}{2}\,. \tag{3.66}$$

But from Equation (3.63)

$$(n\;-\;1) \;\sim\; -\frac{(m+2)}{2} \;+\; \frac{m\Omega_*^2}{2}\,, \tag{3.67}$$

and so

$$a \sim n - 1 + \frac{m}{2}\,\delta_o\,(2\kappa)^s\,. \tag{3.68}$$

Using the Reflection formula for the gamma function (Abramowitz and Stegun, 1965; p.256)

$$\Gamma(z)\Gamma(1-z) = \frac{\pi}{\sin(\pi z)}\,, \quad (0 < Re(z) < 1)\,, \tag{3.69}$$

$\Gamma(-a)$ becomes

$$\Gamma(-a) \sim \frac{\pi}{\sin(-\pi a)\Gamma(1+a)}\,. \tag{3.70}$$

Also, by using (3.68), Equation (3.70) may be written as

$$\Gamma(-a) \sim \frac{\pi}{\sin(-\pi a)\Gamma(n)}\,. \tag{3.71}$$

Now, substituting $\delta = (2\kappa)^s\delta_o$,

$$\begin{aligned}
\sin(\pi a) &\sim \sin\left\{\pi(n-1) + \frac{\pi m\delta}{2}\right\} \\
&= \sin\pi(n-1)\cos\left(\frac{\pi m\delta}{2}\right) + \cos\pi(n-1)\sin\left(\frac{\pi m\delta}{2}\right) \\
&= \cos\pi(n-1)\sin\left(\frac{\pi m\delta}{2}\right) \\
&\sim (-1)^{(n-1)}\frac{\pi m\delta}{2}\,, \qquad \text{(since } \delta \text{ is small)}\,.
\end{aligned} \tag{3.72}$$

Thus, in terms of δ_o, $\Gamma(-a)$ can be written as

$$\Gamma(-a) \sim \frac{2(-1)^n(2\kappa)^{-s}}{m\;\delta_o\;\Gamma(n)} \text{ as } \kappa \to 0. \tag{3.73}$$

Equation (3.56) combined with (3.58) now reads as

$$(\kappa)\left\{1 - \frac{a_8\Omega_*^8 + a_4\Omega_*^4 + a_0}{\Omega_*^2(\Omega_*^4 - 1)}\right\} + O(\kappa^2) \sim -(1+m)\left[\frac{\mathcal{D}_1 - (2\kappa)^{(m+2)}\mathcal{D}_2(-a)\Gamma(-a)}{\mathcal{D}_3 - (2\kappa)^{(m+1-s)}\mathcal{D}_4\Gamma(-a)}\right]$$

$$\sim -(1 + m)\left[\frac{\mathcal{D}_1 + (2\kappa)^{(m+2-s)}\mathcal{D}_2\, a\, \mathcal{G}}{\mathcal{D}_3 - (2\kappa)^{(m+1-s)}\mathcal{D}_4\mathcal{G}}\right] , \quad (3.74)$$

where the following have been used:

$$\Gamma(-a) \sim \frac{2(-1)^n(2\kappa)^{-s}}{m\ \delta_o\ \Gamma(n)} = \mathcal{G}(2\kappa)^{-s} , \quad (3.75)$$

$$\mathcal{D}_1 = M(-1-a-m,-m-1,2\kappa) , \quad \mathcal{D}_2 = \frac{M(1-a,m+3,2\kappa)\Gamma(-m-1)}{\Gamma(-a-m-1)\Gamma(m+3)} ,$$

$$\mathcal{D}_3 = M(-1-a-m,-m,2\kappa) , \quad \mathcal{D}_4 = \frac{M(-a,m+2,2\kappa)\Gamma(-m)}{\Gamma(-a-m-1)\Gamma(m+2)} . \quad (3.76)$$

Thus, the choice $s = m + 2$, provided that m is not an integer, gives

$$(2\kappa)^{(m+1-s)}\mathcal{G} \sim \mathcal{G}(2\kappa)^{-1} , \quad (3.77)$$

and (3.74) (on noting that $\mathcal{D}_4\mathcal{G}(2\kappa)^{-1} \gg \mathcal{D}_3$) reads as

$$(\kappa)\left\{1 - \frac{a_8\ \Omega_\star^8 + a_4\ \Omega_\star^4 + a_0}{\Omega_\star^2(\Omega_\star^4 - 1)}\right\} + O(\kappa^2) = (1+m)\frac{\mathcal{D}_1 + \mathcal{D}_2\ a\ \mathcal{G}}{\mathcal{D}_4\mathcal{G}}(2\kappa) . \quad (3.78)$$

This then gives the unknown δ_o, the correction due to a field-free isothermal atmosphere as (see Appendix A3, Section 5)

$$\delta_o = \frac{-\Gamma(1+m+n)}{m\ (m+1)\ \Gamma(n)\ \Gamma(m+1)\Gamma(m+2)}\left[\frac{(a_8\ \Omega_\star^8 + a_4\ \Omega_\star^4 + a_0)}{\Omega_\star^2(\Omega_\star^4 - 1)} - \frac{m\ \Omega_\star^2}{(m+2)}\right] . \quad (3.79)$$

Returning to Equation (3.65),

$$\Omega^2 \sim \Omega_*^2 - \frac{\Gamma(1+m+n)}{m(m+1)\Gamma(n)\Gamma(m+1)\Gamma(m+2)}$$

$$\times \left[\frac{(a_8\Omega_*^8 + a_4\Omega_*^4 + a_0)}{\Omega_*^2(\Omega_*^4 - 1)} - \frac{m\Omega_*^2}{(m+2)}\right](2\kappa)^{m+2}. \tag{3.80}$$

Thus, the correction to Ω^2 depends upon κ^{m+2}.

In terms of temperatures T_p and T_c, the constants a_8, a_4 and a_o are given as follows:

$$a_8 = \frac{1}{\gamma}\frac{T_c}{T_p}\,, \qquad a_4 = 2\frac{T_c}{T_p}\left(1 - \frac{1}{\gamma}\right) - 1\,, \qquad a_o = \frac{T_c}{T_p}\left(\frac{1}{\gamma} - 2\right) + 1\,. \tag{3.81}$$

On assuming $T_p = T_c$, the constants a_8, a_4 and a_o reduce to

$$a_8 = \frac{1}{\gamma}\,, \qquad a_4 = 1 - \frac{1}{\gamma}\,, \qquad a_o = \frac{1}{\gamma} - 1\,, \tag{3.82}$$

giving a thermally independent correction in the absence of a magnetic field. Since the thermal effects are an important concern of this chapter, it is Equation (3.80) and the coefficients a_8, a_4 and a_o given by (3.81) that will be considered for further discussion. Equation (3.80) with coefficients given by Equation (3.82) was obtained by Campbell and Roberts (1989) when they examined the field-free limit of a magnetic chromosphere. It may be observed from Equation (3.80) that all the p-modes suffer a frequency decrease as T_c increases in the absence of a magnetic field (a decrease caused by there being an isothermal atmosphere (in $z < 0$)).

It is of interest to consider the behaviour of higher order frequencies in the limit $n \to \infty$ (see also Evans and Roberts, 1992; Evans, 1991). This can be done by fixing ω_*^2 and expressing n as a function of k_x as follows:

$$n = \frac{m}{2}\left(\frac{\omega_*^2}{gk_x} - 1\right)\,. \tag{3.83}$$

After some algebra, Equation (3.79) can be written as (see Appendix A3, Section 6)

$$\delta_o \sim -\frac{2}{(m+1)m^2\Gamma(m+1)\Gamma(m+2)}\left(\frac{m\omega_*^2 z_o}{g}\right)^{m+2}\left(a_8 - \frac{m}{m+2}\right)\,. \tag{3.84}$$

Thus, in the limit of large n with $\kappa \to 0$, the cyclic frequency ν of p-modes in the presence of a field-free atmosphere is given by

$$\nu \sim \nu_* - \frac{\left(a_8 - \frac{m}{m+2}\right)}{4\pi^2 \nu_* (m+1) m^2 \Gamma(m+1)\Gamma(m+2)} \left(\frac{4\pi^2 m \nu_*^2 z_o}{g}\right)^{m+2} \left(\frac{g\ l}{R_{sun}}\right) , \quad (3.85)$$

where,

$$\nu = \frac{\omega}{2\pi} , \qquad \nu_* = \frac{\omega_*}{2\pi} , \qquad k_x \sim \frac{l}{R_{sun}} ; \quad (3.86)$$

and l is the degree and R_{sun} is the radius of the Sun.

It should be noted that the term $a_8 - \frac{m}{m+2}$ is always positive when $T_c > T_p$. Thus in a field-free atmosphere, p-mode frequencies are less than the mode frequencies given by Equation (3.64) (this shift being due to the non-zero temperature of the atmosphere). In the limiting case where the order n becomes large, the discrepancy varies as a power function of frequency. It is also interesting to note from Equation (3.85) that $\nu - \nu_* \propto l$ i.e. the frequency shift is proportional to the degree l.

3.3.2 Solutions for the field inclusive case in the limit as $\kappa \to 0$

More general than a field-free atmosphere, is an atmosphere containing a magnetic field. This subsection is concerned with carrying out an asymptotic analysis for such an atmosphere. To find the asymptotic solutions for this case, it is necessary to examine the dimensionless dispersion relation (3.45) in the limit $\kappa \to 0$.

Once again it will be assumed, as in subsection (3.3.1), that $\Omega^2 \to \Omega_*^2$ and $\Omega_*^2 \neq 0$ as $\kappa \to 0$. Thus, it is clear from Equation (3.46) that as $\kappa \to 0$

$$p \to 0 , \qquad q \to 1 , \qquad r \to 1 , \qquad -\frac{\mathcal{A}_1}{\mathcal{A}_2} \to -\beta ,$$

and so

$$\phi \to 1 - \beta \left\{ 1 + \left(\frac{\gamma - 1}{\gamma}\right) \frac{1}{\Omega_*^2} + \frac{\Omega_*^2}{\gamma} \right\} \frac{F(1,2;2;-\beta)}{F(0,1;1;-\beta)} . \quad (3.87)$$

On noting the special case of the hypergeometric function (Abramowitz and Stegun, 1965; p.556)

$$F(\alpha, \beta; \beta; z) \;=\; (1-z)^{-\alpha}\,, \tag{3.88}$$

Equation (3.87) becomes

$$\phi \rightarrow \frac{1 - \left(\frac{\gamma-1}{\gamma}\right)\frac{\beta}{\Omega_\star^2} - \beta\frac{\Omega_\star^2}{\gamma}}{\beta+1} \quad \text{as} \quad \kappa \rightarrow \;\; 0\,. \tag{3.89}$$

Thus, the right hand side of the dispersion relation (3.45) is given by

$$\text{rhs. of Equation(3.45)} = \left(\frac{T_c}{T_p}\right)\frac{\gamma^2\beta \wedge \Omega_\star^2(1-\Omega_\star^4)}{\Gamma\left[\beta(1-\Omega_\star^4)+\gamma\Omega_\star^2\right]}\,, \quad \text{as} \quad \kappa \rightarrow \;\; 0\,. \tag{3.90}$$

Noting that the asymptotic behaviour of the confluent hypergeometric U- function is given by (Abramowitz and Stegun, 1965; p.508)

$$U(a,b,z) \sim \frac{\Gamma(b-1)}{\Gamma(a)} z^{1-b}\,, \quad z \rightarrow 0\,, \tag{3.91}$$

the left hand side of the dispersion relation (3.45) reduces to zero in the limit as $\kappa \rightarrow 0$, provided $(-a)$ does not tend to 1, 0, or any negative integer. Then, given this priviso,

$$\left(\frac{T_p}{T_c}\right)\frac{\gamma^2\beta \wedge \Omega_\star^2(1-\Omega_\star^4)}{\Gamma\left[\beta(1-\Omega_\star^4)+\gamma\Omega_\star^2\right]} \;=\; 0\,. \tag{3.92}$$

The solutions to Equation (3.92) are $\Omega_\star^2 = 0, \pm 1$. The solution $\Omega_\star^2 = 0$ is not allowed as it violates the basic assumption at the beginning of the subsection; $\Omega_\star^2 = -1$ gives complex roots which are not of interest here. The only interesting solution, then, is $\Omega_\star^2 = 1$ which would mean $a = -1$. The solution $\Omega_\star^2 = 1$ is the f-mode. The analysis for the f-modes will not be taken further as our main concern here lies with the p-modes.

It is then interesting to consider the remaining cases, $a \rightarrow 0, 1, 2, 3, ...$, i.e. $a \rightarrow n-1$ where $n = 1, 2, 3, ...$ For the special case of adiabatic stratification a is given by Equation (3.62) and so

$$n - 1 \;\sim\; -\frac{(m+2)}{2} + \frac{m\Omega_\star^2}{2}\,. \tag{3.93}$$

Hence

$$\Omega_\star^2 \;\sim\; 1 + \frac{2n}{m}\,, \qquad n = 1, 2, 3...\,, \tag{3.94}$$

a result also obtained in subsection (3.3.1). These are the p-modes. The solutions given by (3.94) must give a non-contradictory statement for the limit of the dispersion relation. It is thus necessary to expand the left hand side of the dispersion relation (3.45) for a small κ, as in Equation (3.58), and examine the case $a \rightarrow 0, 1, 2, 3, ...$

Once again, consider

$$\Omega^2 \sim \Omega_\star^2 + \delta_b (2\kappa)^s , \tag{3.95}$$

where s and δ_b are as yet to be determined. Then

$$a \sim (n-1) + \frac{m}{2}\delta_b (2\kappa)^s . \tag{3.96}$$

Thus, in terms of δ_b,

$$\Gamma(-a) \sim \frac{2(-1)^n (2\kappa)^{-s}}{m\ \delta_b\ \Gamma(n)} \equiv \mathcal{H}(2\kappa)^{-s} , \tag{3.97}$$

and

$$-(1+m)\left[\frac{\mathcal{D}_1 + (2\kappa)^{(m+2-s)}\mathcal{D}_2 a\mathcal{H}}{\mathcal{D}_3 - (2\kappa)^{(m+1-s)}\mathcal{D}_4\mathcal{H}}\right] = \left(\frac{T_c}{T_p}\right)\frac{\gamma^2\beta \wedge (1-\Omega_\star^4)}{\Gamma\left[\beta(1-\Omega_\star^4) + \gamma\Omega_\star^2\right]} - (m+1). \tag{3.98}$$

This then determines δ_b, the correction due to the presence of a magnetic atmosphere, valid for small κ, which is given by (see Appendix A3, Section 7; see also Evans and Roberts, 1992)

$$\delta_b = \frac{2\Gamma(m+n+1)\gamma\left(1-\Omega_\star^4-2\Omega_\star^2\right)}{m\Gamma(n)\Gamma(m+1)\Gamma(m+2)(2\beta+\gamma)(1-\Omega_\star^4)} . \tag{3.99}$$

Substituting δ_b into Equation (3.95) yields

$$\Omega^2 \sim \Omega_\star^2 + \frac{2\Gamma(m+n+1)\gamma\left(1-\Omega_\star^4-2\Omega_\star^2\right)}{m\Gamma(n)\Gamma(m+1)\Gamma(m+2)(2\beta+\gamma)(1-\Omega_\star^4)}(2\kappa)^{m+1} . \tag{3.100}$$

It may be noted that Ω^2 here depends upon κ^{m+1} and the frequency of the p-modes suffer an increase due to the presence of a magnetic atmosphere.

Taking the limit $n \to \infty$, and rearranging in terms of cyclic frequency, it can be shown that (see Appendix A3, Section 8)

$$\nu \sim \nu_\star + \frac{\gamma}{4\pi^2 \nu_\star m \Gamma(m+1)\Gamma(m+2)(\gamma+2\beta)} \left(\frac{4\pi^2\ m\ \nu_\star^2 z_o}{g}\right)^{m+1} \left(\frac{g\ l}{R_{sun}}\right) . \quad (3.101)$$

Thus, the presence of a magnetic field causes each p-mode frequency to be greater than it would be in the field-free case, this frequency shift varying as a positive power of the frequency.

3.4 Numerical Solutions

Although the analysis of Section 3.3 gives some useful information about the nature of theoretical frequency shifts, in order to find actual numerical values for such shifts (which can be compared with the observed values) a computational approach must be used to solve Equation (3.44). In this work the computer programs have been written in the language Fortran 77 and make use of double precision arithmetic. The aim is to find a value of ω which satisfies Equation (3.44) when all other quantities are supplied.

The p-modes are the main interest in Equation (3.44). As has been seen, in the absence of an upper atmosphere the frequencies of p-modes in an adiabatically stratified polytropic medium are given by

$$\omega_\star \ \sim \ (gk_x)^{1/2} \left(1 \ + \ \frac{2n}{m}\right)^{1/2} , \quad (3.102)$$

where $n(= 1, 2, 3, \ldots)$, the order of a mode, is the number of nodes of a mode in the vertical, or radial, direction. Equation (3.102) provides a convenient starting point for a numerical search for the modes given by dispersion relation (3.44).

In this investigation, the hypergeometric function has been evaluated by using the integral formula (Abramowitz and Stegun, 1965; p.558)

$$F(p,q;r;Z) \ = \ \frac{\Gamma(r)}{\Gamma(q)\Gamma(r-q)} \int_0^1 t^{q-1}(1-t)^{r-q-1}(1-Zt)^{-p} dt,$$

$$(Re(r) > Re(q) > 0) . \quad (3.103)$$

The quantities q and r (together with all other variables, parameters, etc.) are assumed to be real. This integral is evaluated by means of the NAG Fortran Library,

Mark 14. The confluent hypergeometric function U is evaluated by using the routine written by Temme (1983). This is a very reliable routine and is written in Pascal language. The fortran interface for this was supplied by courtesy of Mr. A. Macdonald. Finally, it is desirable to assign a suitable set of parameters for the model to make it resemble the atmospheric structure of the Sun as closely as possible, given the simplicity of the model. The non-availability of precise values for the temperature, pressure, density, polytropic index, etc. and uncertainties in their variation with depth in the Sun, make it difficult to choose parameters which exactly mimic the solar atmosphere. However we are able to use averages of the various parameters from H.S.R.A. (Gingerich et al. 1971) and the chosen values are listed in Table 3.1 (see also Evans and Roberts, 1990). The atmosphere is assumed to be marginally stable, so that $m = 1/(\gamma - 1)$. The spherical harmonic degree l is related to horizontal wavenumber k_x by $k_x = \sqrt{l(l+1)}/R_{sun}$, R_{sun} being the solar radius.

Parameters	Values
T_p	4170K
p_p	86.82 kg $m^{-1}s^{-2}$
γ	1.8
m	1.25
$\mathcal{R}$	6425.97 m^2 s^{-2} K^{-1}
g	274.0 m s^{-2}
R_{sun}	6.96×10^8 m

Table 3.1: Parameters used for the atmospheric model.

In the subsequent subsections, graphs of frequency shift $\Delta\nu$ against frequency are plotted. The procedure employed is as follows. The dispersion relation (3.44) is solved for chosen values of the chromospheric temperature T_c and magnetic field strength B_c (referred to as the 'base temperature' and 'base field strength') and the resulting frequency $\nu(T_c, B_c)$ is known as the 'base frequency'. The dispersion relation is then solved again with the chromospheric temperature T_c' and/or field strength B_c' having been increased from their 'base' value(s). The cyclic frequency thus obtained are referred to as $\nu(B_c', T_c')$. The frequency shift $\Delta\nu$ is the difference between the resulting cyclic frequency and the cyclic base frequency. The graphs which follow show this frequency shift,

$$\Delta\nu \equiv \nu(B_c', T_c') - \nu(B_c, T_c)\ , \tag{3.104}$$

plotted as a function of the base frequency.

3.4.1 Field-free case for arbitrary κ- effects of changing chromospheric temperature

Before the solution of the full dispersion relation (Equation (3.44)) is carried out, the non-magnetic case is considered. In the absence of a magnetic field, the dispersion relation is given by Equation (3.52). Equation (3.52) is solved for various chromospheric temperatures. The objective is to investigate the influence of chromospheric temperature and hence the set of parameters $(T_p, p_p, m, \gamma, z_o)$ describing the convection zone is fixed. The computer program evaluating the cyclic frequency $\nu(=\omega/2\pi)$ of the p-modes has an inbuilt search routine to ensure that the term inside the square root in Equation (3.53) is positive. This corresponds to the solution in the chromosphere $(z < 0)$ being evanescent. If it is negative, then the mode will propagate away to $-\infty$ and no trapping occurs. Thus, there exists a cut-off frequency which separates the modes that propagate from those modes that evanesce. This cut-off frequency is given by

$$1 - \frac{4\kappa}{\gamma^2 \Lambda}\left[\frac{(\gamma-1) + \Omega^2(\Omega^2 - \frac{\kappa}{\Lambda})}{\Omega^2}\right] = 0\,. \tag{3.105}$$

In terms of angular frequency ω this simply gives (for small κ)

$$\omega^2 = \omega_{cut}^2 \equiv \frac{\gamma^2 g^2}{4c_{sc}^2}\,, \tag{3.106}$$

where ω_{cut} is the acoustic cut-off frequency in a field-free isothermal atmosphere (Lamb, 1932). The curves in the following figures stop when they reach such cut-off values.

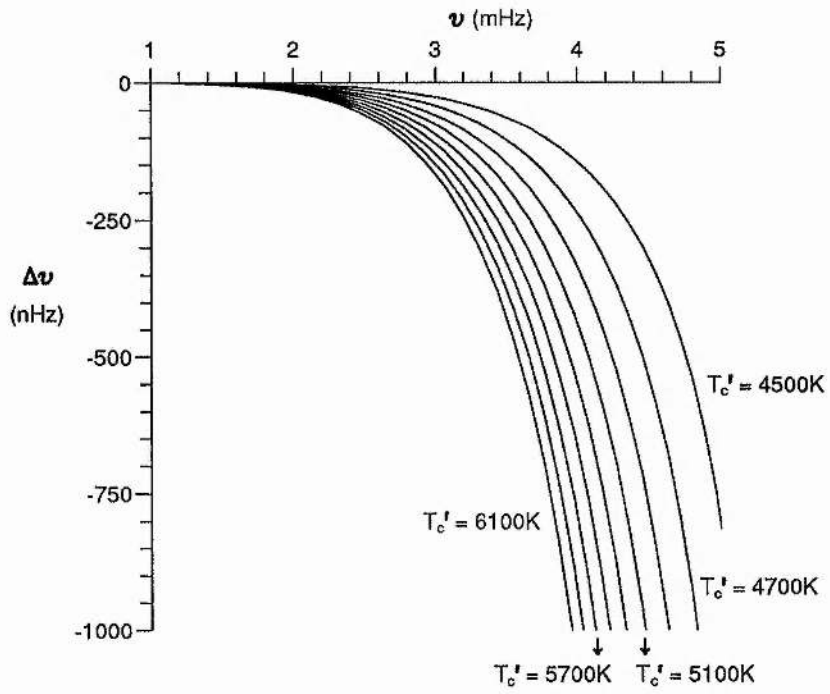

Figure 3.3: The frequency shift $\Delta\nu \equiv \nu(T_c') - \nu(4170K)$ as a function of solar p-mode frequency ν as determined by the dispersion relation (3.44) pertaining to the non-magnetic case. The various curves shown correspond to various chromospheric temperatures (T_c'), ranging from 4500K to 6100K at intervals of 200K. The degree l is set equal to 50. The decrease in frequency shift with mode frequency is consistent with the predictions of Equation (3.80).

Figure 3.3 illustrates the change in cyclic frequency $\Delta\nu$ for several p-modes as a function of base frequency. Here $B_c = B_c' = 0$. The base frequency is calculated for $T_c = T_p = 4170$K. The various curves shown correspond to various chromospheric temperatures T_c' ranging from 4500K to 6100K at intervals of 200K. The degree l is set equal to 50. It is clear that the frequencies of all the p-modes decrease with increasing T_c'. The frequency shift $\Delta\nu$ is almost zero for small frequencies and becomes increasingly negative as the frequency is increased. This is consistent with the findings of the asymptotic formulae (see Equations (3.80) and (3.85)). The modes of higher radial order n and hence higher frequency (since the spherical harmonic degree l is fixed) are very sensitive to changes in chromospheric temperature.

Figure 3.4 displays the effect of changing the degree l of the mode. The chromospheric temperature is now taken to be $T_c' = 5100$K with the base temperature remaining as 4170K. The magnitude of the negative frequency shift $\Delta\nu = \nu(5100K) - \nu(4170K)$ increases with the increasing l. In fact, Equation (3.85) shows that $\Delta\nu \propto l$ as an asymptotic property of the modes at high frequency. The general conclusion from this section is that an increase in the chromospheric temperature decreases the frequencies of p-modes (see also Campbell and Roberts, 1989; Goldreich et. al., 1991; Evans and Roberts, 1991).

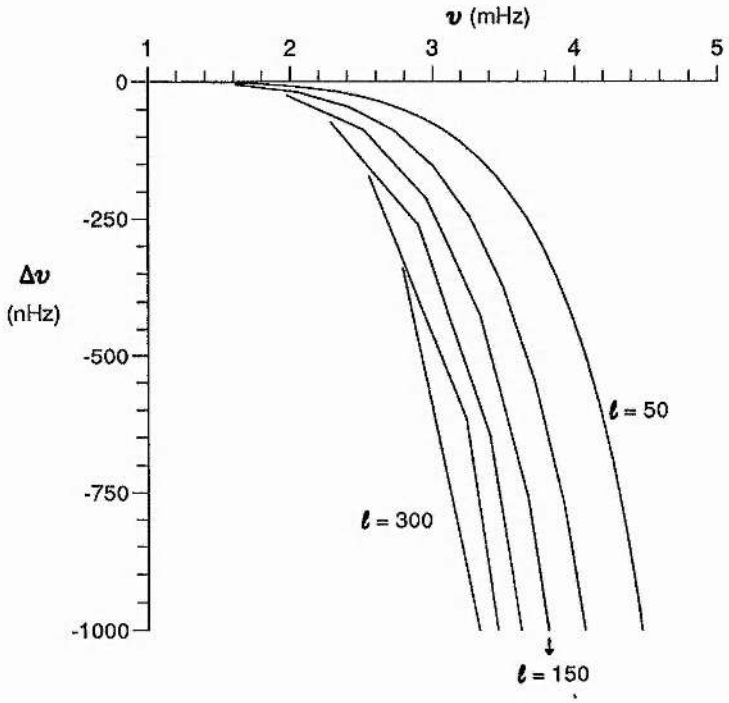

Figure 3.4: The calculated frequency shift $\Delta\nu \equiv \nu(5100K) - \nu(4170K)$ in the absence of a magnetic field for modes of degree $l = 50, 100, .., 300$ as a function of mode frequency ν. For all values of l the shift decreases with mode frequency ν and the magnitude of the frequency shift $\Delta\nu$ increases with increasing l. This is consistent with the asymptotic property of the p-modes calculated for higher order n (see Equation (3.85)).

3.4.2 Field inclusive case for arbitrary κ - effects of changing chromospheric magnetic field

In order to bring out the effects of changing the chromospheric magnetic field strength, the dispersion relation (3.44) is solved numerically. The set of parameters given in Table 3.1 has been used and the solution for a chromospheric temperature $T_c = 4170$K is used as a 'base' frequency. As in the previous subsection, the convection zone is assumed

to be marginally stable. The purpose of the current subsection is to investigate the effects of changes in chromospheric magnetic field strength while the chromospheric temperature remains constant. In practice, the chromospheric temperature is likely to rise as a response to an increase in the local magnetic field strength but this effect will not be considered here as we wish to isolate the effects of changing the magnetic field. The combined effects of increasing both the field strength and the temperature will be discussed in the next section.

Figure 3.5 shows the change in frequency $\Delta\nu = \nu(B_c') - \nu(B_c = 10G)$ when the frequency in the presence of a chromospheric magnetic field $B_c'(= 25G,\ 50G,\ 100G)$ is compared with the frequency when the magnetic field is $10G$. For each value of B_c', $\Delta\nu$ is plotted as a function of the base frequency i.e. the frequency in the presence of a magnetic field of $10G$. The spherical harmonic degree l is set equal to 50. It is clear that the frequency shift increases with an increase in magnetic field strength. This behaviour is to be expected from the asymptotic solutions of the p-modes for small K (see Equations (3.100) and (3.101)).

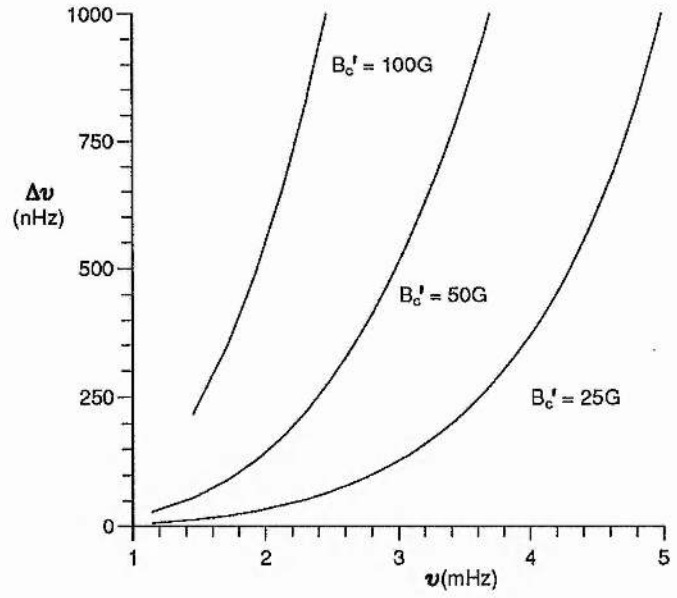

Figure 3.5: The frequency shift $\Delta\nu \equiv \nu(B_c') - \nu(B_c = 10G)$ as a function of solar p-mode frequency ν as determined by Equation (3.44) for three different values of B_c' (= 25G, 50G, 100G). The degree l is set equal to 50. Consistent with the predictions of Equation (3.100), the frequency shift increases with the increase in magnetic field strength.

Figure 3.6 illustrates the effect of varying l. Here, the frequency in the presence of a magnetic field strength of 50G is compared with the frequency when the magnetic field is 10G. The various curves shown represent different values of the degree l. Once again, it can be noted that the magnitude of the frequency shift $\Delta\nu$ increases with increasing l; this is consistent with the asymptotic property of the p-modes calculated for higher order n (see Equation (3.101)). Thus an increase in the magnetic field strength increases the p-mode frequencies, while an increase in chromospheric temperature causes a decrease. Section 3.5 investigates the effect of changing these two quantities simultaneously with a view to reproducing the observed behaviour of the p-modes frequencies.

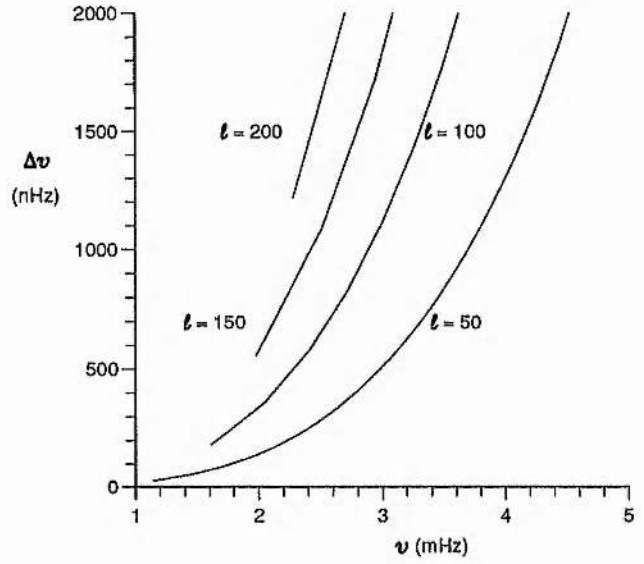

Figure 3.6: The calculated frequency shift $\Delta\nu \equiv \nu(B_c' = 50G) - \nu(B_c = 10G)$ as a function of mode frequency ν for modes of degree $l = 50, 100, .., 200$. For all values of l the shift increases with mode frequency ν and the magnitude of the frequency shift $\Delta\nu$ increases with increasing l; this is consistent with the asymptotic property of the p-modes for higher order n (see Equation (3.101)).

3.5 Comparison with Observations

The observational data provided by Libbrecht and Woodard (1990) and Woodard and Libbrecht (1991) consist of p-mode frequencies for the same set of spherical harmonic degree, l, and radial order, n, but calculated at different epochs, 1986, 1988 and 1989 (1986 was a period of low magnetic activity, while 1988 was a period of substantially increased magnetic activity on the rise to the 1989 solar maximum). They found that the p-mode frequency shifts $\Delta\nu$ between 1986 and 1988, as well as between 1986 and

1989, increased with increasing frequency followed by a drop around $\nu = 3.9$ mHz. It is here speculated that this increase in magnetic activity causes a rise in mean chromospheric magnetic field strength and mean chromospheric temperature.

To compare the numerical predictions of Equation (3.44) with the observational frequency shifts given by Libbrecht and Woodard (1990) and Woodard and Libbrecht (1991) the following procedure has been adopted. The cyclic frequency $\nu(\equiv \omega/2\pi)$ for each mode (n, l) is calculated from Equation (3.44) for a given chromospheric temperature T_c and magnetic field strength B_c. These frequencies are taken as 'base' frequencies for 1986 : $\nu(1986) = \nu(B_c, T_c)$. The calculation is repeated for higher values of chromospheric temperature ($T_c' > T_c$) and magnetic field strength ($B_c' > B_c$) for the same pairs (n, l), and the cyclic frequencies thus obtained are considered as frequencies for 1988 : $\nu(1988) = \nu(B_c', T_c')$. The calculated shift $\Delta\nu$ in cyclic frequency ν between 1986 and 1988 is obtained by taking the difference between these two sets : $\Delta\nu \equiv \nu(1988) - \nu(1986)$. The change in cyclic frequency $\Delta\nu$ between 1986 and 1989 is found in a similar manner: $\nu(1989) = \nu(B_c'', T_c'')$, where $B_c'' > B_c'$ and $T_c'' > T_c'$.

Figure 3.7 shows how the calculated frequency shift $\Delta\nu$ depends on the frequency ν. The chromospheric magnetic field at solar minimum (1986) is taken as $B_c = 40$G and the magnetic field at a time of greater solar activity (1988) as $B_c' = 50$G. The chromospheric temperature at solar minimum is assumed to be $T_c = 4170$K and values of the temperature T_c' (chromospheric temperature at a period of greater solar activity) between 4170K and 6100K are used. The spherical harmonic degree l is set equal to 100. The parameters modelling the field-free zone are as given in Table 3.1.

The aim here is to compare the calculated frequency shifts with the measured frequency shifts between 1986 and 1988, 1989 (Libbrecht and Woodard, 1990; Woodard and Libbrecht, 1991). For all values of the chromospheric temperature T_c', the calculated p-mode frequency shifts begin to increase as a function of frequency ν with an increase in the mean chromospheric magnetic field strength. For lower values of T_c' ($\leq$ 5100K) this increase continues beyond 4mHz; but for higher values of T_c', there comes a frequency where the shift begins to decrease. For $T_c' = 5900$K the turnover in frequency shift occurs at 3.9 mHz, which corresponds well with the observational data. The increase in the frequency shift with mode frequency is consistent with an increase in magnetic field strength while the drop in frequency shift for certain chromospheric temperatures at high frequencies may be evidence of a hotter chromosphere in 1988.

If the same procedure is carried out with $B_c' = B_c = 50$G (i.e. with no change in the chromospheric magnetic field strength) but changing the chromospheric temperature, then negative frequency shifts are found (see Figure 3.8). This suggests that a change in the chromospheric temperature alone cannot reproduce the observed frequency shifts.

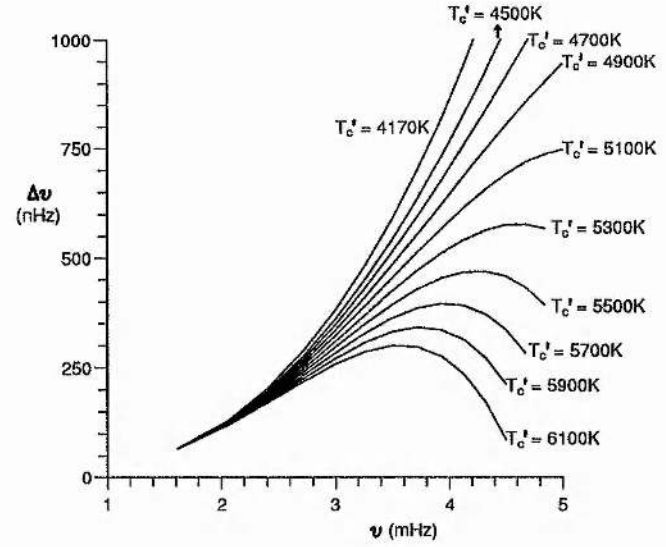

Figure 3.7: The frequency shift $\Delta\nu \equiv \nu(B_c', T_c') - \nu(B_c, T_c)$ as a function of solar p-mode frequency ν as determined by Equation (3.44). The base frequencies $\nu(B_c, T_c)$, corresponding to 1986, are calculated for a chromospheric magnetic field B_c = 40G and a chromospheric temperature T_c = 4170K. The 1988 mode frequencies are calculated by taking the magnetic field strength B_c' to be 50 G. The various curves shown correspond to various chromospheric temperatures (T_c'). The degree l is set equal to 100. The curves stop at atmospheric cut-off frequencies

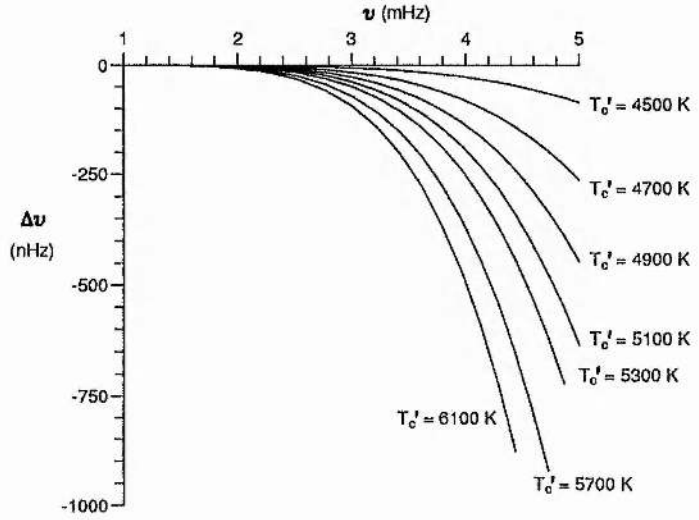

Figure 3.8: As Figure 3.7 but with the same chromospheric magnetic field strengths for 1986 and 1988, i.e. $B_c = B_c'$ = 50 G. The chromospheric base temperature is T_c = 4170K. The negative frequency shifts indicate that a change in chromospheric temperature alone cannot reproduce the observed frequency shifts.

It is interesting to choose $T_c' = 5900$K and investigate the effect of changing the degree l of the mode. The results are shown in Figure 3.9a for values of l between 10 and 140. Included in Figure 3.9a are the observational data points of Libbrecht and Woodard (1990), for the frequency shifts between 1986 and 1988. Libbrecht and Woodard's data points (shown here as crosses ($\times$)) are for frequencies (for $n_{max} = 27$) averaged over l between 5 and 140, to reduce scatter. The calculated frequency shifts show the occurrence of turnover at around 3.7 to 3.9mHz, for all values of l. The magnitude of the frequency shift $\Delta\nu$ increases with increasing l, this being consistent with the findings of Libbrecht and Woodard (1990). Evans and Roberts (1992) show that $\Delta\nu \propto l$ follows from Equation (3.44), with $T_c = T_p$, as an asymptotic property of the modes at high frequency (see also Goldreich et al, 1991).

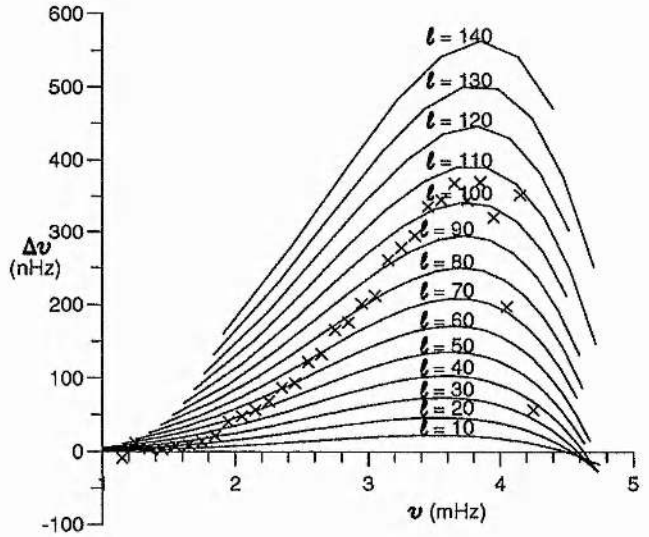

Figure 3.9a: The calculated frequency shift $\Delta\nu \equiv \nu(B_c', T_c') - \nu(B_c, T_c)$ for modes of degree l between 10 and 140. The observational data points (taken from Libbrecht and Woodard, 1990; Woodard and Libbrecht, 1991) are shown as crosses ($\times$) for 1988. For all values of l the shift increases at low frequency before decreasing sharply at around $\nu = 3.7$ to 3.9 mHz. The base frequency $\nu(B_c, T_c)$, representative of 1986, is calculated for $B_c = 40$G and $T_c = 4170$K. The curves are drawn for $B_c' = 50$ G and $T_c' = 5900$ K, corresponding (speculatively) to 1988 data.

To model the frequency changes between 1986 and 1989, values of B_c'' and T_c'' of 55G and 6700K were used. Figure 3.9b shows the results (in a format similar to that for 3.9a); again all curves show a turnover around 3.9 mHz and the magnitude of the frequency shift increases with l.

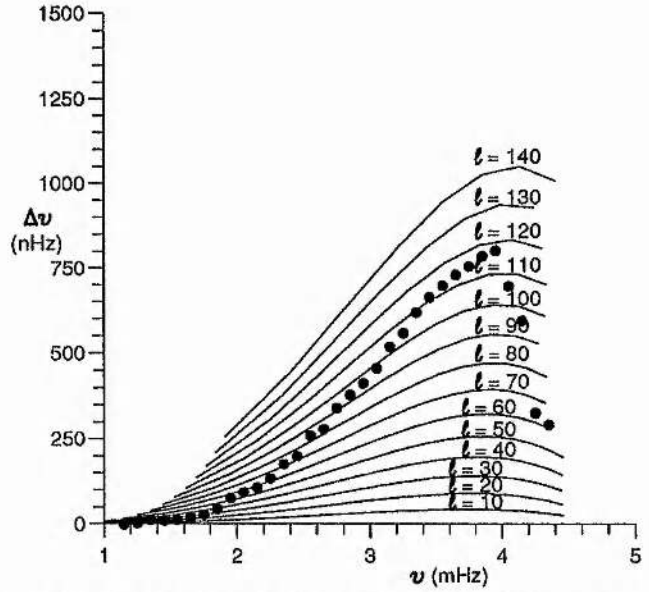

Figure 3.9b: The calculated frequency shift $\Delta\nu$ for modes of degree l between 10 and 140. The observational data points (Libbrecht and Woodard, 1990; Woodard and Libbrecht, 1991) are shown as filled circles (•) for 1989. For all values of l the shift increases at low frequency before decreasing sharply at around $\nu = 3.9$ mHz. The base frequency $\nu(B_c, T_c)$, representative of 1986, is calculated for $B_c = 40$G and $T_c = 4170$K. The curves are drawn for $B_c'' = 55$ G and $T_c'' = 6700$ K, corresponding (speculatively) to 1989 data. Note the change of scale in $\Delta\nu$ between Figures 3.9a and 3.9b.

Finally, Figure 3.10 displays the result of averaging the various curves of Figure 3.9a,b over all values of the degree l between 5 and 140 (for $n = 1 to 27$). This allows a closer comparison with the data points which were also averaged. Figure 3.10a shows the results for 1988, corresponding to Fig. 3.9a; Figure 3.10b is for 1989, corresponding to Fig. 3.9b. The averaged values of the calculated curves agree well with the data for frequencies up to about 3.0 mHz, and reproduce the turnover around $\nu = 3.9$ mHz. However, the calculated curves do not show such a sharp peak as the data points. This may be a consequence of the simplicity of the present model atmosphere. Thus, for both 1988 and 1989, theoretical frequency shift curves have been drawn. These reproduce the general trend of the observed curves.

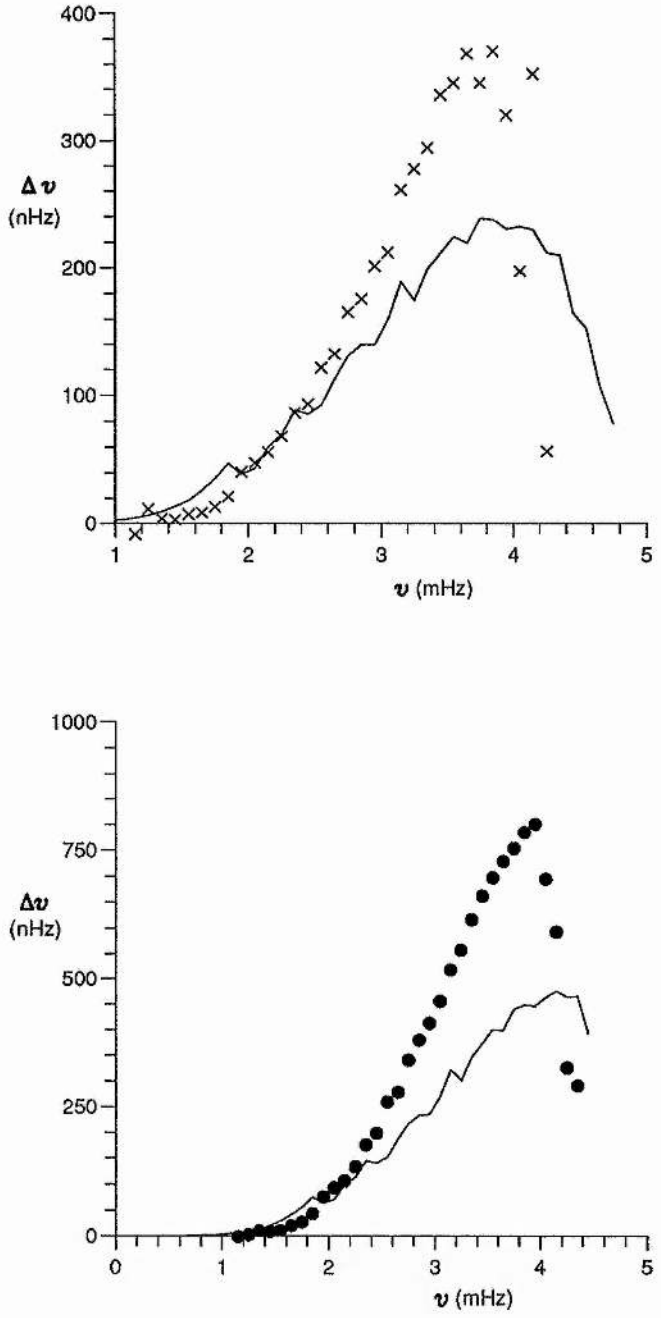

Figure 3.10: As Figure 3.9a,b, but here the calculated frequency shifts are averaged over values of l between 5 and 140. Also shown for comparison are Libbrecht and Woodard's averaged observational data points. Fig. 3.10(a) shows $\Delta\nu$ for 1988 minus 1986 (crosses, $\times$), and Fig. 3.10(b) shows $\Delta\nu$ for 1989 minus 1986 (filled circles, $\bullet$).

3.6 Further Results

As shown in Figure 3.7, the calculated frequency shift curve depends significantly upon the changes in chromospheric magnetic field strengths and chromospheric temperatures between two different epochs. The calculated frequency shifts initially increase as a function of frequency but for higher temperatures T_c' this increase in frequency shift is reversed.

Similar trends are found when magnetic field strengths are considerably lower than those used in Figure 3.7. Figure 3.11a displays the corresponding curves for magnetic field strengths of $B_c = 5G$ and $B_c' = 15G$. The degree l is set equal to 100. For low values of chromospheric temperatures T_c', the frequency shift increases with frequency ν, this increase continuing beyond 4mHz. For higher temperatures ($T_c' \geq 4900K$) the frequency begins to increase as before but a turnover occurs and the frequency shift decreases to reach negative values. It is interesting to note that while the magnitude of the calculated frequency shifts for such temperatures are much less than the observed frequency shifts, the general trend in the curves has been retained.

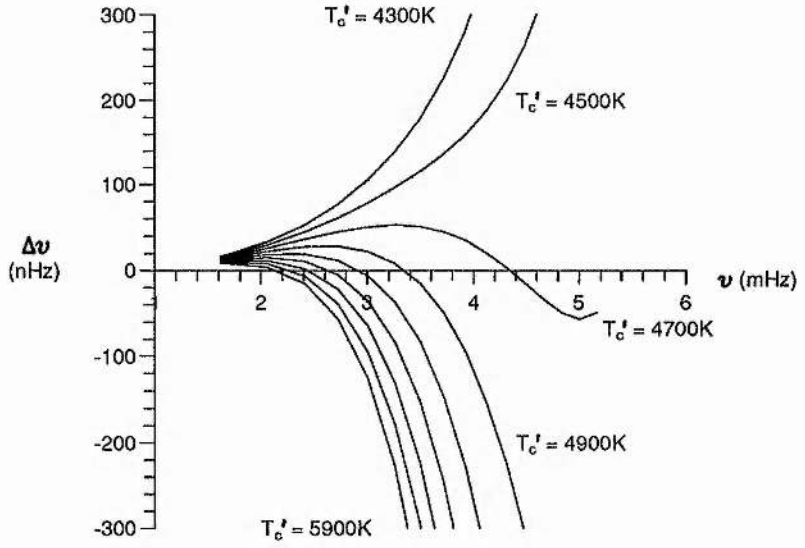

Figure 3.11a: The frequency shift $\Delta\nu \equiv \nu(B_c', T_c') - \nu(B_c, T_c)$ as a function of solar p-mode frequency ν as determined by Equation (3.44). The base frequencies $\nu(B_c, T_c)$ are calculated for a chromospheric magnetic field B_c = 5G and a chromospheric temperature T_c = 4170K. The frequencies $\nu(B_c', T_c')$ are calculated by taking the magnetic field strength B_c' to be 15 G. The various curves shown correspond to various chromospheric temperatures (T_c'). The degree l is set equal to 100.

The curve for $T_c' = 4700K$ is an interesting case and will be studied further. In common with the curves for higher temperatures, the frequency shift decreases after 3.2 mHz but for this particular case the frequency shift rises again after about 4.7 mHz. Figure 3.11b shows the curves for values of T_c' close to 4700K, namely from 4500K to 4900K in steps of 20K. It is seen that the curves for $T_c' = 4640$K to 4720K represent a transition between those calculated frequency shift curves which increase indefinitely ($T_c' \leq 4620K$) and those curves where the frequency shift decreases indefinitely after a turnover ($T_c' \geq 4760K$).

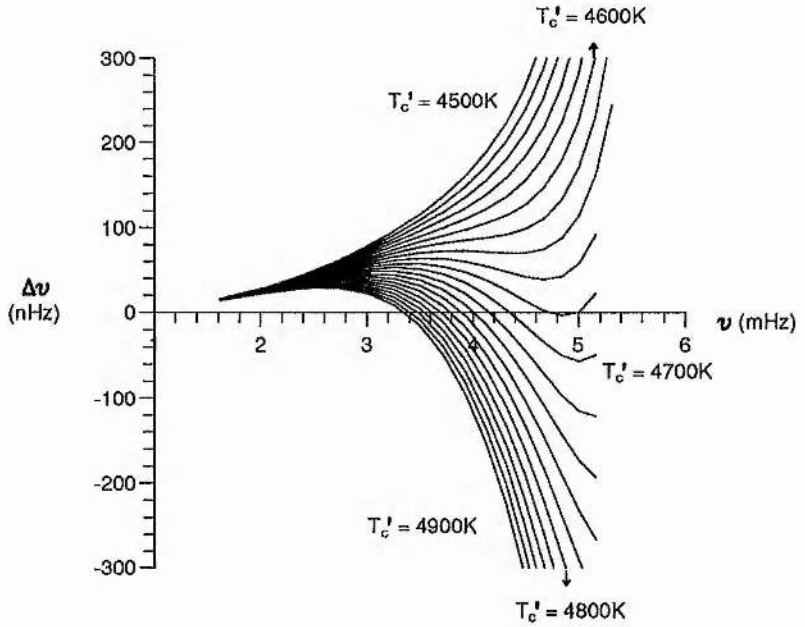

Figure 3.11b: Similar to Figure 3.11a except that the chromospheric temperature T_c' here varies from 4500K to 4860K in steps of 20K. The curve for $T_c' = 4700$K represents a transition between those calculated frequency shift curves which increase indefinitely ($T_c' \leq 4640$K) and those curves where the frequency shift decreases indefinitely after a turnover ($T_c' \geq 4760$K).

It is interesting to note that this late upturn in the frequency shift curves occurs at a frequency which does not vary greatly as degree l is changed. Figure 3.11c concentrates on chromospheric temperature $T_c' = 4700$K but considers different values of l between 50 and 150. For each value of l the frequency shift begins to decrease after about 3.2 mHz but the shift begins to increase again once the frequency reaches about 4.9 mHz. This frequency 4.9 mHz is largely independent of degree l and if the curves of different values of l were to be averaged (as is the case for observed data points) the behaviour of the downturn at 3.2 mHz and an upturn at 4.9 mHz would be retained.

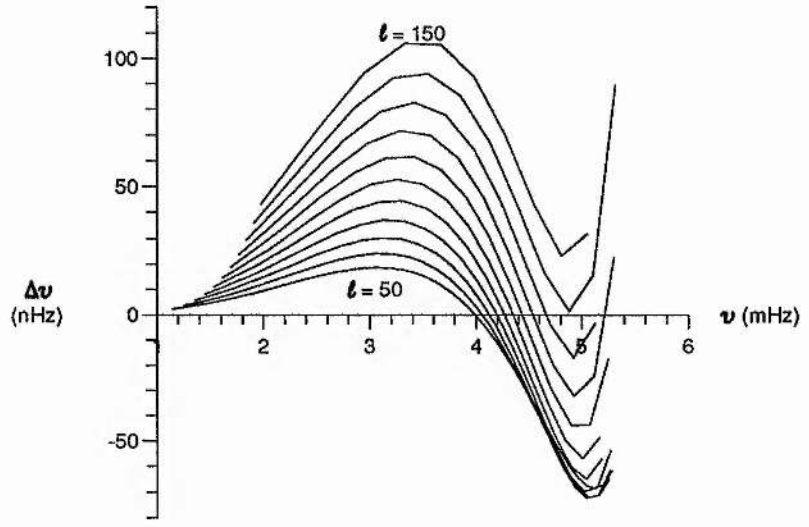

Figure 3.11c: Similar to Figure 3.11b except that the degree l here varies from 50 to 150 in steps of 10. These curves are drawn for $T_c' = 4700$K.

The general conclusion of Figure 3.11 is that the trend of the observed frequency shift curve can be reproduced even by using smaller values of chromospheric magnetic field strengths. For a limited range of chromospheric temperature T_c', the calculated frequency shift curves increase after having decreased.

To date frequency shift curves exhibiting such behaviour have not been observed. However, the upper limit for observed frequencies currently lies at around 4.4 mHz. Many other factors would make observations of this behaviour, difficult, if indeed it occurs in the Sun at all; a late upturn in the frequency shift occurs at frequencies where errors in the observed frequency shift are comparable with the shift themselves. Such errors could easily obscure the existence of a late upturn.

3.7 Discussion

The qualitative behaviour of the observed p-mode frequency shifts has been reproduced by modelling the solar atmosphere as consisting of two distinct layers, an upper isothermal layer containing a uniform horizontal magnetic field and a lower layer being field-free but having a temperature increasing linearly with depth. In particular, the observed turnover at around 3.9mHz in the frequency shift as a function of frequency has been reproduced qualitatively by our models. The turnover in the present model is a consequence of the combined effects of an *increase* in both chromospheric magnetic

field strength and chromospheric temperature. How can one understand the frequency shifts given by this model ? It can be done most simply by considering first the special case $T_c = T_p$. Evans and Roberts (1990, 1992) have been able to obtain analytically the asymptotic behaviour of $\Delta\nu$ as a function of ν and l by examining the behaviour of the dispersion relation (3.44) in the limit of small $k_x z_o$. This limit becomes $lz_o \ll R_{sun}$; with the solar radius as $R_{sun} = 6.96 \times 10^8$m and $z_o = 220$ km this corresponds to $l \ll 3200$, and so all observed data sets satisfy this property. It follows from Equation (3.101) that for large n the frequency shift $\Delta\nu$ satisfies (see also Evans and Roberts, 1992)

$$\frac{\Delta\nu}{\nu} = A_m \left(\frac{B_c'^2 - B_c^2}{2\mu p_p}\right) \left(\frac{\nu}{\nu_c}\right)^{2m} \left(\frac{H_o}{R_{sun}}\right) l \,, \tag{3.107}$$

where

$$A_m = \frac{m+1}{\Gamma(m+1)\Gamma(m+2)} \left(\frac{\gamma m(m+1)}{4}\right)^m \,, \tag{3.108}$$

is positive and $\nu_c = \frac{1}{2\pi}\left(\frac{\gamma g}{4H_o}\right)^{1/2}$ is the cyclic cutoff frequency for an isothermal atmosphere with scale height H_o. Notice the direct proportionality of $\Delta\nu$ with degree l and the change in magnetic pressure (from $B_c^2/2\mu$ at one time to $B_c'^2/2\mu$ at a more active time). Observe too the flat increase in $\Delta\nu$ at low ν given by the power ν^{2m}.

In a similar fashion the frequency shift $\Delta\nu$ due to a change in chromospheric temperature can be considered. In the absence of any magnetic field, Equation (3.85) shows

$$\frac{\Delta\nu}{\nu} = -C_m \left(\frac{\nu}{\nu_c}\right)^{2m+2} \left(\frac{H_o}{R_{sun}}\right) l \,, \tag{3.109}$$

where

$$C_m = \frac{\left(\frac{\gamma m}{2}\right)^{2m+2}}{\gamma(m+1)\Gamma(m+1)\Gamma(m+2)} \left(\frac{T_c' - T_c}{T_p}\right) \,. \tag{3.110}$$

It is clear that $C_m > 0$ if $T_c' > T_c$ and $C_m < 0$ if $T_c' < T_c$ (see Campbell and Roberts, 1989; Evans, 1991 for the special case $T_p = T_c$). Thus, $\Delta\nu$ becomes more negative or less positive with increasing chromospheric temperature and the decline is directly proportional to l.

In Equation (3.107) $\Delta\nu$ is proportional to the frequency raised to the power $2m$. In Equation (3.109) the power increases to $2m + 2$. Hence the frequency increase caused

by magnetic field is expected to dominate at low frequencies, whereas the decrease caused by increasing temperature is expected to dominate for higher frequencies.

Finally, a combination of results (3.107) and (3.109) *suggests* a behaviour in $\Delta\nu$ of the form

$$\frac{\Delta\nu}{\nu} = A_m \left(\frac{\nu}{\nu_c}\right)^{2m} \left(\frac{H_o\, l}{R_{sun}}\right) \left\{ \left(\frac{B_c'^2 - B_c^2}{2\mu p_p}\right) - \left(\frac{\nu^2}{\nu_c^2} D_m\right) \right\}, \qquad (3.111)$$

where D_m is dependent both upon changes in magnetic pressure and on thermal effects; D_m is non-zero even in the absence of a magnetic-field. Equation (3.111) shows that $\Delta\nu$ follows a similar structure to that presented in the numerical results (Figures 3.7-3.10). It should be added, however, that while Equation (3.111) is made plausible by the special cases that lead to Equation (3.107) and (3.109), the complexity of the full dispersion relation (3.44) has hampered a derivation of a result of the form (3.111).

It should be noted that for certain values of the chromospheric temperature, the frequency shift curve shows a late upturn ($\nu > 4.4$ mHz); see Figure 3.11. To explain this behaviour, further orders of the asymptotic solution may be required.

The lack of specific observational evidence for the required rise in chromospheric temperature and the simplicity of the theoretical model combine to make it difficult to determine the precise change in the chromospheric magnetic field strengths and the temperatures that might be causing the frequency shifts in the p-modes. The assumption of adiabaticity is reasonable as a first approximation for the study of the complicated effects of magnetic fields, but the value of adiabatic index γ (and consequently the polytropic index m) is uncertain. In the numerical solutions discussed in Section 3.4, $\gamma = 1.8$ ($m = 1.25$) was used. A slight change in the value of γ changes the values of mode frequencies and the magnitude of the frequency shifts. This is illustrated in Figure 3.12. One further avenue of research would be to relax the assumption of adiabaticity by using standard solar models e.g. Christensen-Dalsgaard's model 1 (see Christensen Dalsgaard, 1991).

With the chromospheric layer having a constant magnetic field, the Alfven speed increases indefinitely with height. This over-estimates the effects of magnetism. It was suggested (Evans and Roberts, 1991) that this drawback may be overcome by considering a three layer model, similar to that discussed here, where the middle layer is permeated by a uniform horizontal magnetic field and the upper layer has a horizontal magnetic field such that the Alfvén speed is constant. Such a model is investigated in Chapter 5. The frequency shifts of the p-modes determined for such a three layer model differ little from the ones found here using the simpler two layer model. Nonetheless, it

is important to progress beyond the simple isothermal magnetic atmosphere discussed here. The relative simplicity of the present model, however, affords one the convenience and insights of an analytical calculation, as embodied in the dispersion relation (3.44) and its subsequent asymptotic reductions. Future developments (largely numerical) which include the non-isothermality of the chromosphere will be needed as more detailed frequency data sets become available for various stages in the solar cycle.

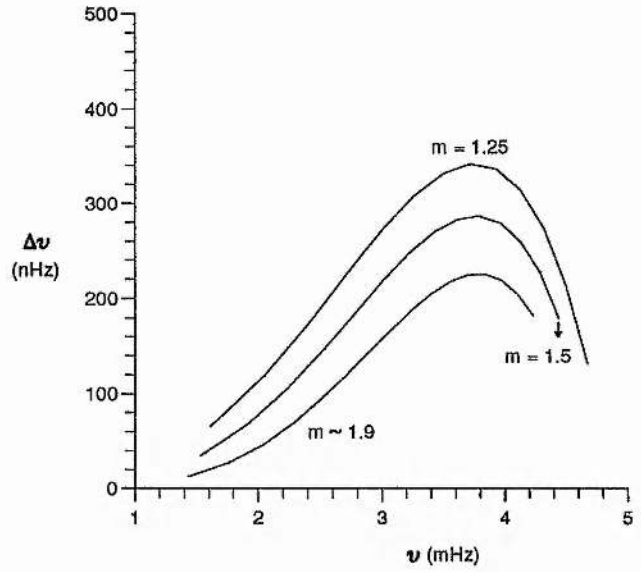

Figure 3.12: The frequency shift $\Delta\nu \equiv \nu(B_c' = 50G, T_c' = 5900K) - \nu(B_c = 40G, T_c = 4170K)$ as a function of solar p-mode frequency ν as determined by dispersion relation (3.44) for various m (= 1.25, 1.5, 1.9). The degree l is set equal to 100. For all three values of m the base frequency is calculated for $B_c = 40$G and $T_c = 4170$K, and the chromospheric temperature T_c' when $B_c' = 50G$ is taken to be $T_c' = 5900$K. A change in the value of m changes the magnitude of the frequency shift.

The chromospheric temperature rises that have been invoked to explain the observed downturn in frequency shifts are as follows: 1700K between 1986 and 1988; 2500K between 1986 and 1989. There is no observational evidence for or against chromospheric temperature changes over the solar cycle. Nonetheless, the changes adduced here are rather large and it may be that a more realistic non-isothermal model atmosphere will allow smaller temperature changes to produce frequency shifts of the observed magnitude.

3.8 Summary

In this *chapter* the p-mode frequency changes have been discussed for a simple model atmosphere. The upper part of the atmosphere is taken to be isothermal, with temperature T_c, within which is embedded a uniform horizontal magnetic field of strength B_c. This region models the chromospheric canopy; the base of the magnetic field is assumed to be at the temperature minimum. The region below the magnetic chromosphere, modelling the convection zone, is assumed to be field-free and to have a temperature $T_p\left(1+\frac{z}{z_o}\right)$ varying linearly with depth z. Here z_o is the temperature scale-height and T_p is the temperature at the top ($z=0$) of this region.

This model of the solar atmosphere gave the possibility of examining, both analytically and numerically, the frequency shifts in p-modes that occur as a result of changes in the magnetic chromosphere. What happens to the frequency of a p-mode if the chromospheric magnetic field strength B_c and the chromospheric temperature T_c change ? In practice, one expects that as the chromospheric field strength increases while the solar cycle progresses from minimum towards maximum, so also will the chromospheric temperature rise, as a response to increasing magnetic activity. But precisely how these changes occur, and what their magnitudes are, is not currently known. Indeed, it may well be that a close monitoring of p-mode frequency shifts over a solar cycle will ultimately provide an answer to this question.

The model atmosphere considered in this *chapter* is the same as that investigated by Evans and Roberts (1990). However, except for the special case of zero magnetic field, Evans and Roberts did not explore the consequences of a change in chromospheric temperature. In the absence of a magnetic field ($B_c=0$), an increase in chromospheric temperature leads to a *decrease* in frequency, and so to a negative frequency shift (see also Campbell and Roberts, 1989; Evans and Roberts, 1990; Goldreich et al., 1991). This is precisely opposite to the observed frequency shift at low ν but suggestive of the observed sharp fall-off at high frequencies. In the presence of a magnetic chromosphere, however, an increase of magnetic field strength, at fixed T_c, leads to an *increase* in frequency and so to a positive frequency shift, in accordance with the observations at low ν (see also Evans and Roberts, 1990; 1992).

These diametrically opposing results, of a positive frequency shift for an increase in field strength and a negative shift for a temperature increase when $B_c \equiv 0$, suggest that a combination of the two effects may serve to reproduce the observed frequency shifts. It was shown in this chapter that this is indeed the case, i.e. the observed p-mode frequency shifts may be reproduced qualitatively by a theoretical model involving simultaneous increases in both magnetic field strength and chromospheric temperature.

CHAPTER 4

EFFECTS OF NON-PARALLEL PROPAGATION ON SOLAR *P*- AND *F*- MODES

4.1 Introduction

The effects of changes in chromospheric canopy fields and chromospheric temperatures on the frequencies of solar p modes were investigated in chapter 3. The chromospheric canopy fields were considered to be uniform and horizontal. It was found that an increase in the magnetic field strength led to an increase in the frequencies of p-modes (see also Evans and Roberts, 1990, 1991, 1992). The changes in such canopy fields from one time to another modify the distribution of gas within the atmosphere, and thus change the wave motions from one time to another. The increase in magnetic field strength with time raises the wave propagation speed through the increase in the fast magnetoacoustic speed. It is quite likely that besides the effects of magnetic pressure there is magnetic tension, due to the distortion in magnetic field lines, which can modify the frequencies of p- and f- modes of oscillation.

The distribution of magnetic fields in the chromospheric canopies is not well known. From the earlier studies (see Campbell and Roberts, 1989; Evans and Roberts, 1990) of chromospheric canopies, it is clear that the distribution of horizontal magnetic fields is very crucial. In the work of Campbell and Roberts (1989) the magnetic fields were decreasing with height so as to maintain a constant Alfvén speed in that region. This led to a decrease in the frequencies of p-modes of oscillation whereas the effect of a uniform field (chapter 3; see also Evans and Roberts, 1990) gave an increase in the frequencies of p-modes. These previous analyses were for waves propagating in a direction parallel to the magnetic field. It would be more general to include the effects of non-parallel propagation (for which the wave vector is at an angle to the magnetic field) in the studies of the chromospheric canopy field changes on p- and f-modes. This chapter is concerned with investigating this aspect, not explored previously, by concentrating mainly on the magnetic field strength changes rather than temperature changes in the chromospheric canopies.

4.2 The Governing Equation

The effects of a chromospheric magnetic field on the solar f- and p- modes are studied in the case where the propagation vector is at an angle to the magnetic field direction. This is achieved by using the idealised model, where the reference level $z = 0$ is chosen to correspond to the base of the chromosphere (i.e. the temperature minimum), the region $z > 0$ to the convection zone and the region $z < 0$ to the chromosphere. The solar plasma is assumed to be an ideal, perfectly conducting gas, permeated by a horizontal magnetic field $B_o(z)\hat{\mathbf{x}}$. The equilibrium state is stationary and is described by the equations:

$$\frac{d}{dz}\left(p_o + \frac{B_o^2}{2\mu}\right) = \rho_o(z)g\,, \tag{4.1}$$

$$p_o = \mathcal{R}\rho_o T_o\,, \tag{4.2}$$

where $p_o(z)$ and $\rho_o(z)$ are the gas pressure and density respectively. Gravity acts in the +ve z-direction and is assumed to be constant. The gas constant $\mathcal{R}$, is taken to be k_B/m_p, where k_B is Boltzmann's constant and m_p is the mean particle mass of the plasma.

The equations governing the motion are the same as those mentioned in chapter 3, but are given again for convenience:

$$\frac{\partial \rho}{\partial t} + \rho\nabla\cdot\mathbf{v} + \mathbf{v}\cdot\nabla\rho = 0, \tag{4.3}$$

$$\rho\left[\frac{\partial \mathbf{v}}{\partial t} + (\mathbf{v}\cdot\nabla)\,\mathbf{v}\right] = -\nabla p + \frac{1}{\mu}(\nabla\times\mathbf{B})\times\mathbf{B} + \rho\mathbf{g}\,, \tag{4.4}$$

$$\frac{\partial \mathbf{B}}{\partial t} = \nabla\times(\mathbf{v}\times\mathbf{B})\,, \tag{4.5}$$

$$\frac{\partial}{\partial t}\left(\frac{p}{\rho^\gamma}\right) + (\mathbf{v}\cdot\nabla)\left(\frac{p}{\rho^\gamma}\right) = 0\,. \tag{4.6}$$

The quantity $\mathbf{v} = (v_x, v_y, v_z)$ is the velocity field, $\mathbf{B} = (B_o(z), 0, 0)$ is the magnetic field

and γ is the adiabatic index. Here, in contrast to chapter 3, $v_y \neq 0$. The velocities etc are assumed to be of the form $\mathbf{v} = (v_x, v_y, v_z)\, exp\,[i(\omega t - \mathbf{k.r})]$ for angular frequency ω with $\mathbf{k.r} = k_x x + k_y y$. After some algebra (see Appendix A3, Section 1) the x, y and z components of the momentum Equation (4.4) are given by

$$ik_x v_x = \frac{g k_x^2}{\omega^2} v_z + \frac{k_x^2 c_s^2}{\omega^2} \Delta \,, \tag{4.7a}$$

$$ik_y v_y = \frac{g k_y^2}{(\omega^2 - K^2 v_A^2)} v_z - \frac{k_y^2 c_s^2}{(\omega^2 - K^2 v_A^2)} \Delta - \frac{k_y^2 v_A^2}{(\omega^2 - K^2 v_A^2)} \frac{dv_z}{dz} \,, \tag{4.7b}$$

$$\left(k_x^2 v_A^2 - \omega^2\right) v_z + g \frac{dv_z}{dz} = c_s^2 \frac{d\Delta}{dz} - (\gamma - 1) g \Delta - \frac{\gamma B_o B_o'}{\mu \rho_o} \Delta + \frac{1}{\rho_o} \frac{d}{dz} \left[v_A^2 \rho_o \left(\frac{dv_z}{dz} - i k_y v_y \right) \right] , \tag{4.7c}$$

where

$$k = \left(k_x^2 + k_y^2\right)^{1/2} \,, \qquad \Delta = \text{div } \mathbf{v} \,, \tag{4.8}$$

and the dash $'$ denotes differentiation with respect to z.

On eliminating Δ from the above three components of the momentum equation (4.7a,b,c), the following second order ordinary differential equation for the vertical velocity v_z is obtained (see also Goedbloed, 1971 for a similar analysis):

$$\begin{aligned} &\frac{d}{dz} \left\{ \frac{\rho_o(z) \left(k_x^2 v_A^2(z) - \omega^2\right)}{m_o^2(z) + k_y^2} \frac{dv_z}{dz} \right\} + \left\{ \rho_o(z) \left(\omega^2 - k_x^2 v_A^2(z)\right) + \frac{\rho_o(z) g^2 k_x^2}{(k_x^2 c_s^2(z) - \omega^2)} \right. \\ &\qquad + \left. \frac{\rho_o(z)\; g^2\; k_y^2\; \omega^4}{\left(m_o^2(z) + k_y^2\right) \left(c_s^2(z) + v_A^2(z)\right) \left(k_x^2 c_T^2(z) - \omega^2\right) \left(k_x^2 c_s^2(z) - \omega^2\right)} \right. \\ &\left. - g k_x^2 \frac{d}{dz} \left\{ \frac{\rho_o(z) c_s^2(z) m_o^2(z)}{\left(m_o^2(z) + k_y^2\right) \left(k_x^2 c_s^2(z) - \omega^2\right)} \right\} - g k_y^2 \frac{d}{dz} \left\{ \frac{\rho_o(z)}{m_o^2(z) + k_y^2} \right\} \right\} v_z = 0 \,, \end{aligned} \tag{4.9}$$

where

$$m_o^2(z) = \frac{(k_x^2 v_A^2(z) - \omega^2)(k_x^2 c_s^2(z) - \omega^2)}{(c_s^2(z) + v_A^2(z))(k_x^2 c_T^2(z) - \omega^2)}\,, \qquad c_T^2(z) = \frac{c_s^2(z) v_A^2(z)}{c_s^2(z) + v_A^2(z)}\,; \tag{4.10}$$

with v_z and P_T related by

$$P_T = \frac{i}{\omega} \frac{\rho_o(z)}{\left(m_o^2(z) + k_y^2\right)} \left\{ (k_x^2 v_A^2(z) - \omega^2) \frac{dv_z}{dz} - \left[g k_y^2 + g k_x^2 \frac{c_s^2(z) m_o^2(z)}{(k_x^2 c_s^2(z) - \omega^2)} \right] v_z \right\}$$

$$- g \rho_o(z) v_z\,. \tag{4.11}$$

Equation (4.9) is clearly complicated for arbitrary atmospheric profiles. It possesses two singularities, referred to as the "cusp singularity" at $\omega^2 = k_x^2 c_T^2(z)$ and the "Alfvén singularity" at $\omega^2 = k_x^2 v_A^2(z)$. In any domain (z_1, z_2), the set of frequencies defined by $\omega \in \{k_x c_T(z), k_x v_A(z); z_1 \leq z \leq z_2\}$ corresponds to the set of continuous spectra associated with Equation (4.9). Frequencies which are members of this set are associated with the cusp continuum or the Alfvén continuum. Here they shall not be discussed further (see Goedbloed, 1983).

It should be noted that wherever a discontinuity occurs in either the sound speed, Alfvén speed, or the density, surface waves may exist. Across such a discontinuity it is necessary that the vertical component of velocity v_z be continuous. Furthermore, a careful inspection of Equation (4.9); in particular its first integral reveals a second quantity namely

$$\frac{\rho_o(z)\left(k_x^2 v_A^2(z) - \omega^2\right)}{m_o^2(z) + k_y^2} \frac{dv_z}{dz} - g k_x^2 \frac{\rho_o(z) c_s^2(z) m_o^2(z)}{\left(m_o^2(z) + k_y^2\right)\left(k_x^2 c_s^2(z) - \omega^2\right)} - \frac{g k_y^2 \rho_o(z)}{m_o^2(z) + k_y^2} \tag{4.12}$$

which must be continuous. This second condition is equivalent to the requirement that $i\omega P_T + g\rho_o v_z$ be continuous (see Equation (4.11)).

4.3 Interfacial Aspects

4.3.1 Incompressible limit

When $c_s \to \infty$ (see Chapter 2, Subsection 2.3.2), Equation (4.9) reduces to

$$\frac{d}{dz}\left\{ \rho_o(z) \left(k_x^2 v_A^2(z) - \omega^2\right) \frac{dv_z}{dz} \right\} + K^2 \left\{ \rho_o(z) \left(\omega^2 - k_x^2 v_A^2(z)\right) - g\rho_o'(z) \right\} v_z = 0, \tag{4.13}$$

where the dash ′ denotes differentiation with respect to z. Equation (4.11) takes the form

$$P_T = \frac{i}{\omega}\frac{\rho_o(z)}{\left(k_x^2+k_y^2\right)}\left\{(k_x^2 v_A^2(z)-\omega^2)\frac{dv_z}{dz} - \left[gk_y^2 - gk_x^2\right]v_z\right\} - g\rho_o(z)v_z\,. \tag{4.14}$$

Equation (4.13) may be analysed for the Rayleigh Taylor instability. The density $\rho_o(z)$ is assumed to be of the form

$$\rho_o(z) \;=\; \begin{cases} \rho_p\,, & z>0, \\ \rho_c\,, & z<0, \end{cases} \tag{4.15}$$

corresponding to a fluid of constant density ρ_c resting on top of a fluid of constant density ρ_p. The magnetic field is assumed to be uniform so that the Alfvén speed in $z>0$ is $v_{Ap} = B_o/\left(\mu\rho_p\right)^{1/2}$ and in the region $z<0$ is $v_{Ac} = B_o/\left(\mu\rho_c\right)^{1/2}$. On either side of the interface $z=0$, the medium is uniform and so the coefficients of dv_z/dz and v_z in Equation (4.13) are constant for the regions $z<0$ and $z>0$. Thus Equation (4.13) has solution

$$v_z(z) \;=\; \begin{cases} \alpha_p e^{-\left(k_x^2+k_y^2\right)^{1/2}z}\,, & z>0, \\ \alpha_c e^{\left(k_x^2+k_y^2\right)^{1/2}z}\,, & z<0, \end{cases} \tag{4.16}$$

where it is assumed that $\left(k_x^2+k_y^2\right)^{1/2}>0$ and $v_z\to 0$ as $|z|\to\infty$.

It is necessary that v_z and P_T be continuous across the interface $z=0$. The continuity of P_T is apparent from the integral of the Equation (4.13) and assures that there are no unbalanced forces at the interface. Note that this second condition can also be obtained from (4.12) by taking the limit $c_s\to\infty$. Thus, the boundary condition that v_z is continuous across $z=0$ together with the second condition that

$$\rho_o(z)\left(k_x^2 v_A^2(z)-\omega^2\right)\frac{dv_z}{dz} - g\left(k_x^2+k_y^2\right)\rho_o(z)v_z \tag{4.17}$$

is continuous across $z=0$ yields the following dispersion relation:

$$\omega^2 \;=\; k_x^2 c_k^2 - g\left(k_x^2+k_y^2\right)^{1/2}\left[\frac{\rho_c-\rho_p}{\rho_c+\rho_p}\right]\,, \tag{4.18}$$

where

$$c_k = \left(\frac{\rho_p v_{Ap}^2 + \rho_c v_{Ac}^2}{\rho_p + \rho_c} \right)^{1/2} , \tag{4.19}$$

is the well known mean speed with which a surface wave propagates in an incompressible medium in the absence of gravity (see, for example, the reviews by Spruit, 1983; Spruit and Roberts, 1983; Thomas, 1985; Roberts, 1986; Ryutova, 1990). In the absence of a magnetic field ($v_{Ap} = v_{Ac} = 0$), Equation (4.18) shows that if $\rho_c > \rho_p$, i.e. the fluid on the top is denser than at the bottom, the interface is unstable ($\omega^2 < 0$). Thus the effect of the magnetic field is to stabilize the interface against short wavelength modes. Also to be noted is that in a direction perpendicular to the magnetic field (where $\theta = \pi/2$ and so $k_x = K \cos\theta = 0$, $k_y = K \sin\theta = K$), Equation (4.18) gives

$$\omega^2 = -gK \left(\frac{\rho_c - \rho_p}{\rho_c + \rho_p} \right) , \tag{4.20}$$

which shows that if $\rho_c > \rho_p$, the wave is unstable ($\omega^2 < 0$) even in the presence of magnetic field.

Now consider a non-magnetic case with a non-uniform density. In the absence of magnetic field, Equation (4.13) reduces to

$$\frac{d^2 v_z}{dz^2} + \frac{\rho_o'(z)}{\rho_o(z)} \frac{dv_z}{dz} + \left\{ \frac{g\left(k_x^2 + k_y^2\right)}{\omega^2} \left(\frac{\rho_o'(z)}{\rho_o(z)} \right) - \left(k_x^2 + k_y^2\right) \right\} v_z = 0 . \tag{4.21}$$

Consider two semi-infinite regions separated at $z = 0$ having densities exponentially varying as follows

$$\rho_o(z) = \begin{cases} \rho_p e^{z/H_p} , & z > 0, \\ \rho_c e^{z/H_c} , & z < 0, \end{cases} \tag{4.22}$$

and ρ_p and ρ_c are densities at lower and upper regions of the interface $z = 0$, $H_p = p_p/\rho_p g$ and $H_c = p_c/\rho_c g$ are the constant scale heights in the regions $z > 0$ and $z < 0$ respectively. Thus, Equation (4.21) has the solution

$$v_z(z) = \begin{cases} \alpha_p e^{-\lambda_p z} , & z > 0, \\ \alpha_c e^{\lambda_c z} , & z < 0. \end{cases} \tag{4.23}$$

Here

$$2\lambda_p H_p = 1 \mp \left[1 - 4\left(k_x^2 + k_y^2\right)\left(\frac{gH_p}{\omega^2} - H_p^2\right)\right]^{1/2},$$

$$2\lambda_c H_c = -1 \pm \left[1 - 4\left(k_x^2 + k_y^2\right)\left(\frac{gH_c}{\omega^2} - H_c^2\right)\right]^{1/2}. \quad (4.24)$$

It is important to have finite energy density for large z i.e. $\rho_o(z)v_z^2 \to 0$ as $|z| \to \infty$. This is achieved provided

$$2\lambda_p H_p = 1 + \left[1 - 4\left(k_x^2 + k_y^2\right)\left(\frac{gH_p}{\omega^2} - H_p^2\right)\right]^{1/2},$$

$$2\lambda_c H_c = -1 + \left[1 - 4\left(k_x^2 + k_y^2\right)\left(\frac{gH_c}{\omega^2} - H_c^2\right)\right]^{1/2}. \quad (4.25)$$

It is also assumed that the terms in square brackets [ ] are positive, which implies a restriction on the solution (see Roberts, 1991):

$$\left(k_x^2 + k_y^2\right) + \frac{1}{4H_p^2} > \frac{g\left(k_x^2 + k_y^2\right)}{\omega^2 H_p}, \quad \left(k_x^2 + k_y^2\right) + \frac{1}{4H_c^2} > \frac{g\left(k_x^2 + k_y^2\right)}{\omega^2 H_c}. \quad (4.26)$$

If ω^2 exceeds the squared buoyancy (Brunt Väisälä) frequency $\omega_g^2 = g/H$ in each region then the inequalities (4.26) are satisfied for all $K\left[= \left(k_x^2 + k_y^2\right)^{1/2}\right]$. If $\omega^2 < \omega_g^2$ in either or both regions, then inequalities (4.26) imply a restriction

$$0 < \frac{gK^2}{\omega^2 H_p} - K^2 < \frac{1}{4H_p^2} \text{ or/and } 0 < \frac{gK^2}{\omega^2 H_c} - K^2 < \frac{1}{4H_c^2}. \quad (4.27)$$

If the second inequality in Equation (4.26) is not satisfied in the upper region ($z < 0$), then oscillatory v_z arises, growing in amplitude for $z < 0$. Thus although the solution (4.23) was constructed under the restriction of decaying kinetic energy density, another restriction (4.27) which arises quite naturally, allows the possibility of a mode with a growing v_z in the upper region ($z < 0$).

Imposing the conditions that v_z must be continuous across the interface $z = 0$ and that (see Equation (4.17) with $v_A = 0$)

$$\rho_o(z)\omega^2 \frac{dv_z}{dz} + g\left(k_x^2 + k_y^2\right)\rho_o(z)v_z \tag{4.28}$$

is also continuous at $z = 0$, the following dispersion relation is obtained

$$\omega^2 \;=\; -g\left(k_x^2 + k_y^2\right)\left[\frac{\rho_c - \rho_p}{\lambda_p\rho_p + \lambda_c\rho_c}\right] . \tag{4.29}$$

Since λ_p and λ_c are non-polynomial functions of ω, Equation (4.29) is transcendental. When compared with Equation (4.18) (for $v_A = 0$ so that $c_k = 0$), it can be noted that ω^2 no longer varies linearly with $\left(k_x^2 + k_y^2\right)^{1/2}$.

The transcendental nature of Equation (4.29) can be removed by squaring it twice. This was first noted by Bernstein and Book (1983) in their investigation of the Rayleigh-Taylor instability (see also Miles, 1991; Miles and Roberts, 1992 for the case $k_y = 0$). After detailed but straightforward algebra Equation (4.29) can be written as a polynomial in $\Omega^2 \left(= \omega^2/gK, \text{where } K = \left(k_x^2 + k_y^2\right)^{1/2}\right)$ as follows:

$$\left(\Omega^4 - 1\right)\left\{K\left(\rho_p + \rho_c\right)^2\Omega^4 - \left(\frac{\rho_p}{H_c} + \frac{\rho_c}{H_p}\right)\left(\rho_p + \rho_c\right)\Omega^2 - K\left(\rho_p - \rho_c\right)^2\right\} = 0. \tag{4.30}$$

The process of squaring (4.29) in obtaining (4.30) may introduce spurious roots which satisfy the Equation (4.30) but not the dispersion relation (4.29).

The solutions to Equation (4.30) are given by

$$\Omega^2 = \pm 1 \;\text{ or }\; K\left(\rho_p + \rho_c\right)^2\Omega^4 - \left(\frac{\rho_p}{H_c} + \frac{\rho_c}{H_p}\right)\left(\rho_p + \rho_c\right)\Omega^2 - K\left(\rho_p - \rho_c\right)^2 = 0. \tag{4.31}$$

The solution $\Omega^2 = 1$ (i.e. $\omega^2/gK = 1$) is termed the *f*-mode. This will be discussed in later sections. The solutions to the Ω^2 quadratic in Equation (4.31) are

$$\frac{\omega^2}{gK} \;=\; \frac{1 \pm (1 + \mathcal{D}^2)^{1/2}}{\mathcal{S}} , \tag{4.32}$$

where

$$\mathcal{S} = KH_p\left(\rho_p + \rho_c\right)\left(\frac{\rho_p}{\rho_c}\right) , \qquad \mathcal{D} = KH_p\left(\rho_p - \rho_c\right)\left(\frac{\rho_p}{\rho_c}\right) . \tag{4.33}$$

In the long wavelength limit ($KH_p, KH_c << 1$), Equation (4.32) for the positive root gives (using the pressure balance requirement that $\rho_p H_p = \rho_c H_c$)

$$\omega^2 = g\left\{\frac{4 + K^2\rho_p^2\left(H_c - H_p\right)^2}{2\rho_p\left(H_c + H_p\right)}\right\}, \tag{4.34}$$

showing that $\omega^2 > 0$. For the negative root, Equation (4.32) gives

$$\omega^2 = -\frac{gK^2H_c\left(\rho_p - \rho_c\right)^2}{2\left(\rho_p + \rho_c\right)} = -\frac{gK^2\rho_p\left(H_c - H_p\right)^2}{2\left(H_p + H_c\right)}, \tag{4.35}$$

showing that this is an unstable ($\omega^2 < 0$) solution.

In the short wavelength limit ($KH_p, KH_c >> 1$) Equation (4.29) yields

$$\omega^2 = -gK\left(\frac{\rho_c - \rho_p}{\rho_c + \rho_p}\right); \tag{4.36}$$

this is Equation (4.18) with $c_k = 0$ ($v_A = 0$). Equation (4.36) is the dispersion relation that governs the non-magnetic, incompressible Rayleigh - Taylor instability in the short wavelength limit. An instability occurs if $\rho_c > \rho_p$, while the interface is able to support a surface wave if the interfacial densities are such that $\rho_c < \rho_p$ (i.e. when the lighter fluid rests on top of the heavier fluid). Thus in the constant density case, a magnetic field acts to stabilise perturbations propagating parallel to it but when the densities are varying in non-magnetic regions, the nature of solutions depend on the wavelength of the relevant perturbation.

4.3.2 Compressible case

In the following section, the assumption of incompressibility is removed. The case considered here is the non-magnetic one. In the absence of magnetic field, Equation (4.9) reduces to

$$\frac{d}{dz}\left\{\frac{\rho_o(z)\omega^2c_s^2(z)}{\left(K^2c_s^2(z) - \omega^2\right)}\frac{dv_z}{dz}\right\} - \left\{\rho_o(z)\omega^2 + \frac{\rho_o(z)g^2k_x^2}{\left(k_x^2c_s^2(z) - \omega^2\right)}\right.$$

$$\left. - \frac{\rho_o(z)\ g^2\ k_y^2\omega^2}{\left(K^2c_s^2(z) - \omega^2\right)\left(k_x^2c_s^2(z) - \omega^2\right)} - gK^2\frac{d}{dz}\left[\frac{\rho_o(z)c_s^2(z)}{\left(K^2c_s^2(z) - \omega^2\right)}\right]\right\} v_z = 0\,. \tag{4.37}$$

With the assumption of a constant sound speed, Equation (4.37) can be written as

$$\frac{d^2v_z}{dz^2} + \frac{\rho_o'(z)}{\rho_o(z)}\frac{dv_z}{dz} + \left\{ \frac{gK^2}{\omega^2}\left(\frac{\rho_o'(z)}{\rho_o(z)}\right) - \frac{(K^2c_s^2 - \omega^2)}{c_s^2} - \frac{g^2K^2}{\omega^2 c_s^2} \right\} v_z = 0 \,. \qquad (4.38)$$

Now consider a density profile of the form

$$\rho_o(z) \;=\; \begin{cases} \rho_p e^{z/H_p} \,, & z > 0, \\ \rho_c e^{z/H_c} \,, & z < 0, \end{cases} \qquad (4.39)$$

where $H_c = c_{sc}^2/\gamma g$ and $H_p = c_{sp}^2/\gamma g$ are the constant density scale heights in the isothermal atmospheres above and below the interface, respectively; $\rho_p = \rho_p(0_+)$ and $\rho_c = \rho_c(0_-)$ are the densities either side of the interface. Then Equation (4.38) has the solution

$$v_z(z) \;=\; \begin{cases} \alpha_p e^{-\eta_p z} \,, & z > 0, \\ \alpha_c e^{\eta_c z} \,, & z < 0, \end{cases} \qquad (4.40)$$

where

$$2\eta_p H_p \;=\; 1 + \left[1 - 4A_pH_p^2\right]^{1/2} \,,$$

$$2\eta_c H_c \;=\; -1 + \left[1 - 4A_cH_c^2\right]^{1/2} \,. \qquad (4.41)$$

Here

$$A_p = \frac{\left(\omega^2 - K^2c_{sp}^2\right)}{c_{sp}^2} + \frac{(\gamma-1)}{g^2K^2}\omega^2 c_{sp}^2 \,, \quad A_c = \frac{(\omega^2 - K^2c_{sc}^2)}{c_{sc}^2} + \frac{(\gamma-1)}{g^2K^2}\omega^2 c_{sc}^2 \,. \qquad (4.42)$$

Equation (4.41) is chosen so that the parts of Equation (4.40) satisfy the necessary requirement that the energy density $\rho_o(z)v_z^2 \to 0$ as $|z| \to \infty$.

Boundary conditions across the interface are that both the vertical component of velocity, v_z, and the expression

$$\frac{\rho_o(z)\omega^2 c_s^2(z)}{(K^2c_s^2(z)-\omega^2)}\frac{dv_z}{dz} - \frac{g\rho_o(z)K^2c_s^2(z)}{(K^2c_s^2(z)-\omega^2)}v_z \tag{4.43}$$

must be continuous across the interface $z = 0$. Application of these conditions leads to the dispersion relation

$$\omega^2 \;=\; -gK^2\left[\frac{C_p - C_c}{\eta_p C_p + \eta_c C_c}\right], \tag{4.44}$$

where

$$C_c = \frac{\rho_c c_{sc}^2}{(K^2c_{sc}^2-\omega^2)} \quad \text{and} \quad C_p = \frac{\rho_p c_{sp}^2}{\left(K^2c_{sp}^2-\omega^2\right)}. \tag{4.45}$$

Equation (4.44) is the compressible counterpart of the incompressible limit dispersion relation (4.29). In fact if the same analysis as in subsection (4.3.1) is carried out to remove the transcendentality of (4.44) the solutions of the resulting polynomial are (see Miles, 1991)

$$\omega^2 = K^2c_{sp}^2\,,\quad \omega^2 = K^2c_{sc}^2\,,\quad \omega^2 = gK\,,\quad \frac{\omega^2}{gK} = \frac{1\pm(1+\mathcal{D}^2)^{1/2}}{\mathcal{S}}\,, \tag{4.46}$$

where

$$\mathcal{S} = K\frac{\left(c_{sp}^2+c_{sc}^2\right)}{g} \quad \text{and} \quad \mathcal{D} = K\frac{\left(c_{sp}^2-c_{sc}^2\right)}{g}. \tag{4.47}$$

Of the above solutions, $\omega = Kc_{sp}$ and $\omega = Kc_{sc}$ (also called Lamb modes) are not solutions of the dispersion relation (4.44). The solution $\omega^2 = gK$ is the *f*-mode and is discussed separately in a later section. As in the previous subsection, the dispersion relation in the short wavelength limit ($KH_p, KH_c >> 1$) is

$$\omega^2 \;=\; -gK\left(\frac{\rho_c-\rho_p}{\rho_c+\rho_p}\right). \tag{4.48}$$

Thus, if $\rho_c < \rho_p$, the interface supports a stable surface wave whose frequency is

proportional to $\sqrt{g|K|}$, while if $\rho_c > \rho_p$ the interface is once again unstable with growth rate proportional to $\sqrt{g|K|}$. A similar analysis with the inclusion of magnetic field would be of interest but the details are more involved than for the non-magnetic case and are not discussed any further.

From the analysis of this section it is clear that the presence of a magnetic field and gravity introduce quite different wavenumber dependences in the frequency of a surface wave or in the growth rate of an instability. The presence of a horizontal uniform magnetic field can also act to stabilise an otherwise unstable interface.

It is apparent from the analysis of Bernstein and Book (1983) that the compressible and incompressible surface waves and their associated instabilities share the same functional dependences on the wavenumber K in the long and short wavelength limits. Contrary to this it was shown in the above analysis that the incompressible surface wave frequency (or the growth rate of the instability) in a plasma of uniform density exhibits a different wavenumber dependence to that in a plasma of exponential density stratification. Thus the general inference from this section is that care must be taken in making deductions about the behaviour of waves and instabilities in stratified plasmas from an analysis of a constant density plasma (see also Campbell, 1987).

Before the problem of p- and f-modes is considered, it is worth pointing out that Equation (4.37) can give surface wave solutions when applied to a magnetic field discontinuity. A magnetic field region above a field-free atmosphere is of particular interest for the modelling of *running penumbral waves*. Running penumbral waves are observed to propagate out (largely in a horizontal direction) from sunspots. It is possible that these waves are examples of a surface wave propagating on the curved interface between the magnetic field and the field-free gas. See Nye and Thomas (1976), Small and Roberts (1984) for the discussion of Running penumbral waves. An attempt to understand the surface waves in the presence of gravity, will be considered in a later section .

Returning to the problem of p- and f-modes, it is desired to model the chromosphere and the convection zone with as much reality as possible although, as pointed out in Chapter 3, dealing with arbitrary profiles of magnetic field and temperatures is not always convenient mathematically. Nevertheless, it is planned to discuss some of the aspects of Equation (4.9) when some complexities like non-parallel (wave vector at an angle to magnetic field direction) propagation is introduced. The convection zone and the chromosphere are described in the following section.

4.4 The Model

(a) The Chromosphere

The region $z < 0$ is taken to correspond to the chromosphere. It is assumed that the temperature $T_o(z)$ is constant. Hence

$$T_o(z) \;=\; T_c\,, \qquad z<0\,. \tag{4.49}$$

There are two possible configurations for the horizontal magnetic field $B_o(z)\hat{\mathbf{x}}$ consistent with static equilibrium. They are:
(i) uniform magnetic field, $B_o(z) = B_o$.
(ii) a magnetic field that varies with height z.

First consider the case (i) of isothermal atmosphere with a uniform horizontal magnetic field. Since the magnetic field is constant along the z-direction, it has no effect on the hydrostatic equilibrium of the atmosphere. The equilibrium pressure and density both decrease exponentially with height. The Alfvén speed increases exponentially with height due to the decreasing density. Thus,

$$c_s = (\gamma \mathcal{R} T_c)^{1/2} = \text{constant}\,, \qquad H = \frac{\mathcal{R}T_c}{g} = \text{constant}\,, \tag{4.50}$$

and

$$\rho_o(z) = \rho_c e^{-z/H}\,, \qquad v_A(z) = v_{Ac} e^{z/2H}\,, \qquad z<0\,, \tag{4.51}$$

where ρ_c and v_{Ac} are the unperturbed density and Alfvén speed at $z = 0$. For such an equilibrium state, Equation (4.9) reduces to

$$\frac{d^2 v_z}{dz^2} + A(z)\frac{dv_z}{dz} + B(z) v_z \;=\; 0\,, \tag{4.52}$$

where the coefficients $A(z)$ and $B(z)$ are given by

$$A(z) = \frac{1}{H} - \frac{1}{D(z)}\left\{-\omega^4 + (k_x^2 c_s^2 - \omega^2)(k_x^2 v_A^2(z) - \omega^2)\left(1 + \frac{\omega^4}{E(z)}\right)\right\}\frac{v_A^2(z)}{H}\,, \tag{4.53}$$

$$B(z) \;=\; \frac{1}{D(z)}\left\{\omega^6 - \left[\left(c_s^2 + v_A^2(z)\right)K^2 + k_x^2 v_A^2(z)\right]\omega^4\right.$$

$$+\left[k_x^2 v_A^2(z) K^2 \left(2c_s^2 + v_A^2(z)\right) - gK^2\left(g - \frac{c_s^2}{H}\right) + \frac{g}{H} k_y^2 v_A^2(z)\right]\omega^2$$

$$-k_x^2 v_A^2(z) K^2 \left[k_x^2 c_s^2 v_A^2(z) - g\left(g - \frac{c_s^2}{H}\right)\right] - \frac{\omega^6}{E(z)} g k_y^2 \frac{v_A^2(z)}{H}\Bigg\} , \qquad (4.54)$$

$$D(z) \;=\; \left[k_x^2 c_s^2 v_A^2(z) - \omega^2\left(c_s^2 + v_A^2(z)\right)\right]\left(k_x^2 v_A^2(z) - \omega^2\right) , \qquad (4.55)$$

$$E(z) = \omega^4 + K^2\left[k_x^2 c_s^2 v_A^2(z) - \omega^2\left(c_s^2 + v_A^2(z)\right)\right] , \qquad K^2 = k_x^2 + k_y^2 . \qquad (4.56)$$

A similar propagation equation has been obtained previously by Nye and Thomas (1976) for arbitrary vertical distributions of c_s^2, v_A^2 and H, where the coefficients $A(z)$ and $B(z)$ are more complicated than in Equations (4.53) and (4.54) because of terms related to $dc_s^2(z)/dz$ present in them. Here c_s and H are considered constant (see Equation (4.50)) which simplifies $A(z)$ and $B(z)$ slightly but even then the complexity of Equation (4.52) is evident and it is in general solvable only by numerical methods. However, for the case $k_y = 0$, corresponding to wave propagation in the magnetic field direction, it can be transformed into a standard hypergeometric differential equation by using appropriate transformations and the solutions then expressed in terms of hypergeometric functions (Adam 1975; Nye and Thomas, 1976b). This approach was considered in chapter 3.

Now consider the case (ii) of an isothermal atmosphere with magnetic field varying in the z-direction. Following Yu (1965) and Campbell and Roberts (1989) for the analysis, consider the equilibrium magnetic field $B_o(z)$ and density $\rho_o(z)$ being structured in such a way that

$$B_o^2(z) \;\sim\; \rho_o(z) , \qquad (4.57)$$

so that the Alfvén speed $v_A(z) = B_o(z)/\left(\mu\rho_o(z)\right)^{1/2}$ is constant and denoted by v_{Ac}. Since the temperature is constant throughout the chromospheric atmosphere, the sound speed c_{sc} is also constant. With such an atmospheric structuring, the general equilibrium Equation (4.1) reduces to the form

$$\frac{\rho_o'}{\rho_o} \;=\; \frac{\Gamma g}{c_{sc}^2} , \qquad (4.58)$$

where

$$\Gamma \;=\; \frac{2\gamma c_{sc}^2}{2c_{sc}^2+\gamma v_{Ac}^2}\;(\leq \gamma)\;, \tag{4.59}$$

is the magnetically modified adiabatic exponent. The equilibrium pressure, density and magnetic field are then of the form

$$p_o(z)=p_c e^{z/H_c}\;,\quad \rho_o(z)=\rho_c e^{z/H_c}\;,\quad B_o(z)=B_c e^{z/2H_c}\;, \tag{4.60}$$

where $H_c = c_{sc}^2/\Gamma g$ is the magnetically modified scale height of the chromosphere; p_c, ρ_c and B_c are the equilibrium pressure, density and magnetic field strength at the base of the chromosphere.

For the above equilibrium profiles, Equation (4.9) reduces to

$$\frac{d^2v_z}{dz^2}+\frac{1}{H_c}\frac{dv_z}{dz}+A_c v_z \;=\; 0\;, \tag{4.61}$$

where

$$\begin{aligned} A_c \;=\; & -(m_o^2+k_y^2)\;+\;\frac{g^2K^2}{(c_{sc}^2+v_{Ac}^2)(k_x^2c_{Tc}^2-\omega^2)} \\ & -\frac{gk_y^2}{H_c(c_{sc}^2+v_{Ac}^2)(k_x^2c_{Tc}^2-\omega^2)}-\frac{gk_x^2c_{sc}^2}{H_c(c_{sc}^2+v_{Ac}^2)(k_x^2c_{Tc}^2-\omega^2)} \end{aligned} \tag{4.62}$$

and

$$m_o^2=\frac{(k_x^2v_{Ac}^2-\omega^2)(k_x^2c_{sc}^2-\omega^2)}{(c_{sc}^2+v_{Ac}^2)(k_x^2c_{Tc}^2-\omega^2)}\;,\qquad c_{Tc}^2=\frac{c_{sc}^2v_{Ac}^2}{c_{sc}^2+v_{Ac}^2}\;. \tag{4.63}$$

Equation (4.61) possesses solutions of the form

$$v_z \;\propto\; \exp\left\{\frac{z}{2H_c}\left[-1\pm(1-4A_cH_c^2)^{1/2}\right]\right\}\;. \tag{4.64}$$

Thus, for the energy density ($\frac{1}{2}\rho_o v_z^2$) to tend to zero as $z \to -\infty$, the frequency and wavenumber of each mode need to satisfy the inequality $1 > 4A_cH_c^2$ and hence it is necessary to choose

$$v_z = C_3 \exp\left\{\frac{z}{2H_c}\left[-1+(1-4A_cH_c^2)^{1/2}\right]\right\}, \tag{4.65}$$

where C_3 is an arbitrary constant.

Those modes with frequency and wavenumber such that $1 < 4A_cH_c^2$ will propagate energy out of the chromosphere. The equation $1 = 4A_cH_c^2$ provides the cut-off frequency between propagating and evanescent modes. In terms of the original variables, it is given by (for small K)

$$\omega^2 = \frac{c_{sc}^2\left(c_{sc}^2+v_{Ac}^2\right)}{\left(c_{sc}^2+\frac{\gamma}{2}v_{Ac}^2\right)^2}\omega_{cut}^2 + O\left(K^2\right) \tag{4.66}$$

where $\omega_{cut} = \gamma g/2c_{sc}$ is the acoustic cut-off for a field-free isothermal atmosphere (Lamb, 1932).

(b) The Convection Zone

The convection zone ($z > 0$) is assumed to be the same as in chapter 3 (see Figure 4.1). Thus it is field-free and the temperature $T_o(z)$ varies linearly with depth, i.e.

$$T_o(z) = T_p\left(1+\frac{z}{z_o}\right), \quad z > 0, \tag{4.67}$$

where T_p is the temperature at the top of the convection zone, and z_o is the temperature scale height.

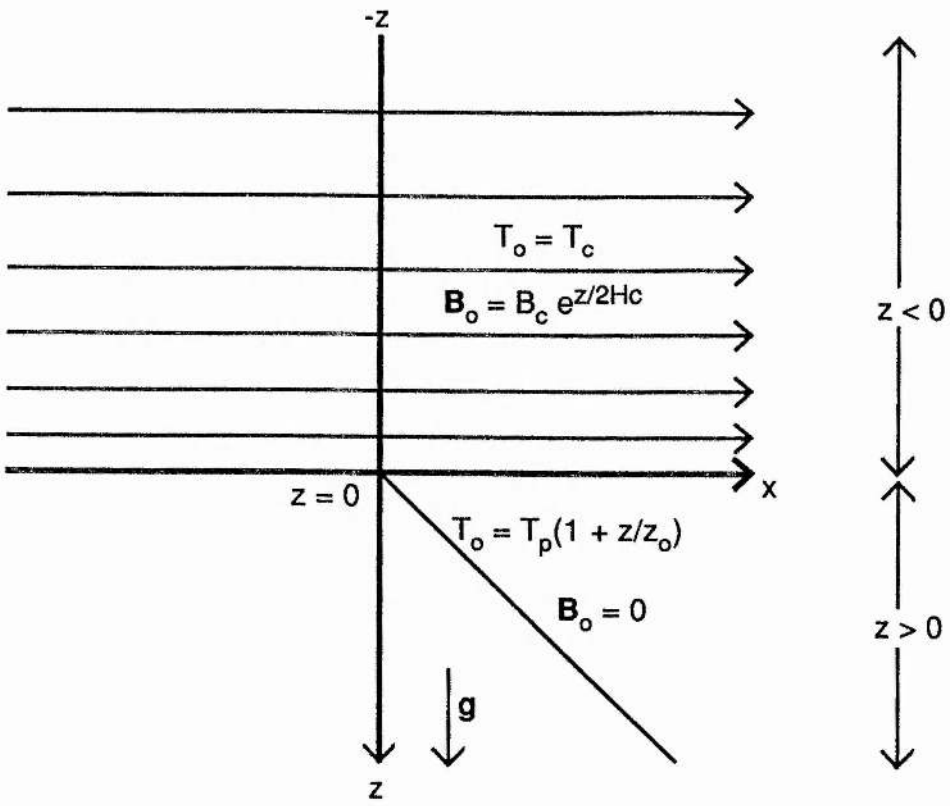

Figure 4.1: The equilibrium atmosphere of the model.

Then, from Equations (4.1) and (4.2), the equilibrium pressure and density are found to be

$$p_o(z) = p_p\left(1 + \frac{z}{z_o}\right)^{(m+1)}, \qquad \rho_o(z) = \frac{p_p}{\mathcal{R}T_p}\left(1 + \frac{z}{z_o}\right)^{m}, \tag{4.68}$$

where

$$m \;=\; \frac{g z_o}{\mathcal{R}T_p} - 1\,, \tag{4.69}$$

is the polytropic index, and p_p is the gas pressure at the top of the convection zone ($z = 0_+$). Note that for an atmosphere in 'convective equilibrium' , where $p_o \propto \rho_o^\gamma$,

$$m\gamma = m + 1\,, \qquad \text{or} \qquad m = \frac{1}{\gamma - 1}\,. \tag{4.70}$$

The vertical component of velocity, v_z, in the convection zone is given by (see chapter 3)

$$(\omega^4 - g^2k_x^2)v_z e^{k_x(z+z_o)} = C_5\left\{\left[k_x c_{sp}^2(\omega^2 + gk_x) - \gamma g\omega^2\right] U(-a, m+2, 2k_x(z+z_o)) - 2a\omega^2 c_{sp}^2 k_x\, U(-a+1, m+3, 2k_x(z+z_o))\right\} . \quad (4.71)$$

Magnetohydrostatic pressure balance across the interface $z = 0$ requires that

$$p_p = p_c + \frac{B_c^2}{2\mu} , \quad (4.72)$$

which may be expressed in terms of the interfacial density ratios as

$$\frac{\rho_p}{\rho_c} = \frac{(c_{sc}^2 + \frac{\gamma}{2}v_{Ac}^2)}{c_{sp}^2} . \quad (4.73)$$

4.5 The Dispersion Relation

The motions in the convection zone and the chromosphere are described by the solutions (4.65) and (4.71). These are matched across the interface $z = 0$ by imposing the boundary conditions that the vertical velocity v_z and the total gravitational pressure perturbation, namely

$$\frac{\rho_o\left(k_x^2 v_A^2(z) - \omega^2\right)}{\left(m_o^2(z) + k_y^2\right)}\frac{dv_z}{dz} - \frac{gk_x^2\rho_o c_s^2 m_o^2(z)}{\left(m_o^2(z) + k_y^2\right)\left(k_x^2c_s^2 - \omega^2\right)}v_z - \frac{gk_y^2\rho_o}{\left(m_o^2(z) + k_y^2\right)}v_z , \quad (4.74)$$

be continuous at $z = 0$ (see Equation (4.12)). Application of these boundary conditions yield the following dispersion relation which relates the frequency and wavenumber in the form

$$2aK\omega^2 c_{sp}^2\frac{U(-a+1, m+3, 2Kz_o)}{U(-a, m+2, 2Kz_o)} + \gamma g\omega^2 - Kc_{sp}^2(\omega^2 + gK)$$

$$= \left(\frac{\rho_p}{\rho_c}\right)\frac{(m_o^2 + k_y^2)(g^2K^2 - \omega^4)c_{sp}^2}{\left\{(k_x^2v_{Ac}^2 - \omega^2)\lambda_+ + \frac{gk_x^2c_{sc}^2m_o^2}{(\omega^2 - k_x^2c_{sc}^2)} - gk_y^2\right\}} , \quad (4.75)$$

where

$$\lambda_+ = \frac{1}{2H_c}\left[-1 + (1 - 4A_cH_c^2)^{1/2}\right] . \quad (4.76)$$

The constant A_c is given by Equation (4.62); m_o^2 and c_{Tc}^2 are given by Equation (4.63). The ratio of $\rho_p\,[=\rho_p(0_+)]$ to $\rho_c\,[=\rho_c(0_-)]$ is given by Equation (4.73).

A similar dispersion relation to (4.75) has been derived by Campbell and Roberts (1989) for the case when wave vector is parallel to the applied magnetic field direction. For $k_y = 0$, $K = k_x$ and Equation (4.75) reduces to

$$2a\omega^2 c_{sp}^2 k_x \frac{U\left(-a+1, m+3, 2k_x z_o\right)}{U\left(-a, m+2, 2k_x z_o\right)} \; + \; \gamma g \omega^2 \; - \; k_x c_{sp}^2 (\omega^2 + g k_x)$$

$$= \left(\frac{\rho_p}{\rho_c}\right) \frac{m_o^2 \left(g^2 k_x^2 - \omega^4\right) c_{sp}^2}{\left\{(k_x^2 v_{Ac}^2 - \omega^2)\lambda_+ + \frac{g k_x^2 c_{sc}^2 m_o^2}{(\omega^2 - k_x^2 c_{sc}^2)}\right\}}\,, \qquad (4.77)$$

where A_c (occurring in λ_+) is now given by

$$A_c(k_y = 0) \;\; = \;\; \frac{(\Gamma - 1) g^2 k_x^2 + (k_x^2 v_{Ac}^2 - \omega^2)\left(k_x^2 c_{sc}^2 - \omega^2\right)}{\left(c_{sc}^2 + v_{Ac}^2\right)\left(\omega^2 - k_x^2 c_{Tc}^2\right)}\,. \qquad (4.78)$$

The reduced form (4.77) is, as expected, in agreement with Campbell and Roberts (1989).

The general dispersion relation (4.75) may be rewritten in dimensionless form:

$$2a\kappa\Omega^2 \frac{U\left(-a+1, m+3, 2\kappa\right)}{U\left(-a, m+2, 2\kappa\right)} \; + (m+1)\Omega^2 \; - \; \kappa(1+\Omega^2) =$$

$$\frac{\wedge(1-\Omega^4)\left\{K'_\beta\left(\kappa\cos^2\theta - \wedge\Omega^2\right) + \kappa\sin^2\theta\left(\frac{1+\beta}{\beta}\right)\left(\frac{\kappa\cos^2\theta}{1+\beta} - \wedge\Omega^2\right)\right\}}{\mathcal{X}\left\{K'_\beta\left[\left(\frac{1+\beta}{\beta}\right)\left(\frac{\kappa\cos^2\theta}{1+\beta} - \wedge\Omega^2\right)\Phi - \wedge\cos^2\theta\right] - \wedge\sin^2\theta\left(\frac{1+\beta}{\beta}\right)\left(\frac{\kappa\cos^2\theta}{1+\beta} - \wedge\Omega^2\right)\right\}}\,, \qquad (4.79)$$

where

$$K'_\beta = \left(\frac{\kappa\cos^2\theta}{\beta} - \wedge\Omega^2\right)\,, \quad \kappa = K z_o\,, \quad k_x = K\cos\theta\,, \quad k_y = K\sin\theta\,, \qquad (4.80)$$

$$\Omega^2 = \frac{\omega^2}{gK}\,, \quad \mathcal{X} = \left(\frac{T_p}{T_c}\right)\frac{\Gamma}{\gamma} = \left(\frac{T_p}{T_c}\right)\frac{2\beta}{2\beta+\gamma}\,, \quad \beta = \frac{c_{sc}^2}{v_{Ac}^2}\,, \quad \wedge = \frac{m+1}{\gamma}\frac{c_{sp}^2}{c_{sc}^2}\,, \qquad (4.81)$$

$$\Phi = \frac{\Gamma\Lambda}{2\kappa}\left[-1+(1-4A_cH_c^2)^{1/2}\right]\,, \tag{4.82}$$

$$A_cH_c^2 = -\kappa\left\{\frac{\left(\frac{\kappa\cos^2\theta}{\beta}-\Lambda\Omega^2\right)\left(\kappa\cos^2\theta-\Lambda\Omega^2\right)+\kappa\sin^2\theta\left(\frac{1+\beta}{\beta}\right)\left(\frac{\kappa\cos^2\theta}{1+\beta}-\Lambda\Omega^2\right)}{\Gamma^2\,\Lambda^2\left(\frac{1+\beta}{\beta}\right)\left(\frac{\kappa\cos^2\theta}{1+\beta}-\Lambda\Omega^2\right)}\right.$$

$$\left.-\frac{\beta}{(1+\beta)\left(\frac{\kappa\cos^2\theta}{1+\beta}-\Lambda\Omega^2\right)\Gamma^2}+\frac{\sin^2\theta}{\left(\frac{\kappa\cos^2\theta}{\beta}-\Lambda\Omega^2\right)\Gamma}+\frac{\cos^2\theta}{\left(\frac{\kappa\cos^2\theta}{1+\beta}-\Lambda\Omega^2\right)\left(\frac{1+\beta}{\beta}\right)\Gamma}\right\}. \tag{4.83}$$

The dimensionless dispersion relation for a field-free atmosphere can be obtained from Equation (4.79) by taking the limit of zero field strength, i.e. $\beta \to \infty$. This yields (Chapter 3, Equation (3.52); see also Evans and Roberts, 1990)

$$2a\frac{U(-a+1,m+3,2\kappa)}{U(-a,m+2,2\kappa)} = -\frac{(m+1)}{\kappa}+\frac{\Omega^2+1}{\Omega^2}+\frac{(m+1)(\Lambda\Omega^2-\kappa)(1-\Omega^4)}{\gamma\,X\,\Omega^2}, \tag{4.84}$$

where (see Equation (4.81) for Ω^2 and Λ)

$$X = \Lambda\kappa+\frac{\gamma\,\Lambda^2\,\Omega^2}{2}\left[-1+\left\{1-\frac{4\kappa}{\gamma^2\Lambda}\left[\frac{(\gamma-1)+\Omega^2(\Omega^2-\frac{\kappa}{\Lambda})}{\Omega^2}\right]\right\}^{1/2}\right]\,. \tag{4.85}$$

Equations (4.79) and (4.84) are derived in a general way so that they allow for different temperatures T_c and T_p in the chromosphere and convection zone and hence different sound speeds ($c_{sc} \neq c_{sp}$). However, in the following sections, the solutions to (4.79) are discussed for $T_p = T_c$ and $c_{sp} = c_{sc}$ for which the dimensionless terms $\mathcal{X}$ and Λ in Equation (4.81) reduce to

$$\mathcal{X} = \frac{2\beta}{2\beta+\gamma}\,, \qquad \Lambda = \frac{(m+1)}{\gamma}\,. \tag{4.86}$$

Further, it is assumed that the equilibrium is marginally stable, i.e. $m = \frac{1}{\gamma-1}$, and hence $\Lambda = m$.

Equation (4.84) is also in agreement with Campbell and Roberts (1989) when $T_p = T_c$.

4.6 Solutions To The Dispersion Relation

4.6.1 Asymptotic Solution for field-free case in the limit as $\kappa \to \infty$

The dispersion relation for the field-free case is given by Equation (4.84). The left hand side of this dispersion relation can be simplified in the limit as $\kappa(= Kz_o) \to \infty$ (short wavelength limit) by using the following expansion (see Abramowitz and Stegun, 1965; p. 508)

$$U(a,b,z) = z^{-a} \sum_{n=0}^{R-1} \left\{ \frac{(a)_n(1+a-b)}{n!}(-z)^{-n} + O\left(|z|^{-R}\right) \right\} ,$$

$$\left(\frac{-3}{2}\pi < \arg z < \frac{3}{2}\pi\right) . \tag{4.87}$$

Thus considering only the first term (i.e. $n = 0$), the left hand side of the dispersion relation (4.84) can be written as

$$2a\frac{U(-a+1,m+3,2\kappa)}{U(-a,m+2,2\kappa)} \sim 2a\ \frac{(2\kappa)^{a-1}(1-a)_0(1+(1-a)-(m+3))}{(2\kappa)^a(-a)_0(1-a-(m+2))} ,$$

$$\sim 2a\ \frac{1}{(2\kappa)}\frac{(-1-a-m)}{(-1-a-m)} , \tag{4.88}$$

and so

$$2a\frac{U(-a+1,m+3,2\kappa)}{U(-a,m+2,2\kappa)} \sim \frac{a}{\kappa} \to 0 \text{ as } \kappa \to \infty . \tag{4.89}$$

Consider the right hand side of the dispersion relation (4.84). As $\kappa \to \infty$

$$\text{r.h.s of Equation (4.84)} = \frac{\Omega^2+1}{\Omega^2} - \frac{(m+1)(1-\Omega^4)}{\gamma\Omega^2\left[\Lambda + \frac{\gamma\Lambda^2\Omega^2}{2\kappa}\left\{1 - \frac{4\kappa}{\gamma^2\Lambda}\left[\frac{(\gamma-1)+\Omega^2(\Omega^2-\frac{\kappa}{\Lambda})}{\Omega^2}\right]\right\}^{1/2}\right]} .$$

(4.90)

Now

$$\frac{\gamma\,\Lambda^2\,\Omega^2}{2\kappa}\left\{1 - \frac{4\kappa}{\gamma^2\Lambda}\left[\frac{(\gamma-1)+\Omega^2(\Omega^2-\frac{\kappa}{\Lambda})}{\Omega^2}\right]\right\}^{1/2}$$

$$\sim \frac{\gamma \Lambda^2 \Omega^2}{2\kappa} \left\{ 1 + \frac{4\kappa^2}{\gamma^2 \Lambda} \right\}^{1/2} \sim \Lambda \Omega^2 \text{ as } \kappa \to \infty \tag{4.91}$$

and so Equation (4.90) becomes

$$\text{r.h.s of Equation (4.84)} = \frac{\Omega^2 + 1}{\Omega^2} - \frac{(m+1)(1-\Omega^4)}{\gamma \Lambda \Omega^2 (1+\Omega^2)} . \tag{4.92}$$

But (see Equations (4.81) and (4.73))

$$\frac{(m+1)(1-\Omega^4)}{\gamma \Lambda \Omega^2} = \frac{\rho_p}{\rho_c} .$$

Thus, the dispersion relation (4.84) in the limit as $\kappa \to \infty$ becomes

$$\left(\Omega^2 + 1\right) = \frac{\rho_p}{\rho_c} \left(1 - \Omega^2\right) , \tag{4.93}$$

that is

$$\Omega^2 = \frac{(\rho_p - \rho_c)}{(\rho_p + \rho_c)} \text{ or equivalently } \omega^2 = gK \frac{(\rho_p - \rho_c)}{(\rho_p + \rho_c)} . \tag{4.94}$$

Several conclusion can be drawn from the dispersion relation (4.94). The frequency ω is real (i.e. the interface is stable) if $\rho_p > \rho_c$, i.e. the plasma lying below the interface is denser than that above the interface; if however, $\rho_p < \rho_c$, the interface is unstable. It is particularly interesting to note that the stability of the interface depends merely on the values of the densities at the interface itself and is completely independent of the density variation away from the interface.

The dispersion relation (4.94) is identical to the dispersion relation (4.48) valid for an atmosphere with constant sound speed either side of $z = 0$. Thus, as the details of an atmosphere are changed, the short wavelength limit dispersion relation remains unchanged and depends only on the plasma densities at the interface. The mode responds only to the interface conditions and not to the temperature or density distributions away from the interface.

4.6.2 Asymptotic Solution in the limit as $\kappa \to 0$

It is possible to derive an asymptotic solution to Equation (4.79), valid for $\kappa \ (= Kz_o) \to 0$, in exactly the same way as in the previous chapter. Asymptotic results of this type

are particularly useful in determining the effects of non-parallel propagation (i.e. when the wave vector is at an angle to the magnetic field) on the frequency dependence of the f- and p-modes upon the general wavenumber K and the magnetism β. The two types of solution of Equation (4.79), the f-modes and p-modes, are considered separately.

(a) The p-modes

The same approach as carried out in Chapter 3 (Section 3.3) is used to find the asymptotic solution in the limit $\kappa \to 0$. The dimensionless dispersion relation (4.79) is expanded in powers of κ to obtain the correction to the p-mode frequency due to the magnetic field. To do this, consider writing the dimensionless dispersion relation (4.79) in the following form :

$$2a\frac{U(-a+1,m+3,2\kappa)}{U(-a,m+2,2\kappa)} = -\frac{(m+1)}{\kappa} + \frac{(1+\Omega^2)}{\Omega^2}$$

$$-\frac{\wedge(1-\Omega^4)\left\{K'_\beta\left(\kappa\cos^2\theta - \wedge\Omega^2\right) + \kappa\sin^2\theta\left(\frac{1+\beta}{\beta}\right)\left(\frac{\kappa\cos^2\theta}{1+\beta} - \wedge\Omega^2\right)\right\}}{\mathcal{X}\kappa\Omega^2\left\{K'_\beta\left[\left(\frac{1+\beta}{\beta}\right)\left(\frac{\kappa\cos^2\theta}{1+\beta} - \wedge\Omega^2\right)\Phi - \wedge\cos^2\theta\right] - \wedge\sin^2\theta\left(\frac{1+\beta}{\beta}\right)\left(\frac{\kappa\cos^2\theta}{1+\beta} - \wedge\Omega^2\right)\right\}} . \tag{4.95}$$

In the limit $\kappa \to 0$, the Taylor series expansion of the right hand side of Equation (4.95) is given by

$$\text{rhs. of Equation(4.95)} = 1 - \frac{a_8\,\Omega^8 + a_4\,\Omega^4 + a_0}{\Omega^2(\Omega^4 - 1)} + O(\kappa)\,, \tag{4.96}$$

where

$$a_8 = \frac{(\gamma+2\beta)^2}{4\gamma\beta(\beta+1)}\,, \quad a_4 = \frac{2\gamma}{\Gamma}\sin^2\theta - \frac{\gamma}{\beta}\cos^2\theta + \frac{2\gamma\beta(\cos^2\theta\Gamma - 1)}{(\beta+1)\Gamma^2} - 1\,,$$

$$a_o = \frac{\gamma\left\{(1+\beta)\Gamma\sin^2\theta + 2\beta\Gamma\cos^2\theta - 2\beta - \Gamma\right\}\sin^2\theta}{\beta\Gamma}$$

$$+\frac{\gamma\beta(\cos^4\theta\Gamma^2 - 2\Gamma\cos^2\theta + 1)}{(\beta+1)\Gamma^2} + 1 - \gamma\,. \tag{4.97}$$

But the left hand side of Equation (4.79), i.e.

$$2a\frac{U\left(-a+1,m+3,2\kappa\right)}{U\left(-a,m+2,2\kappa\right)} = -\frac{(m+1)}{\kappa}\left\{\frac{M(-1-a-m,-m-1,2\kappa)-\mathcal{M}_2}{M(-1-a-m,-m,2\kappa)-\mathcal{M}_4}\right\}, \quad (4.98)$$

would appear to become infinite as $\kappa \to 0$. See Equation (3.58) and thereafter of Chapter 3, Section 3.3 for $\mathcal{M}_2$ and $\mathcal{M}_4$. Using the same arguments as shown in Section 3.3 of Chapter 3, it follows that

$$\Omega^2 = \Omega_\star^2 \equiv 1 + \frac{2n}{m}, \qquad n = 1, 2, 3..., \quad (4.99)$$

where n is the radial order of the mode. Solution (4.99) is the first approximation to the Equation (4.79) and is independent of magnetic field or atmospheric effects. This is not surprising since the modes possessing extremely small values of K will be the modes that have turning points deep within the solar interior. Thus, the frequency of such modes will be dominated by the temperature profile of the convection zone, rather than by any chromospheric structuring.

The effect, then, of a lower chromospheric magnetic field on these p-mode frequencies having small but finite wavenumbers that satisfy the inequality $\kappa \ll 1$ may be calculated by assuming that the accuracy of the first approximation to the frequency given by (4.99) is increased by setting $\Omega^2 \sim \Omega_\star^2 + \delta$. Thus (after an analysis similar to that of Section 3.3, Chapter 3), in the presence of magnetic field the p-modes are described by

$$\Omega^2 \sim \Omega_\star^2 + \mathcal{P}_n(2KH_o)^{m+2}, \quad (4.100)$$

with $\mathcal{P}_n$ given by

$$-\frac{(m+1)^{m+1}\Gamma(1+m+n)}{m\Gamma(m+1)\Gamma(m+2)\Gamma(n)\Omega_\star^2(\Omega_\star^4-1)}\left[a_8\Omega_\star^8 + a_4\Omega_\star^4 + a_o - \left(\frac{m}{m+2}\right)\Omega_\star^4(\Omega_\star^4-1)\right] \quad (4.101)$$

where $H_o = c_{sp}^2/(\gamma g)$ is the pressure scale height at the top of the convection zone.

It may be noted that the frequency corrections given in Equation (4.100) are of order K^{m+2}, the same order as obtained by Campbell and Roberts (1989) except that here $K = \left(k_x^2 + k_y^2\right)^{1/2}$ whereas in Campbell and Roberts (1989) $K = k_x$, $k_y = 0$. Thus, for $K = k_x$ (i.e. $\theta = 0$ so that $k_y = 0$) the two results are in agreement.

After some algebra (see Appendix A3, Section 6) the behaviour of high order frequencies in the limit $n \to \infty$ is found to be

$$\nu \sim \nu_* - \frac{\left(a_8 - \frac{m}{m+2}\right)}{(m+1)m^2\Gamma(m+1)\Gamma(m+2)} \left(\frac{\gamma m}{2}\right)^{2m+2} \nu_* \left(\frac{\nu}{\nu_c}\right)^{2m+2} \left(\frac{H_o}{R_{sun}}\right) l \,, \quad (4.102)$$

where

$$\nu = \frac{\omega}{2\pi} \,, \qquad \nu_* = \frac{\omega_*}{2\pi} \,, \qquad \nu_c = \frac{1}{2\pi}\left(\frac{\gamma g}{4H_o}\right)^{1/2} \,, \qquad k_x \sim \frac{l}{R_{sun}} \,. \quad (4.103)$$

Note that $\nu - \nu_* \propto l$, i.e. the frequency shift of high order modes is proportional to the degree l.

In the absence of a magnetic field, the coefficients a_8, a_4, and a_o reduce to

$$a_8' = \frac{1}{\gamma} \,, \qquad a_4' = 1 - \frac{2}{\gamma} \,, \qquad a_o' = \frac{1}{\gamma} - 1 \,, \quad (4.104)$$

giving a correction due to a field-free isothermal atmosphere (see also, Equation (3.82) in Chapter 3). Thus the frequency shift due purely to changes in magnetic field strength can be found by considering the differences in the coefficients between (4.97) and (4.104). Therefore the asymptotic formula for the frequency shift is

$$\Delta\nu = -\frac{(m+1)^{m+1}\Gamma(1+m+n)}{4\pi m(m+2)\Gamma(m+1)\Gamma(m+2)\Gamma(n)\Omega_*^3(\Omega_*^4-1)} \times$$

$$\left[\left(a_8 - \frac{m}{\gamma}\right)\Omega_*^8 + \left(a_4 + m + \frac{2}{\gamma}\right)\Omega_*^4 + \left(a_o(m+2) - \frac{1}{\gamma} + 2\right)\right](2KH_o)^{m+2}\,(gK)^{\frac{1}{2}}. \quad (4.105)$$

Note that the coefficients a_8, a_4 and a_0 are dependent on the propagation angle θ and hence $\Delta\nu$ also depends on θ. Also to be noted is the minus sign on the right hand side of Equation (4.105), suggesting that p-modes undergo a *decrease* in frequency due to the presence of a chromosphere within which the horizontal magnetic fields are structured in such a way that the Alfvén speed remains constant with height.

(b) The *f*-mode

In the absence of a magnetic field and in the incompressible limit, i.e. $\Delta(=\text{div }\mathbf{v}) \to 0$, Equations (4.7a,b,c) possess the solution $v_z \propto e^{\left(k_x^2+k_y^2\right)^{1/2} z}$ with $\omega^2 = g\left(k_x^2+k_y^2\right)^{1/2}$ (i.e. $\Omega^2 = 1$). The solution $\Omega^2 = 1$ is the *f*-mode. The *f*-mode is incompressible and its frequency is independent of the thermal stratification. In the presence of a magnetic field the *f*-mode no longer remains incompressible and its frequency is influenced by the magnetic forces and the compressibility of the gas (see Campbell and Roberts, 1989; Evans and Roberts, 1990; Miles and Roberts, 1991). It would be interesting to investigate the effects of non-parallel propagation on the *f*-mode frquency in the presence of a magnetic field.

Since the *f*-mode has a solution Ω^2 close to unity, the analysis of part (a) cannot be used for finding out the corrections due to the magnetic field. Returning to the dimensionless dispersion relation, note that

$$2a\frac{U\left(-a+1,m+3,2\kappa\right)}{U\left(-a,m+2,2\kappa\right)} = -\frac{(m+1)}{\kappa}\left\{\frac{M(-1-a-m,-m-1,2\kappa)-\mathcal{M}_2}{M(-1-a-m,-m,2\kappa)-\mathcal{M}_4}\right\}, \quad (4.106)$$

where

$$\mathcal{M}_2 = (2\kappa)^{(m+2)}\frac{M(1-a,m+3,2\kappa)\Gamma(1-a)\Gamma(-m-1)}{\Gamma(-a-m-1)\Gamma(m+3)}, \quad (4.107)$$

$$\mathcal{M}_4 = (2\kappa)^{(m+1)}\frac{M(-a,m+2,2\kappa)\Gamma(-a)\Gamma(-m)}{\Gamma(-a-m-1)\Gamma(m+2)}. \quad (4.108)$$

Here it is assumed that m is not an integer. Expanding the M-functions in power series in $\kappa(=Kz_o)$, Equation (4.106) gives

$$2a\frac{U\left(-a+1,m+3,2\kappa\right)}{U\left(-a,m+2,2\kappa\right)} = \frac{-(m+1)}{\kappa}\left[1-\frac{2(1+a+m)}{m(m+1)}(\kappa)\right.$$
$$\left.-\frac{4(1+a+m)(1+a)}{m^2(m^2-1)}(\kappa)^2+\mathcal{Y}_o(\kappa)^{m+1}\right], \quad (4.109)$$

where

$$\mathcal{Y}_o = \frac{2^{m+1}\Gamma(-a)\Gamma(-m)}{\Gamma(m+2)\Gamma(-1-a-m)}. \quad (4.110)$$

(This expansion is not valid for the p-modes, since for them a is close to an integer and then $\mathcal{Y}_o$ is large. Also note that in writing Equation (4.109), the terms of order $(\kappa)^3$ (leading ignored term) and $(\kappa)^{m+2}\,\Gamma(1-a)$ have been ignored. This means that $1 < m < 2$; otherwise, additional terms should be added to Equation (4.109)).

Equation (4.79) can now be written as

$$\left[\frac{2(1+a+m)}{m}\Omega^2 - 1 - \Omega^2 + \frac{4(1+a+m)(1+a)}{m^2(m-1)}\Omega^2\,(\kappa) - \mathcal{Y}_o(m+1)\Omega^2(\kappa)^m\right]\mathcal{Z}$$

$$= \Gamma_m\left\{K'_\beta\left(\kappa\cos^2\theta - m\Omega^2\right) + \kappa\sin^2\theta\left(\frac{1+\beta}{\beta}\right)\left(\frac{\kappa\cos^2\theta}{1+\beta} - m\Omega^2\right)\right\}\,, \qquad (4.111)$$

where

$$\Gamma_m = \frac{(m+1)}{\Gamma}\left(1-\Omega^4\right)\,, \quad \kappa = Kz_o\,, \quad k_x = K\cos\theta\,, \quad k_y = K\sin\theta\,,$$

$$\mathcal{Z} = \kappa\left\{K'_\beta\left[\left(\frac{1+\beta}{\beta}\right)\left(\frac{\kappa\cos^2\theta}{1+\beta} - m\Omega^2\right)\left(\Phi - \frac{m\sin^2\theta}{K'_\beta}\right) - m\cos^2\theta\right]\right\}\,. \qquad (4.112)$$

From the definition of a under the adiabatic condition (see Chapter 3, Equations (3.37) and (3.38))

$$1 + a + m \;=\; \frac{m}{2}\left(\Omega^2+1\right)\,, \qquad (4.113)$$

and so Equation (4.111) gives

$$\left[\left(\Omega^4-1\right) + \frac{2(1+a)\left(\Omega^4+\Omega^2\right)\kappa}{m(m-1)}\mathcal{Y}_o(m+1)\Omega^2(\kappa)^m\right]\mathcal{Z} =$$

$$\Gamma_m\left\{K'_\beta\left(\kappa\cos^2\theta - m\Omega^2\right) + \kappa\sin^2\theta\left(\frac{1+\beta}{\beta}\right)\left(\frac{\kappa\cos^2\theta}{1+\beta} - m\Omega^2\right)\right\}\,. \qquad (4.114)$$

Expanding $\mathcal{Z}$ in a Taylor series in κ gives

$$\mathcal{Z} \;=\; -\left\{\frac{m\left(\Omega^4-1\right)\kappa}{\Gamma} + \frac{(\kappa)^2}{\Omega^2}\left(d_8\Omega^8 + d_4\Omega^4 + d_o\right)\right\} + ... \qquad (4.115)$$

where

$$d_8 = \frac{\beta}{(\beta+1)\Gamma^3},$$

$$d_4 = \frac{(2\beta-(\beta+1)\Gamma)\sin^2\theta}{\beta\Gamma^2} - \frac{(\beta+1)\cos^2\theta}{\beta\Gamma} + \frac{2\beta(\Gamma\cos^2\theta-1)}{(\beta+1)\Gamma^3},$$

$$d_o = \frac{\left((1+\beta)\Gamma\sin^2\theta + 2\beta\Gamma\cos^2\theta - 2\beta\right)\sin^2\theta}{\beta\Gamma^2} + \frac{\beta\left(\Gamma^2\cos^4\theta - 2\Gamma\cos^2\theta + 1\right)}{(\beta+1)\Gamma^3} \quad (4.116)$$

Note that as $\kappa \to 0$, $\mathcal{Z} \to 0$ and so from Equation (4.111) $\Omega^4 \to 1$ as $\kappa \to 0$.

To obtain the correction due to the magnetic field, set

$$\Omega^2 \sim 1 + f_o(\kappa)^s, \quad (4.117)$$

where s and f_o are to be determined. From the definition of a

$$a \sim -1 + \frac{m}{2} f_o(\kappa)^s. \quad (4.118)$$

The dispersion relation (4.79) is expanded in powers of κ in order to find a solution with $\Omega^2 \to 1$ as $\kappa \to 0$. The result is

$$\Omega^2 \sim 1 + f_o(\kappa)^{m+2}, \quad (4.119)$$

where

$$f_o = \frac{2^m \cos^2\theta\left\{(1+\sin^2\theta)+2\beta\right\}}{\beta(\beta+1)m\Gamma(m+2)}. \quad (4.120)$$

Thus, in the presence of a magnetic field, the f-mode frequency *increases* in a manner dependent on $(\kappa)^{m+2}$. The shift in frequency *decreases* with increasing θ but is positive for all field-strengths. For $\theta = \pi/2$, corresponding to propagation perpendicular to the magnetic field, $f_o = 0$. For $\theta = 0$, corresponding to propagation parallel to the magnetic field,

$$f_o(\theta = 0) \;=\; \frac{(1+2\beta)2^m}{\beta(\beta+1)m\Gamma(m+2)}\,. \tag{4.121}$$

The result (4.121) was first obtained by Campbell and Roberts (1989).

4.6.3 Numerical Solutions

In this subsection the numerical solutions of the dispersion relations (4.79) and (4.84) are considered. It is important to assess how well the asymptotic solutions derived in the previous subsection agree with the numerical solutions to the full dispersion relation. For this reason, some of the following figures are shown with solid curves representing the solutions to the full dispersion relation and dotted curves representing the results obtained from the asymptotic formula, this formula being valid for small Kz_o. For spherical degree l restricted to 500 (i.e. $l < 500$), the two solutions are expected to agree closely. Since the interest is in the trapped modes, only those frequencies less than the magnetoacoustic cut-off frequencies are considered. Also, one of the main concerns here is to investigate the effects of non-parallel propagation on the frequencies of *f*- and *p*- modes, and so, for ease of comparison, the figures are drawn using the same set of parameters as given in Table 3.1 (see Chapter 3) except for the values of γ and m which here are taken to be $\gamma = 5/3$, $m = 1.5$.

In the following figures, the frequency shift $\Delta\nu$ is plotted against various other parameters. The quantity $\Delta\nu$ for the *p*-modes is obtained by taking the difference between the cyclic frequency ν_b (obtained by solving the dispersion relation (4.79)) in the presence of a magnetic field and the cyclic frequency ν_f in a field-free atmosphere (obtained by solving the dispersion relation (4.84)). The result is shown by solid curves. The asymptotic formula for the frequency shift $\Delta\nu$ is given by Equation (4.105). The result is shown by dotted curves. The cyclic frequency ν_f is also referred to as the 'base' frequency. For the *f*-mode ($n = 0$), once again the dispersion relation (4.79) is used to evaluate the cyclic frequency ν_b in the presence of a magnetic field. Thus the frequency shift for the *f*-mode is obtained by taking the difference between this cyclic frequency ν_b and the field-free frequency $\nu_\star(= \frac{(gK)^{1/2}}{2\pi})$. The result is shown by solid curves. For asymptotic solutions, Equation (4.120) is used and the results are represented by dotted curves.

Figures 4.2a,b illustrate the change in cyclic frequency $\Delta\nu$ as a function of base frequency for *p*-modes of degree $l = 100$, 200, 300. The Alfvén speed is (a) $v_{Ac} = 0.4967$ km/sec, corresponding to $B_c = 10$G at the base of the chromosphere and (b) $v_{Ac} = 6.773$ km/sec, corresponding to $B_c = 100$G. Here, the angle θ is set to 0, corresponding

to propagation in the direction of the magnetic field. The solid curves represent the frequency shifts obtained from the full dispersion relations (4.79) and (4.84) whereas the dotted curves represent the solutions to asymptotic formula (4.105).

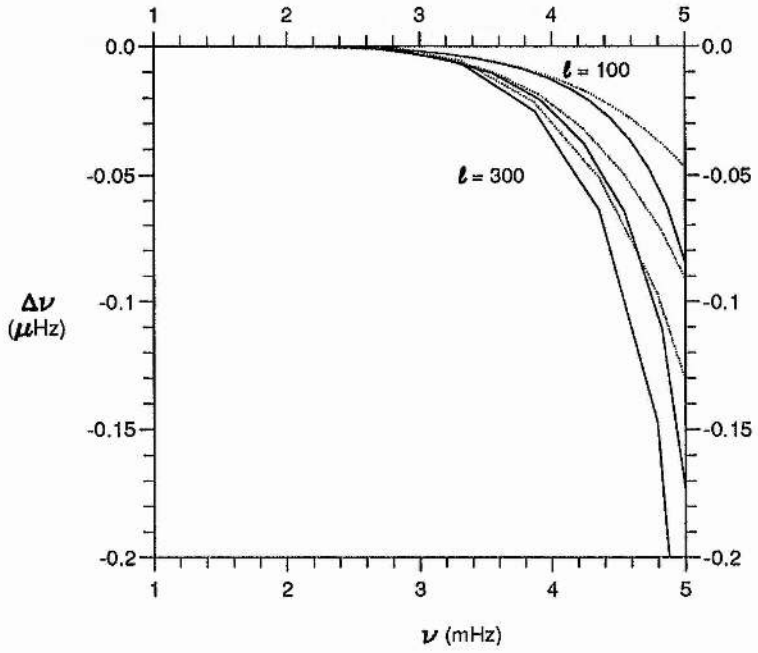

Figure 4.2a

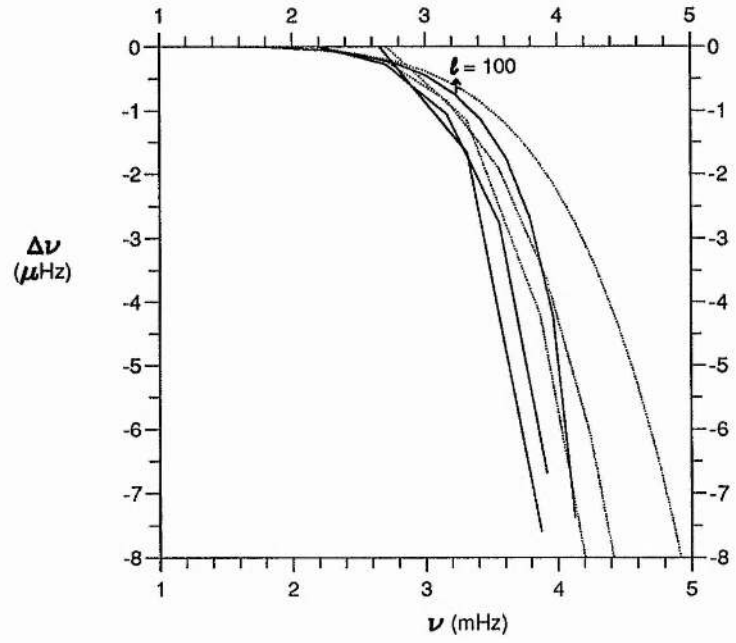

Figure 4.2: The frequency shift $\Delta\nu$ as a function of frequency ν for different values of the degree l when the propagation angle $\theta = 0$. The solid curves show the numerical solutions to Equations (4.79) and (4.84) while the dotted curves illustrate the asymptotic formula (4.105). The case illustrated here is for (a) $v_{Ac} = 0.4967$ km/sec. (corresponding to a magnetic field of $B_c = 10$G at the base of the chromosphere) and (b) $v_{Ac} = 6.7335$ km/sec. (corresponding to a magnetic field of $B_c = 100$G at the base of the chromosphere).

In Figure 4.2(a) the dotted curves and the solid curves (for each l) are in good agreement up to a frequency $\nu \sim 4$ mHz. Beyond this frequency, the dotted curves lie well above the solid curves suggesting that the asymptotic formula underestimates the effects of magnetism. In Figure 4.2(b) the dotted curves agree well with the solid curves up to 3 mHz, beyond which the dotted curves lie above the solid curves. Thus for higher frequencies and higher magnetic field strengths, it is necessary to consider the numerical solutions to the full dispersion relations. Nonetheless, it is interesting to note that the asymptotic results and the exact solutions show similar trends in the frequency shifts, i.e. the negative frequency shifts increase with the increase in frequency. Furthermore, the magnitudes of the negative frequency shifts increase with the increase in the value of degree l. The property $\Delta\nu \propto l$ is consistent with Equation (4.102).

It is of interest to assess the dependence of a varying propagation angle θ on the frequency shifts. Figure 4.3 shows the frequency shifts plotted against frequency for

three different propagation angles θ (=0°, 45°, 90°). Here the degree l is set to be 200. Figures 4.3a,b display the frequency shift curves for v_{Ac} = 0.4967 km/sec and v_{Ac} = 6.733 km/sec, respectively. As in Figure 4.2, the asymptotic solutions agree well with the solutions to the full dispersion relation up to about 4 mHz in Figure 4.3(a) and 3 mHz in Figure 4.3(b). Beyond these frequencies the asymptotic formula underestimates the effects of magnetism for all propagation angles θ. In each case the top curve represents $\theta = 0$ and the bottom one $\theta = 90°$. It is also clear from these figures that there is no significant variation in the frequency shift of p-modes due to changing propagation angles θ. This lack of noticeable variation may be restricted to intermediate degree l and hence it would be advisable to consider the situation for other values of the degree l.

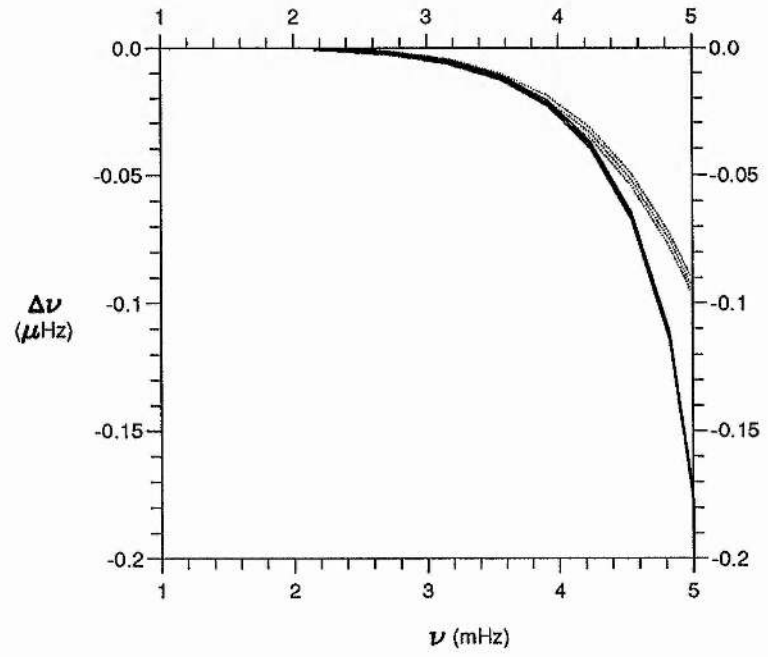

Figure 4.3a

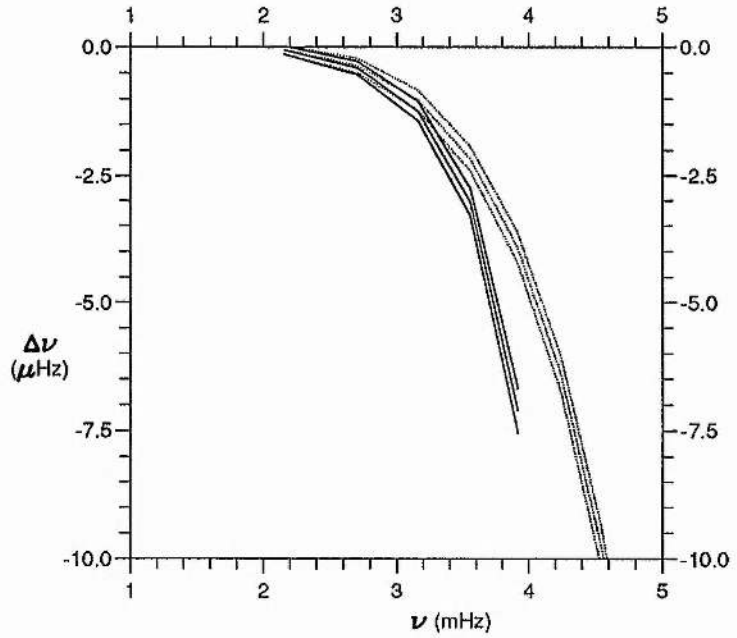

Figure 4.3: The frequency shift $\Delta\nu$ as a function of frequency ν for three different values of the propagation angle θ (= 0, 45°, 90°). The numerical solutions are displayed by solid lines while the asymptotic solutions are represented by the dotted lines. The top curve in each set corresponds to θ = 0 and the bottom one to $\theta = 90°$. The curves are for degree $l = 200$. Case (a)$v_{Ac} = 0.4967$ km/sec, and (b)$v_{Ac} = 6.7735$ km/sec. Note the change in scale in $\Delta\nu$ from (a) to (b).

Figure 4.4 shows the dependence of non-parallel propagation on the frequency shifts of the 1st p-mode ($n = 1$) as a function of degree l for three different propagation angles θ (=0°, 45°, 90°). Obviously as l is changed the frequencies change accordingly. Figures 4.4a,b display results for chromospheric Alfvén speeds $v_{Ac} = 0.496$ km/sec and $v_{Ac} = 6.7735$ km/sec, respectively. Note the change in scale in $\Delta\nu$ from case (a) to case (b). Comparing Figures 4.4(a) and 4.4(b), it is clear that there is a significant change in the frequency shifts for higher l values, suggesting that the effects of non-parallel propagation are important when high degree ($l > 500$) p-modes are considered. It may also be observed that the magnitude of this change in frequency shift increases with an increase in Alfvén speed v_{Ac}.

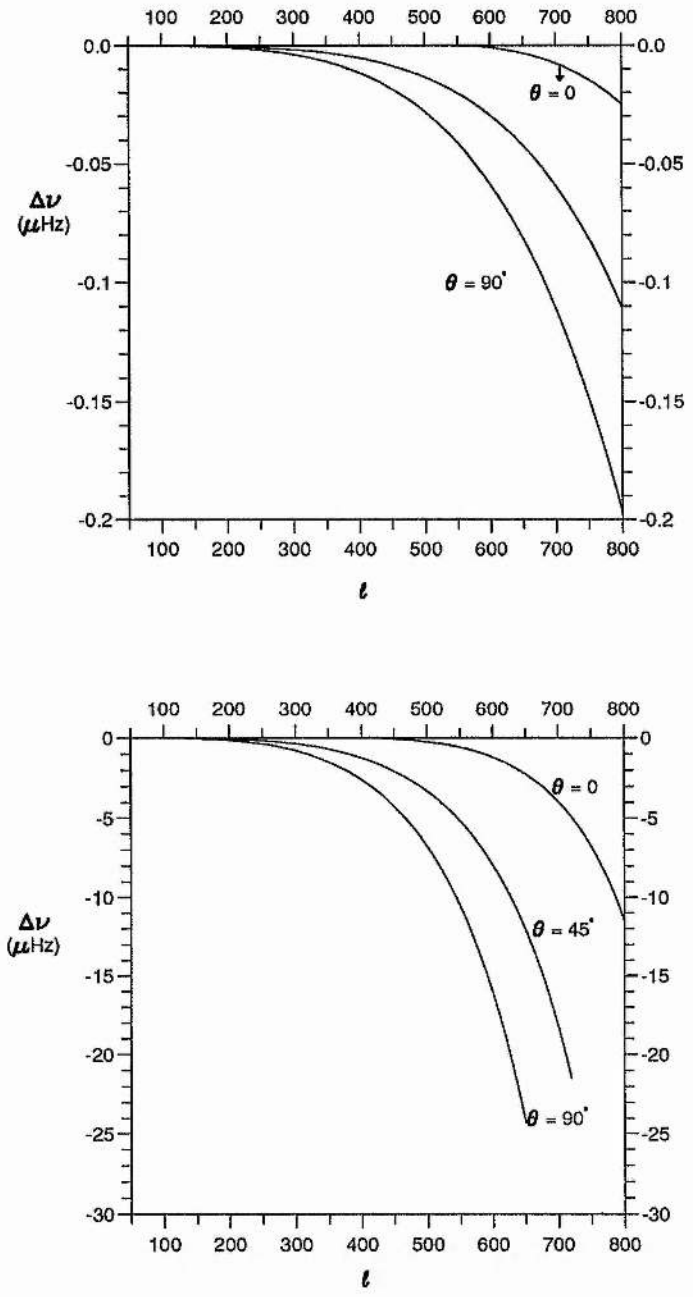

Figure 4.4: The frequency shift $\Delta\nu$ for the first p-mode as a function of frequency ν of degree l for propagation angles $\theta = 0,\ 45°,\ 90°$. (a)$v_{Ac} = 0.4967$ km/sec and (b)$v_{Ac} = 6.773$ km/sec. Note the change of scale in $\Delta\nu$ from (a) to (b).

It is rewarding to examine the first p-mode ($n = 1$) for angle $\theta = 0$ in Figures 4.4a,b in detail. Figure 4.5a,b display the frequency shift curves for the $n = 1$ p-mode for v_{Ac}

= 0.4967 km/sec and v_{Ac} = 6.733 km/sec, respectively. It is surprising to note that in Figure 4.5(a), the $n = 1$ p-mode shows positive frequency shift up to $l \sim 580$ followed by a drop thereafter. In Figure 4.5(b), the frequency shifts are positive up to about $l \sim 410$ after which they are negative in accordance with the asymptotic formula. Note the decrease in the value of degree l with the increase in magnetic field strength at which the frequency shift is maximum. In Figure 4.5a, the maximum frequency shift $\Delta\nu_{max}$ = 1.23 nHz at $l = 460$, while in Figure 4.5b $\Delta\nu_{max}$ = 40.2 nHz at $l = 330$.

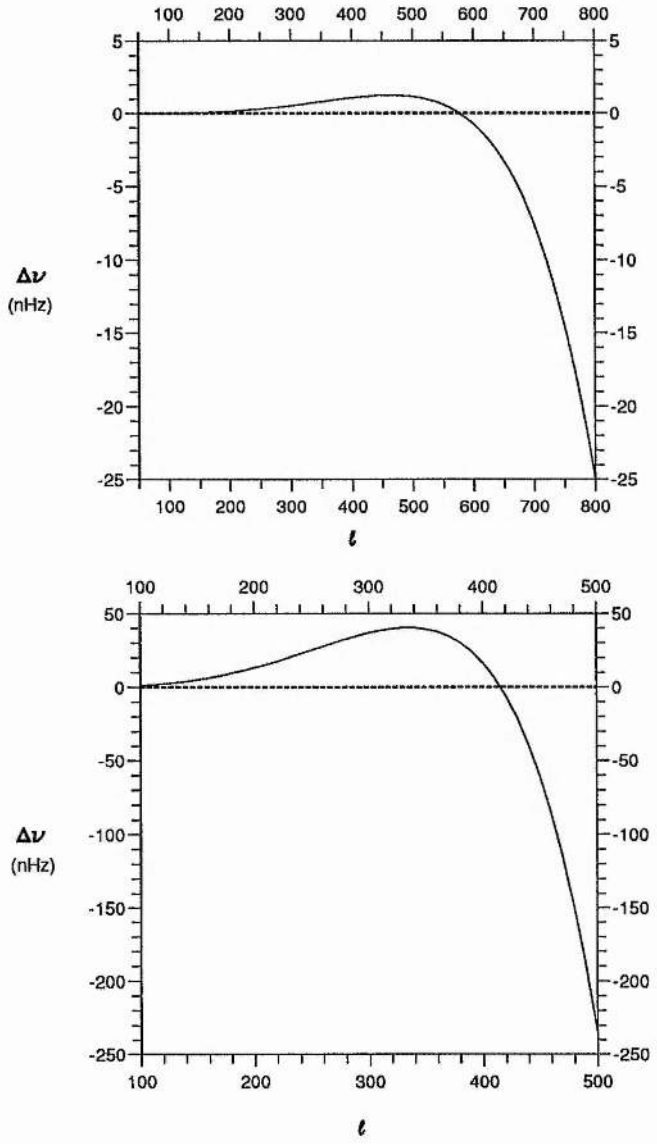

Figure 4.5: A closer look at the curves for prop. angle $\theta = 0$ in Figure 4.4 in which the frequency shift $\Delta\nu$ is plotted as a function of degree l. (a)v_{Ac} = 0.4967 km/sec, (b) v_{Ac} = 6.773 km/sec.

Figures 4.6a,b display the frequency shifts as functions of degree l, illustrating the effects of varying the propagation angle θ for a higher value of the radial order n (=5 in this case). The curves stop at the magnetoacoustic cut-off frequencies. It can be observed that for higher magnetic field strengths the changes in the frequency shift due to varying propagation angle become significant (i.e. ≥ 1 μHz) for higher values of l. However, the effects of non-parallel propagation can be neglected for low degree p-modes in the presence of weak magnetic fields (see, e.g., Figures 4.4a and 4.6a).

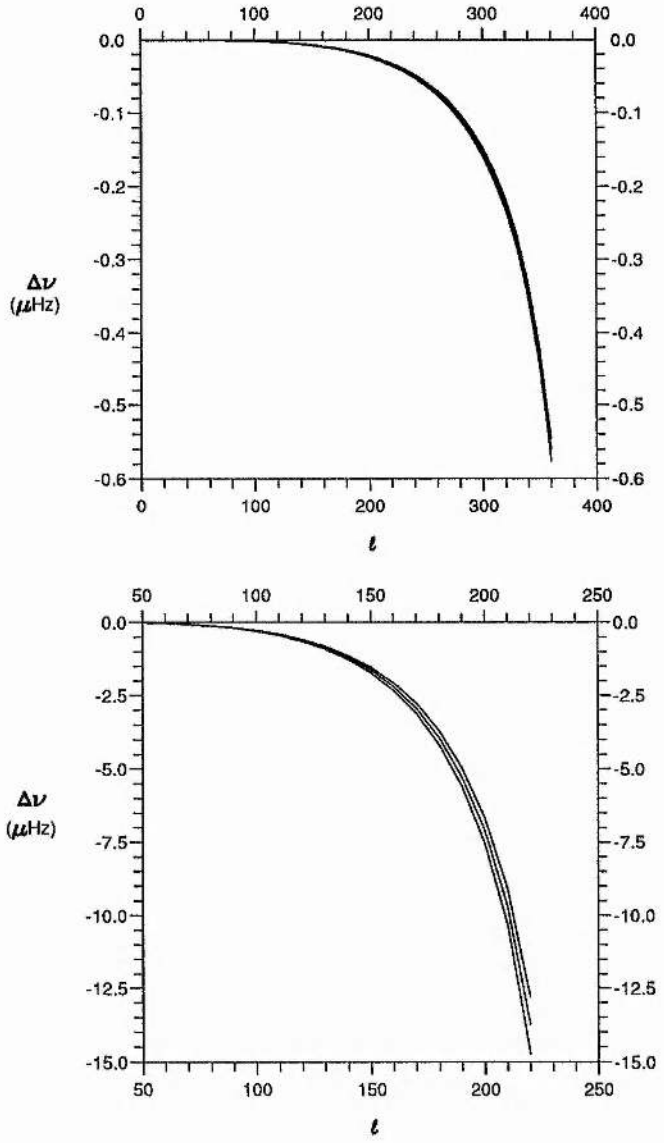

Figure 4.6: The frequency shift $\Delta\nu$ for the fifth p-mode (i.e. the solution for $n = 5$ in Equation (4.79) and (4.84)) as a function of degree l. Curves for three different values of the propagation angle (namely $\theta = 0$, 45° and 90°) are displayed, with $\theta = 0$ giving the uppermost curve and $\theta = 90°$ the lowest curve. The curves shown are for (a) $v_{Ac} = 0.4967$ km/sec and (b) $v_{Ac} = 6.773$ km/sec.

Thus, from the above figures it can be concluded that the effects of non-parallel propagation are significant for low radial order and high degree p-modes. Also apparent is the fact that the asymptotic solutions provide a good guide to understand the trends in frequency shifts but for precise values numerical solutions to the full dispersion relation are necessary.

Finally there remains an investigation of the effects of magnetism on the f-mode. In Figures 4.7a,b are plotted the frequency shifts for the f-mode as a function of degree l for propagation angles $\theta = 0, 45°, 60°$ (recall that when $\theta = 90°$, $f_o = 0$ and so the frequency shifts of the f-mode is zero). Figure 4.7a is for $v_{Ac} = 0.4967$ km/sec and Figure 4.7b is for $v_{Ac} = 6.977$ km/sec. The dotted curves represent the asymptotic solutions given by Equation (4.120), while solid curves were obtained by solving the dispersion relation (4.79) for $n = 0$. For both the asymptotic solutions and for the full solutions from the dispersion relation, the base frequency is taken to be $\Omega^2 = 1$ (corresponding, in terms of cyclic frequency, to $\nu_\star = \frac{(gK)^{1/2}}{2\pi}$). It may be noted in the graphs that although the asymptotic solutions lie above the exact solutions of the dispersion relation, the trend of positive frequency shift increasing with the increase in degree l for all three values of θ is clear. As the wave vector becomes more and more perpendicular to the magnetic field direction (i.e., as the value of θ increases) the frequency shift (for a given l and v_{Ac}) decreases and eventually becomes zero for $\theta = 90°$.

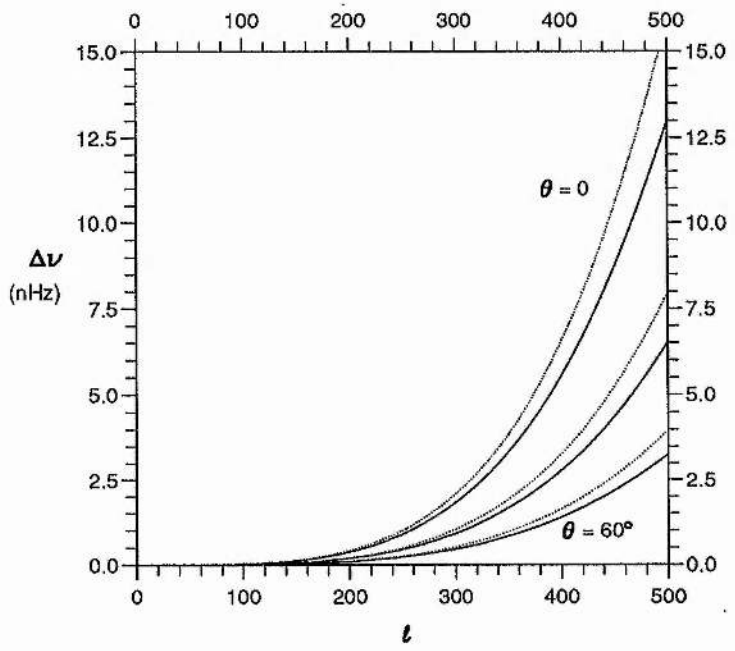

Figure 4.7a

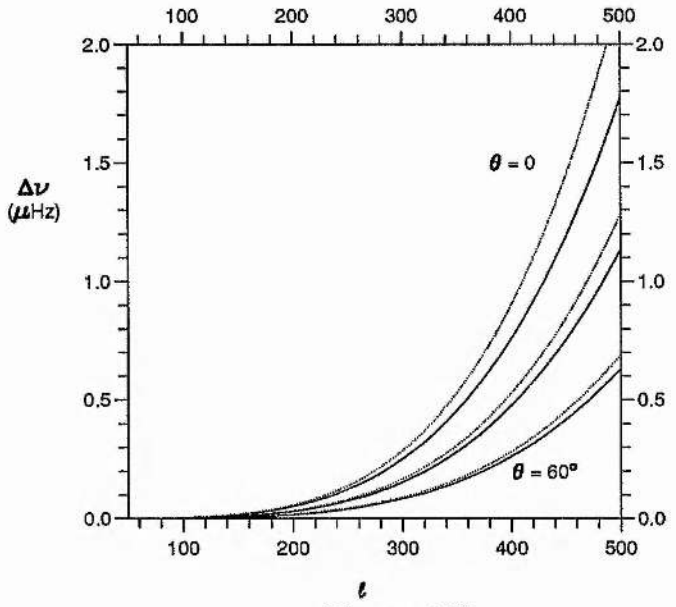

Figure 4.7b

Figure 4.7: The frequency shift $\Delta\nu$ for the f-mode as a function of degree l. Curves for three different values of the propagation angle (namely $\theta = 0$, 45° and 60°) are displayed. The curves are shown for case (a)$v_{Ac} = 0.4967$ km/sec and case (b)$v_{Ac} = 6.773$ km/sec. Solid curves are full numerical solutions of the dispersion relation (4.79) and dotted curves correspond to the asymptotic results given by Equation (4.120).

4.7 Isothermal Atmospheres

The analysis of the preceeding section was for a convection zone where the temperature increases with depth. If the convection zone is considered as isothermal so that the temperature, instead of varying linearly with depth (see Equation (4.67)), is constant i.e.

$$T_o(z) \;=\; T_p\,, \qquad\qquad z > 0\,, \tag{4.122}$$

then the square of the sound speed $c_{sp}^2 = \gamma \mathcal{R} T_p$ is constant and the general equilibrium Equation (4.1) reduces to

$$\frac{\rho_o'}{\rho} \;=\; \frac{\gamma g}{c_{sp}^2}\,. \tag{4.123}$$

On integrating (4.123) the equilibrium pressure and density profiles obtained are

$$p_o(z) = p_p e^{z/H_p}\,, \quad \rho_o(z) = \rho_p e^{z/H_p}\,, \tag{4.124}$$

where $H_p = c_{sp}^2/\gamma g$ is the constant density scale height and p_p and ρ_p are the values of pressure and density at $z = 0$. For such an equilibrium profile, the governing equation for v_z reduces to (see also Equations (4.37) and (4.38))

$$\frac{d^2 v_z}{dz^2} + \frac{1}{H_p}\frac{dv_z}{dz} + A_p v_z = 0 , \tag{4.125}$$

where

$$A_p = \frac{(\gamma-1)g^2K^2 + \omega^2\left(\omega^2 - K^2 c_{sp}^2\right)}{\omega^2 c_{sp}^2} . \tag{4.126}$$

Note that Equation (4.125) can also be obtained from the reduction of Lamb's Equation (see Equation (3.34) in Chapter 3).

Equation (4.125) has a solution of the form

$$v_z = e^{-\lambda_p z} , \qquad z > 0 , \tag{4.127}$$

where

$$2\lambda_p H_p = 1 + \left[1 - 4\left\{\frac{(\gamma-1)g^2K^2 + \omega^2\left(\omega^2 - K^2c_{sp}^2\right)}{\omega^2 c_{sp}^2}\right\}\right]^{1/2} . \tag{4.128}$$

Thus the energy density $\rho(z)v_z^2 \to 0$ as $z \to \infty$ provided the square bracket of (4.128) is positive.

The chromosphere or the upper region is considered the same as in Figure 4.1 i.e. isothermal with constant Alfvén speed. The vertical velocity v_z in the chromosphere is thus given by Equation (4.65). Matching the solutions (4.65) and (4.127) by imposing the boundary conditions that v_z and the total pressure perturbation (see equation (4.74)) are continuous at $z = 0$, the following dispersion relation is obtained

$$\left(\omega^2 - k_x^2 v_{Ac}^2\right)\left\{\frac{1}{2H_c}\left[1 - \left(1 - 4A_c H_c^2\right)^{1/2}\right]\right\} - gk_y^2 - \frac{gk_x^2 m_o^2 c_{sc}^2}{\left(k_x^2 c_{sc}^2 - \omega^2\right)}$$

$$= \left(\frac{\rho_p}{\rho_c}\right)\left(\frac{m_o^2 + k_y^2}{m_e^2 + k_y^2}\right)\left[\left\{\frac{\omega^2}{2H_p}\left[1 + \left(1 - 4A_p H_p^2\right)^{1/2}\right]\right\} - gk_y^2 - \frac{gk_x^2}{\left(k_x^2 c_{sp}^2 - \omega^2\right)}\right] , \tag{4.129}$$

where

$$m_e^2 \;=\; \frac{\left(k_x^2 c_{sp}^2 - \omega^2\right)}{c_{sp}^2} \,. \tag{4.130}$$

Equation (4.129) possesses two distinct stable modes, the magnetoacoustic (gravity modified) surface mode and the *f*-mode. Note that the dispersion relation (4.129) allows for different temperatures in the chromosphere and the convection zone (i.e., $T_p \neq T_c$).

In the absence of gravity (i.e., when $g \to 0$, $H_c^{-1} = H_p^{-1} \to 0$),

$$A_c \to -\left(m_o^2 + k_y^2\right) \;,\quad A_p \to -\left(m_e^2 + k_y^2\right) \;,$$

and so

$$\frac{1}{2H_c} - \frac{1}{2}\left(\frac{1}{H_c^2} - 4A_c\right)^{1/2} \to -\left(m_o^2 + k_y^2\right)^{1/2} \;,$$

$$\frac{1}{2H_p} + \frac{1}{2}\left(\frac{1}{H_p^2} - 4A_p\right)^{1/2} \to \left(m_e^2 + k_y^2\right)^{1/2} \;. \tag{4.131}$$

Thus, in the absence of gravity, the dispersion relation (4.129) reduces to

$$\rho_c \left(k_x^2 v_{Ac}^2 - \omega^2\right)\left(m_e^2 + k_y^2\right)^{1/2} - \rho_p\, \omega^2 \left(m_o^2 + k_y^2\right)^{1/2} \;=\; 0 \,, \tag{4.132}$$

where $\left(m_o^2 + k_y^2\right)^{1/2}$ and $\left(m_e^2 + k_y^2\right)^{1/2} > 0$. This recovers the dispersion relation describing the non-parallel propagation of the surface waves on a single magnetic interface one side of which is field-free (see Equation (2.22), Chapter 2).

Defining

$$\mathcal{L}_c = \frac{c_{sc}}{c_{sp}} \,,\quad \mathcal{V}_c = \frac{v_{Ac}}{c_{sp}} \,,\quad \mathcal{H}_p = K H_p \,,\quad \varphi = \frac{\omega}{K c_{sp}} \,, \tag{4.133}$$

the dimensionless form of the general dispersion relation (4.129) can be written as

$$\frac{\left(\mathcal{L}_c^2 \mathcal{V}_c^2 \cos^2\theta - \varphi^2\left(\mathcal{L}_c^2 + \mathcal{V}_c^2\right)\right)\left\{\left(\varphi^2 - \mathcal{V}_c^2\cos^2\theta\right)\frac{\Gamma}{2\mathcal{L}_c^2}\left[1 - \left(1 - 4A_c H_c^2\right)^{1/2}\right] - \sin^2\theta\right\} + \mathcal{C}_c}{\left(\mathcal{V}_c^2\cos^2\theta - \varphi^2\right)\left(\mathcal{L}_c^2\cos^2\theta - \varphi^2\right) + \sin^2\theta\left(\mathcal{L}_c^2\mathcal{V}_c^2\cos^2\theta - \varphi^2\left(\mathcal{L}_c^2 + \mathcal{V}_c^2\right)\right)}$$

$$= \left(\mathcal{L}_c^2 + \frac{\gamma}{2}\mathcal{V}_c^2\right)\left\{\frac{\gamma\varphi^2}{2\left(1-\varphi^2\right)}\left[1-\left(1-4A_pH_p^2\right)^{1/2}\right]-\frac{1}{\left(1-\varphi^2\right)}\right\}, \qquad (4.134)$$

where

$$\mathcal{C}_c = \mathcal{L}_c^2\cos^2\theta\left(\varphi^2-\mathcal{V}_c^2\cos^2\theta\right), \qquad A_pH_p^2 = \frac{(\gamma-1)}{\gamma^2\varphi^2}+\mathcal{H}_p^2\left(\varphi^2-1\right),$$

$A_cH_c^2 =$

$$\frac{\mathcal{L}_c^4}{\Gamma^2}\left\{\frac{\left(\mathcal{V}_c^2\cos^2\theta-\varphi^2\right)\left[(\Gamma-1)+\gamma^2\mathcal{H}_p^2\left\{\left(\mathcal{L}_c^2\cos^2\theta-\varphi^2\right)\left(\mathcal{V}_c^2\cos^2\theta-\varphi^2\right)+\mathcal{C}_l\right\}\right]+\frac{\Gamma}{\mathcal{L}_c^2\mathcal{C}_l}}{\left(\mathcal{V}_c^2\cos^2\theta-\varphi^2\right)\left(\varphi^2\left(\mathcal{L}_c^2+\mathcal{V}_c^2\right)-\mathcal{L}_c^2\mathcal{V}_c^2\cos^2\theta\right)}\right\},$$

and

$$\mathcal{C}_l = \sin^2\theta\left[\mathcal{L}_c^2\mathcal{V}_c^2\cos^2\theta-\varphi^2\left(\mathcal{L}_c^2+\mathcal{V}_c^2\right)\right]. \qquad (4.135)$$

It is clear from Equation (4.134) that to avoid singularities, $\varphi^2 \neq 1$ and

$$\left(\mathcal{V}_c^2\cos^2\theta-\varphi^2\right)\left(\mathcal{L}_c^2\cos^2\theta-\varphi^2\right)+\sin^2\theta\left(\mathcal{L}_c^2\mathcal{V}_c^2\cos^2\theta-\varphi^2\left(\mathcal{L}_c^2+\mathcal{V}_c^2\right)\right)\neq 0. \qquad (4.136)$$

These conditions lead to restrictions on the non-dimensionalised phase-speed $\varphi\,(=\omega/Kc_{sp})$ for the magnetoacoustic gravity modified surface waves. The restriction (4.136) becomes $\varphi \neq \varphi_\pm^2$, where

$$2\varphi_\pm^2 = \left(\mathcal{L}_c^2+\mathcal{V}_c^2\right)\pm\left[\left(\mathcal{L}_c^2+\mathcal{V}_c^2\right)^2-4\mathcal{L}_c^2\mathcal{V}_c^2\cos^2\theta\right]^{1/2}. \qquad (4.137)$$

Also, in order to avoid complex roots, it is required that

$$\left(1-4A_pH_p^2\right)\geq 0. \qquad (4.138)$$

This leads to the restriction $\varphi_1^2 \leq \varphi^2 \leq \varphi_2^2$, where

$$\varphi^2_{1,2} = \frac{\left(1+4\mathcal{H}_p^2\right) \mp \left[\left(1+4\mathcal{H}_p^2\right)^2 - 16\frac{(\gamma-1)}{\gamma^2}\mathcal{H}_p^2\right]^{1/2}}{8\mathcal{H}_p^2} . \tag{4.139}$$

Similarly, the requirement

$$\left(1-4A_cH_c^2\right) \geq 0 \tag{4.140}$$

suggests that if $\varphi > (c_{Tc}/c_{sp})\cos\theta$, then

$$\left(\varphi^2-\varphi_3^2\right)\left(\varphi^2-\varphi_4^2\right) \leq \frac{4\Gamma\mathcal{L}_c^2\mathcal{V}_c^2\sin^2\theta}{(\mathcal{V}_c^2\cos^2\theta-\varphi^2)}\varphi^2 ; \tag{4.141}$$

however, if $\varphi < (c_{Tc}/c_{sp})\cos\theta$ then

$$\left(\varphi^2-\varphi_3^2\right)\left(\varphi^2-\varphi_4^2\right) \geq \frac{4\Gamma\mathcal{L}_c^2\mathcal{V}_c^2\sin^2\theta}{(\mathcal{V}_c^2\cos^2\theta-\varphi^2)}\varphi^2 . \tag{4.142}$$

Here

$$\varphi^2_{3,4} = \frac{\mathcal{L}_v \mp \left\{\frac{\mathcal{L}_v^2}{(\mathcal{L}_c^2+\mathcal{V}_c^2)} - 16\mathcal{H}_p^2\gamma^2\mathcal{L}_c^6\left[\Gamma^2\mathcal{V}_c^2\cos^2\theta + 4\mathcal{L}_c^2(\Gamma-1) + 4\mathcal{H}_p^2\mathcal{V}_c^2\gamma^2\mathcal{L}_c^4\cos^4\theta\right]\right\}^{1/2}}{8\mathcal{H}_p^2\gamma^2\mathcal{L}_c^4} ,$$

where

$$\mathcal{L}_v = \left(\mathcal{L}_c^2+\mathcal{V}_c^2\right)\left[\Gamma^2+4\mathcal{H}_p^2\gamma^2\mathcal{L}_c^4\right] . \tag{4.143}$$

Thus, the conclusion is that the magnetoacoustic gravity modified surface waves will propagate along the interface with the above mentioned constraints. The *f*-mode will be a solution to the dispersion relation (4.134) in the field-free limit provided the mode satisfies the condition on v_z under which the dispersion relation was derived. To examine this it is necessary to rewrite the Equation (4.134) in the limit of zero field. Equation (4.134) in the case of a zero magnetic field (so that $\mathcal{V}_c = 0$, $\Gamma = \gamma$, $H_c = H_{co}$) becomes

$$\frac{\left(\frac{\gamma\varphi^2}{2\mathcal{L}_c^2}\right)\left[1-(1-4A_cH_{co}^2)^{1/2}\right]+1}{(\mathcal{L}_c^2-\varphi^2)} = \frac{\frac{\gamma\varphi^2}{2}\left[1+\left(1-4A_pH_p^2\right)^{1/2}\right]-1}{(1-\varphi^2)} . \tag{4.144}$$

On noting that $\varphi^2 = \Omega^2/K\mathcal{H}_p$, Equation (4.144) with $\Omega^2 = 1$ reduces to

$$\frac{\left\{\frac{1}{2\mathcal{H}_p\mathcal{L}_c^2}\left[1 \mp (1 - 2\mathcal{H}_p\mathcal{L}_c^2)\right] - 1\right\}}{(\gamma\mathcal{H}_p\mathcal{L}_c^2 - 1)} = \frac{\left\{\frac{1}{2\mathcal{H}_p}\left[1 \pm (2\mathcal{H}_p - 1)\right] - 1\right\}}{(\gamma\mathcal{H}_p - 1)} . \tag{4.145}$$

After careful examination it is found that Equation (4.145) is satisfied only if $1 < 2\mathcal{H}_p < c_{sp}^2/c_{sc}^2$; that is, Equation (4.145) is satisfied only if the wavenumber $k \left(= \left(k_x^2 + k_y^2\right)^{1/2}\right)$ lies in the interval

$$\frac{1}{2H_p} < \left(k_x^2 + k_y^2\right)^{1/2} < \frac{1}{2H_{co}} . \tag{4.146}$$

With K lying in this interval there is a mode with $\omega^2 = gK$ and $v_z \propto e^{\left(k_x^2+k_y^2\right)^{1/2}z}$ that has bounded kinetic energy density but an unbounded vertical velocity in the chromosphere ($z > 0$). The inequality (4.146) states that the f-mode can propagate only if $H_p > H_{co}$, i.e. if $c_{sp} > c_{sc}$. Thus the field-free region must be warmer than the overlying atmosphere for the f-mode to propagate in an isothermal non-magnetic region. This same condition was obtained for the fast magnetoacoustic surface waves to exist (see chapter 2; see also Roberts, 1981, 1991; Miles and Roberts, 1989 for the special case $K = k_x$ i.e. $\theta = 0$).

In order to find the influence of a magnetic field on the f-mode an approximate solution to the dispersion relation (4.144) is sought with the property that $\Omega^2 \to 1$ as $v_{Ac}/c_{sp} \to 0$. Setting

$$\Omega^2 \to 1 + \delta\,\frac{v_{Ac}^2}{c_{sp}^2} , \tag{4.147}$$

for constant δ. Substituting $\varphi^2 = \Omega^2/K\mathcal{H}_p$ and expanding the dispersion relation (4.134) for small v_{Ac}/c_{sp} allows a determination of δ. After some detailed algebra, it is found that

$$\delta = \frac{\gamma}{2}\cos^2\theta\frac{(2KH_p - 1)}{\left(1 - \frac{c_{sc}^2}{c_{sp}^2}\right)} . \tag{4.148}$$

Since the dispersion relation (4.144) was derived under the conditions $2KH_p > 1$ and

$c_{sc}^2/c_{sp}^2 < 1$, the correction δ is positive. Thus, in terms of the original variables, the first order correction to the f-mode in the presence of a magnetic field gives the result

$$\frac{\omega^2}{gK} \sim 1 + \frac{\gamma}{2}\cos^2\theta \frac{(2KH_p - 1)}{\left(c_{sp}^2 - c_{sc}^2\right)} v_{Ac}^2 , \tag{4.149}$$

valid for $c_{sp} > c_{sc}$ and $2KH_p > 1$. It is clear from (4.149) that in the presence of a magnetic field the frequency of the f-mode is *increased*. Other studies (for $K = k_x$) of the effect of a magnetic field on the f-mode frequency have also found an increase (Campbell and Roberts, 1989; Evans and Roberts, 1990; Miles and Roberts, 1991).

4.8 Discussion

The investigation of the influence of a non-uniform field (with constant Alfvén speed v_A), considered in this chapter, has brought out several important aspects. Firstly, the frequencies of f- and p-modes change in the presence of a magnetic atmosphere. The behaviour of the p-mode frequencies for the current model presents a very different scenario when compared with that of the uniform field model (see chapter 3). The f-mode frequencies change in a manner similar to that for the uniform field model although the magnitudes are different. Secondly a consideration of non-parallel propagation yields some interesting results. In the case of parallel propagation ($\theta = 0$), the frequency of the first p-mode ($n = 1$) increases for small degrees l (see Figure 4.5) but at large values it once again decreases and indeed becomes negative. When non-parallel propagation is taken into account (e.g., with $\theta = 45°$, $90°$) the frequencies of the first p-mode show a decrease even for small degree l (see Figure 4.4). The modes with $n \geq 2$ show a frequency decrease for all values of l, although the magnitudes differ for modes with different propagation angles and for different degrees l. Generally the frequency decreases slightly as the propagation angle θ increases.

It should be mentioned that the results presented in Campbell and Roberts (1989) and Evans and Roberts (1990) assumed the wave vector to be parallel to the magnetic field. This assumption was made for mathematical convenience. However, the effects of non-parallel propagation were speculated upon by Evans and Roberts (1991) on the basis of a previous investigation by Jain and Roberts (1990). Evans and Roberts suggested that the change in the f-mode frequencies in the presence of a magnetic atmosphere is due to magnetic tension and so for the case of non-parallel propagation this will result in a reduction in field-line bending. Accordingly, it is expected that the frequency shift in the f-mode will be reduced as the wave vector becomes more nearly perpendicular to the magnetic field. This was also the finding of Jain and Roberts

(1990). The detailed analysis laid out in this chapter (see in particular Figure 4.7) supports the earlier findings of Jain and Roberts (1990).

A decrease in frequency shift with an increase in propagation angle θ is also expected for the $n = 1$ p-mode since it is also affected by magnetic tension. This is confirmed in Figure 4.4 of this chapter showing that the effects of non-parallel propagation are quite significant. For higher radial order p-modes, only small effects are expected since the p-modes of higher radial order have frequency shifts that are believed to be caused mainly by changes in the 'rigidity' of the chromosphere, which in turn affects the rate of evanescence of the modes. Since this depends strongly on temperature and magnetic pressure in the chromosphere, the orientation of the wavevector is less critical. While accepting that the effects of non-parallel propagation are small for high radial orders, these effects cannot be ignored for low radial order and strong magnetic fields (compare Figures 4.4 and 4.6).

4.9 Summary

In this *chapter* the effects of a chromospheric magnetic field on the solar p- and f-modes are studied for the case when the propagation vector is at an angle to the magnetic field direction. A general equation governing the motion has been derived and some of its interfacial aspects are discussed in the limit of incompressibity as well as for the compressible case.

The problem of p- and f-modes was considered in some detail after deriving the dispersion relation for a simple model atmosphere. This model essentially examined the effects of changes in chromospheric canopy fields on solar p- and f-modes. The model had two distinct layers, the upper layer being isothermal with a magnetic field that was decreasing in height in such a manner so as to keep a constant Alfvén speed in that layer. The lower layer represented a field-free convection zone with temperature increasing linearly with depth. Various asymptotic and numerical results were obtained and discussed for this model. It was shown that for an atmosphere with constant Alfvén speed the p-mode frequency *decrease* in the presence of a chromosphere. In the case of the f-mode, the mode frequency $\omega^2 = gK$ *increased* in the presence of the magnetic field, although this increase became less significant in a direction almost perpendicular to the magnetic field. The asymptotic solutions and the solutions to the full dispersion relation were compared for both f- and p-modes. It was found that for higher frequencies and higher magnetic field strengths, the effects of non-parallel propagation are important.

CHAPTER 5

SURFACE EFFECTS OF A MAGNETIC FIELD ON P-MODES: THREE LAYER MODEL

5.1 Introduction

In the two previous chapters the solar atmosphere was modelled as possessing two layers, namely a field-free convection zone where the temperature decreases in a downward direction and an isothermal chromosphere incorporating a horizontal magnetic field. For each model the frequencies of p-modes have been calculated, and in particular the effects of changes in chromospheric temperature and/or magnetic field on these frequencies determined.

The major difference between the models of Chapter 3 and Chapter 4 is the distribution of magnetic field in the chromosphere. Chapter 3 involved a magnetic field which did not vary with height in the chromosphere. One consequence is that as one moves upwards in the chromosphere, the Alfvén speed increases. The frequency shifts (the differences between p-mode frequencies at conditions indicative of solar maximum and solar minimum) are positive and increase with frequency for low frequencies before (for some values of chromospheric temperatures) decreasing at higher frequencies (see Figure 3.7). This behaviour matches qualitatively that of the observed frequency shifts.

On the other hand, Chapter 4 assumed that the magnetic field decreased as one moved upwards in the chromosphere. This decrease was assumed to be such that the Alfvén speed remained constant. The resulting frequency shifts were negative and became increasingly negative as the frequency was increased.

The purpose of this chapter is to combine the approaches of the two previous chapters. A three layer model is used with the bottom layer being, as before, the field-free convection zone with the temperature increasing with depth. Immediately above this lies a region of constant magnetic field. This region in turn is surmounted by a layer in which the Alfvén speed is constant. The top layer is thus similar to the magnetic layer considered in Chapter 4.

It is hoped to retain the more favourable points of each model. One drawback of the model of Chapter 3 is that, on moving upwards, the Alfvén speed increases without limit. The addition of the upper atmosphere (of constant Alfvén speed) overcomes this shortcoming.

Part of the motivation for the three layer model is to combine aspects of the frequency shift curve which match the observations. In particular, it is hoped that at low frequencies the positive, increasing frequency shifts of Chapter 3 will be retained whereas at higher frequencies it is desired to reproduce the decreasing frequency shifts as in the model of Chapter 4.

The aim of this chapter therefore is to combine, in a realistic manner, certain aspects of the preceeding two chapters in an attempt to match the observed frequency shift curves.

5.2 The Equilibrium Model

The reference level $z = 0$ corresponds to the base of the chromosphere (i.e. the temperature minimum). The chromosphere and the convection zone are represented by the regions $z < 0$ and $z > 0$, respectively. The chromosphere is assumed to consist of two regions, a lower chromosphere $-h < z < 0$ and an upper chromosphere $z < -h$. The medium is stratified by gravity acting in the positive z-direction (see Figure 5.1).

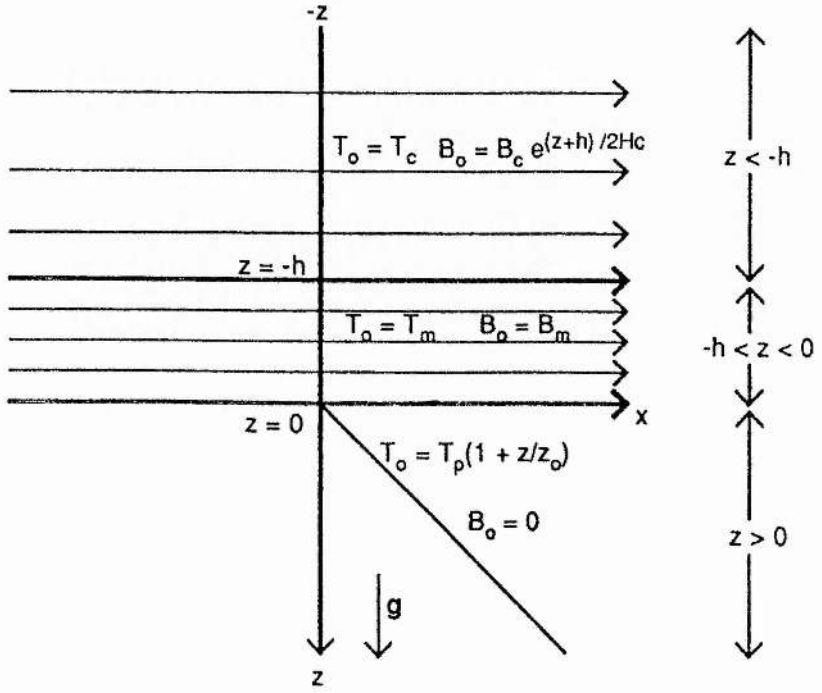

Figure 5.1: The equilibrium atmosphere of the model.

The solar plasma is assumed to be an ideal, perfectly conducting gas, permeated by a horizontal magnetic field $\mathbf{B} = B_o(z)\hat{\mathbf{x}}$. The unperturbed state is one of magnetohydrostatic equilibrium described by the equation

$$\frac{d}{dz}\left(p_o(z) + \frac{B_o^2(z)}{2\mu}\right) = \rho_o(z)g \,. \tag{5.1}$$

The plasma pressure $p_o(z)$ and temperature $T_o(z)$ are related by the ideal gas law :

$$p_o(z) = \mathcal{R}\rho_o(z)T_o(z) \,. \tag{5.2}$$

Here $\mathcal{R}$ $(=\frac{k_B}{m_p}$ where k_B is Boltzmann's constant, and m_p is the mean particle mass) is the gas constant. The temperature $T_o(z)$ is taken to increase linearly with depth in the convection zone ($z > 0$) and to be constant in each of the two regions of the chromosphere ($z < 0$) :

$$T_o(z) = \begin{cases} T_p\left(1 + \frac{z}{z_o}\right) \,, & z > 0, \\ T_m \,, & -h < z < 0, \\ T_c \,, & z < -h, \end{cases} \tag{5.3}$$

Here, T_p is the temperature at the top of the convection zone, T_m is the temperature in the middle region (lower chromosphere) and T_c is the temperature in the upper region of the chromosphere. The temperature scale height at the top of the convection zone is z_o.

The magnetic field profile is taken to be of the form

$$B_o(z) = \begin{cases} 0 \,, & z > 0, \\ B_m \,, & -h < z < 0, \\ B_c e^{(z+h)/2H_c} \,, & z < -h, \end{cases} \tag{5.4}$$

where the uniform field B_m is confined to the region $-h < z < 0$. In the upper region ($z < -h$), the density scale height $H_c = c_{sc}^2/\Gamma g$ where

$$\Gamma = \frac{2\gamma c_{sc}^2}{2c_{sc}^2 + \gamma v_{Ac}^2} (\leq \gamma) \tag{5.5}$$

is the magnetically modified adiabatic exponent (see Section 4.4, Chapter 4). Note

that Γ is generally less than the adiabatic exponent γ, with $\Gamma = \gamma$ in the absence of a magnetic field. The equilibrium magnetic field $B_o(z)$ is structured in such a way that

$$B_o^2(z) \sim \rho_o(z) \,, \tag{5.6}$$

so that the Alfvén speed $v_{Ac}\left(= B_o(z)/(\mu\ \rho_o(z))^{1/2}\right)$ there is constant.

Thus, with $T_o(z)$ and $B_o(z)$ specified by Equations (5.3) and (5.4), the gas pressure distribution is

$$p_o(z) \;=\; \begin{cases} p_p\left(1+\frac{z}{z_o}\right)^{(m+1)} \,, & z > 0, \\ p_m e^{z/H_m} \,, & -h < z < 0, \\ p_c e^{(z+h)/H_c} \,, & z < -h, \end{cases} \tag{5.7}$$

with density scale heights $H_m(= \mathcal{R}T_m/g)$ and $H_c(= c_{sc}^2/\Gamma g)$, and polytropic index $m\,[= gz_o/\mathcal{R}T_p - 1]$.

The density distribution $\rho_o(z)$ is given by

$$\rho_o(z) \;=\; \begin{cases} \rho_p\left(1+\frac{z}{z_o}\right)^{m} \,, & z > 0, \\ \rho_m e^{z/H_m} \,, & -h < z < 0, \\ \rho_c e^{(z+h)/H_c} \,, & z < -h. \end{cases} \tag{5.8}$$

where, ρ_m and ρ_p are the densities at $z = 0_-$ and $z = 0_+$ respectively; ρ_c is the density at the base of the uppermost region (i.e. $z = -h_-$).

The gas pressure p_p at the top of the convection zone ($z = 0_+$) is related to the pressure p_m at the base of the middle region ($z = 0_-$) through continuity of total pressure

$$p_m + \frac{B_m^2}{2\mu} \;=\; p_p \,, \tag{5.9}$$

and so, using the ideal gas law (5.2), the interfacial density ratio may be expressed as

$$\frac{\rho_m}{\rho_p} \;=\; \frac{c_{sp}^2}{(c_{sm}^2 + \frac{\gamma}{2}v_{Am}^2)} \,. \tag{5.10}$$

Here, $c_{sp}\left\{= (\gamma p_p/\rho_p)^{1/2}\right\}$ is the sound speed at the temperature minimum($z = 0_+$), and $c_{sm}\left\{= (\gamma p_m/\rho_m)^{1/2}\right\}$, $v_{Am}\left\{= B_m/(\mu\rho_m)^{1/2}\right\}$ are the sound and Alfvèn speeds at the base ($z = 0_-$) of the middle region ($-h < z < 0$).

Similarly, magnetohydrostatic pressure continuity across the interface $z = -h$ requires that

$$p_c + \frac{B_c^2}{2\mu} = p_m e^{-h/H_m} + \frac{B_m^2}{2\mu} . \tag{5.11}$$

On coupling Equation (5.11) with the ideal gas law (see Equation (5.2)), the density ratio at $z = -h$ is given by

$$\frac{\rho_c}{\rho_m e^{-h/H_m}} = \frac{(c_{sm}^2 + \frac{\gamma}{2} v_{Am}^2 e^{h/H_m})}{(c_{sc}^2 + \frac{\gamma}{2} v_{Ac}^2)} , \tag{5.12}$$

where $c_{sc}\left(= (\gamma p_c/\rho_c)^{1/2}\right)$ and $v_{Ac}\left(= B_c/(\mu\rho_c)^{1/2}\right)$ are the sound and Alfvèn speeds in the region $z < -h$.

5.3 The Dispersion Relation

The equations of motion describing small oscillations about a general stratified equilibrium of the kind discussed in Section 5.2 are given in Chapter 3. The velocity field is taken to be two dimensional : $\mathbf{v} = (v_x, 0, v_z)$. For small displacements, each physical quantity is assumed to change by a small perturbation from its equilibrium value. It is also assumed that the perturbation quantities can be expressed in the form $\mathbf{v} = (v_x(z), 0, v_z(z)) \exp\ i(\omega t - k_x x)$, etc, where ω is the angular frequency and k_x is the wavenumber along the x-axis. After some algebra (see Equation (3.12)), the following governing equation (Goedbloed 1971; Adam 1977; Roberts 1985) is obtained:

$$\frac{d}{dz}\left\{\frac{\rho_o(c_s^2 + v_A^2)(\omega^2 - k_x^2 c_T^2)}{(\omega^2 - k_x^2 c_s^2)} \frac{dv_z}{dz}\right\}$$

$$= \left\{\frac{\rho_o g^2 k_x^2}{(\omega^2 - k_x^2 c_s^2)} - \rho_o(\omega^2 - k_x^2 v_A^2) - g k_x^2 \frac{d}{dz}\left(\frac{\rho_o c_s^2}{(\omega^2 - k_x^2 c_s^2)}\right)\right\} v_z , \tag{5.13}$$

where $c_s(z)\left(= (\gamma p_o(z)/\rho_o(z))^{1/2}\right)$ is the local sound speed, $v_A(z)\left(= B_o(z)/(\mu\rho_o(z))^{1/2}\right)$ is the local Alfvén speed and $c_T(z) = c_s v_A/(c_s^2 + v_A^2)^{1/2}$ is the MHD cusp speed. Equation (5.13) is a general equation and is valid in all three layers of the atmosphere.

The middle region ($-h < z < 0$) is isothermal and has a uniform magnetic field and so the governing Equation (5.13) reduces to

$$\{\mathcal{A}_1 + \mathcal{A}_2\ exp(-\mathcal{A}_3 z)\}\frac{d^2 v_z}{dz^2} + \mathcal{A}_1\mathcal{A}_3\frac{dv_z}{dz} + \left\{\mathcal{A}_4 - k_x^2\mathcal{A}_2\ exp(-\mathcal{A}_3 z)\right\} v_z = 0\ , \quad (5.14)$$

where

$$\mathcal{A}_1 = \omega^2 c_{sm}^2\ , \qquad \mathcal{A}_2 = v_{Am}^2(\omega^2 - k_x^2 c_{sm}^2)\ , \qquad \mathcal{A}_3 = \frac{1}{H_m} = \frac{\gamma g}{c_{sm}^2}\ ,$$

$$\mathcal{A}_4 = (\gamma - 1)g^2 k_x^2 + \omega^2(\omega^2 - k_x^2 c_{sm}^2)\ . \quad (5.15)$$

Equation (5.14) has the solution (see Equation (3.20), Chapter 3)

$$\begin{aligned} v_z \;=\; & C_1\left(\frac{-\mathcal{A}_1}{\mathcal{A}_2}\right)^{\frac{k_x}{\mathcal{A}_3}} e^{k_x z} F\left(p, q; r; \frac{-\mathcal{A}_1}{\mathcal{A}_2} e^{\mathcal{A}_3 z}\right) \\ & + C_2\left(\frac{-\mathcal{A}_1}{\mathcal{A}_2}\right)^{\frac{-k_x}{\mathcal{A}_3}} e^{k_x z} F\left(p - r + 1, q - r + 1; 2 - r; \frac{-\mathcal{A}_1}{\mathcal{A}_2} e^{\mathcal{A}_3 z}\right)\ , \\ & -h < z < 0\ . \quad (5.16) \end{aligned}$$

For the equilibrium profiles in the upper region ($z < -h$) with its constant Alfvén and sound speed, Equation (5.13) reduces to (see Chapter 4)

$$\frac{d^2 v_z}{dz^2} + \frac{1}{H_c}\frac{dv_z}{dz} + A_c v_z \;=\; 0\ , \quad (5.17)$$

where

$$H_c = \frac{c_{sc}^2}{\Gamma g}\ , \qquad \Gamma = \frac{2\beta\gamma}{2\beta + \gamma}\ , \qquad \beta = \frac{c_{sc}^2}{v_{Ac}^2}\ , \quad (5.18)$$

$$A_c \;=\; \frac{(\Gamma - 1)g^2 k_x^2 + (\omega^2 - k_x^2 v_{Ac}^2)(\omega^2 - k_x^2 c_{sc}^2)}{(c_{sc}^2 + v_{Ac}^2)(\omega^2 - k_x^2 c_{Tc}^2)}\ . \quad (5.19)$$

The solution to Equation (5.17) may be written as

$$v_z \;=\; C_4\ exp\ (\lambda_+ z) \;+\; C_5\ exp\ (\lambda_- z)\ , \qquad z < -h\ , \quad (5.20)$$

where

$$\lambda_\pm \;=\; \frac{1}{2H_c}\left[-1 \pm (1 - 4A_c H_c^2)^{1/2}\right]\ . \quad (5.21)$$

Thus, the solution with energy density $\rho_o v_z^2$ tending to zero as $z \to -\infty$ is given by

$$v_z \;=\; \mathcal{C}_4 \;\exp\left\{\frac{z}{2H_c}\left[-1 \;+\; (1-4A_cH_c^2)^{1/2}\right]\right\}\;. \tag{5.22}$$

The vertical velocity v_z in the convection zone satisfies (see Chapters 3 and 4)

$$\begin{aligned}(\omega^4 - g^2k_x^2)v_z e^{k_x(z+z_o)} \;=\; & \mathcal{C}_5\left\{\left[k_xc_{sp}^2(\omega^2+gk_x)-\gamma g\omega^2\right]\; U(-a,m+2,2k_x(z+z_o))\right.\\ & \left.-2a\omega^2c_{sp}^2k_xU(-a+1,m+3,2k_x(z+z_o))\right\},\; z>0. \end{aligned}\tag{5.23}$$

To obtain the dispersion relation relating ω and k_x the solutions for v_z given by Equations (5.16) and (5.23) are matched at the interface $z = 0$, and those given by Equations (5.16) and (5.22) are matched at the interface $z = -h$. Also, integrating Equation (5.13) across each interface yields a second condition, namely that

$$\left\{\frac{\rho_o(c_s^2+v_A^2)(\omega^2-k_x^2c_T^2)}{(\omega^2-k_x^2c_s^2)}\right\}\frac{dv_z}{dz} \;+\; \left\{\frac{gk_x^2\rho_oc_s^2}{(\omega^2-k_x^2c_s^2)}\right\}v_z\;, \tag{5.24}$$

or equivalently $i\omega P_T \;+\; g\rho_o v_z$, is continuous at each interface. Application of these two conditions to the solutions (5.16), (5.22) and (5.23) yields the dispersion relation

$$\mathcal{J} = \frac{(\omega^2-k_x^2c_{sm}^2)(c_{sm}^2+\frac{\gamma}{2}v_{Am}^2)\left\{(\mathcal{X}_1\mathcal{M}-\mathcal{X}_2\mathcal{L}) \;+\; (\mathcal{L}-\mathcal{M})/\Re_B\right\}}{(\omega^2-k_x^2c_{sc}^2)(c_{sm}^2+v_{Am}^2)(\omega^2-k_x^2c_{Tm}^2)\left\{(\mathcal{M}\mathcal{Z}_2\mathcal{X}_1-\mathcal{L}\mathcal{Z}_1\mathcal{X}_2)+(\mathcal{L}\mathcal{Z}_1-\mathcal{M}\mathcal{Z}_2)/\Re_B\right\}}, \tag{5.25}$$

where

$$\mathcal{J} = \frac{-2a\omega^2c_{sp}^2k_x\frac{U(-a+1,m+3,2k_xz_o)}{U(-a,m+2,2k_xz_o)} \;+\; k_xc_{sp}^2(\omega^2+gk_x)-\gamma g\omega^2}{(\omega^2-k_x^2c_{sm}^2)(g^2k_x^2 \;-\; \omega^4)}\;, \tag{5.26}$$

$$\mathcal{X}_1 = \left\{k_x \;+\; \frac{F'\left(p,q;r;\frac{-\mathcal{A}_1}{\mathcal{A}_2}e^{-\mathcal{A}_3h}\right)}{F\left(p,q;r;\frac{-\mathcal{A}_1}{\mathcal{A}_2}e^{-\mathcal{A}_3h}\right)} \;+\; \frac{gk_x^2c_{sm}^2}{(c_{sm}^2+v_{Am}^2e^{h/H_m})(\omega^2-k_x^2c_{Tmc}^2)}\right\}\;, \tag{5.27}$$

$$\mathcal{X}_2 = \left\{ -k_x + \frac{F'\left(p-r+1, q-r+1; 2-r; \frac{-\mathcal{A}_1}{\mathcal{A}_2} e^{-\mathcal{A}_3 h}\right)}{F\left(p-r+1, q-r+1; 2-r; \frac{-\mathcal{A}_1}{\mathcal{A}_2} e^{-\mathcal{A}_3 h}\right)} + \frac{g k_x^2 c_{sm}^2}{(c_{sm}^2 + v_{Am}^2 e^{h/H_m})(\omega^2 - k_x^2 c_{Tmc}^2)} \right\}, \tag{5.28}$$

$$\mathcal{L} = \frac{e^{k_x h} F\left(p-r+1, q-r+1; 2-r; \frac{-\mathcal{A}_1}{\mathcal{A}_2} e^{-\mathcal{A}_3 h}\right)}{e^{-k_x h} F\left(p, q; r; \frac{-\mathcal{A}_1}{\mathcal{A}_2} e^{-\mathcal{A}_3 h}\right)}, \tag{5.29}$$

$$\mathcal{M} = \frac{F\left(p-r+1, q-r+1; 2-r; \frac{-\mathcal{A}_1}{\mathcal{A}_2}\right)}{F\left(p, q; r; \frac{-\mathcal{A}_1}{\mathcal{A}_2}\right)}, \tag{5.30}$$

$$\mathcal{Z}_1 = \left\{ k_x + \frac{F'\left(p, q; r; \frac{-\mathcal{A}_1}{\mathcal{A}_2}\right)}{F\left(p, q; r; \frac{-\mathcal{A}_1}{\mathcal{A}_2}\right)} + \frac{g k_x^2 c_{sm}^2}{(c_{sm}^2 + v_{Am}^2)(\omega^2 - k_x^2 c_{Tm}^2)} \right\}, \tag{5.31}$$

$$\mathcal{Z}_2 = \left\{ -k_x + \frac{F'\left(p-r+1, q-r+1; 2-r; \frac{-\mathcal{A}_1}{\mathcal{A}_2}\right)}{F\left(p-r+1, q-r+1; 2-r; \frac{-\mathcal{A}_1}{\mathcal{A}_2}\right)} + \frac{g k_x^2 c_{sm}^2}{(c_{sm}^2 + v_{Am}^2)(\omega^2 - k_x^2 c_{Tm}^2)} \right\}, \tag{5.32}$$

$$\Re_B = \frac{2\beta+\gamma}{2\beta} \frac{(c_{sm}^2 + v_{Am}^2 e^{h/H_m})(\omega^2 - k_x^2 c_{Tmc}^2)(\omega^2 - k_x^2 c_{sc}^2)}{(\omega^2 - k_x^2 c_{sm}^2)(c_{sm}^2 + \frac{\gamma}{2} v_{Am}^2 e^{h/H_m}) \left\{ g k_x^2 + \phi \left[-1 + \sqrt{1 - 4 A_c H_c^2} \right] \right\}}, \tag{5.33}$$

$$c_{Tmc}^2 = \frac{c_{sm}^2 v_{Am}^2 e^{h/H_m}}{(c_{sm}^2 + v_{Am}^2 e^{h/H_m})}, \quad c_{Tc}^2 = \frac{c_{sc}^2 v_{Ac}^2}{(c_{sc}^2 + v_{Ac}^2)}, \quad \phi = \frac{(\beta+1)(\omega^2 - k_x^2 c_{Tc}^2)}{2\beta H_c}. \tag{5.34}$$

$$F'(a, b; c; z) = \frac{ab}{c} F(a+1, b+1; c; z) \tag{5.35}$$

The dispersion relation (5.25) is clearly complicated. Consider the two extremes of $h \to 0$ and $h \to \infty$. In the limit of $h \to 0$, the dispersion relation (5.25) reduces to (see Appendix A5, Section 1)

$$2a\omega^2 c_{sp}^2 k_x \frac{U(-a+1, m+3, 2k_x z_o)}{U(-a, m+2, 2k_x z_o)} + \gamma g \omega^2 - k_x c_{sp}^2 (\omega^2 + g k_x)$$

$$= \left(\frac{\rho_p}{\rho_c}\right) \frac{m_o^2 (g^2 k_x^2 - \omega^4) c_{sp}^2}{\left\{(k_x^2 v_{Ac}^2 - \omega^2)\lambda_+ + \frac{g k_x^2 c_{sc}^2 m_o^2}{(\omega^2 - k_x^2 c_{sc}^2)}\right\}}. \qquad (5.36)$$

This is identical to Equation (4.75) of Chapter 4. With $h \to 0$ the present model becomes the model in Figure 4.1 and hence the reduction of (5.25) to (4.75) is expected.

When $h \to \infty$ the present model becomes the model used in Chapter 3 (see Figure 3.2) and hence in the limit $h \to \infty$ the dispersion relation (5.25) must reduce to the dispersion relation (3.44) of Chapter 3. This is indeed the case. In the limit of $h \to \infty$, the dispersion relation (5.25) reduces to (see Appendix A5, Section 2)

$$2a\omega^2 c_{sp}^2 k_x \frac{U(-a+1, m+3, 2k_x z_o)}{U(-a, m+2, 2k_x z_o)} + \gamma g \omega^2 - k_x c_{sp}^2 (\omega^2 + g k_x)$$

$$= \left(\frac{\rho_p}{\rho_m}\right) \frac{(g^2 k_x^2 - \omega^4)(\omega^2 - k_x^2 c_{sm}^2)}{g k_x^2 c_{sm}^2 + (c_{sm}^2 + v_{Am}^2)(\omega^2 - k_x^2 c_{Tm}^2)\left\{k_x - \frac{pq}{r}\frac{\mathcal{A}_1 \mathcal{A}_3}{\mathcal{A}_2}\frac{F\left(p+1, q+1; r+1; \frac{-\mathcal{A}_1}{\mathcal{A}_2}\right)}{F\left(p, q; r; \frac{-\mathcal{A}_1}{\mathcal{A}_2}\right)}\right\}}, \qquad (5.37)$$

which is the dispersion relation (3.44) of Chapter 3.

The dimensionless form of the general dispersion relation (5.25) is given by

$$2a\kappa\Omega^2 \frac{U(-a+1, m+3, 2\kappa)}{U(-a, m+2, 2\kappa)} + (m+1)\Omega^2 - (\Omega^2 + 1)\kappa$$

$$= \frac{(1-\Omega^4)\left(\Omega^2 - \frac{\kappa}{\tau\wedge}\right)\left\{(\overline{\mathcal{X}}_1 \mathcal{M} - \overline{\mathcal{X}}_2 \mathcal{L}) + (\mathcal{L} - \mathcal{M})/\overline{\Re}_B\right\}}{\left(\frac{\gamma}{m+1}\right)\left(\frac{1+\beta_m}{\beta_m}\right)\left(\Omega^2 - \frac{\kappa}{\tau\wedge(1+\beta_m)}\right)\left\{(\overline{\mathcal{X}}_1 \overline{\mathcal{Z}}_2 \mathcal{M} - \overline{\mathcal{X}}_2 \overline{\mathcal{Z}}_1 \mathcal{L}) + (\mathcal{L}\overline{\mathcal{Z}}_1 - \mathcal{M}\overline{\mathcal{Z}}_2)/\overline{\Re}_B\right\}}, \qquad (5.38)$$

where

$$\overline{\mathcal{X}}_1 = \frac{\mathcal{X}_1}{k_x} = \left\{1 + \frac{F'\left(p, q; r; \frac{-\mathcal{A}_1}{\mathcal{A}_2} e^{-\mathcal{A}_3 h}\right)}{k_x F\left(p, q; r; \frac{-\mathcal{A}_1}{\mathcal{A}_2} e^{-\mathcal{A}_3 h}\right)} + \frac{\beta_m}{(1 + \beta_m e^{-h/H_m})\left(\Omega^2 - \frac{\kappa}{\tau\wedge(1+\beta_m e^{-h/H_m})}\right)}\right\},$$

(5.39)

$$\overline{\mathcal{X}}_2 = \frac{\mathcal{X}_2}{k_x} = \left\{ -1 \; + \; \frac{F'\left(p-r+1, q-r+1; 2-r; \frac{-\mathcal{A}_1}{\mathcal{A}_2} e^{-\mathcal{A}_3 h}\right)}{k_x F\left(p-r+1, q-r+1; 2-r; \frac{-\mathcal{A}_1}{\mathcal{A}_2} e^{-\mathcal{A}_3 h}\right)} \right.$$
$$\left. + \; \frac{\beta_m}{(1+\beta_m e^{-h/H_m})\left(\Omega^2 - \frac{\kappa}{\tau\wedge(1+\beta_m e^{-h/H_m})}\right)} \right\} , \qquad (5.40)$$

$$\overline{\mathcal{Z}}_1 = \frac{\mathcal{Z}_1}{k_x} \; = \; \left\{ 1 \; + \; \frac{F'\left(p, q; r; \frac{-\mathcal{A}_1}{\mathcal{A}_2}\right)}{k_x F\left(p, q; r; \frac{-\mathcal{A}_1}{\mathcal{A}_2}\right)} \; + \; \frac{\beta_m}{\left(\Omega^2(1+\beta_m) - \frac{\kappa}{\tau\wedge}\right)} \right\} , \qquad (5.41)$$

$$\overline{\mathcal{Z}}_2 = \frac{\mathcal{Z}_2}{k_x} = \left\{ -1 + \frac{F'\left(p-r+1, q-r+1; 2-r; \frac{-\mathcal{A}_1}{\mathcal{A}_2}\right)}{k_x F\left(p-r+1, q-r+1; 2-r; \frac{-\mathcal{A}_1}{\mathcal{A}_2}\right)} + \frac{\beta_m}{\left(\Omega^2(1+\beta_m) - \frac{\kappa}{\tau\wedge}\right)} \right\} ,$$

(5.42)

$$\mathcal{L} \; = \; \frac{e^{K\Upsilon} F\left(p-r+1, q-r+1; 2-r; \frac{-\mathcal{A}_1}{\mathcal{A}_2} e^{-\mathcal{A}_3 h}\right)}{e^{-K\Upsilon} F\left(p, q; r; \frac{-\mathcal{A}_1}{\mathcal{A}_2} e^{-\mathcal{A}_3 h}\right)} , \qquad (5.43)$$

$$\mathcal{M} \; = \; \frac{F\left(p-r+1, q-r+1; 2-r; \frac{-\mathcal{A}_1}{\mathcal{A}_2}\right)}{F\left(p, q, r, \frac{-\mathcal{A}_1}{\mathcal{A}_2}\right)} , \qquad (5.44)$$

$$\overline{\Re}_B = k_x \Re_B = \frac{2\beta+\gamma}{2\beta} \frac{\left(1+\frac{1}{\beta_m} e^{h/H_m}\right)\left(\Omega^2 - \frac{\kappa}{(1+\beta_m e^{-h/H_m})}\right)\left(\Omega^2 - \frac{\kappa}{\wedge}\right)}{\left(\Omega^2 - \frac{\kappa}{\tau\wedge}\right)\left(1+\frac{\gamma}{2\beta_m} e^{h/H_m}\right)\left\{1 + \Phi\left(1+\frac{1}{\beta}\right)\left(\Omega^2 - \frac{\kappa}{(1+\beta)\wedge}\right)\right\}} .$$

(5.45)

Here

$$\beta_m = \frac{c_{sm}^2}{v_{Am}^2} , \quad \tau = \frac{c_{sc}^2}{c_{sm}^2} , \quad \kappa = k_x z_o , \quad \frac{k_x}{\mathcal{A}_3} = \frac{\kappa}{\gamma\tau\wedge} , \quad \Upsilon = h/z_o ,$$

$$\mathcal{A}_3 h = \Upsilon\gamma\tau\wedge , \quad \frac{-\mathcal{A}_1}{\mathcal{A}_2} = \frac{-\Omega^2\beta_m}{\left(\Omega^2 - \frac{\kappa}{\tau\wedge}\right)} , \quad \Phi = \frac{\Gamma\wedge}{2\kappa}\left[-1 + \sqrt{1 - 4A_c H_c^2}\right] ,$$

$$\wedge = \frac{(m+1)}{\gamma} \frac{c_{sp}^2}{c_{sc}^2} , \quad A_c H_c^2 = \frac{\kappa}{\Gamma^2\wedge}\left\{ \frac{(\Gamma-1) + \left(\Omega^2 - \frac{\kappa}{\beta\wedge}\right)\left(\Omega^2 - \frac{\kappa}{\wedge}\right)}{\left(\Omega^2 - \frac{\kappa}{(1+\beta)\wedge}\right)\left(1+\frac{1}{\beta}\right)} \right\} . \qquad (5.46)$$

The dispersion relation (5.25), or alternatively its non-dimensional form (5.38), can be solved to find the frequencies of p-modes in a three layer atmosphere.

5.4 The Magnetoacoustic Cut-Off Frequency

Note that Equation (5.33) contains a square root term, namely $(1-4A_cH_c^2)^{1/2}$. In order for all quantities to remain real (for mathematical convenience) it is necessary for this term to be positive. This term is identical with the term $\mathcal{D}(\omega,k_x)$ mentioned in Section 3.2 of Chapter 3. The term $\mathcal{D}(\omega,k_x)$ should be positive for the mode to be evanescent. If it is negative, the mode will propagate and the energy density associated with the perturbation will be an oscillatory function of height z. Thus, the nature of a mode's motion in the chromosphere is determined by the sign of $\mathcal{D}(\omega,k_x)$. The solution $\mathcal{D}(\omega,k_x)=0$ corresponds to the borderline between the two cases and provides the magnetoacoustic cut-off frequency for the mode with wavenumber k_x and frequency ω. The expression for $\mathcal{D}(\omega,k_x)$ is given by

$$\mathcal{D}(\omega,k_x) \;=\; 1-4\left\{\frac{(\Gamma-1)\,g^2k_x^2 \;+\; (\omega^2-k_x^2c_{sc}^2)(\omega^2-k_x^2v_{Ac}^2)}{(c_{sc}^2+v_{Ac}^2)\,(\omega^2-k_x^2c_{Tc}^2)}\right\}H_c^2\;. \qquad (5.47)$$

In terms of the non-dimensional frequency $\Omega\left(=\omega/(gk_x)^{1/2}\right)$ and wavenumber $\kappa(=k_xz_o)$, Equation (5.47) can be written as

$$\mathcal{D}(\Omega,\kappa) \;=\; 1-4\left\{\frac{\kappa}{\Gamma^2\wedge}\frac{(\Gamma-1)\;+\left(\Omega^2\;-\;\frac{\kappa}{\beta\wedge}\right)\left(\Omega^2\;-\;\frac{\kappa}{\wedge}\right)}{\left(1+\frac{1}{\beta}\right)\left(\Omega^2-\frac{\kappa}{(1+\beta)\wedge}\right)}\right\}\;. \qquad (5.48)$$

Equation (5.47) for $\mathcal{D}(\omega,k_x)=0$ may be reduced to a quadratic in ω^2 :

$$\omega^4-\left(c_{sc}^2+v_{Ac}^2\right)\left(k_x^2+\frac{1}{4H_c^2}\right)\omega^2+\left(k_x^4c_{sc}^2v_{Ac}^2+(\Gamma-1)g^2k_x^2+\frac{k_x^2c_{sc}^2v_{Ac}^2}{4H_c^2}\right)=0. \qquad (5.49)$$

For small k_x Equation (5.49) becomes

$$\omega^2 \;=\; \frac{c_{sc}^2\,(c_{sc}^2+v_{Ac}^2)\,\omega_a^2}{\left(c_{sc}^2+\frac{\gamma}{2}v_{Ac}^2\right)^2}+O(k_x^2H_c^2)\;, \qquad (5.50)$$

where

$$\omega_a \;=\; \frac{\gamma g}{2c_{sc}} \qquad (5.51)$$

is the acoustic cut-off frequency for a field-free, isothermal atmosphere (Lamb, 1932). Relation (5.50) gives the magnetoacoustic cut-off frequency for small k_x. In the limit

of zero magnetic field it reduces to the acoustic cut-off frequency given by (5.51). In solving Equation (5.49), due to its quadratic nature, there were two potential roots. These represent the minimum and maximum values of frequency for which the term under the square root sign in Equation (5.47) is positive. It is the greater of those two roots which is considered and the corresponding cyclic frequency denoted by ν_{cut}.

Before displaying the behaviour of the magnetoacoustic cut-off frequency it is necessary to examine the nature of the Alfvén speed in the model. The Alfvén speed in the upper chromosphere is constant and is taken to be equal to the Alfvén speed at the top of the middle region (i.e. $z = -h_+$). The Alfvén speed at the base of the middle region ($z > 0_-$) is calculated from a given magnetic field strength B_m and density ρ_m and is increasing exponentially with height up to $z = -h$. Thus the (effective) Alfvén speed in the chromosphere can be varied by varying the thickness h of the middle (uniform field) region. It is instructive to plot the Alfvén speeds as functions of height. In Figure 5.2 are plotted the Alfvén speeds (in km/sec.) versus the height $-z$ (in km) for two different values of the magnetic field strength B_m (=20G, 40G). Note that for height $h \to 0$, the middle region of uniform field strength becomes extremely thin and the Alfvén speed shown in Figure 5.2a is for $B_c(= B_m) = 20$G (or 40 G as appropriate), the magnetic field strength at the base of the constant v_{Ac} region. As the distance z increases, the Alfvén speed increases. The value of Alfvén speed at $z = -h_+$ is the Alfvén speed taken for the uppermost region ($z < -h$) and is kept constant throughout this region. Thus there is a discontinuity in the magnetic field strength (B_m and B_c) at $z = -h$, this discontinuity being a reflection of the discontinuities in temperature and density.

Consider the case when the magnetic field strength B_m at $z = 0_-$ is 20G. In this case the Alfvén speed is 1.0 km/sec for a density of $\rho_m \sim 3.18 \times 10^{-6}$ kg/m^3 (T_m = 4170K); the Alfvén speed at $-z$ = 1300 km is 770.34 km/sec for a density of 3.63 $\times 10^{-5}$ kg/m^3 (the density scale height is H_m = 97.79 km). It is this Alfvén speed (770.34 km/sec.) which is kept constant throughout $z < -h$. When the magnetic field strength B_m at $z = 0_-$ is 40G, then the Alfvén speed is 2.5 km/sec for a density of $\rho_m \sim 2.02 \times 10^{-6}$ kg/m^3 (T_m = 6200K); the Alfvén speed at $-z$ = 1300 km is 219.41 km/sec. for a density of 2.64 $\times$ 10^{-10} kg/m^3, lower than the previous case despite the stronger field because the density scale height has increased to H_m = 145.40 km and so the density falls off less rapidly with height. It is this Alfvén speed (219.41 km/sec., when B_m = 40G) which is kept constant throughout $z < -h$.

It may seem surprising that the Alfvén speed for B_m = 20G, T_m = 4170K are greater than those for B_m = 40G, T_m = 6200K (see Figure 5.2b). Note from Figure 5.2a that the value of the Alfvén speed at the base ($z = 0_-$) of the middle region is, as expected,

greater when $B_m = 40$G than when $B_m = 20$G. However, the rate at which the Alfvén speed increases with height in the middle region is greater when $B_m = 20$G, $T_m = 4170$K than when $B_m = 40$G, $T_m = 6200$K. This is because of a higher temperature and hence a larger density scale height applies in the middle region for $B_m = 40$G.

Turning now to a consideration of magnetoacoustic cut-off, note that the cut-off frequency exhibits complicated dependence on the magnetic field strength (see also Campbell and Roberts, 1989) Equation (5.49) is solved to show the dependence of magnetoacoustic cut-off frequency ($\nu_{cut} = \omega/2\pi$) on the chromospheric Alfvén speed for various values of the degree l.

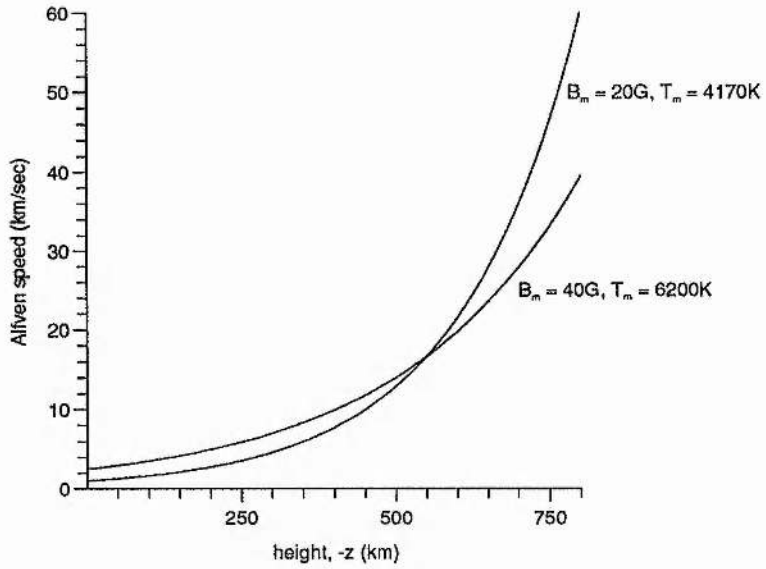

Figure 5.2a: The Alfvén speed $v_A(z) = v_{Am}e^{z/2H_m}$ as a function of height, $-z$, in the middle region $-h < z < 0$. The chromospheric temperature in the middle region $(-h < z < 0)$ is taken to be T_m = 4170K when the magnetic field strength B_m = 20G, and T_m = 6200K when B_m = 40G. At $z = 0$, v_{Am} = 1.1 km/sec for B_m = 20G, and v_{Am} = 2.5 km/sec for B_m = 40G.

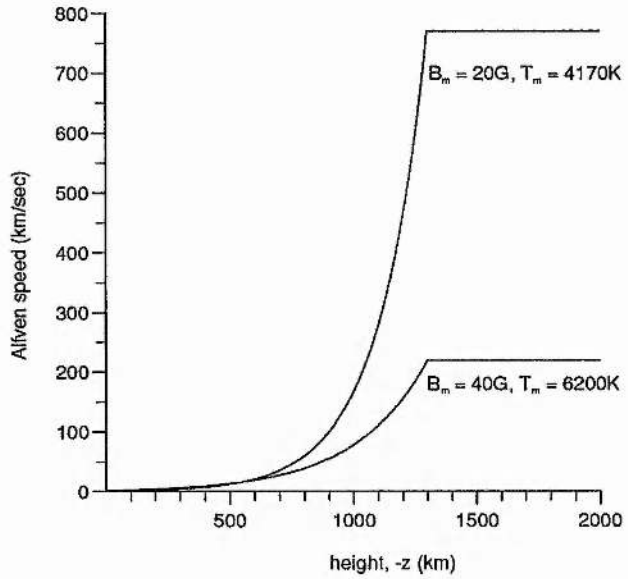

Figure 5.2b: The Alfvén speed $v_A(z)$ as a function of height, $-z$ in the region $z < 0$. The chromospheric temperature in the middle region $(-h < z < 0)$ is taken to be T_m = 4170K when the magnetic field strength B_m = 20G, and T_m = 6200K when B_m = 40G.

In Figure 5.3, the horizontal axis denotes the value of the thickness h and the vertical axis represents the magnetoacoustic cut-off frequencies for different l values. Figure 5.3a is plotted for magnetic field strength $B_m = 20G$. The chromospheric temperature in the middle region is $T_m = 4170$K and in the uppermost region the chromospheric temperature T_c is assumed to be 5000K. In Figure 5.3b the magnetic field strength B_m is increased to 40 G and chromospheric temperatures $T_m = 6200$K and $T_c = 7000$K are considered. It is clear from this figure that the magnetoacoustic cut-off frequency is not a monotonic function of h; but declines to a minimum value before increasing indefinitely. Thus it is possible for a mode of fixed degree l to have an evanescent nature (with its frequency ν being less than the magnetoacoustic cut-off frequency (ν_{cut}) for a particular Alfvén speed) and a propagating nature (with its frequency ν being greater than the magnetoacoustic cut-off frequency (ν_{cut})) for another Alfvén speed (i.e. another value of h). For example, in Figure 5.3a the mode with frequency $\nu \sim 3$ mHz for $l = 100$ has an evanescent nature for $h = 1000$ km ($v_{Ac} = 166.18$ km/sec) but will propagate in the chromosphere if h is between 500 km ($v_{Ac} = 12.89$ km/sec) and 900 km ($v_{Ac} = 104.88$ km/sec). In Figure 5.3b the same mode (i.e. $\nu \sim 3$ mHz) will have a propagating nature at thicknesses h between 450 km ($v_{Ac} = 11.79$ km/sec) and 1100 km ($v_{Ac} = 110.3$ km/sec) but an evanescent nature otherwise.

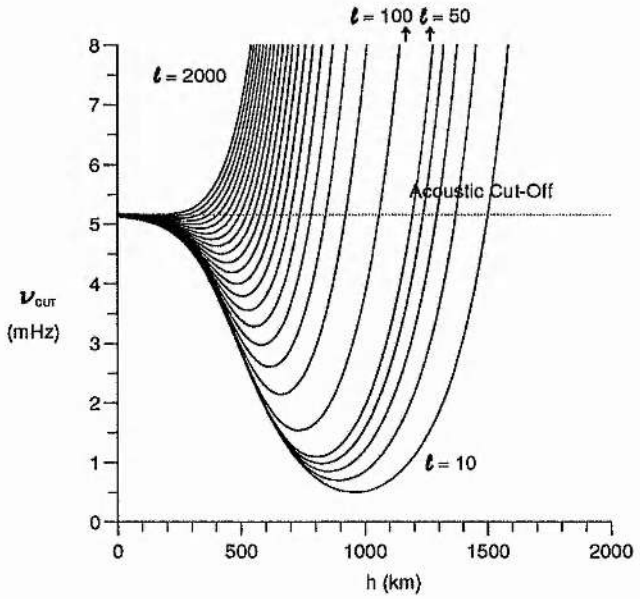

Figure 5.3a

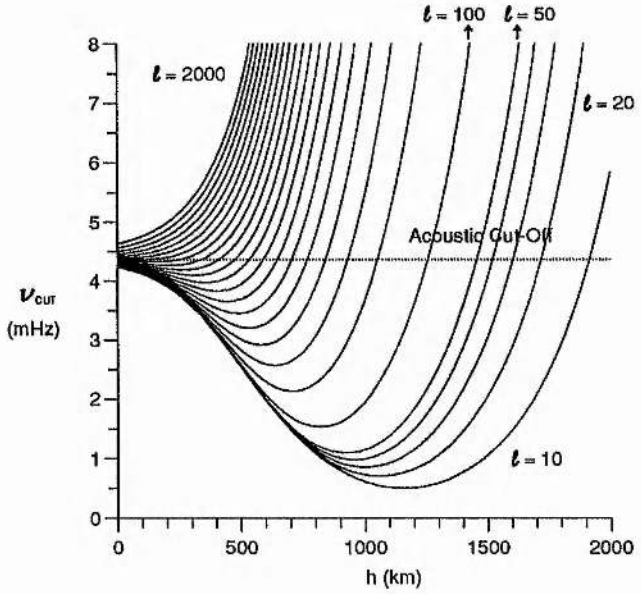

Figure 5.3b

Figure 5.3b: The magnetoacoustic cut-off frequency ν_{cut} as a function of thickness h for different values of the degree l. (a) The chromospheric temperature T_m in the middle region ($-h < z < 0$) is taken to be 4170K and the magnetic field strength B_m to be 20G. The chromospheric temperature T_c for the uppermost region ($z < -h$) is considered to be 5000K. (b) The chromospheric temperature T_m in the middle region ($-h < z < 0$) is taken to be 6200K and the magnetic field strength B_m to be 40G. The chromospheric temperature T_c for the upper most region ($z < -h$) is considered to be 7000K. Note the different values of acoustic cut-off frequency $\nu_a (= \omega_a/2\pi)$ given by Equation (5.51): (a) $\nu_a \sim 5.16$mHz for $h = 0$, and (b)$\nu_a \sim 4.36$mHz for $h = 0$.

Also, it is interesting to note the turning points of the curves. The magnetoacoustic cut-off frequency has a minimum (ν_{cut}^{min}) whose value increases and moves to smaller values of h with an increase in l, disappearing altogether for $l \geq 1800$. The height $h = 0$ corresponds to an Alfven speed at the base of the chromosphere. Thus, it is apparent from the figure that ν_{cut}^{min} depends on Alfvén speed and the degree l.

5.5 Numerical solutions

The dispersion relation (5.25) can be rearranged to give

$$\left\{2a\omega^2 c_{sp}^2 k_x U\left(-a+1, m+3, 2k_x z_o\right) + \left[\gamma g\omega^2 - k_x c_{sp}^2(\omega^2 + g k_x)\right] U\left(-a, m+2, 2k_x z_o\right)\right\} \times$$

$$\left\{(c_{sm}^2 + v_{Am}^2)(\omega^2 - k_x^2 c_{Tm}^2)\left[(\mathcal{M}\mathcal{Z}_2\mathcal{X}_1 - \mathcal{L}\mathcal{Z}_1\mathcal{X}_2) + (\mathcal{L}\mathcal{Z}_1 - \mathcal{M}\mathcal{Z}_2)/\Re_B\right]\right\} - (c_{sm}^2 + \frac{\gamma}{2}v_{Am}^2) \times$$

$$(\omega^2 - k_x^2 c_{sm}^2)(g^2 k_x^2 - \omega^4)\left[(\mathcal{X}_1\mathcal{M} - \mathcal{X}_2\mathcal{L}) + (\mathcal{L} - \mathcal{M})/\Re_B\right] U\left(-a, m+2, 2k_x z_o\right) = 0 \quad (5.52)$$

This form of the dispersion relation is solved numerically, using Fortran 77 programming and double precision arithmetic with an inbuilt routine to ensure that the condition $(1 - 4A_cH_c^2) \geq 0$ is satisfied. This condition corresponds to the solution in the chromosphere ($z < 0$) being evanescent. If the condition is not met, then modes will propagate away to $-\infty$ and no trapping exist.

It is of interest to assess how the present results differ from the ones obtained in Chapter 3. It is expected that for large thickness h the two results should be in agreement as the model of Chapter 3 can be considered to be the case of the current model where the thickness of the middle region is infinite. The graphs are drawn here using the same basic parameters as in Table 3.1. The temperature for the uppermost region ($z < -h$) is taken to be higher than the temperature of the middle region, i.e. $T_c > T_m$.

The procedure employed is as follows. The dispersion relation (5.52) is solved for chosen values of the chromospheric temperatures T_m and T_c and magnetic field strength B_m (referred to as the 'base temperatures' and 'base field strength') and the resulting frequency is known as the 'base frequency'. The dispersion relation is then solved again with the chromospheric temperatures T_m', T_c' and field strength B_m' having been increased from their 'base' values. The frequency shift $\Delta\nu$ is the difference between the resulting cyclic frequency and the cyclic base frequency. The graphs which follow show this frequency shift,

$$\Delta\nu \equiv \nu\left(B_m', T_m', T_c'\right) - \nu\left(B_m, T_m, T_c\right) \ , \tag{5.53}$$

plotted as a function of the base frequency.

Figure 5.4 gives a comparison between the results of the current model and the two layer model described in Chapter 3. Figure 5.4a considers the model of Chapter 3. This is a frequency shift curve, drawn considering the chromospheric magnetic field strength $B_c = 20$G and the chromospheric temperature $T_c = 4170$K. The cyclic frequencies obtained are taken as base frequencies $\nu(B_c, T_c)$. The dispersion relation (3.44) is solved again, this time for higher values of the magnetic field strength (B_c' = 40G) and the temperature ($T_c' = 6200$K). The cyclic frequencies thus obtained are denoted as $\nu(B_c', T_c')$. The difference between $\nu(B_c', T_c')$ and $\nu(B_c, T_c)$ is $\Delta\nu$, which is displayed in Figure 5.4a as a function of ν.

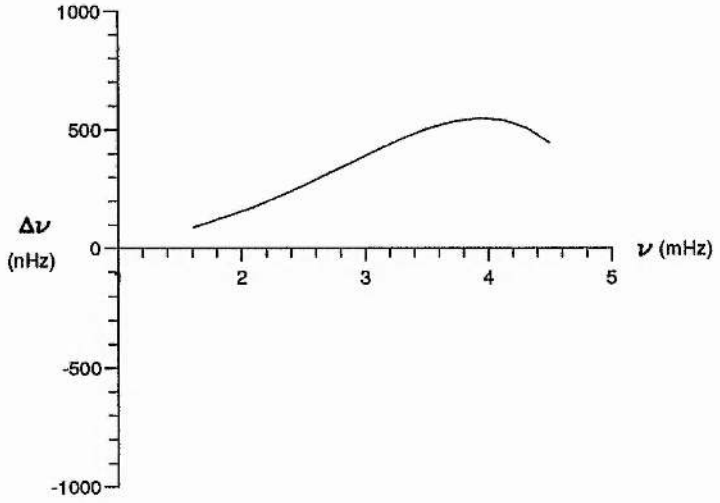

Figure 5.4a: The frequency shifts $\Delta\nu$ for a two layer atmosphere (see Chapter 3) as a function of frequency ν for degree $l = 100$. The base chromospheric temperature T_c is taken to be 4170K and the magnetic field strength B_c to be 20G. The chromospheric temperature T_c' is considered as 6200K and the magnetic field strength B_c' to be 40G. The curve stops at the magnetoacoustic cut-off frequency.

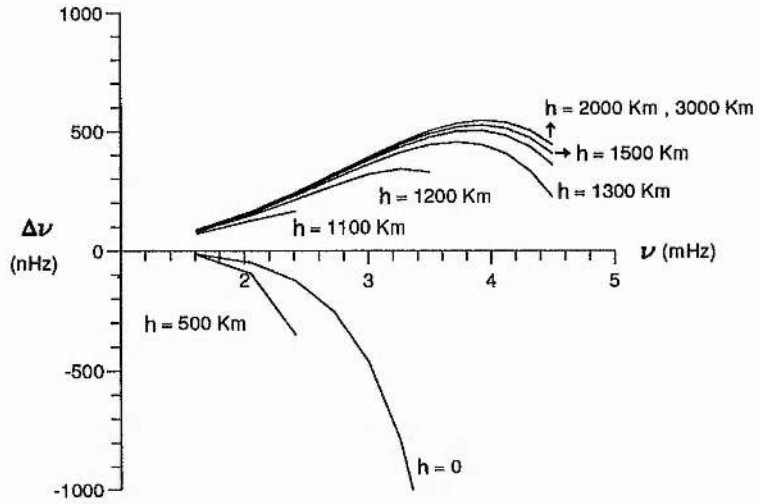

Figure 5.4b: The frequency shift $\Delta\nu$ for a three layer atmosphere as functions of frequency ν for the degree $l = 100$. The base chromospheric temperatures T_m and T_c are taken to be 4170K and 5000K respectively. The base magnetic field strength B_m is taken to be 20G. The chromospheric temperatures T_m' and T_c' are considered to be 6200K and 7000K respectively. The magnetic field strength B_m' is taken to be as 40G. The curves stop at the magnetoacoustic cut-off frequency for that case.

Figure 5.4b deals with the three layer model described in the current chapter. There are several curves in Figure 5.4b, corresponding to various thicknesses h. For small values of h negative frequency shifts are found whereas for higher values of h the frequency shifts are positive. The frequency shift curve for $h = 0$ is a special case and, as expected (see Equation (5.36)), resembles the p-mode frequency shift curves of Chapter 4.

As a finite value of h is introduced and increased, the frequency shift curves evolve in several ways. The magnetoacoustic cut-off frequency (at which the curves stop) at first decreases with increasing h, but for values of h in excess of about 1000 km it increases again (see Figure 5.3). Thus, the curve for $h = 500$ km stops at about 2.4 mHz while the curve for $h = 1300$ km reaches a frequency of about 4.5 mHz.

It may seem surprising that the curve for $h = 500$ km should lie below that for a zero value of h. However the curve for $h = 500$ km is influenced by the larger values of Alfvén speed in the uppermost region. It should be noted that (see Figures 4.2a, b) an increase in the Alfvén speed causes the frequency shift curve to move to larger negative values.

For the larger values of h (> 1000 km) the shifts are dominated by the thick middle region ($-h < z < 0$) of atmosphere and the curves resemble those shown in Chapter 3. In fact, as h becomes large the frequency shift curves become identical with the corresponding curve for the two layer model (see Figure 5.4a). For $h = 2000$ km or 3000 km the curves start to merge and coincide with the curve of Figure 5.4a. A turnover in the frequency shift becomes evident for values of h greater than about 1200 km.

There is an intermediate range of h for which frequency shift curves cannot be drawn simply because the magnetoacoustic cut-off frequency is too low. It is likely that this range contains the height at which the values of the frequency shift change from being negative to positive.

The situation for $h = 1300$ km is examined further for different values of degree l. The results are displayed in Figure 5.5. For all values of l the frequency shifts are positive and the magnitude of frequency shifts increase with increasing l. For lower values of l the magnetoacoustic cut-off frequency is lower (e.g. $\nu_{cut} = 1.9$ mHz for $l = 40$) and hence the curves stop before reaching 4.0 mHz. The curves for $l > 80$ exhibit a turnover at around 3.8 mHz.

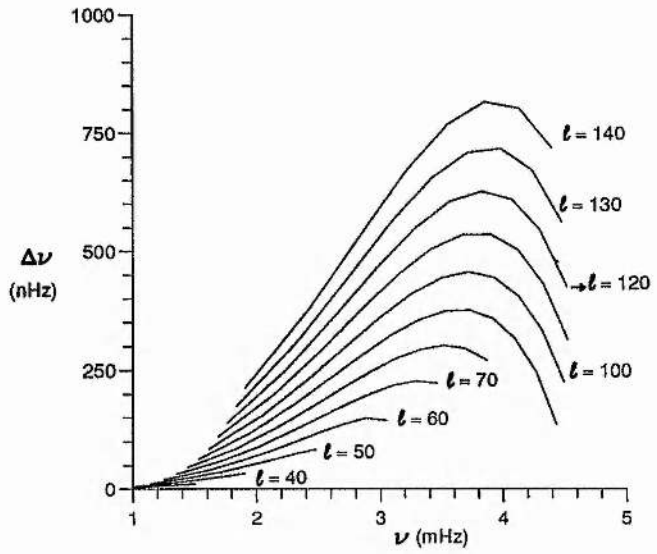

Figure 5.5: The frequency shifts $\Delta\nu$ as functions of frequency ν for thickness $h = 1300$ km. The various curves correspond to the marked values of l. All other parameters remain same as in Figure 5.4b.

5.6 Conclusions

The frequencies of p-modes have been calculated for a three layer atmosphere. These have been calculated for conditions resembling both solar maximum and solar minimum (see Chapter 3 for the assumptions and speculations made about the variations of the magnetic field and chromospheric temperature over the solar cycle). One important quantity derived from the model is the frequency shift - the difference between the frequencies of a given p-mode at solar maximum and solar minimum.

The nature of the frequency shift curve depends greatly upon the extent of the middle layer of the atmosphere, i.e. the layer containing the constant magnetic field. When this layer is very thin the frequency shifts are negative, and resemble those obtained in Chapter 4; when the thickness of this layer is zero, the current model becomes identical to that of Chapter 4. Thus when the region of constant magnetic field is thin, the p-mode frequencies at solar minimum are greater than those at solar maximum.

At the other extreme, when the middle layer (constant magnetic field) is thick enough to dominate, the frequency shift curve will resemble that from Chapter 3, i.e. if the chromospheric temperatures and other parameters are chosen properly, the frequency shifts will be low and positive and increasing for low frequencies followed

by a turnover for higher frequencies. In the limit where the thickness of this region is infinite, the model is identical with the model of Chapter 3 and the frequency shift curve is also identical. When the thickness h of the middle region is large but not infinite, the drop in the frequency shift after the turnover is steeper, and thus more like the observed frequency shifts, although the magnitudes of the calculated frequency shifts are less than the magnitudes of their observed counterparts.

It had initially been thought that as the thickness of the middle layer was increased from zero to infinity, the resultant frequency shift curve would evolve from one extreme to the other. This, however, is not the case as for intermediate values of the thickness of the middle layer, the magnetoacoustic cut-off frequency is small, so small that very few (if any) p-modes have frequencies less than the cut-off frequency. It had also been hoped to reproduce qualitatively the previously mentioned aspects of the observed frequency shift curve (i.e. the rise for low frequencies and the turnover for higher frequencies) by changing the magnetic fields alone, with no change in the chromospheric temperatures. Figure 5.6 shows the result of such changes in the magnetic fields alone; the field B_m is increased from 20G to $B'_m = 40$G with the temperatures $T_m = T'_m$ and $T_c = T'_c$ remaining as 4170K and 5000K, respectively. The thickness h is set equal to 1300 km, and the degree of the mode is $l = 100$. This figure reproduces the observed behaviour for low frequencies but, clearly, no turnover takes place at high frequencies, and so there the calculated curve does not match the observed one.

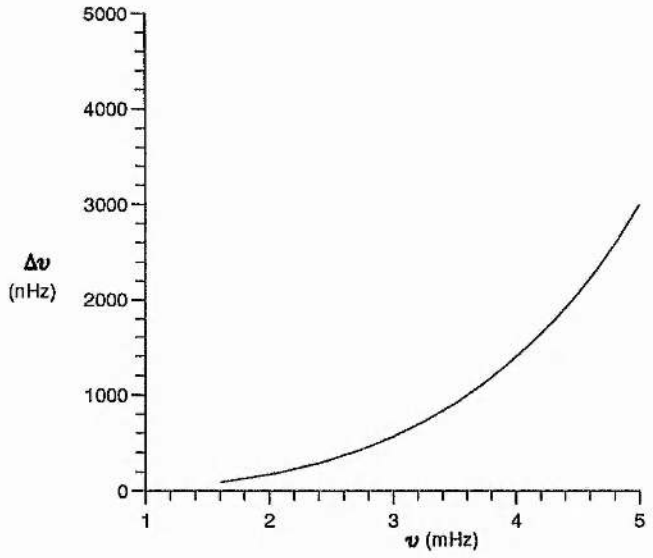

Figure 5.6: The frequency shifts $\Delta\nu$ as functions of frequency ν for changes in the chromospheric magnetic fields but for the chromospheric temperatures remaining constant. Here $B_m = 20$G, $B'_m = 40$G; $T_m = T'_m = 4170$K and $T_c = T'_c = 5000$K. The thickness $h = 1300$ km and the degree $l = 100$.

Therefore, for a middle layer of thickness $h \geq 1300$ km, changes in chromospheric temperature as well as in magnetic field strength are necessary to give a turnover in the frequency shift curve. For these values of h the thick middle region dominates; for a much smaller value of h (e.g. $h \leq 500$ km) the upper chromosphere would dominate and the resultant frequency shifts would always be negative. The small magnetoacoustic cut-off frequency prevents a corresponding investigation of intermediate values of h; otherwise changes in magnetic field alone may well have produced a frequency shift curve which increases for small frequencies but turns over and reduces for larger frequencies.

For this model, one drawback of the two layer model of Chapter 3, namely the arbitrary large value of the Alfvén speed with height, has been overcome. Instead, for the current model, the Alfvén speed reaches a constant value in the high chromosphere.

Thus, in principle, the three layer model is more realistic than the two layer model of Chapter 3. However, the parameters one is compelled to choose for the uppermost region (in order to allow the frequency to range from say $\sim$1 mHz to $\sim$4.5 mHz) are rather unphysical. In reality, one would expect the chromospheric temperatures T_c and T_c' in the uppermost region (which corresponds to the upper chromosphere) to be larger than the values chosen ($T_c = 5000$K, $T_c' = 7000$K) in the preceeding sections. Since the acoustic cut-off frequency reduces with the increase in temperature, it is not possible to investigate the frequency changes for the real situation (the analysis discussed here is for real frequency ω).

The other problem with the chosen parameters is the thickness of the middle region. For the thickness $h = 1300$ km, the Alfvén speed in the uppermost region is quite different (see Figure 5.2b) in the two cases $B_m = 20$G and $B_m = 40$G. This large discontinuity in the value of Alfvén speed at $h = 1300$ km combined with large temperature discontinuity (and hence large discontinuity in the sound speeds) gives very large values of scale heights ($\sim$ 108 Mm and $\sim$ 1100 Mm).

Accepting the advantages and defects of the three layer model, an analysis allowing for an imaginary part of the frequency ω would be very interesting. It is likely that such an analysis would reflect physical aspects more realistically. Here, the analysis was restricted to the case of real frequency ω. It was felt that concentrating on a simpler case would be more useful.

Figure 5.7 illustrates the density distribution $\rho_o(z)$ as a function of distance z for the three layers considered in the current model. Since the condition for the convection zone remains unchanged from one time to another, the density profile for this region remains the same. Since the middle region consists of uniform magnetic field, the

density at $z = 0_-$ now depends on magnetic field strength B_m (or B'_m) as well as the temperature T_m (or T'_m) in this region. Greater magnetic field strength and temperature changes give a larger discontinuity in the value of density at $z = 0$. In fact it can be seen from Figure 5.7 that the value of density near the interface $z = 0_-$ reduces with the increases in temperature and magnetic field strength. This is because the total pressure is continuous across this interface. However it may seem surprising that the densities high in the atmosphere (for large negative z) are smaller for the case when the temperature is low (e.g. $T_m = 4170$K) than when the temperature is higher. This is because the value of the density for a given z is affected more by the scale height than by its value ρ_m near the interface. The scale height is $H_m \sim 97$ km for $B_m = 20$G and $T_m = 4170$K, and $H_m \sim 145$ km for $B_m = 40$G and $T_m = 6200$K. Thus the density $\rho_o(z)\left(= \rho_m e^{z/H_m} \text{ in } -h < z < 0\right)$ falls off more rapidly with height when $H_m \sim 97$ km than when $H_m \sim 145$ km. As mentioned earlier, the density scale heights for the uppermost region are quite high.

The general conclusion is that for a three layer model atmosphere, there exists a frequency shift curve, qualitatively similar to the corresponding observed curve.

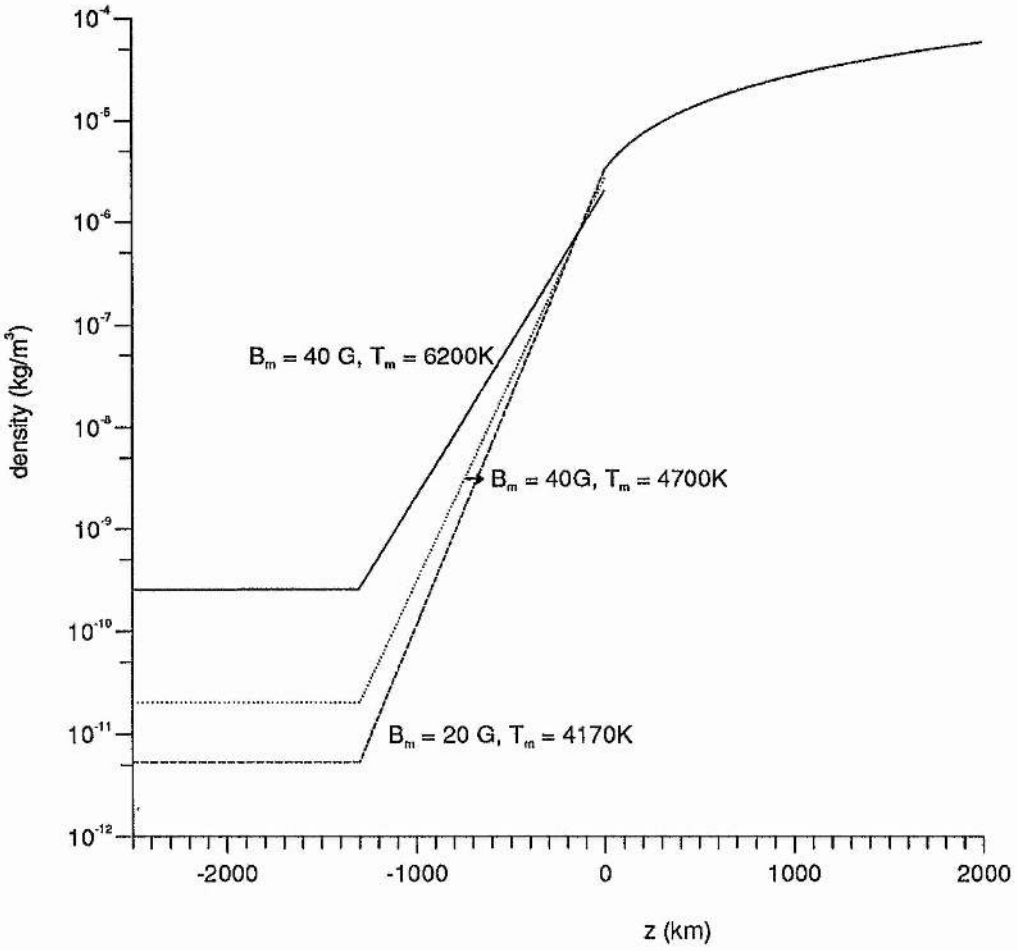

Figure 5.7: The variation of the gas density (plotted logarithmically) with z for B_m = 20G, T_m = 4170K and T_c = 5000K; B_m = 40G, T_m = 4700K and T_c = 7000K; and B_m = 40G, T_m = 6200K and T_c = 7000K. In this Figure the thickness h of the middle region is set equal to 1300 km. The three curves are identical for $z > 0$.

CHAPTER 6

CONCLUDING REMARKS AND SUGGESTIONS FOR FURTHER WORK

This thesis has concentrated on the effects of magnetic atmospheres on solar oscillations, paying particular attention to solar p- and f-modes. Various investigations have been carried out, through a magnetohydrodynamic formalism, involving effects of changes in the chromospheric magnetic field strengths and the chromospheric temperatures. In these investigations, the main aim has been to model some basic aspects of the solar atmosphere and study their influences on the frequencies of the oscillations. Each model can be refined by adding further effects. However, it is important to first understand simple models before adding refinements.

In Chapter 2, surface waves have been discussed for the case of non-parallel propagation and three dimensional motions. Information was obtained about the nature of slow and fast magnetoacoustic surface waves and the conditions for their existence. These conditions are found to be similar to those previously explored in Roberts (1981), Somasundaram and Uberoi(1982), Uberoi(1982) and Miles and Roberts (1989). The model in Chapter 2 extends previous models to include the case of non-parallel propagation. However, many simplifications have been made in constructing the model and generalisations should include at least some of the following aspects.

1) The effects of gravity have been ignored. Clearly, the role of gravity is vital in the solar atmosphere and any discussion of surface waves in the context of the Sun should include stratification due to gravity. An attempt to improve the model of Chapter 2 has been made in Chapter 4 (see Section 4.7) and the relevant dispersion relation has been obtained. However, the properties of magnetoacoustic surface waves need to be explored further.

2) Another important point to note is that the analysis in Chapter 2 has been carried out for semi-infinite regions on either side of a sharp discontinuity. Steady state flows have been ignored. A model taking into account such motions would be more general and of relevance to the Sun.

The model used in Chapter 3 to investigate the influence of chromospheric canopy fields on solar p-mode frequencies confirms and extends the work of Evans and Roberts

(1990). It was found that an increase in magnetic field strength from one time to another increased the frequencies of p-modes, whereas an increase in chromospheric temperature lead to a decrease in the frequencies. A combination of these two effects leads to a situation qualitatively similar to that found by observations. Thus, frequency shifts may be due to changes in the reflective properties of the chromosphere.

Since the observational frequency shifts of the solar p-modes (Libbrecht and Woodard, 1990) are believed to depend on the structure and dynamics of the solar interior and atmosphere, an attempt was made to compare the theoretically calculated frequency shifts (defined to be the difference between the frequencies at solar minimum and solar maximum, for an assumed increase in the chromospheric magnetic field strength and chromospheric temperature) with the observed frequency shifts. Efforts to explain the observational data have enjoyed some success in reproducing the observed frequency shifts qualitatively but unfortunately the model is too simple to explain the observations quantitatively. Many assumptions have been made in the model. A more realistic model would include the removal of at least some of these assumptions. These include the following:

1) The convection zone is assumed to be field-free and the canopy fields are assumed to lie above it in the form of a purely horizontal magnetic field with constant strength. Obviously the magnetic fields in the solar chromosphere are non-uniform and so the uniform field assumption needs to be modified. Also, the magnetic fields in and below the photosphere are believed to exist in the form of magnetic flux tubes. In the current model, these fields are ignored. While the magnetic field and temperature profiles chosen in the current model satisfy several physical requirements and provide very interesting analytical and numerical results, the model can be improved by adapting a field profile which agrees more closely with that expected in magnetic flux tubes that spread to form canopies (i.e. when the fields of the tubes spread out at some height above the photosphere). How can this be done ? One possible way is as follows.

Each field line is assumed to be hyperbolic in shape and described in cylindrical coordinates by $z = \frac{A}{r} - cr$, where r measures horizontal distance from the center of a flux tube and c and A are constant along each field line. When r is large, z tends to $-cr$ and hence the field lines radiate out in all directions (into the chromosphere). When r is small, $z \to \frac{A}{r}$ and the field lines are vertical and close together (i.e. for z being positive they resemble a flux tube). Figure 6.1 illustrates the configuration.

The parameter c denotes the gradient of each field line as it radiates into the chromosphere. The parameter A depends on c, and the correct choice of the form of A allows the equation $\nabla \cdot \mathbf{B} = 0$ to be satisfied. Once the components of magnetic field are known, a plasma pressure can be added to satisfy the magnetostatic equation. When

the pressures and magnetic fields are known at all points, the p-mode modelling can begin.

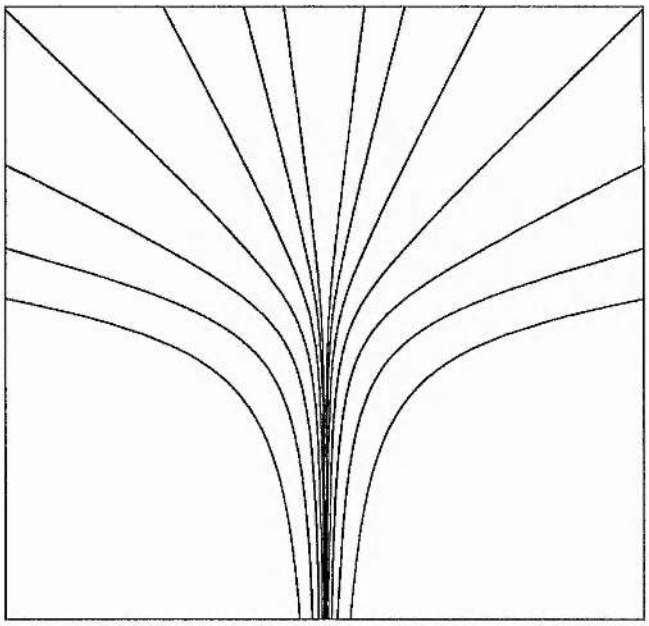

Figure 6.1: An idealised magnetic field profile including a convection zone, where the magnetic field is confined to a single flux tube, and a chromosphere with a magnetic field radiating out in all directions.

Recently, Goldreich et. al (1991) have suggested that the observed frequency shifts (see Figure 3.1) can be divided into two components: a positive component (for which frequency shifts are increasing with an increase in frequency) and a negative component (for which the frequency shift curves suffer a sharp drop at a frequency of $\sim$ 4mHz). According to these authors the changes in photospheric fields may be responsible for the positive signal, while an increase in chromospheric temperature, from solar minimum to solar maximum, together with the presence of a chromospheric resonance could be the reason for the sharp drop in the frequency shift.

The presence of a chromospheric cavity for p-mode oscillation is predicted by the theory of solar atmospheric structure (Ando and Osaki, 1977; Leibacher and Stein, 1981; Deubner and Gough, 1984). This chromospheric cavity is formed by the temperature minimum at the bottom and by the steep temperature rise of the transition region above. However, the observational evidence for the existence of such a cavity is

not yet fully confirmed. Also, at present this cavity is not well understood theoretically. Observations with accurate height discrimination and spatial resolution are needed to clarify the dynamical processes in this layer (see Hill et. al, 1990). However, it is in this cavity that the magnetic field takes control over most of the plasma and the flux emerging from active regions connects to coronal structures. It would be interesting to investigate the influence of such a chromospheric cavity on the solar p-modes. In the light of the models discussed in this thesis, the effects of such a cavity on p-mode frequencies can be studied by allowing for a discontinuous temperature at a certain height (say $\sim$ 2000 km from the temperature minimum).

In Chapter 4 the effects of a *weak* chromosphere were examined by constraining the chromospheric magnetic fields to decline exponentially with height. It was recognised that the assumption of parallel propagation (wave vector parallel to magnetic field direction) in Chapter 3 should be relaxed and a more general approach to take into account non-parallel propagation was considered in Chapter 4. The f-mode frequencies were found to be the most affected by the change of propagation angle. The p-mode frequencies remained, by and large, unchanged. In this model the dispersion relation was derived to allow for a discontinuous temperature (between chromosphere and photosphere) profile so that it is possible to investigate the effects of a hot chromosphere. However, the asymptotic and numerical results were obtained for a continuous temperature profile. It would be more complete to include the effects of temperature changes from one time to another.

The magnetic structure of the chromosphere considered in Chapter 4 may underestimate the effects of magnetism on p-mode frequencies. However, the two models (those of Chapter 3 and Chapter 4) may represent extreme cases of real magnetic fields in the solar chromosphere.

It is worth mentioning that generally observers use the f-mode for calibrating the spatial scale of disk observations because this mode has a simple theoretical dispersion relation $\omega = (gK)^{1/2}$ or $\nu = 3159(l/1000)^{1/2}\mu$Hz (see Hill et. al, 1991). A spatial scale is determined by adjusting it until this relation is satisfied. However, care must be taken with this procedure as the results in Chapter 4 suggest that the frequency of the f-mode is affected by the presence of a magnetic field and non-parallel propagation.

In Chapter 5, the models of Chapter 3 and Chapter 4 were combined in the sense that a region of constant Alfvén speed was added on the top of a uniform field region. This was advantageous in that it prevented the Alfvén speed from becoming very large. Unfortunately it led to the problem of magnetoacoustic cut-off (with frequency shift curves stopping at this cut-off), which hampered attempts to study the combined effects of the two layers. A potential further development would be to investigate the

situation where the frequency exceeds the magnetoacoustic cut-off frequency and wave leakage occurs.

The dispersion relation obtained for the three layer model was rather complicated and hence only numerical solutions were discussed. One alternative to this analysis would be to derive asymptotic solutions, as was the case for the previous chapters.

Finally, it should be emphasised that in this thesis the effects of an isothermal chromosphere on solar oscillations have been considered but it should be recognised that a logical development would be to consider a non-isothermal chromosphere.

One major achievement of this thesis has been to produce a frequency shift curve qualitatively similar to those found from observations (i.e. a curve which increases for low frequencies but turns over and decreases for higher frequencies). This has been achieved both with a simple two layer model (see Chapter 3) and with a slightly more sophisticated and realistic model incorporating a third layer (see Chapter 5).

Two of the model atmospheres examined (namely those in Chapters 2 and 4) considered non-parallel propagation. The f-mode frequencies in the presence of a magnetic field were found to be greater in the case of parallel propagation and as the propagation angle (i.e. deviation from parallel case) increased the magnetic correction to the f-mode frequency decreased.

The work in this *thesis* has investigated two factors not previously considered in models of this nature (Evans and Roberts, 1990; Campbell and Roberts, 1989), namely the effect of a simultaneous change in the chromospheric magnetic field and temperature on p-mode frequencies and the effect of non-parallel propagation. Having identified which parameters play significant roles and which parameters the frequency shift curve is not particularly sensitive to, this model opens the way for fully numerical, two dimensional model atmospheres where the effects of many parameters may be considered.

APPENDIX A2 : DERIVATION OF THE VELOCITY EQUATION AND DISPERSION RELATION

Section 1 : Velocity Equation

The equlibrium state of the plasma is

$$p_o = p_o(z)\,, \quad \rho_o = \rho_o(z)\,, \quad \frac{d}{dz}\left(p_o + \frac{B_o^2}{2\mu}\right) = 0\,. \tag{A2.1}$$

Linear perturbations about this equilibrium state give the equations of continuity (2.2), momentum (2.3), induction (2.4) and the energy equation (2.5) for isentropic disturbances as follows:

$$\frac{\partial \rho}{\partial t} + \nabla \cdot (\rho_o \mathbf{v}) \;=\; 0, \tag{A2.2}$$

$$\rho_o \frac{\partial \mathbf{v}}{\partial t} \;=\; -\nabla\left(p + \frac{1}{\mu}\mathbf{B_o}\cdot\mathbf{B}\right) + \frac{1}{\mu}(\mathbf{B_o}\cdot\nabla)\,\mathbf{B} + \frac{1}{\mu}(\mathbf{B}\cdot\nabla)\,\mathbf{B_o}\,, \tag{A2.3}$$

$$\frac{\partial \mathbf{B}}{\partial t} \;=\; \nabla \times (\mathbf{v}\times\mathbf{B_o})\,, \tag{A2.4}$$

$$\frac{\partial p}{\partial t} + \mathbf{v}\cdot\nabla p_o \;=\; c_s^2\left(\frac{\partial \rho}{\partial t} + \mathbf{v}\cdot\nabla\rho_o\right)\,, \tag{A2.5}$$

where $\rho, p, \mathbf{v}$ and $\mathbf{B}$ (satisfying $\nabla\cdot\mathbf{B} = 0$) are the perturbations in density, pressure, velocity and induction field, respectively. The sound speed in the equilibrium state is $c_s(z) = (\gamma p_o(z)/\rho_o(z))^{1/2}$, where γ is the ratio of specific heats.

Differentiating the momentum equation (A2.3) with respect to time t gives

$$\rho_o \frac{\partial^2 \mathbf{v}}{\partial t^2} \;=\; -\nabla\left(\frac{\partial P_T}{\partial t}\right) + \frac{1}{\mu}(\mathbf{B_o}\cdot\nabla)\frac{\partial \mathbf{B}}{\partial t} + \frac{1}{\mu}\left(\frac{\partial \mathbf{B}}{\partial t}\cdot\nabla\right)\mathbf{B_o}\,, \tag{A2.6}$$

where

$$P_T \;=\; p \;+\; \frac{1}{\mu}(\mathbf{B_o}\cdot\mathbf{B}) \;. \tag{A2.7}$$

On using the induction equation (A2.4) and the energy equation (A2.5), the x, y, and z components of the momentum equation (A2.6) are given as

$$\frac{\partial^2 v_x}{\partial t^2} \;=\; c_s^2\frac{\partial \Delta}{\partial x}\;, \tag{A2.8a}$$

$$\left(\frac{\partial^2}{\partial t^2} \;-\; v_A^2\frac{\partial^2}{\partial x^2}\right)v_y \;=\; \frac{\partial}{\partial y}\left[\left(c_s^2+v_A^2\right)\Delta - v_A^2\frac{\partial v_z}{\partial z}\right]\;, \tag{A2.8b}$$

$$\left(\frac{\partial^2}{\partial t^2} \;-\; v_A^2\frac{\partial^2}{\partial x^2}\right)v_z \;=\; \frac{\partial}{\partial z}\left[\left(c_s^2+v_A^2\right)\Delta - v_A^2\frac{\partial v_z}{\partial z}\right]\;, \tag{A2.8c}$$

where

$$\Delta \;=\; \frac{\partial v_x}{\partial x}+\frac{\partial v_y}{\partial y}+\frac{\partial v_z}{\partial z} \tag{A2.9}$$

On Fourier analysing (see Equation (2.8) of the main text), equations (A2.8) can be reduced to a simple ordinary differential equation for $v_z(z)$:

$$\frac{d}{dz}\left\{\frac{\rho_o(z)(k_x^2v_A^2(z)-\omega^2)}{(m^2(z)+k_y^2)}\frac{dv_z}{dz}\right\} - \rho_o(z)\left(k_x^2v_A^2(z)-\omega^2\right)v_z \;=\; 0\;. \tag{A2.10}$$

where $m^2(z)$ is defined by

$$m^2(z) = \frac{(k_x^2c_s^2(z)-\omega^2)\,(k_x^2v_A^2(z)-\omega^2)}{(c_s^2(z)+v_A^2(z))\,(k_x^2c_T^2(z)-\omega^2)}\;, \qquad c_T^2(z) = \frac{c_s^2(z)v_A^2(z)}{(c_s^2(z)+v_A^2(z))}\;. \tag{A2.11}$$

Equation (A2.10) is Equation (2.9) of the main text.

Section 2 : Dispersion Relation

The energy equation (A2.5) on using the continuity equation (A2.2) can be written as (since $p_o = p_o(z)$)

$$\frac{\partial p}{\partial t} = -\rho_o c_s^2 \Delta - \frac{dp_o}{dz} v_z \, . \tag{A2.12}$$

Using equations (A2.12), (2.4) and (A2.7)

$$\frac{\partial P_T}{\partial t} = \rho_o v_A^2 \frac{\partial v_x}{\partial x} - \rho_o \left(c_s^2 + v_A^2 \right) \Delta \, . \tag{A2.13}$$

Fourier analysis of equation (A2.13) then gives the total perturbed pressure as (using equation (A2.8))

$$P_T = \frac{i\rho_o}{\omega} \frac{(k_x^2 v_A^2 - \omega^2)}{(m^2 + k_y^2)} \frac{dv_z}{dz} \, . \tag{A2.14}$$

Across the interface $z = 0$, $v_z(z)$ and $P_T(z)$ must be continuous. Thus $\alpha_e = \alpha_o$ (see Equation (2.20) of the main text) while the continuity of P_T at $z = 0$ gives

$$\rho_o (k_x^2 v_A^2 - \omega^2)(m_e^2 + k_y^2)^{1/2} + \rho_e (k_x^2 v_{Ae}^2 - \omega^2)(m_o^2 + k_y^2)^{1/2} = 0 \, , \tag{A2.15}$$

where m_o^2 and m_e^2 denote the values of m^2 in the regions ($z < 0$) and ($z > 0$), respectively. Equation (A2.15) is the dispersion relation (2.22) of the main text.

APPENDIX A3 : DERIVATION OF THE DISPERSION RELATION AND VARIOUS ASYMPTOTIC FORMULAE

Section 1: The Governing Differential Equation

The basic equilibrium state of the plasma has

$$\mathbf{B} = B_o(z)\,, \quad \mathbf{V} = 0\,, \quad p = p_o(z)\,, \quad \rho = \rho_o(z)\,, \quad \frac{d}{dz}\left(p_o + \frac{B_o^2}{2\mu}\right) = \rho_o(z)g\,. \tag{A3.1}$$

Linear perturbations about this equilibrium state modify the equations of continuity (3.8), momentum (3.9), induction (3.10), and the energy equation (3.11) for isentropic disturbances as follows:

$$\frac{\partial \rho}{\partial t} + \nabla \cdot (\rho_o \mathbf{v}) \;=\; 0, \tag{A3.2}$$

$$\rho_o \frac{\partial \mathbf{v}}{\partial t} \;=\; -\nabla\left(p + \frac{1}{\mu}\mathbf{B_o}\cdot\mathbf{B}\right) + \frac{1}{\mu}\left(\mathbf{B_o}\cdot\nabla\right)\mathbf{B} + \frac{1}{\mu}\left(\mathbf{B}\cdot\nabla\right)\mathbf{B_o} + \rho\mathbf{g}\,, \tag{A3.3}$$

$$\frac{\partial \mathbf{B}}{\partial t} \;=\; \nabla \times (\mathbf{v} \times \mathbf{B_o})\,, \tag{A3.4}$$

$$\frac{\partial p}{\partial t} + \mathbf{v}\cdot\nabla p_o \;=\; c_s^2\left(\frac{\partial \rho}{\partial t} + \mathbf{v}\cdot\nabla\rho_o\right)\,, \tag{A3.5}$$

where $\rho, p, \mathbf{v}$ and $\mathbf{B}$ (satisfying $\nabla \cdot \mathbf{B} = 0$) are the perturbations in density, pressure, velocity and magnetic field, respectively. The sound speed in the equilibrium state is $c_s(z) = (\gamma p_o(z)/\rho_o(z))^{1/2}$, where γ is the ratio of specific heats.

Differentiating the momentum equation (A3.3) with respect to time t gives

$$\rho_o \frac{\partial^2 \mathbf{v}}{\partial t^2} = -\nabla\left(\frac{\partial P_T}{\partial t}\right) + \frac{1}{\mu}(\mathbf{B_o}\cdot\nabla)\frac{\partial \mathbf{B}}{\partial t} + \frac{1}{\mu}\left(\frac{\partial \mathbf{B}}{\partial t}\cdot\nabla\right)\mathbf{B_o} + \mathbf{g}\frac{\partial \rho}{\partial t}\,, \quad \text{(A3.6)}$$

where

$$P_T = p + \frac{1}{\mu}(\mathbf{B_o}\cdot\mathbf{B})\,. \quad \text{(A3.7)}$$

On using the induction equation (A3.4) and the energy equation (A3.5), the x and z components of the momentum equation (A3.6) are given by

$$\frac{\partial^2 v_x}{\partial t^2} = c_s^2\frac{\partial \Delta}{\partial x} + g\frac{\partial v_z}{\partial x}\,, \quad \text{(A3.8a)}$$

$$\left(\frac{\partial^2}{\partial t^2} - v_A^2\frac{\partial^2}{\partial x^2}\right)v_z = \frac{1}{\rho_o}\frac{\partial}{\partial z}\left[\rho_o\left(c_s^2+v_A^2\right)\Delta - \rho_o v_A^2\frac{\partial v_x}{\partial x}\right] + g\left(\frac{\partial v_z}{\partial z} - \Delta\right), \quad \text{(A3.8b)}$$

where (since here $v_y = 0$)

$$\Delta = \frac{\partial v_x}{\partial x} + \frac{\partial v_z}{\partial z}\,. \quad \text{(A3.9)}$$

On Fourier analysis, expressing the perturbed quantities in the form

$$\mathbf{v} = (v_x(z), 0, v_z(z))\, e^{i(\omega t - k_x x)}\,,$$

etc, where ω is the angular frequency and k_x is the wavenumber along x-axis, Equations (A3.8a,b) can be reduced to a second order ordinary differential equation for $v_z(z)$:

$$\frac{d}{dz}\left\{\frac{\rho_o(c_s^2+v_A^2)(\omega^2 - k_x^2c_T^2)}{(\omega^2 - k_x^2c_s^2)}\frac{dv_z}{dz}\right\}$$

$$= \frac{\rho_o g^2 k_x^2}{(\omega^2 - k_x^2c_s^2)} - \rho_o(\omega^2 - k_x^2v_A^2) - gk_x^2\frac{d}{dz}\left(\frac{\rho_o c_s^2}{(\omega^2 - k_x^2c_s^2)}\right)v_z\,. \quad \text{(A3.10)}$$

This is Equation (3.12) of the main text.

Section 2: The Non-Magnetic Case

On Fourier analysis, Equation (A3.8a) gives

$$-\omega^2\left(\Delta - \frac{dv_z}{dz}\right) = -k_x^2\left(c_{sp}^2\Delta + gv_z\right) , \tag{A3.11}$$

which can also be written as

$$(\omega^2 - k_x^2 c_{sp}^2)\Delta = gk_x^2 v_z + \omega^2 \frac{dv_z}{dz} . \tag{A3.12}$$

This is Equation (3.33a) of the main text.

When the magnetic field $B_o = 0$, Equation (A3.8b) becomes

$$\frac{\partial^2 v_z}{\partial t^2} = \frac{\rho_o'}{\rho_o}c_s^2\Delta + c_s'^2\Delta + c_s^2\frac{\partial \Delta}{\partial z} + g\frac{\partial v_z}{\partial z} - g\Delta , \tag{A3.13}$$

where the dash $'$ denotes differentiation with respect to z. On Fourier analysing as above and using the equilibrium constraint

$$\frac{c_s'^2}{c_s^2} = \frac{\gamma g}{c_s^2} - \frac{\rho_o'}{\rho_o} , \tag{A3.14}$$

Equation (A3.13) gives

$$-\omega^2 v_z + gv_z' = c_s^2\Delta' - (\gamma - 1)g\Delta . \tag{A3.15}$$

Finally, using (A3.12) gives

$$(\omega^4 - g^2k_x^2)v_z = g(k_x^2c_{sp}^2 - \gamma\omega^2)\Delta - \omega^2 c_{sp}^2\frac{d\Delta}{dz} , \tag{A3.16}$$

which is Equation (3.33b) of the main text.

Section 3: The Field-free Dispersion Relation

Consider Equation (3.45) in the limit $\beta \to \infty$ to obtain the dispersion relation for the field-free case. Thus, as $\beta \to \infty$, Equation (3.45) reduces to (on noting that $\Gamma \to \gamma$ as $\beta \to \infty$).

$$2a\kappa\Omega^2\frac{U(-a+1, m+3, 2\kappa)}{U(-a, m+2, 2\kappa)} + (m+1)\Omega^2 - \kappa(1 + \Omega^2)$$

$$= \left(\frac{T_c}{T_p}\right) \frac{(\wedge\Omega^2 - \kappa)(1 - \Omega^4)}{[1 + \phi\Omega^2]}, \qquad \text{(A3.17)}$$

where

$$\phi = 1 - \beta\Omega^2 \left\{ \frac{\left[1 + \frac{\gamma-1}{\gamma}\frac{1}{\Omega^2} + \frac{\Omega^2}{\gamma}\right]}{\left[\frac{2\kappa}{\gamma\wedge} + 1\right]\left[\Omega^2 - \frac{\kappa}{\wedge}\right]} \frac{F\left(p+1, q+1; r+1; \frac{-\mathcal{A}_1}{\mathcal{A}_2}\right)}{F\left(p, q; r; \frac{-\mathcal{A}_1}{\mathcal{A}_2}\right)} \right\}. \qquad \text{(A3.18)}$$

But as $\beta \to \infty$

$$\frac{\mathcal{A}_1}{\mathcal{A}_2} = -\frac{\Omega^2\beta}{(\Omega^2 - \frac{\kappa}{\wedge})} \to -\infty . \qquad \text{(A3.19)}$$

Using the following identity (Abramowitz and Stegun, 1965; p.559) for $|\arg(1-z)| < \pi$

$$\begin{aligned} F\left(a, b; c; \frac{-\mathcal{A}_1}{\mathcal{A}_2}\right) &= \frac{\Gamma(c)\Gamma(b-a)}{\Gamma(b)\Gamma(c-a)}(-z)^{-a} F\left(a, 1-c+a; 1-b+a; \frac{1}{z}\right) \\ &+ \frac{\Gamma(c)\Gamma(a-b)}{\Gamma(a)\Gamma(c-b)}(-z)^{-b} F\left(b, 1-c+b; 1-a+b; \frac{1}{z}\right), \qquad \text{(A3.20)} \end{aligned}$$

it is possible to write

$$\frac{F\left(p+1, q+1; r+1; -\frac{\mathcal{A}_1}{\mathcal{A}_2}\right)}{F\left(p, q; r; -\frac{\mathcal{A}_1}{\mathcal{A}_2}\right)} = \left(\frac{\mathcal{A}_1}{\mathcal{A}_2}\right)^{-1} \frac{\frac{\Gamma(r+1)\Gamma(q-p)}{\Gamma(q+1)\Gamma(r-p)}\left(\frac{\mathcal{A}_1}{\mathcal{A}_2}\right)^{-p} + \frac{\Gamma(r+1)\Gamma(p-q)}{\Gamma(p+1)\Gamma(r-q)}\left(\frac{\mathcal{A}_1}{\mathcal{A}_2}\right)^{-q}}{\frac{\Gamma(r)\Gamma(q-p)}{\Gamma(q)\Gamma(r-p)}\left(\frac{\mathcal{A}_1}{\mathcal{A}_2}\right)^{-p} + \frac{\Gamma(r)\Gamma(p-q)}{\Gamma(p)\Gamma(r-q)}\left(\frac{\mathcal{A}_1}{\mathcal{A}_2}\right)^{-q}} \qquad \text{(A3.21)}$$

On assuming that $p > q$, Equation (A3.21) can be written as

$$\begin{aligned} \frac{F\left(p+1, q+1; r+1; -\frac{\mathcal{A}_1}{\mathcal{A}_2}\right)}{F\left(p, q; r; -\frac{\mathcal{A}_1}{\mathcal{A}_2}\right)} &= \left(\frac{\mathcal{A}_1}{\mathcal{A}_2}\right)^{-1} \left\{\frac{\Gamma(r+1)\Gamma(p-q)}{\Gamma(p+1)\Gamma(r-q)} \times \frac{\Gamma(p)\Gamma(r-q)}{\Gamma(r)\Gamma(p-q)}\right\} \\ &= \left(\frac{\mathcal{A}_1}{\mathcal{A}_2}\right)^{-1} \frac{\Gamma(p)}{\Gamma(p+1)} \times \frac{\Gamma(r+1)}{\Gamma(r)} \\ &= \left(\frac{\mathcal{A}_1}{\mathcal{A}_2}\right)^{-1} \left(\frac{r}{p}\right). \qquad \text{(A3.22)} \end{aligned}$$

Thus, Equation (A3.18) becomes

$$\phi \;\rightarrow\; 1 \;-\; 2\frac{\left[1 \;+\; \frac{\gamma-1}{\gamma}\frac{1}{\Omega^2} + \frac{\Omega^2}{\gamma}\right]}{\left[\frac{2\kappa}{\gamma\Lambda} \;+\; 1\right]}\left(\frac{r}{p}\right) \quad \text{as } \beta \rightarrow \infty\,. \tag{A3.23}$$

Since

$$r = \frac{2\kappa}{\gamma\Lambda} + 1\;, 2p = \left(\frac{2\kappa}{\gamma\Lambda} + 1\right) \pm \left\{1 - \frac{4\kappa}{\Omega^2\gamma^2\Lambda}\left[(\gamma-1) + \Omega^2\left(\Omega^2 - \frac{\kappa}{\Lambda}\right)\right]\right\}^{1/2}\;, \tag{A3.24}$$

Equation (A3.23) is equivalent to

$$\phi \;\rightarrow\; 1 \;-\; 2\frac{\left[1 \;+\; \frac{\gamma-1}{\gamma}\frac{1}{\Omega^2} + \frac{\Omega^2}{\gamma}\right]}{\left[\left(\frac{2\kappa}{\gamma\Lambda} + 1\right) + \left(1 - \frac{4\kappa}{\Omega^2\gamma^2\Lambda}\left[(\gamma-1) + \Omega^2\left(\Omega^2 - \frac{\kappa}{\Lambda}\right)\right]\right)^{1/2}\right]}\,. \tag{A3.25}$$

On rationalising, Equation (A3.25) becomes

$$\phi \rightarrow 1 - 2\frac{\left[1 + \frac{\gamma-1}{\gamma}\frac{1}{\Omega^2} + \frac{\Omega^2}{\gamma}\right]\left[\left(\frac{2\kappa}{\gamma\Lambda} + 1\right) + \left(1 - \frac{4\kappa}{\Omega^2\gamma^2\Lambda}\left[(\gamma-1) + \Omega^2\left(\Omega^2 - \frac{\kappa}{\Lambda}\right)\right]\right)^{1/2}\right]}{\left[\left(\frac{2\kappa}{\gamma\Lambda} + 1\right)^2 - \left(1 - \frac{4\kappa}{\Omega^2\gamma^2\Lambda}\left[(\gamma-1) + \Omega^2\left(\Omega^2 - \frac{\kappa}{\Lambda}\right)\right]\right)^{1/2}\right]} \tag{A3.26}$$

After some algebra

$$\phi \;\rightarrow\; 1 \;-\; 2\frac{\left[\left(\frac{2\kappa}{\gamma\Lambda} \;+\; 1\right) + \left(1 - \frac{4\kappa}{\Omega^2\gamma^2\Lambda}\left[(\gamma-1) + \Omega^2\left(\Omega^2 - \frac{\kappa}{\Lambda}\right)\right]\right)^{1/2}\right]}{\frac{4\kappa}{\gamma\Lambda}}\,. \tag{A3.27}$$

Thus,

$$\phi \;\rightarrow\; \frac{\gamma\Lambda}{2\kappa}\left\{-1 + \left[1 - \frac{4\kappa}{\Omega^2\gamma^2\Lambda}\left\{(\gamma-1) + \Omega^2\left(\Omega^2 - \frac{\kappa}{\Lambda}\right)\right\}\right]^{1/2}\right\} \tag{A3.28}$$

After substituting ϕ in Equation (A3.17) and rearranging,

$$2a\frac{U(-a+1, m+3, 2\kappa)}{U(-a, m+2, 2\kappa)} = -\frac{(m+1)}{\kappa} + \frac{\Omega^2+1}{\Omega^2} + \frac{(m+1)(\Lambda\Omega^2 - \kappa)(1-\Omega^4)}{\gamma\; X\; \Omega^2}, \tag{A3.29}$$

where

$$X = \wedge\kappa + \frac{\gamma\wedge^2\Omega^2}{2}\left[-1+\left\{1-\frac{4\kappa}{\gamma^2\wedge}\left[\frac{(\gamma-1)+\Omega^2(\Omega^2-\frac{\kappa}{\wedge})}{\Omega^2}\right]\right\}^{1/2}\right] . \quad \text{(A3.30)}$$

Equation (A3.29) is the same equation as (3.52) of the main text.

Section 4: Taylor Series for the Field-free Dispersion Relation

The Taylor series expansion of (A3.30) namely,

$$X = \wedge\kappa + \frac{\gamma\wedge^2\Omega^2}{2}\left[-1+\left\{1-\frac{4\kappa}{\gamma^2\wedge}\left[\frac{(\gamma-1)+\Omega^2(\Omega^2-\frac{\kappa}{\wedge})}{\Omega^2}\right]\right\}^{1/2}\right] \quad \text{(A3.31)}$$

around $\kappa = 0$ is given by

$$X = -\frac{\wedge\kappa(\Omega^4-1)}{\gamma} - \frac{\kappa^2}{\Omega^2}\left\{d_8\Omega^8 + d_4\Omega^4 + d_o\right\} , \quad \text{(A3.32)}$$

where

$$d_8 = \frac{1}{\gamma^3} , \qquad d_4 = \frac{2(\gamma-1)}{\gamma^3} - \frac{1}{\gamma} , \qquad d_o = \frac{(\gamma-1)^2}{\gamma^3} . \quad \text{(A3.33)}$$

So, the right-hand side of Equation (3.52) of the main text becomes

$$-\frac{(m+1)}{\kappa} + \frac{(\Omega^2+1)}{\Omega^2} - \frac{(m+1)(\wedge\Omega^2-\kappa)(1-\Omega^4)}{\wedge\kappa\Omega^2(\Omega^4-1)+\gamma\kappa^2(d_8\Omega^8+d_4\Omega^4+d_o) + \ldots}, \quad \text{(A3.34)}$$

which after some algebra can be written as

$$\frac{(m+1)\gamma(d_8\Omega^8+d_4\Omega^4+d_o) - \wedge(\Omega^4-1)(\Omega^2+1) + (m+1)(\Omega^4-1)}{-\wedge\Omega^2(\Omega^4-1) + \gamma\kappa(d_8\Omega^8+d_4\Omega^4+d_o)} + O(\kappa) \quad \text{(A3.35)}$$

where the order κ term has the form

$$\frac{\gamma\kappa(\Omega^2+1)(d_8\Omega^8+d_4\Omega^4+d_o)}{\Omega^2} . \quad \text{(A3.36)}$$

On further analysis, the expression (A3.35) becomes

$$\frac{(1+\Omega^2)}{\Omega^2} - \frac{(m+1)}{\Lambda\Omega^2} - \frac{\gamma(m+1)(d_8\Omega^8 + d_4\Omega^4 + d_o)}{\Lambda\Omega^2(\Omega^4-1)} + O(\kappa)\,, \qquad \text{(A3.37)}$$

which can be written in the form

$$1 - \frac{a_8\,\Omega^8 + a_4\,\Omega^4 + a_0}{\Omega^2(\Omega^4-1)} + O(\kappa)\,, \qquad \text{(A3.38)}$$

where

$$a_8 = \frac{(m+1)}{\gamma^2\Lambda}\,, \quad a_4 = -1 + 2(\gamma-1)a_8\,,$$

$$a_0 = 1 + \frac{(m+1)}{\Lambda}\frac{(1-2\gamma)}{\gamma^2}\,. \qquad \text{(A3.39)}$$

Equation (A3.38) provides the desired right hand side of Equation (3.54) of the main text.

Section 5: The Field-free Thermal Correction

In order to determine δ_o, the correction due to the thermal effects in the absence of magnetic field, consider Equation (3.78) of the main text which, on division by κ, is as follows:

$$1 - \frac{(a_8\,\Omega_\star^8 + a_4\,\Omega_\star^4 + a_0)}{\Omega_\star^2(\Omega_\star^4-1)} + O(\kappa) = \frac{2(m+1)(\mathcal{D}_1 + \mathcal{D}_2\,a\,\mathcal{G})}{\mathcal{D}_4\mathcal{G}}\,. \qquad \text{(A3.40)}$$

Since

$$\mathcal{G} = \frac{2(-1)^n}{m\,\delta_o\,\Gamma(n)}\,, \qquad \text{(A3.41)}$$

Equation (A3.40) can be written as

$$\frac{(-1)^n}{m\delta_o\,\Gamma(n)}\left[\mathcal{D}_4\left\{1 - \frac{(a_8\,\Omega_\star^8 + a_4\,\Omega_\star^4 + a_0)}{\Omega_\star^2(\Omega_\star^4-1)}\right\} - 2(m+1)\mathcal{D}_2\,a\right] = (m+1)\mathcal{D}_1\,. \qquad \text{(A3.42)}$$

Using the definition of the confluent hypergeometric M-function (Abramowitz and Stegun, 1965; p.504)

$$M(c,d,z) \;=\; 1+\frac{c}{d}z+\frac{c(c+1)}{d(d+1)}\frac{z^2}{2!}+\dots\,, \tag{A3.43}$$

it can be noticed that $\mathcal{D}_1 \approx 1$ in the limit
kappa $\rightarrow 0$; specifically,

$$\begin{aligned}\mathcal{D}_1 \;&=\; M(-1-a-m,-m-1,2\kappa)\approx 1 \;+\; \frac{m+n}{m+1}(2\kappa)\\ &\quad+\frac{(m+n)(m+n-1)}{m(m+1)}\frac{(2\kappa)^2}{2!} \;+\; O(\kappa^3)\,,\end{aligned} \tag{A3.44}$$

Thus, (A3.42) yields,

$$\delta_o=\frac{(-1)^n\mathcal{D}_4}{m\;\Gamma(n)(m+1)}\left[1-\frac{(a_8\;\Omega_\star^8+a_4\;\Omega_\star^4+a_0)}{\Omega_\star^2(\Omega_\star^4-1)}-2(m+1)\;a\;\frac{\mathcal{D}_2}{\mathcal{D}_4}\right]\,. \tag{A3.45}$$

But

$$\begin{aligned}\mathcal{D}_4 \;&=\; \frac{\Gamma(-m)}{\Gamma(-1-a-m)\Gamma(m+2)}\\ &=\; \frac{\Gamma(-m)}{\Gamma(-m-n)\Gamma(m+2)}\,, \qquad \text{since a } \rightarrow \text{ n}-1\,.\end{aligned} \tag{A3.46}$$

Also

$$\begin{aligned}\mathcal{D}_2 \;&=\; \frac{\Gamma(-1-m)}{\Gamma(-1-a-m)\Gamma(m+3)}\\ &=\; \frac{\Gamma(-1-m)}{\Gamma(-m-n)\Gamma(m+3)}\,, \qquad \text{since a } \rightarrow \text{ n}-1\,.\end{aligned} \tag{A3.47}$$

Thus, substituting for

$$\frac{\mathcal{D}_2}{\mathcal{D}_4} \;=\; -\frac{\Gamma(m+2)}{(m+1)\Gamma(m+3)} \;=\; -\frac{1}{(m+1)(m+2)}\,, \tag{A3.48}$$

in Equation (A3.45) yields

$$\delta_o = \frac{(-1)^n \Gamma(-m)}{m\Gamma(n)(m+1)\Gamma(-m-n)\Gamma(m+2)} \left[1 - \frac{(a_8\Omega_*^8 + a_4\Omega_*^4 + a_0)}{\Omega_*^2(\Omega_*^4 - 1)} + \frac{2a}{(m+2)}\right] \quad \text{(A3.49)}$$

Noting that

$$\frac{(-1)^n \Gamma(-m-n)}{\Gamma(-m)} = \frac{\Gamma(1+m)}{\Gamma(1+m+n)}, \quad \text{(A3.50)}$$

and $a \rightarrow n - 1$, Equation (A3.49) can be written as

$$\delta_o = \frac{-\Gamma(1+m+n)}{m(m+1)\Gamma(n)\Gamma(m+1)\Gamma(m+2)} \left[\frac{(a_8\Omega_*^8 + a_4\Omega_*^4 + a_0)}{\Omega_*^2(\Omega_*^4 - 1)} - 1 - \frac{2(n-1)}{(m+2)}\right]. \quad \text{(A3.51)}$$

In terms of Ω_*^2, Equation (A3.51) can be written as

$$\delta_o = \frac{-\Gamma(1+m+n)}{m(m+1)\Gamma(n)\Gamma(m+1)\Gamma(m+2)} \left[\frac{(a_8\Omega_*^8 + a_4\Omega_*^4 + a_0)}{\Omega_*^2(\Omega_*^4 - 1)} - \frac{m\,\Omega_*^2}{(m+2)}\right], \quad \text{(A3.52)}$$

since

$$\begin{aligned} -1 - \frac{2(n-1)}{(m+2)} &= \frac{-(m+2) - 2n + 2}{(m+2)}, \\ &= \frac{-m\left(1 + \frac{2n}{m}\right)}{(m+2)}, \\ &= \frac{-m\Omega_*^2}{(m+2)}, \end{aligned} \quad \text{(A3.53)}$$

using the Equation (3.64) of the main text.

Equation (3.79) of the main text then follows.

Section 6: High Frequency Limit of the Zero Field Correction

We wish to obtain the limit $n \to \infty$ of the correction δ_o. Consider Equation (3.79) of the main text, viz.

$$\delta_o = \frac{-\Gamma(1+m+n)}{m(m+1)\Gamma(n)\ \Gamma(m+1)\Gamma(m+2)} \left[\frac{(a_8\Omega_\star^8 + a_4\Omega_\star^4 + a_0)}{\Omega_\star^2(\Omega_\star^4 - 1)} - \frac{m\ \Omega_\star^2}{(m+2)} \right], \quad \text{(A3.54)}$$

Using Stirling's formula (Abramowitz and Stegun, 1965; p.256, 257)

$$\Gamma(1+x) \sim (2\pi x)^{1/2} x^x e^{-x}, \qquad x \to \infty, \quad \text{(A3.55)}$$

it can be noted that

$$\begin{aligned} \frac{\Gamma(1+m+n)}{m\ (m+1)\ \Gamma(n)\ \Gamma(m+1)\Gamma(m+2)} &= \frac{n\Gamma(1+m+n)}{m\ (m+1)\ \Gamma(1+n)\ \Gamma(m+1)\Gamma(m+2)}, \\ &\sim \frac{n\sqrt{2\pi(m+n)}(m+n)^{m+n}e^{-(m+n)}}{n^n e^{-n} m(m+1)\Gamma(m+1)\Gamma(m+2)}, \\ &\sim \frac{e^{-m}(1+\frac{m}{n})^{1/2} n^{m+1}(1+\frac{m}{n})^{m+n}}{m(m+1)\Gamma(m+1)\Gamma(m+2)}, \quad \text{(A3.56)} \end{aligned}$$

as $n \to \infty$. But

$$\left(1+\frac{m}{n}\right)^{1/2}\left(1+\frac{m}{n}\right)^{m+n} = \left(1+\frac{m}{n}\right)^{m+1/2}\left(1+\frac{m}{n}\right)^{n} \sim e^m \ (\text{since } n \to \infty),$$

and so the Equation (A3.56) can be written as

$$\frac{\Gamma(1+m+n)}{m\ (m+1)\ \Gamma(n)\ \Gamma(m+1)\Gamma(m+2)} \sim \frac{n^{m+1}}{m\ (m+1)\ \Gamma(m+1)\Gamma(m+2)}. \quad \text{(A3.57)}$$

Now consider the remaining terms of (A3.54) namely,

$$\frac{(a_8\ \Omega_\star^8 + a_4\ \Omega_\star^4 + \ a_0)}{\Omega_\star^2(\Omega_\star^4 - 1)} - \frac{m\ \Omega_\star^2}{(m+2)}\ , \tag{A3.58}$$

which in terms of $\omega_\star$ can be written as (by substituting $\Omega_\star^2 = \frac{\omega_\star^2}{gk_x}$)

$$\frac{\left(a_8 - \frac{m}{m+2}\right)\frac{\omega_\star^8}{g^4k_x^4} + \left(a_4 + \frac{m}{m+2}\right)\frac{\omega_\star^4}{g^2k_x^2} + a_o}{\frac{\omega_\star^2}{gk_x}\left(\frac{\omega_\star^4}{g^2k_x^2} - 1\right)}\ . \tag{A3.59}$$

On further analysis, Equation (A3.59) can be rearranged as

$$\frac{\omega_\star^2}{gk_x}\left(a_8 - \frac{m}{m+2}\right)\ +\ O(k_x)\ . \tag{A3.60}$$

Thus, Equation (A3.54) now becomes

$$\delta_o\ \sim\ \frac{n^{m+1}}{m\ (m+1)\ \Gamma(m+1)\Gamma(m+2)}\frac{\omega_\star^2}{gk_x}\left(a_8 - \frac{m}{m+2}\right)(2k_xz_o)^{m+2}\ , \tag{A3.61}$$

which on using the Equation (3.83) of the main text further simplifies to

$$\delta_o\ =\ \frac{-(m)^{m+1}(2k_x)^{-m-1}\left(\frac{\omega_\star^2}{g}\right)^{m+1}\left(\frac{\omega_\star^2}{gk_x}\right)\left(a_8 - \frac{m}{m+2}\right)}{m(m+1)\Gamma(m+1)\Gamma(m+2)}\ (2k_xz_o)^{m+2}\ . \tag{A3.62}$$

Thus,

$$\delta_o\ =\ \frac{-2\left(\frac{m\omega_\star^2}{g}\right)^{m+2}(2k_x)^{-(m+2)}\left(a_8 - \frac{m}{m+2}\right)}{m^2(m+1)\Gamma(m+1)\Gamma(m+2)}\ (2k_xz_o)^{m+2}\ , \tag{A3.63}$$

giving

$$\delta_o\ =\ -\frac{2}{(m+1)m^2\Gamma(m+1)\Gamma(m+2)}\left(\frac{m\omega_\star^2z_o}{g}\right)^{m+2}\left(a_8 - \frac{m}{m+2}\right)\ . \tag{A3.64}$$

This is Equation (3.84) of the main text.

Section 7: The Magnetic Correction

In order to determine δ_b, the correction due to a magnetic-field, consider the dispersion relation in the presence of the magnetic field i.e. Equation (3.45):

$$2a\kappa\frac{U\left(-a+1,m+3,2\kappa\right)}{U\left(-a,m+2,2\kappa\right)} \;+\; (m+1) \;-\; \kappa\frac{(1\;+\;\Omega^2)}{\Omega^2}$$

$$= \left(\frac{T_c}{T_p}\right)\frac{\gamma\wedge(\wedge\Omega^2\;-\;\kappa)(1\;-\;\Omega^4)}{\Gamma\Omega^2\left[\wedge\;+\;\phi\left(\frac{1\;+\;\beta}{\beta}\right)\left(\wedge\Omega^2\;-\;\frac{\kappa}{1\;+\;\beta}\right)\right]}\,. \qquad \text{(A3.65)}$$

In the limit $\kappa \to 0$, it may be shown that (A3.65) becomes

$$2a\kappa\frac{U\left(-a+1,m+3,2\kappa\right)}{U\left(-a,m+2,2\kappa\right)} = \left(\frac{T_c}{T_p}\right)\frac{\gamma^2\beta\wedge(1-\Omega_*^4)}{\Gamma\left[\beta(1-\Omega_*^4)+\gamma\Omega_*^2\right]} - (m+1)\,. \qquad \text{(A3.66)}$$

Noting the expansion of left hand side of (A3.66) in the limit of $\kappa \to 0$ from Section 3.3.1,

$$-(1+m)\left[\frac{\mathcal{D}_1+(2\kappa)^{(m+2-s)}\mathcal{D}_2 a\mathcal{H}}{\mathcal{D}_3-(2\kappa)^{(m+1-s)}\mathcal{D}_4\mathcal{H}}\right] = \left(\frac{T_c}{T_p}\right)\frac{\gamma^2\beta\wedge(1-\Omega_*^4)}{\Gamma\left[\beta(1-\Omega_*^4)+\gamma\Omega_*^2\right]} - (m+1), \qquad \text{(A3.67)}$$

where

$$\mathcal{H} \;=\; \frac{2(-1)^n}{m\;\delta_b\;\Gamma(n)}\,. \qquad \text{(A3.68)}$$

With $s = m+1$, (A3.67) becomes

$$-(m+1)\left[\frac{\mathcal{D}_1}{\mathcal{D}_3\;-\;\mathcal{D}_4\mathcal{H}}\right] = \left(\frac{T_c}{T_p}\right)\frac{\gamma^2\beta\wedge(1-\Omega_*^4)}{\Gamma\left[\beta(1-\Omega_*^4)+\gamma\Omega_*^2\right]} \;-\; (m+1)\,. \qquad \text{(A3.69)}$$

Substituting for $\mathcal{D}_1$, $\mathcal{D}_3$ and $\mathcal{D}_4$ from Section 3.3.1, equation (A3.69) yields

$$\frac{-(m+1)}{\left[1\;-\;\frac{\Gamma(-m)}{\Gamma(-m-n)\Gamma(m+2)}\mathcal{H}\right]} \;=\; \left(\frac{T_c}{T_p}\right)\frac{\gamma^2\beta\wedge(1-\Omega_*^4)}{\Gamma\left[\beta(1-\Omega_*^4)+\gamma\Omega_*^2\right]} \;-\; (m+1)\,, \qquad \text{(A3.70)}$$

which after further simplification gives

$$1 \; - \; \frac{\Gamma(-m)\mathcal{H}}{\Gamma(-m-n)\Gamma(m+2)} = \frac{2\left[\gamma\Omega_\star^2 \; + \; \beta(1-\Omega_\star^4)\right]}{2\left[\gamma\Omega_\star^2 + \beta(1-\Omega_\star^4)\right] - (2\beta+\gamma)(1-\Omega_\star^4)} \; . \quad \text{(A3.71)}$$

Using (A3.68) and (A3.50), equation (A3.71) can be written as

$$\frac{2\Gamma(m+n+1)}{m\delta_b\Gamma(n)\Gamma(m+1)\Gamma(m+2)} = \frac{(2\beta+\gamma)(1-\Omega_\star^4)}{\left[\gamma(1-\Omega_\star^4) - 2\gamma\Omega_\star^2\right]} \; , \quad \text{(A3.72)}$$

which then determines δ_b as follows:

$$\delta_b \;\; = \;\; \frac{2\Gamma(m+n+1)\gamma\left[1-\Omega_\star^4-2\Omega_\star^2\right]}{m\Gamma(n)\Gamma(m+1)\Gamma(m+2)(2\beta+\gamma)(1-\Omega_\star^4)} \; . \quad \text{(A3.73)}$$

This is Equation (3.99) of the main text.

Section 8: High Frequency Limit of the Magnetic Correction

In order to take the limit $n \rightarrow \infty$, consider the correction δ_b due to the presence of a magnetic field given above Equation (A3.73). As shown in Section 5,

$$\frac{\Gamma(m+n+1)}{\Gamma(n)} \sim n^{m+1} \sim -(m)^{m+1}(2k_x)^{-m-1}\left(\frac{\omega_\star^2}{g}\right)^{m+1}\left(\frac{\omega_\star^2}{gk_x}\right) \; . \quad \text{(A3.74)}$$

Now consider the term

$$\frac{\Omega_\star^4 + 2\;\Omega_\star^2 - 1}{(\Omega_\star^4 - 1)} \; . \quad \text{(A3.75)}$$

This can be written in terms of $\omega_\star$ as

$$\frac{\omega_\star^4 + 2\;\omega_\star^2 gk_x - g^2k_x^2}{\omega_\star^4 - g^2k_x^2} \approx \left(1 + 2\frac{gk_x}{\omega_\star^2} - \frac{g^2k_x^2}{\omega_\star^4}\right)\left(1 - \frac{g^2k_x^2}{\omega_\star^4}\right)^{-1} \; . \quad \text{(A3.76)}$$

Thus,

$$\frac{\Omega_\star^4 + 2\;\Omega_\star^2 - 1}{(\Omega_\star^4 - 1)} \sim 1 + \frac{2gk_x}{\omega_\star^2} \; + \; O(k_x^3) \; . \quad \text{(A3.77)}$$

Putting Equations (A3.74) and (A3.77) together into Equation (A3.73) gives

$$\delta_b = \frac{2\gamma\left(\frac{m\omega_*^2}{g}\right)^{m+1}(2k_x)^{-m-1}\left(1-\frac{gk_x}{\omega_*^2}\right)^{m+1}}{m\Gamma(m+1)\Gamma(m+2)(\gamma+2\beta)}\left\{1+\frac{2gk_x}{\omega_*^2}+O(k_x^3)\right\} . \quad \text{(A3.78)}$$

Noting that

$$\Omega^2 \sim \Omega_*^2 + \frac{2\gamma(2k_x)^{-m-1}}{m\Gamma(n)\Gamma(m+1)\Gamma(m+2)(\gamma+2\beta)}\left(\frac{m\omega_*^2}{g}\right)^{m+1}(2k_x z_o)^{m+1} , \quad \text{(A3.79)}$$

Thus,

$$\Omega^2 \sim \Omega_*^2 + \frac{2\gamma}{m\Gamma(n)\Gamma(m+1)\Gamma(m+2)(\gamma+2\beta)}\left(\frac{m\omega_*^2}{g}\right)^{m+1}(z_o)^{m+1} , \quad \text{(A3.80)}$$

In terms of cyclic frequency $\nu(=\omega/2\pi)$ this can be approximated to

$$\nu \sim \nu_*\left[1 + \frac{(m+1)}{\Gamma(m+1)\Gamma(m+2)}\left(\frac{\gamma\, m(m+1)}{4}\right)^m\left(\frac{\gamma}{\gamma+2\beta}\right)\left(\frac{\nu_*}{\nu_c}\right)^{2m}\left(\frac{H_o}{R_{sun}}\right)l\right] \quad \text{(A3.81)}$$

This leads to Equation (3.101) of the main text.

APPENDIX A5 : DERIVATION OF DISPERSION RELATIONS FOR EXTREME VALUES OF h

Section 1: The Limit h → 0

The dispersion relation is given by (see Equation (5.25))

$$\mathcal{J} = \frac{(\omega^2 - k_x^2 c_{sm}^2)(c_{sm}^2 + \frac{\gamma}{2} v_{Am}^2)\left\{(\mathcal{X}_1\mathcal{M} - \mathcal{X}_2\mathcal{L}) \; + \; (\mathcal{L} - \mathcal{M})/\Re_B\right\}}{(\omega^2 - k_x^2 c_{sc}^2)(c_{sm}^2 + v_{Am}^2)(\omega^2 - k_x^2 c_{Tm}^2)\left\{(\mathcal{M}\mathcal{Z}_2\mathcal{X}_1 - \mathcal{L}\mathcal{Z}_1\mathcal{X}_2) + (\mathcal{L}\mathcal{Z}_1 - \mathcal{M}\mathcal{Z}_2)/\Re_B\right\}}, \tag{A5.82}$$

As $h \to 0$ (see Equation (5.25) - (5.30)), $\mathcal{L} = \mathcal{M} \quad \mathcal{X}_1 = \mathcal{Z}_1 \quad \mathcal{X}_2 = \mathcal{Z}_2$. Thus (A5.82) becomes

$$\mathcal{J} = \frac{(\omega^2 - k_x^2 c_{sm}^2)(c_{sm}^2 + \frac{\gamma}{2} v_{Am}^2)\Re_B}{(\omega^2 - k_x^2 c_{sc}^2)(c_{sm}^2 + v_{Am}^2)(\omega^2 - k_x^2 c_{Tm}^2)} \; , \tag{A5.83}$$

where

$$\Re_B = \frac{2\beta + \gamma}{2\beta} \frac{(c_{sm}^2 + v_{Am}^2 e^{h/H_m})(\omega^2 - k_x^2 c_{Tmc}^2)(\omega^2 - k_x^2 c_{sc}^2)}{(\omega^2 - k_x^2 c_{sm}^2)(c_{sm}^2 + \frac{\gamma}{2} v_{Am}^2 e^{h/H_m})\left\{g k_x^2 + \phi\left[-1 + \sqrt{1 - 4A_c H_c^2}\right]\right\}}. \tag{A5.84}$$

After considerable algebra it is possible to rearrange (A5.83) as

$$2a\omega^2 c_{sp}^2 k_x \frac{U(-a+1, m+3, 2k_x z_o)}{U(-a, m+2, 2k_x z_o)} \; + \; \gamma g \omega^2 \; - \; k_x c_{sp}^2(\omega^2 + g k_x)$$

$$= \left(\frac{\rho_p}{\rho_c}\right) \frac{m_o^2 \left(g^2 k_x^2 - \omega^4\right) c_{sp}^2}{\left\{(k_x^2 v_{Ac}^2 - \omega^2)\lambda_+ + \frac{g k_x^2 c_{sc}^2 m_o^2}{(\omega^2 - k_x^2 c_{sc}^2)}\right\}} \; . \tag{A5.85}$$

This is Equation (5.36) of the main text.

Section 2: The Limit h $\rightarrow \infty$

The dispersion relation (5.25) can also be written as

$$\mathcal{J} = \frac{(\omega^2 - k_x^2 c_{sm}^2)(c_{sm}^2 + \frac{\gamma}{2} v_{Am}^2)\left\{(\frac{\mathcal{X}_1 \mathcal{M}}{\mathcal{L}} - \mathcal{X}_2 + (1 - \frac{\mathcal{M}}{\mathcal{L}})/\Re_B\right\}}{(\omega^2 - k_x^2 c_{sc}^2)(c_{sm}^2 + v_{Am}^2)(\omega^2 - k_x^2 c_{Tm}^2)\left\{(\frac{\mathcal{M}\mathcal{Z}_2 \mathcal{X}_1}{\mathcal{L}} - \mathcal{Z}_1 \mathcal{X}_2) + (\mathcal{Z}_1 - \frac{\mathcal{M}\mathcal{Z}_2}{\mathcal{L}})/\Re_B\right\}}. \tag{A5.86}$$

As $h \rightarrow \infty$, $\mathcal{L} \rightarrow \infty$ and hence the above Equation reduces to

$$\mathcal{J} = \frac{(\omega^2 - k_x^2 c_{sm}^2)(c_{sm}^2 + \frac{\gamma}{2} v_{Am}^2)\{-\mathcal{X}_2) + 1/\Re_B\}}{(\omega^2 - k_x^2 c_{sc}^2)(c_{sm}^2 + v_{Am}^2)(\omega^2 - k_x^2 c_{Tm}^2)\{-\mathcal{Z}_1 \mathcal{X}_2 + \mathcal{Z}_1/\Re_B\}}. \tag{A5.87}$$

Substituting $\mathcal{J}$ after simplifying, the above Equation can be written as

$$2a\omega^2 c_{sp}^2 k_x \frac{U(-a+1, m+3, 2k_x z_o)}{U(-a+1, m+3, 2k_x z_o)} + \gamma g\omega^2 - k_x c_{sp}^2(\omega^2 + g k_x)$$

$$= \frac{(\omega^2 - k_x^2 c_{sm}^2)(c_{sm}^2 + \frac{\gamma}{2} v_{Am}^2)(g^2 k_x^2 - \omega^4)}{(\omega^2 - k_x^2 c_{sc}^2)(c_{sm}^2 + v_{Am}^2)(\omega^2 - k_x^2 c_{Tm}^2) + \mathcal{Z}_1}. \tag{A5.88}$$

But

$$\mathcal{Z}_1 = \left\{ k_x + \frac{F'\left(p, q; r; \frac{-\mathcal{A}_1}{\mathcal{A}_2}\right)}{F\left(p, q; r; \frac{-\mathcal{A}_1}{\mathcal{A}_2}\right)} + \frac{g k_x^2 c_{sm}^2}{(c_{sm}^2 + v_{Am}^2)(\omega^2 - k_x^2 c_{Tm}^2)} \right\}. \tag{A5.89}$$

Thus the dispersion relation (A5.86) becomes

$$2a\omega^2 c_{sp}^2 k_x \frac{U(-a+1, m+3, 2k_x z_o)}{U(-a, m+2, 2k_x z_o)} + \gamma g\omega^2 - k_x c_{sp}^2(\omega^2 + g k_x)$$

$$= \left(\frac{\rho_p}{\rho_m}\right) \frac{(g^2 k_x^2 - \omega^4)(\omega^2 - k_x^2 c_{sm}^2)}{g k_x^2 c_{sm}^2 + (c_{sm}^2 + v_{Am}^2)(\omega^2 - k_x^2 c_{Tm}^2)\left\{k_x - \frac{pq}{r}\frac{\mathcal{A}_1 \mathcal{A}_3}{\mathcal{A}_2}\frac{F\left(p+1, q+1; r+1; \frac{-\mathcal{A}_1}{\mathcal{A}_2}\right)}{F\left(p, q; r; \frac{-\mathcal{A}_1}{\mathcal{A}_2}\right)}\right\}} \tag{A5.90}$$

This is Equation (5.37) of the main text.

REFERENCES

Abramowitz, M. and Stegun, I. A. 1965, *Handbook of Mathematical Functions*, Dover, New York.

Adam, J. A. 1977, *Solar Phys.* **52**, 293.

Ando, H. and Osaki, Y. 1975, *Publ. Astron. Soc. Japan* **29**, 221.

Bernstein, I. B. and Book, D. L. 1983, *Phys. Fluids* **26**, 453.

Bogdan, T. J. and Cattaneo, F. 1989, *Ap. J.* **342**, 545.

Bogdan, T. J. and Zweibel, E. G. 1985, *Ap. J.* **298**, 867.

Cadez, V. M. and Okretic, V. K. 1989, *J. Plasma Phys.* **41**, 23.

Cally, P. S. and Adam, J. A. 1983, *Solar Phys.* **85**, 97.

Campbell, W. R. 1987, *Ph.D. Thesis*, University of St. Andrews.

Campbell, W. R. and Roberts, B. 1986, in *Advances in Helio- and Asteroseisemology*, ed. J. Christensen Daalsgaard and S. Frandsen, IAU Symp.No.**123**, p.161.

Campbell, W. R. and Roberts, B. 1989, *Ap. J.* **338**, 538.

Chandrasekhar, S. 1961, in *Hydrodynamic and Hydromagnetic Stability*, Clarendon Press, Oxford, Section 97.

Christensen-Dalsgaard, J. 1986, in *Helio- and Asterioseismology*, ed. J. Christensen-Dalsgaard and S. Frandsen, IAU Symp.No.**123**, p.3.

Christensen-Dalsgaard, J. and Berthomieu, G. 1991, in *Solar Interior and Atmosphere*, ed. A. N. Cox, W. C. Livingston and M. S. Matthews, The University of Arizona Press, p.401.

Christensen-Dalsgaard, J. and Gough, D. O. 1980, *Nature* **288**, 544.

Christensen-Dalsgaard, J., Gough, D. O. and Toomre, J. 1985 *Science* **229**, 923.

Cowling, T. G. 1941, *Mon. Not. Roy. Astron. Soc.* **101**, 367.

Davila, J. M. 1990 in *Basic Plasma Processes on the Sun*, ed. E. R. Priest and V. Krishan, IAU Symp.No. **142**, p.149.

Deubner, F.-L. 1972, *Solar Phys.* **22**, 263.

Deubner, F.-L. 1975, *Astron. Astrophys.* **44**, 371.

Deubner, F.-L. and Gough, D. O. 1984, *Ann. Rev. Astron. Astrophys.* **22**, 593.

Dungey, J. W. and Loughhead, R. E. 1954 *Australian J. Phys.* **7**, 5.

Duvall, T. L., Harvey, J. W. and Pomerantz, M. A. 1987, in *The Internal Solar Angular Velocity*, ed. B. R. Durney and S. Sofia, D. Reidel Publishing Co. Holland, p.19.

Elsworth, Y., Howe, R., Isaak, G.R., McLeod, C.P. and New, R. 1990, *Nature* **345**, 322.

Evans, D. J. 1990, *Ph.D. Thesis*, University of St. Andrews.

Evans, D. J. 1991, private comm.

Evans, D. J. and Roberts, B. 1990, *Ap. J.* **356**, 704.

Evans, D. J. and Roberts, B. 1991, *Ap. J.* **371**, 387.

Evans, D. J. and Roberts, B. 1992, *Nature* **355**, 230.

Evans, J. W. and Michard, R. 1962, *Ap. J.* **136**, 493.

Gerwin, R. 1967, *Phys. Fluids.* **10**, 2164.

Gingerich, O., Noyes, R. W., Kalkofen, W. and Cuny, Y. 1971, *Solar Phys.* **18**, 347.

Giovanelli, R. G. 1972, *Solar Phys.* **27**, 71.

Goedbloed, J. P. 1971, *Physica* **53**, 412.

Goldreich, P., Murray, N., Willette, G. and Kumar, P. 1991, *Ap. J.* **370**, 752.

Gough, D. O. and Thompson, M. J. 1986, in *Advances in Helio- and Asteroseismology*, ed. J. Christensen Daalsgaard and S. Frandsen, IAU Symp.No.**123**, p.155.

Hill, F., Deubner, F.-Z. and Isaak, G. 1991, in *Solar Interior and Atmosphere*, ed. A. N. Cox, W. C. Livingston and M. S. Matthews, The University of Arizona Press, p.329.

Hollweg, J. V. 1986, in *Advances in Space Plasma Physics*, ed. B. Buti, World Scientific, p.77.

Hollweg, J. V. 1987a, *Ap. J.* **312**, 880.

Hollweg, J. V. 1987b, *Ap. J.* **320**, 875.

Hollweg, J. V. 1990, *Comp. Phys. Reports* **12**, 205.

Ionson, J. A. 1978, *Ap. J.* **226**, 650.

Ionson, J. A. 1985, *Solar Phys.* **100**, 289.

Jain, R. and Roberts, B. 1990, in *Mechanisms of Chromospheric and Coronal Heating*, ed. P. Ulmschneider, E. R. Priest and R. Rosner, Springer-Verlag, p.511.

Jain, R. and Roberts, B. 1991, *Solar Phys.* **133**, 263.

Kruskal, M. and Schwarzschild, M. 1954, *Proc. Roy. Soc.* **A223**, 348.

Lamb, H. 1932, *Hydrodynamics*, Cambridge University Press, Cambridge.

Lee, M. A. and Roberts, B. 1986, *Ap. J.* **301**, 430.

Leibacher, J. W., Noyes, R. W., Toomre, J. and Ulrich, R. K. 1985 *Scientific Amer.* **253**, 48.

Leibacher, J. W. and Stein, R. F. 1971, *Ap. J.* **7**, L191.

Leibacher, J. W. and Stein, R. F. 1981, in *The Sun as a Star*, ed. S. Jordan, NASA SP-450, p.263.

Leighton, R. B. 1960, Proceedings of IAU Symp., **12**, 321.

Leighton, R. B., Noyes, R. W. and Simon, G. W. 1962, *Ap. J.* **135**, 474.

Libbrecht, K. G. and Kaufman, J. M. 1988, *Ap. J.* **324**, 1172.

Libbrecht, K. G. and Woodard, M. F. 1990, *Nature* **345**, 779.

Libbrecht, K. G., Woodard, M. F. and Kaufman, J. M. 1990, *Ap. J. Suppl.* **74**, 1129.

Mein, P. 1966, *Ann. Astrophys.* **29**, 153.

Miles, A. J. 1991 *Ph.D. Thesis*, University of St. Andrews.

Miles, A. J. and Roberts, B. 1989, *Solar Phys.* **119**, 257.

Miles, A. J. and Roberts, B. 1992, *Solar Phys.* **141**, 205.

Nye, A. H. and Thomas, J. H. 1974, *Solar Phys.* **38**, 399.

Nye, A. H. and Thomas, J. H. 1976, *Ap. J.* **204**, 582.

Priest, E. R. 1982, *Solar Magnetohydrodynamics*, D. Reidel Publ. Co., Holland.

Rabaey, G. F., Hill, H. A. and Barry, C. T. 1988, *Astrophys. and Space Sc.* **143**, 81.

Rae, I. C. and Roberts, B. 1981, *Geophys. Astrophys. Fluid Dyn.* **18**, 197.

Rae, I. C. and Roberts, B. 1983, *Solar Phys.* **84**, 99.

Roberts, B. 1980, *Ann. Phys. Fr.* **5**, 453.

Roberts, B. 1981, *Solar Phys.* **69**, 27.

Roberts, B. 1985, in *Solar System Magnetic Fields*, ed. E. R. Priest, D. Reidel Publ. Co., Holland, chap. 3.

Roberts, B. 1986, in *Small Scale Magnetic Flux Concentrations in the Solar Photosphere*, ed. W. Deinzer, M. Knolker and H. H. Voigt, p.169.

Roberts, B. 1988, in *Symp. on the Physics of Ionised Gases, Sarajevo*, ed. L. Tanović, p.687.

Roberts, B. 1990, in *Mechanisms of Chromospheric and Coronal Heating*, ed. P. Ulmschneider, E. R. Priest and R. Rosner, Springer-Verlag, p.511.

Roberts, B. and Campbell, W. R. 1986, *Nature* **323**, 603.

Roberts, B. and Campbell, W. R. 1988, in *Seismology of the Sun and Sun-like stars*, ed. E. J. Rolfe, ESA SP-286, p.311.

Ryutova, M. P. 1990, in *Solar Photosphere: Structure, Convection and Magnetic Fields*, ed. J. O. Stenflo, IAU Symp. **138**, p.229.

Small, L. M. and Roberts, B. 1984, in *The Hydromagnetics of the Sun*, ESA SP-200, p.257.

Somasundaram, K. and Uberoi, C. 1982, *Solar Phys.* **81**, 19.

Southwood, D. J. and Hughes, J. W. 1983 *Space Sci. Rev.* **35**, 301.

Speigel, E. A. and Unno, W. 1962, *Publ. Astron. Soc. Japan* **14**, 28.

Spruit, H. C. 1983, in *Solar and Stellar Magnetic Fields: Origins and Coronal Effects*, ed. J. O. Stenflo, D. Reidel Publ. Co., Holland, p.41.

Spruit, H. C. and Roberts, B. 1983, *Nature* **304**, 401.

Tarbell, T., Peri, M., Frank, Z., Title, A. 1988, in *Seismology of the Sun and Sun-like Stars*, ed. E. J. Rolfe, ESA SP-286, p.315.

Temme, N. M. 1983, *Numer. Math.* **41**, 63.

Thomas, J. H. 1985, in *Theoretical Problems in High Resolution Solar Physics*,

ed. H. U. Schmidt, Max-Planck-Institut fur Astrophysik, Garching, p.126.
Thompson, M. J. 1988, in *Seismology of the Sun and Sun-like Stars*,
ed. E. J. Rolfe, ESA SP-286, p.321.
Uberoi, C. 1982, *Solar Phys.* **78**, 351.
Ulrich, R. K. 1970, *Ap. J.* **162**, 993.
Vorontsov, S. V. 1986, in *Advances in Helio- and Asteroseismology*,
ed. J. Christensen Dalsgaard and S. Frandsen, IAU Symp.No. **123**, p.151.
Wentzel, D. G. 1979, *Ap. J.* **227**, 319.
Woodard, M.F. and Libbrecht, K.G. 1991, *Ap. J.* **374**, L61.
Woodard, M.F. and Noyes, R. W. 1985, *Nature* **318**, 449.
Wright, A. N. and Thompson, M. J. 1992, *Astron. Astrophys.* **264**, 701.
Zhugzhda, Y. D. and Dzhalilov, N. S. 1984, *Astron. Astrophys.* **133**, 333.
Zirin, H. and Stein, A. 1972, *Ap. J.* **178**, L85.
Zweibel, E. G. and Bogdan, T. J. 1986, *Ap. J.* **308**, 401.
Zweibel, E. G. and Däppen, W. 1989, *Ap. J.* **343**, 994.